

Міністерство освіти і науки України  
Національний університет  
«Полтавська політехніка імені Юрія Кондратюка»

---

Ministry of Education and Science of Ukraine  
National University «Yuri Kondratyuk Poltava Polytechnic»

# **ЗБІРНИК НАУКОВИХ ПРАЦЬ**

ГАЛУЗЕВЕ МАШИНОБУДУВАННЯ,  
БУДІВНИЦТВО

**Випуск 2 (55)' 2020**

---

**ACADEMIC JOURNAL**  
INDUSTRIAL MACHINE BUILDING,  
CIVIL ENGINEERING  
**Issue 2 (55)' 2020**

Полтава – 2020

---

Poltava – 2020



[www.znp.nupp.edu.ua](http://www.znp.nupp.edu.ua)  
<http://journals.nupp.edu.ua/znp>

## Збірник наукових праць. Галузеве машинобудування, будівництво / Національний університет «Полтавська політехніка імені Юрія Кондратюка»

Збірник наукових праць видається з 1999 р., періодичність – двічі на рік.

Засновник і видавець – Національний університет «Полтавська політехніка імені Юрія Кондратюка».

Свідоцтво про державну реєстрацію КВ 24621-14561ПР від 14.12.2020 р.

Збірник наукових праць включений до переліку наукових фахових видань (категорія Б), у яких можуть публікуватися результати дисертаційних робіт (Наказ МОН України №1218 від 07.11.2018 року).

Збірник наукових праць рекомендовано до опублікування вченою радою Національного університету «Полтавська політехніка імені Юрія Кондратюка» протокол №6 від 30.12.2020 р.

У збірнику представлені результати наукових і науково-технічних розробок у галузі машинобудування, автомобільного транспорту та механізації будівельних робіт; із проектування, зведення, експлуатації та реконструкції будівельних конструкцій, будівель і споруд; їх основ та фундаментів; будівельної фізики та енергоефективності будівель і споруд.

Призначений для наукових й інженерно-технічних працівників, аспірантів і магістрів.

### Редакційна колегія:

<i>Пічугін С.Ф.</i>	– <i>головний редактор</i> , д.т.н., професор, Національний університет «Полтавська політехніка імені Юрія Кондратюка» (Україна), pichugin.sf@gmail.com
<i>Винников Ю.Л.</i>	– <i>заступник головного редактора</i> , д.т.н., професор, Національний університет «Полтавська політехніка імені Юрія Кондратюка» (Україна), vnyukov@ukr.net
<i>Ільченко В.В.</i>	– <i>відповідальний секретар</i> , к.т.н., доцент, Національний університет «Полтавська політехніка імені Юрія Кондратюка» (Україна), znpbud@gmail.com
<i>Болтрік М.</i>	– д.т.н., професор, Білостоцький технологічний університет (Польща)
<i>Ємельянова І.А.</i>	– д.т.н., професор, Харківський національний університет будівництва та архітектури (Україна)
<i>Галінська Т.А.</i>	– к.т.н., доцент, Національний університет «Полтавська політехніка імені Юрія Кондратюка» (Україна)
<i>Гасімов А.Ф.</i>	– к.т.н., доцент, Азербайджанський архітектурно-будівельний університет (Азербайджан)
<i>Качинський Р.</i>	– д.т.н., професор, Білостоцький технологічний університет (Польща)
<i>Коробко Б.О.</i>	– д.т.н., професор, Національний університет «Полтавська політехніка імені Юрія Кондратюка» (Україна)
<i>Косіор-Казберук М.</i>	– д.т.н., професор, Білостоцький технологічний університет (Польща)
<i>Камал М.А.</i>	– д.т.н., доцент, Мусульманський університет Алігарха (Індія)
<i>Молчанов П.О.</i>	– к.т.н., доцент, Національний університет «Полтавська політехніка імені Юрія Кондратюка» (Україна)
<i>Назаренко І.І.</i>	– д.т.н., професор, Київський національний університет будівництва та архітектури (Україна)
<i>Павліков А.М.</i>	– д.т.н., професор, Національний університет «Полтавська політехніка імені Юрія Кондратюка» (Україна)
<i>Погрібний В.В.</i>	– к.т.н., с.н.с., Національний університет «Полтавська політехніка імені Юрія Кондратюка» (Україна)
<i>Савик В.М.</i>	– к.т.н., доцент, Національний університет «Полтавська політехніка імені Юрія Кондратюка» (Україна)
<i>Семко О.В.</i>	– д.т.н., професор, Національний університет «Полтавська політехніка імені Юрія Кондратюка» (Україна)
<i>Шаповал В.Г.</i>	– д.т.н., професор, Національний гірничий університет (Україна)
<i>Стороженко Л.І.</i>	– д.т.н., професор, Національний університет «Полтавська політехніка імені Юрія Кондратюка» (Україна)
<i>Сулєвська М.</i>	– д.т.н., професор, Білостоцька політехніка (Польща)
<i>Тур В.В.</i>	– д.т.н., професор, Брестський державний технічний університет (Білорусь)
<i>Васильєв Є.А.</i>	– к.т.н., доцент, Національний університет «Полтавська політехніка імені Юрія Кондратюка» (Україна)
<i>Вінеке-Тумаї Б.</i>	– д.т.н., професор, Університет прикладних наук м. Банденбург (Німеччина)
<i>Панг С.</i>	– к.т.н., професор, Китайський університет нафти – Пекін (Китай)
<i>Жусупбеков А.Ж.</i>	– д.т.н., професор, Євразійський національний університет ім. Л.М. Гумільова (Казахстан)
<i>Зоценко М.Л.</i>	– д.т.н., професор, Національний університет «Полтавська політехніка імені Юрія Кондратюка» (Україна)
<i>Зурло Франческо</i>	– д.т.н., професор, Міланська політехніка (Італія)

Адреса видавця та редакції – Національний університет «Полтавська політехніка імені Юрія Кондратюка»

Науково-дослідницька частина, к. 320Ф, Першотравневий проспект, 24, м. Полтава, 36011.

тел.: (05322) 29875; e-mail: [v171@nupp.edu.ua](mailto:v171@nupp.edu.ua); [www.nupp.edu.ua](http://www.nupp.edu.ua)

Макет та тиражування виконано у поліграфічному центрі

Національного університету «Полтавська політехніка імені Юрія Кондратюка»,

Першотравневий проспект, 24, м. Полтава, 36011.

Свідоцтво про внесення суб'єкта видавничої справи до державного реєстру видавців,

виготовників і розповсюджувачів видавничої продукції (ДК № 3130 від 06.03.2008 р.).

Комп'ютерна верстка – В.В. Ільченко. Коректори – Я.В. Новічкова, Л.А. Ключко.

Підписано до друку 31.12.2020 р.

Папір ксерокс. Друк різнограф. Формат 60x80 1/8. Ум. друк. арк. – 15,11.

Тираж 300 прим.

## Academic journal. Industrial Machine Building, Civil Engineering / National University «Yuri Kondratyuk Poltava Polytechnic»

Academic journal was founded in 1999, the publication frequency of the journal is twice a year.

Founder and Publisher is National University «Yuri Kondratyuk Poltava Polytechnic».

State Registration Certificate KB 24621-14561IIP dated 14.12.2020.

Academic journal is included into the list of specialized academic publications where graduated thesis results could be presented (Order of Department of Education and Science of Ukraine № 1218 dated 07.11.2018).

Academic journal was recommended for publication by the Academic Board of National University «Yuri Kondratyuk Poltava Polytechnic», transactions № 6 of 30.12.2020.

The results of scientific and scientific-technical developments in the sphere of mechanical engineering, automobile transport and mechanization of construction works; designing, erection, operation and reconstruction of structural steels, buildings and structures; its bases and foundations; building physics and energy efficiency of buildings and structures are presented in the collection.

Academic journal is designed for researchers and technologists, postgraduates and senior students.

### Editorial Board:

<i>Pichugin Sergii</i>	– <i>Editor-in-Chief</i> , DSc, Professor, National University «Yuri Kondratyuk Poltava Polytechnic» (Ukraine), pichugin.sf@gmail.com
<i>Vynnykov Yuriy</i>	– <i>Deputy Editor</i> , DSc, Professor, National University «Yuri Kondratyuk Poltava Polytechnic» (Ukraine), vynnykov@ukr.net
<i>Ilchenko Volodymyr</i>	– <i>Executive Secretary</i> , PhD, Associate Professor, National University «Yuri Kondratyuk Poltava Polytechnic» (Ukraine), znpbud@gmail.com
<i>Boltryk Michal</i>	– DSc, Professor, Bialystok Technological University (Poland)
<i>Emeljanova Inga</i>	– DSc, Professor, Kharkiv National University of Construction and Architecture (Ukraine)
<i>Galinska Tatiana</i>	– PhD, Associate Professor, National University «Yuri Kondratyuk Poltava Polytechnic» (Ukraine)
<i>Gasimov Akif</i>	– PhD, Associate Professor, Azerbaijan Architectural and Construction University (Azerbaijan)
<i>Kaczyński Roman</i>	– DSc, Professor, Bialystok Technological University (Poland)
<i>Korobko Bogdan</i>	– DSc, Professor, National University «Yuri Kondratyuk Poltava Polytechnic» (Ukraine)
<i>Kosior-Kazberuk Marta</i>	– DSc, Professor, Bialystok Technological University (Poland)
<i>Kamal Mohammad Arif</i>	– DSc, Associate Professor, Architecture Section, Aligarh Muslim University (India)
<i>Molchanov Petro</i>	– PhD, Associate Professor, National University «Yuri Kondratyuk Poltava Polytechnic» (Ukraine)
<i>Nazarenko Ivan</i>	– DSc, Professor, Kyiv National Civil Engineering and Architecture University (Ukraine)
<i>Pavlikov Andriy</i>	– DSc, Professor, National University «Yuri Kondratyuk Poltava Polytechnic» (Ukraine)
<i>Pohribnyi Volodymyr</i>	– PhD, Associate Professor, National University «Yuri Kondratyuk Poltava Polytechnic» (Ukraine)
<i>Savyk Vasyl</i>	– PhD, Associate Professor, National University «Yuri Kondratyuk Poltava Polytechnic» (Ukraine)
<i>Semko Oleksandr</i>	– DSc, Professor, National University «Yuri Kondratyuk Poltava Polytechnic» (Ukraine)
<i>Shapoval Volodymyr</i>	– DSc, Professor, National Mining University (Ukraine)
<i>Storozhenko Leonid</i>	– DSc, Professor, National University «Yuri Kondratyuk Poltava Polytechnic» (Ukraine)
<i>Sulewska Maria</i>	– DSc, Professor, Bialystok University of Technology (Poland)
<i>Tur Viktor</i>	– DSc, Professor, Brest State Technical University (Belarus)
<i>Vasyliiev Ievgen</i>	– PhD, Associate Professor, National University «Yuri Kondratyuk Poltava Polytechnic» (Ukraine)
<i>Wieneke-Toutaoui Burghilde</i>	– DSc, Professor, President of Brandenburg University of Applied Sciences (Germany)
<i>Pang Xiongqi</i>	– PhD, Professor, China University of Petroleum – Beijing (China)
<i>Zhusupbekov Askar</i>	– DSc, Professor, Eurasia National L.N. Gumiliov University (Kazakhstan)
<i>Zotsenko Mykola</i>	– DSc, Professor, National University «Yuri Kondratyuk Poltava Polytechnic» (Ukraine)
<i>Zurlo Francesco</i>	– DSc, Professor, Polytechnic University of Milan (Italia)

Address of Publisher and Editorial Board – National University «Yuri Kondratyuk Poltava Polytechnic»,

Research Centre, room 320-F, Pershotravnevyi Avenue, 24, Poltava, 36011, Ukraine.

tel.: (05322) 29875; e-mail: v171@pntu.edu.ua; www.pntu.edu.ua

Layout and printing made in the printing center of National University «Yuri Kondratyuk Poltava Polytechnic», Pershotravnevyi Avenue, 24, Poltava, 36011, Ukraine.

Registration certificate of publishing subject in the State Register of Publishers Manufacturers and Distributors of publishing products (DK № 3130 from 06.03.2008).

Desktop Publishing – V. Ilchenko. Corrections – Y. Novichkova, L. Klochko.

Authorize for printing 31.12.2020.

Paper copier. Print rizoğraf. Format 60x80 1/8. Conventionally printed sheets – 15,11.

Circulation 300 copies.

UDK 624.042.42

## Probabilistic basis development of standardization of snow loads on building structures

Pichugin Sergii<sup>1\*</sup>

<sup>1</sup>National University «Yuri Kondratyuk Poltava Polytechnic» <https://orcid.org/0000-0001-8505-2130>

\*Corresponding author E-mail: [pichugin.sf@gmail.com](mailto:pichugin.sf@gmail.com)

Ensuring the reliability and safety of buildings and structures largely depends on a proper understanding of nature and quantitative description and rationing of loads on building structures, including snow loads. Analysis of the evolution of domestic snow load codes together with their statistical substantiation is an urgent task. The article contains a systematic review of codes and publications on the problem of snow load over the 80-year period from the 40s of the twentieth century to the present. The main attention is paid to the tendencies analysis of designing codes development concerning changes of territorial zoning and design coefficients, the appointment of normative and design values of snow load, and involvement in it of experimental statistical data. There is a high scientific level of domestic code DBN B.1.2-2006 "Loads and effects", which have a modern probabilistic basis and are associated with the codes of Eurocode. Scientific results that can be included in subsequent editions of snow load standards are highlighted.

**Keywords:** snow observations, snow load, territorial zoning, normative load, design load

## Розвиток імовірнісних засад нормування снігового навантаження на будівельні конструкції

Пічугін С.Ф.<sup>1\*</sup>

<sup>1</sup>Національний університет «Полтавська політехніка імені Юрія Кондратюка»

\*Адреса для листування E-mail: [pichugin.sf@gmail.com](mailto:pichugin.sf@gmail.com)

Забезпечення надійності та безаварійності будівель і споруд у великій мірі залежить від правильного розуміння природи і кількісного опису та нормування навантажень на будівельні конструкції, в тому числі снігових навантажень. Ці навантаження на споруди мають досить складну фізичну природу і мінливий характер, що вимагають знання термодинамічних процесів в атмосфері і на ґрунті, фізичних властивостей снігу, методики метеорологічних спостережень і кліматологічного опису місцевості, мінливості навантажень, характеру відкладення снігу на конструкціях і спорудах. Такі особливості у певній мірі відображаються в розділах норм проектування будівельних конструкцій, що містять нормативи снігового навантаження. Більшість параметрів норм снігового навантаження мають імовірнісну природу і вимагають для свого обґрунтування застосування статистичних методів. Ці методи постійно змінювалися і розвивалися разом з регулярним переглядом норм будівельного проектування. Аналіз еволюції вітчизняних норм снігового навантаження разом з їх статистичними обґрунтуванням є актуальною задачею. Матеріали, присвячені сніговим навантаженням, опубліковані в різних науково-технічних журналах, збірниках статей, матеріалах конференцій. Стаття містить систематизований огляд норм проектування та публікацій по проблемі снігового навантаження за 80-річний період з 40-х років ХХ століття до теперішнього часу. Головна увага приділяється аналізу тенденцій розвитку норм проектування конструкцій в частині змін територіального районування та розрахункових коефіцієнтів, призначення нормативних і розрахункових значень снігового навантаження і залучення до цього дослідних статистичних даних. Відзначається високий науковий рівень вітчизняних норм ДБН В.1.2-2006 «Навантаження і впливи», які мають сучасний імовірнісний базис і асоціюються з нормами Єврокод. Виділяються наукові результати, що можуть бути включеними в наступні норми снігового навантаження.

**Ключові слова:** снігові спостереження, снігове навантаження, територіальне районування, нормативне навантаження, розрахункове навантаження



## Introduction

Ensuring the reliability and trouble-free operation of buildings and structures depends on a correct understanding of the nature, quantitative description, and regulation of loads on building structures, including snow loads. These loads on structures are of a rather complex physical nature and changeable character, requiring knowledge of thermodynamic processes in the atmosphere and on the ground, physical properties of snow, methods of meteorological observations and climatological description of the terrain, variability of loads, the nature of snow deposition on buildings and structures. These features are reflected to a certain extent in the sections of the codes for the building structures design containing the standards for the snow load. Most of the parameters of the snow load codes are of a probabilistic nature and require the use of statistical methods for their substantiation. These methods have been constantly changing and evolving together with the regular revision of building design codes. Analysis of the evolution of domestic snow load norms, together with their statistical justification, is an urgent problem.

## Review of research sources and publications

Regular snow measurements have been carried out since the end of the 19th century. In the 1930s, their results served as the basis for the compilation of the first normative document on snow load and the first publications on this problem [1]. This process has intensified with the preparation for the transition of structural calculations to the method of limit states [2, 3]. In subsequent years, along with the regular revision of the codes of loads and effects on structures, the regulation of the snow load was improved. The evolution of snow codes was covered in publications of leading scientific and technical journals [4–14]. Reviews of the development of snow codes have been published as sections of monographs and dissertations devoted to loads on buildings and structures [18–21]. Since the 90s of the last century, design standards have been developed by separate states that were previously part of the USSR. In this regard, probabilistic studies of the snow load on the territory of Ukraine became more active [25–30], the result of which was the corresponding section DBN V.1.2-2006 "Loads and effects". In subsequent years, studies of the snow load continued along with the substantiation and refinement of a number of code coefficients [31–35].

## Definition of unsolved aspects of the problem

Materials on snow loads have been published in various scientific and technical journals, collections of articles, and conference proceedings. Access to these publications is difficult; some institutions began to destroy paper magazines of the past years, motivating the transition to electronic editions. However, in reality, the transfer to electronic form has occurred so far only for publications published after 2000. Published reviews of the snow load regulation development are incomplete and do not include the results of studies of the last 15 – 20 years.

## Problem statement

The article contains a systematized review of publications in leading scientific and technical journals on the problem of snow load for the period from the 40s of the twentieth century to the present. The main attention is paid to the analysis of the evolution of structural design codes in terms of changes in territorial zoning and design coefficients, the appointment of normative and design values of the snow load, and the involvement of experimental statistical data. It highlights the scientific results that can be included in subsequent editions of snow load codes.

## Basic material and results

The regulation of snow loads in the USSR was developed based on experience in the operation of buildings and structures, as well as with the improvement of methods for building structures calculating.

One of the first normative documents on the snow load in the USSR was the "Unified Norms" OST / VKS 7626 / B (introduced from June 1, 1933). A certain scientific basis for substantiating the codes at that time already existed: long-term meteorological snow observations; snowdrift research carried out since pre-revolutionary times at the St. Petersburg Institute of Railways and Moscow State University (laboratory of hydrodynamics, N.E. Zhukovsky); the results of snow accumulation studying on the roofs of industrial buildings, obtained by TsNIPS in the early 30s [1]. However, due to the limited source material, it can be assumed that the first domestic snow codes were drawn up based on expert assessments of specialists and taking into account the experience of operating buildings and structures. In this document, the snow load was normalized depending on the height of the snow cover  $h$ , and the average maximum height for the last ten years was taken into account. Thus, the design of snow depth had some statistical justification. At the same time, the density of snow, without sufficient explanation, was taken equal to  $\rho = 100 \text{ kgf/m}^3$ . The design value of the snow load was determined as  $p = 1,6 \rho h$ . On the territory of the Soviet Union, only 4 regions were identified with different snow cover heights and the corresponding snow load, determined from a map or table: the 1st region without permanent snow cover, for which the load was taken  $p = 25 \text{ kgf/m}^2$ ; 2nd region with a snow cover height  $h < 30 \text{ cm}$  and  $p = 40 \text{ kgf/m}^2$ ; 3rd area with a height of  $30 \text{ cm} \leq h \leq 60 \text{ cm}$  and  $p = 80 \text{ kgf/m}^2$ ; 4<sup>th</sup> region with  $h > 80 \text{ cm}$  and  $p = 120 \text{ kgf/m}^2$ . For mountainous areas, the height of the snow cover was presented in tabular form.

These codes determined such features of the snow load distribution on the roofs as the dependence on the roof slope and the presence of lanterns. It is interesting to note that for roofs with a slope of  $20 \dots 30^\circ$  the snow load increased by 25% (in the subsequent versions of the codes, this increase is absent). For roofs with height discontinuity, a scheme was recommended with a 50% decrease in the snow load on elevated areas (but not less than  $25 \text{ kgf/m}^2$ ) with an additional 50% load drift to the lower areas. Possible accumulation of snow (snow bag)

with a maximum height equal to the height of the obstacle, but not more than  $4h$  was taken into account near-vertical obstacles. A triangular shape of snow bags was assumed, but the codes did not contain recommendations for their length. The load from the snow bag was taken into account at the above-mentioned snow density  $\rho = 100 \text{ kg/m}^3$ . For gable and vaulted roofs, the level of snow load was determined according to two options: full uniform loading of the entire span and one-sided loading of the half span.

In the determination of the snow load on the roof, the type of terrain was taken into account. For open areas with frequent strong winds at a speed of 12 m/s and more, the snow load was allowed to be reduced by 50%, but not less than  $25 \text{ kgf/m}^2$ . For areas closed from the wind, the snow load increased by 25%. The codes contained detailed recommendations for accounting for snow melting on roofs, as a result of which a sufficiently large (up to 50 ... 75%) decrease in snow load was allowed depending on the thermal resistance of the roof, internal air temperature, and the amount of heat release. However, in subsequent regulations, these recommendations were omitted.

A serious drawback of these codes was the underestimation of the accepted snow density, although at that time there was already information about its significantly higher values. So, according to TsNIPS [1], the density of freshly fallen snow was  $85 \dots 190 \text{ kg/m}^3$  (on average  $135 \text{ kg/m}^3$ ), the maximum density during the winter –  $240 \dots 250 \text{ kg/m}^3$ . As a result, the design snow loads quite often turned out to be noticeably lower than the actual loads. In addition, the codes included the snow cover height, measured using constant slats, which did not make it possible to fully take into account the terrain peculiarities and the wind regime. Taken by TsNIPS in 1932–1933 measurements of snow accumulation on the roofs of industrial buildings revealed the complex nature of the snow bags, which significantly differed from the simplified recommendations of the first domestic codes. From the height of historical experience, it is possible to assess the conjunctural and political shade of the underestimated loads codes of the 30s (this applied not only to snow loads), aimed at all-round savings in the construction of a country that was experiencing massive industrialization. Despite this, such rationing provided a generally satisfactory operation of buildings and structures, since relatively high safety factors were taken in the methodology for calculating structures for permissible stresses, which was in force at that time.

This was followed by OST 90058-40 (1940), compiled on the research results basis of the building aerodynamics laboratory of the Central Scientific Research Institute of Industrial Construction (TsNIPS). When substantiating the snow load code, the snow density was increased with differentiation depending on the snow cover height. At a height of  $h > 50 \text{ cm}$ , the density  $\rho \approx 200 \text{ kg/m}^3$  was taken, for  $h \approx 30 \text{ cm}$  –  $\rho \approx 230 \text{ kg/m}^3$  and for  $h < 20 \text{ cm}$  –  $\rho \approx 250 \text{ kg/m}^3$ . The territory of the USSR was divided into 5 snow regions with the following values of the snow cover

height and the estimated weight of snow  $p$  on the surface of the earth at a slightly higher level compared to the previous codes: I region – height up to 20 cm, weight  $p = 50 \text{ kgf/m}^2$ ; II region – height from 20 to 40 cm,  $p = 70 \text{ kgf/m}^2$ ; III region – height from 40 to 60 cm,  $p = 100 \text{ kgf/m}^2$ ; IV region – height from 60 to 90 cm,  $p = 150 \text{ kgf/m}^2$ ; V region – height more than 90 cm,  $p = 200 \text{ kgf/m}^2$ . For mountainous areas, the design weight of the snow cover ( $\text{kgf/m}^2$ ) was recommended to be determined as  $p_c = 2h$  (but not less than  $60 \text{ kgf/m}^2$ ), where  $h$  is the average 10-year snow cover height in cm, taken from the data of meteorological observations. In this document, the recommendations for taking into account the coverage profile were slightly changed towards simplification.

The development of methods for calculating building structures, especially for assessing the safety factor of structures, required to objectively identify the parameters of loads and strength of materials [2]. Therefore, the need has increased to use statistical methods to describe snow loads, which have a distinctly random nature. An example of a statistical analysis of the snow cover was the distribution curves of the snow height for the Moscow region, built for the period from 1898 to 1935. N.S. Streletsky was the first who had used this data to numerically assess the reliability of steel truss structures, designed according to the codes in force at that time [3].

Further refinement of the snow load with the justification of the design values based on field observations was carried out in the post-war 50s of the twentieth century. Materials of snow surveys on the roofs of industrial buildings and new data on the features of the drift and melting of snow were obtained, which confirmed the need to adjust this code. Taking into account the new data, in 1954, Codes and Rules SNiP II-B.1-54 "Loads and effects" were introduced, in which the values of the snow load were increased for certain regions, in particular, the snow-covered territory in the region of Perm was assigned to the V snow region, to the IV snow region – the region of Novosibirsk, the need for which was evidenced by the publications of specialists. These codes were consistent with the introduction of structural analysis using the limit state method. When switching to this method, the values of the calculated weight of the snow cover according to the previous norms  $p$  were taken as the normative loads, i.e. average values of annual maximums. The design snow loads, which began to be interpreted as the highest possible during the operation of the structure, began to be determined by multiplying by the overload factor. This coefficient, due to the lack of reliable data on the variability of annual maximums, was taken to be common for the entire territory,  $n = 1.4$ . Thus, the normative load  $p$  increased by 40%. This correction was justified by the fact that  $p$  was determined as the average of the maximum weights of snow for each year (and the weight was determined from the average density of snow). Consequently, the actual values of snow loads can exceed the normative load in about 50% of winters. The design snow load on the buildings' roofs was determined as  $p_c = npc$ , where  $c$  is the coefficient introduced

for the first time, taken depending on the profile of the roof. In this document, the recommendations for taking into account the roof profile were slightly changed towards simplification, which included the range  $c = 0 \dots 1,0$  for simple single-slope and gable roofs,  $c = 0,3 \dots 1,0$  for vaulted roofs,  $c = 0,4 \dots 1,6$  for roofs with skylights, with only the transverse profile of the building taken into account. In buildings with a height difference  $H$  (m), the maximum height of the snow bag was specified  $p_c = 200 H \leq 4q$  with the length of the additional triangular part  $a = 2H$ , with  $5 \text{ m} \leq a \leq 10 \text{ m}$ .

Damages and collapses of roofs in several cities [4–6] showed that the codes of that time did not provide the necessary reliability of roof structures. Therefore, further clarification of snow loads was required, primarily in places of increased snow accumulation. Based on the generalization of the results of mass measurements of snow cover on 50 roofs of various profiles in different regions, carried out in 1958–1959 at TsNIISK [7], in the development of SNiP II-B.1-54, were developed and approved in 1959 SN 69-59 "Guidelines for the determination of snow loads on the roofs of buildings." In these instructions, individual calculation schemes of snow loads, placed in the SNiP, were clarified, and new schemes for the distribution of loads for the most common roof profiles (12 schemes in total) were given [8]. It is taken into account that snow accumulations on vaulted roofs strongly depend on the strength and frequency of winds; snow load on such surfaces is increased by 25%. The loads from snow bags at the lanterns of single-span and multi-span buildings are differentiated, the load at the ends of the lanterns is highlighted and the schemes of snow loads on the roofs of two- and multi-span buildings without lanterns are supplemented. Additional accounting of snow load on parts of the span has been regulated, taking into account possible wind blowing off snow or carrying out snow cleaning operations. At the same time, it is envisaged to reduce the snow load by 20% on surfaces with excessive heat release, as well as for flat and gentle surfaces with a wind speed of at least 4,0 m/s. It is interesting to note that Soviet works of this period in the field of studying snow loads were well known abroad, were translated into English, and taken into account when compiling snow codes for Canada.

Recommendations SN 69-59 were included in the next edition of SNiP II-A.11-62 "Loads and effects" with minor changes. In this edition, the snow zoning of the USSR was clarified – 5 regions of the previous SNiP 1954 with normative values of 50 – 200 kgf/m<sup>2</sup> were left and a 6th region was introduced for Kamchatka with 250 kgf/m<sup>2</sup>. The code developers had used data from 4075 weather stations and posts. They also took into account more reliable maps of the average annual maximum weight of the snow cover on the earth, built based on data from 140 meteorological stations. At the stations simultaneously with the height of the snow cover, its weight was measured and the average density was determined. They used the results of route snow surveys accumulated over the past 15 ... 20 years, the accuracy of which is significantly higher than measurements on three permanently installed rails [9].

It should be noted that in the absence of snow survey data, it was nevertheless allowed that the weight of the snow cover was determined by the formula  $p_0 = 220 H$ , where  $H$  is the height of the snow cover in meters, taken from the data of meteorological observations as the average of the maximum annual heights in a protected place for a long-term period (at least 10 years). SNiP II-A.11-62 specifies the effect of wind on the level of snow loads due to wind drift from the roofs. As in the previously developed "Guidelines", for individual roof profiles of buildings located in areas with an average wind speed of at least 4 m/s for the three coldest months, a reduction in snow load by 20% was provided.

During this period, some researchers continued to work on the clarification and regulation of snow bags on the roofs [10]. A technical and economic comparison of the methods of snow removal from the roofs was carried out [11].

The next revision of SNiP II-6-74 "Loads and effects" was adopted 12 years later and had an almost modern look, including a map of the zoning of the USSR territory by weight of snow cover. These codes took into account the results of further studies of the methodology for determining the weight of snow cover, the study of the drift and transfer of snow under the wind influence, and statistical substantiation of overloading snow loads coefficients on buildings and structures. As in the previous editions of the codes, the regional snow load standard was determined as the average annual maximum obtained over a 10-year period based on long-term snow measurements. In this version of the codes, classification of loads was developed, in which temporary long-term loads were highlighted. They are addressed to structural calculations, taking into account the effect of the loads' action duration on displacements, deformations, and cracking (for example, for reinforced concrete structures). For the snow load without statistical justification, the weight of the snow cover of the III-VI regions, reduced by 70 kgf/m<sup>2</sup>, was taken as the long-term part.

According to Institute "TsNIIPromzdaniya" data for 112 cities, the actual snow loads (kgf/m<sup>2</sup>) in the indicated period exceeded the design ones (shown in brackets): I region 100 (70); II region 132 (98); III region 179 (140); IV region 252 (210) [11]. Considering this situation, as well as the fact that during the period of validity of SNiP II-A.11-62 there were cases of light roof accidents due to overloading with snow, a differentiated increased coefficient of overload was introduced into SNiP II-6-74. It depended on the ratio of the dead load  $q$  (own weight of the roof, including the weight of the suspended stationary equipment) to the normative weight of the snow cover  $p_0$ . For relatively heavy roofs with  $q/p_0 = 1$  or more, the overload factor assumed the previous value of  $n = 1.4$ , with the relative lightening of the roof, it increased: at  $q/p_0 = 0.8 - n = 1.5$ ; at  $q/p_0 = 0.6 - n = 1.55$ ; at  $q/p_0 = 0.4$  and less –  $n = 1.6$ .

In support of this proposal, its author Driving A.Ya. [12] gave the following considerations. The dead-weight of heavy roofs is several times higher than the



normative snow load. So, in region III, the normative snow load was 100 kgf/m<sup>2</sup>, and the roof weight was 4–5 times more. Light roofs, on the contrary, had their own weight less than the normative snow load (in region III, 30–50% of the snow weight). When zoning the territory according to snow loads, their values were taken into account, which is possible once every 10 years. In fact, over a longer period of the structure's existence, snow loads may exceed the normative value (which has been repeatedly observed in practice). This excess for heavy roofs is insignificant and is within the calculation accuracy and tolerances. At the same time, the tolerances and overload factors taken into account in the design of lightweight roofs turn out to be insufficient, and exceeding the normative snow loads becomes dangerous for them.

A significant advantage of these codes edition is a more accurate and specific accounting of snowdrifts by the wind. This was preceded by experimental studies conducted at TsNIISK by Otstavnov V.A. and Rosenberg L.S. [13]. As a result, for flat roofs, the snow load was determined for each year, taking into account the snowdrift:

$$S = (1.24 - 0.13 v_m) S_3 - q I_2 \tau, \quad (1)$$

where  $S_3$  is the maximum weight of snow that fell during the winter;

$v_m$  – wind speed during snowfall;

$q$  – the average intensity of snowdrift per day during a blizzard without snowfalls (depends on the wind speed during blizzards);

$I_2$  – repeatability of wind speeds over 6 m/s in the absence of snowfall;

$\tau$  – the duration of snowdrift during the period of no snowfall.

As can be seen from formula (1), the phenomenon of snowdrift has a clear probabilistic nature, depending on several random factors, which were taken into account by the developers of the codes. As a result, it was substantiated that the normative load on flat and gently sloping roofs without lanterns with slopes of up to 12% and curved roofs with a boom-to-span ratio  $f/l < 0,05$ , designed in areas with an average wind speed for the three coldest months  $v \geq 2$  m/s, it is allowed to reduce it by multiplying by a factor  $k = 1.2 - 0.1v$ . For roofs with slopes from 12 to 20% in areas with  $v \geq 4$  m/s, the normative snow load may be reduced by 15%. For buildings with a width of up to 60 m or a height of more than 20 m, the coefficient  $k$  is additionally reduced by 10%. In addition, the coefficient  $c$  of the transition from the weight of the earth snow cover to the snow load on non-insulated roofs of workshops with excessive heat release has been clarified. With slopes of such roofs of more than 3% and ensuring proper water drainage, this coefficient can be reduced by 20%. In this version of the codes, the schemes of snow loads on the roofs with complex profiles and parapet parts are also clarified.

SNiP II-6-74, which was in operation for 11 years, quite accurately regulated snow loads. However, the peculiarities of snow accumulation on certain types of roofs remained unaccounted, which caused numerous

requests from design organizations. In this regard, TsNIISK 1982 issued "Recommendations for determining the snow load for some types of roofs" (developed by L. S. Rosenberg) as an addition to this version of the codes. They provide recommendations for taking into account the accumulation of snow near the ridge of a gable roof, on pointed arches and sagging cylindrical roofs. However, the questions of the design organizations to the developers of the codes (TsNIISK) continued. One of the most frequent questions was the following: how were the schemes of uneven snow deposition built at differences in the height of the roofs? One of the authors of the load codes Bat A.A. gave the following answer to this question [14]. In the determination of coefficient  $c$ , a single initial condition was used – the total amount of unevenly deposited snow on the surface should be equal to the amount of uniformly deposited snow. Part of the snow is blown down from the upper roof; snow also falls on the lower roof with a different wind direction. Therefore, the coefficient  $c$  increases as the lengths from which snowdrifts and onto which snow is applied increases. In this case, the experimentally established fact was taken into account that unevenness is observed on the lower cover at a length approximately equal to twice the height of the drop. Therefore, the maximum unevenness will decrease as the drop increases, and the height of the drop is in the denominator. The coefficient  $c$  characterizing the unevenness is limited by two conditions:  $c \leq 200 h/p_0$  – the limitation physically reflects the complete filling of the drop with snow;  $c \leq 4$  for buildings and  $c \leq 6$  for awnings – inequality takes economic considerations into account.

In subsequent years, several organizations continued to study the factors influencing the snow load. In particular, field observations of snow bags on various types of shells were carried out in the Krasnoyarsk, Sverdlovsk, and Chelyabinsk [15]. A one-sided trapezoidal scheme of snow loading of pointed arches was proposed, which was taken into account in the next edition of the codes [16]. A study of snow loads on flat surfaces of industrial buildings with skylights was carried out [17].

An active study of the loads on building structures in the 70-80s of the last century contributed to the release in 1985 of SNiP 2.02.07-85 "Loads and effects". This version of the codes, like the previous one, regulated six values of the quantity  $S_0 = 50 - 250$  kgf/m<sup>2</sup>, which corresponded to the number of snow regions on the territory of the former USSR. At the same time, most of the territory belonged to the III and IV snow regions, the areas south of 49° or 50° north latitude corresponded to the I and II snow regions (including Ukraine), the V region was mainly distributed in the Urals, Western Siberia, and Kamchatka, and the VI snow region was found only on Sakhalin. Snow load in mountainous areas was not standardized; it should have been established according to meteorological data. The normative values  $S_0$  were noticeably increased in the foothill areas.

The overload factor, which was renamed "load safety factor" and the new designation  $\gamma_f$  remained at 1.4 for most cases. When calculating the structural roof elements, for which the ratio of the considered normative value of the uniformly distributed load from the weight of the roof to the normative value of the snow cover  $S_0$  weight is less than 0.8, it was prescribed to take  $\gamma_f$  equal to 1.6. For cases that should provide for the consideration of rheological processes in structures, special reduced standard values of the snow load were established without a statistical justification, obtained by multiplying the full design values by coefficients 0.3 for the III snow region; 0.5 – for the IV region; 0.6 – for V and VI regions.

A number of researchers have identified significant shortcomings of SNiP 2.01.07-85 in terms of the snow load regulation [18-20]. With the collapse of the USSR, the new states had the opportunity to move away from the coarse Soviet snow rationing and develop their own, more differentiated snow zoning. Further development of snow codes on the territory of the CIS was realized in the form of national codes of each state.

Russia followed the path of gradual development of SNiP codes. The Code of Rules SP 20.13330.2011 "Loads and effects", an updated version of SNiP 2.01.07-85\*, was developed. It introduced a new principle for standardizing the weight values of the earth's snow cover, in accordance with the highest annual values exceeded, on average, once every 25 years. They are determined according to the data of ten-day route snow surveys on the largest reserves of water in the snow cover in areas protected from direct wind impact (in the forest under tree crowns or forest glades) for at least 20 years. In this case, the data of Roshydromet were used for more than 4600 meteorological stations and posts with a row length of 20 ... 45 years, obtained by directly measuring the weight of the snow cover using a weight snow meter. On the basis of the outlined basic provisions, a new zoning map of the Russian territory was developed according to the estimated weight of snow cover, on which the boundaries of 8 snow regions (instead of 7 in the previous codes) were plotted with regional values in the range of 0.80 ... 5.60 kPa [20, 21]. Region values have increased markedly in comparison with the corresponding design values according to the previous standards. For example, for the III region, the design value became equal to  $S_g = 1.8$  kPa in comparison with the previous calculated value  $S = S_0 \gamma_f = 1.0 \cdot 1.4 = 1.4$  kPa. In this edition of the snow codes, the same principle is applied that was used earlier in the rationing of snow loads when territories with a snow cover weight about 2/3 more and 1/3 less than the accepted regional values were included in one region. SP 20.13330 "Loads and effects" defines the normative value of the snow load on the horizontal projection of the roof as a base value:

$$S_0 = 0.7 c_e c_t \mu S_g, \quad (2)$$

where  $S_g$  is the weight of the snow cover per 1 m<sup>2</sup> of the earth horizontal surface, the procedure for determining which is described above;

$c_e$  – coefficient of the possible drift of snow from the building roof under the influence of wind or other factors (previously indicated as  $k$  and  $k_1$ );

$c_t$  – coefficient of reduction of snow load due to the effect of temperature (previously did not have a special designation);

$\mu$  – coefficient of transition from the weight of the earth snow cover to the snow load on the roof.

To switch to the calculated value of the snow load, the load safety factor  $\gamma_f = 1.4$  is used.

As in SNiP 2.01.07-85, the scope of the explicitly introduced snowdrift coefficient extends to gentle (with slopes up to 12% and with  $f/l \leq 0.05$  roofs of single-span and multi-span buildings without lanterns designed in areas with average wind speed for the three coldest months  $V \geq 2$  m/s. The formula for determining this coefficient has been slightly changed

$$c_e = (1.2 - 0.1V\sqrt{k})(0.8 - 0.002b), \quad (3)$$

where  $k$  is a coefficient that takes into account the change in wind pressure along with the height;

$b$  – the roof width, taken no more than 100 m.

In addition, the coefficient  $c_e$  is introduced for spherical and conical roofs of buildings on a circular plan. The specified Code of Rules for the first time determines the possibility of using the thermal coefficient to take into account the reduction of snow loads on roofs with a high heat transfer coefficient ( $>1W/(m^2\text{ }^\circ\text{C})$ ), leaving its justification for the developers of special recommendations. At the same time, similar to the previous editions of SNiP, the coefficient  $c_t$  is taken equal to 0.8 for non-insulated roofs of workshops with increased heat release, provided that meltwater is removed from the roof with a slope of more than 3%.

Unlike the previous version of the codes, the reduced normative value of the snow load is determined regardless of the snow region by multiplying the full normative value by a factor of 0,7, except for areas with an average January temperature above minus 5C.

Despite a significant increase in the design values of snow loads in the considered version of the Russian codes, there were some critical remarks about the method of snow rationing in Russia. In particular, Maliy V.I. (TsNII Proektstalkonstruktziya) [24] harshly criticized the main criterion of this rationing – the use of a 25-year repetition period of the annual maximum to substantiate the design values of the snow load. In support of this, data was given that in the Moscow region over 100 years of observations, the snow load reached 2.1 kPa at a rate of 1.8 kPa according to SP 20.13330.2011 "Loads and effects". The critic also drew on a well-known independent test scheme to show the high probability of exceeding the design value of 1.8 kPa over a period of 100 years. Taking this into account, as well as the example of the Eurocode standards, which use an additional safety factor of 1.5, a proposal was made to increase the design snow load to 3.0 kPa for the Moscow region. The developers of the codes from TsNIIISK strongly disagree with this [22, 23]. In principle, one can agree with them, since the load standards should be considered not in isolation

for individual loads, but as part of a general assessment of the structures reliability [25]. Maliy V.I. also criticizes the principle of zoning the weight of the snow cover, when points which differ from the regional ones, both to a greater and a lesser extent, are combined into regions for the purpose of unification. A number of publications note that the zoning of the Russian territory according to the design snow loads still does not fully take into account the variability of the snow load in the area, and alternative approaches to snow rationing are proposed [26].

Ukrainian specialists, in contrast to the Russian developers of the codes, prepared the State Norms of Ukraine DBN V.1.2-2006 "Loads and effects", conceptually different from SNiP in terms of snow loads. The probabilistic representation of loads, including snow loads on building structures, was significantly developed. Such mathematical models have been developed as stochastic processes, absolute maxima of stochastic processes, independent test schemes, discrete representation, extremes, and correlated random sequence of overloads [27]. This made it possible for the first time to substantiate a probabilistic model for the snow load in the form of a quasi-stationary differentiable random process with a stationary frequency structure and an annual seasonal trend of the mathematical expectation and standard [28]. For the snow load of Ukraine, which has an unstable nature, a relatively little-known bimodal distribution, called "polynomial-exponential", was successfully applied:

$$f(\gamma) = \exp(C_0 + C_1\gamma + C_2\gamma^2 + C_3\gamma^3), \quad (4)$$

where  $\gamma = (x - \bar{x})/\hat{x}$  is the normalized deviation of the load from its mathematical expectation  $\bar{x}$ ;  
 $\hat{x}$  – standard (standard deviation).

The statistical characteristics of this probabilistic model were calculated based on data from over one hundred meteorological stations located in the territory of Ukraine. They are summarized in publications [19, 29]. Due to sufficient information provision, the probabilistic model of a quasi-stationary random process has been successfully applied to normalize the snow load in the DBN. For this, the results of snow surveys were used, carried out at 222 meteorological stations and posts in Ukraine during 1950 ... 1990 with the duration of climatic series from 21 to 35 years. In general, a representative sample of more than 100 thousand snow survey results was used to normalize the snow load in Ukraine.

The DBN consider the snow load as a variable load with three design values: limiting  $S_m$ , operational  $S_e$ , and quasi-constant  $S_p$  (5):

$$\begin{aligned} S_m &= \gamma_{fm} S_0 C; \\ S_e &= \gamma_{fe} S_0 C; \\ S_p &= (0.4S_0 - 160) C, \end{aligned} \quad (5)$$

where  $S_0$  – the characteristic value of the snow load, equal to the weight of the snow cover per 1 m<sup>2</sup> of the earth surface, which can be exceeded on average once

every 50 years (similar to the Eurocode), is taken from the map of territorial zoning of Ukraine;

$\gamma_{fm}$  and  $\gamma_{fe}$  – respectively, the safety factor for the limiting and operational design value.

The reliability factor for the limiting design value  $\gamma_{fm}$  is presented in tabular form in the range 0.24 – 1.44 depending on the specified repetition period of the snow load  $T = 1 - 500$  years. The reliability factor for the operational design value  $\gamma_{fe}$  is presented in tabular form in the range 0.88 – 0.10, depending on the fraction  $\eta = 0.002 - 0.1$  of the established service life of the structure, during which this value may be exceeded. Giving reason to the quasi-constant design value of the snow load, the phenomenon of concrete creep under load was taken as the basis, as the most common rheological effect, which is taken into account in the calculations of building structures [30]. The values of the coefficients and the design values of the snow load in the formula (5) have a statistical justification [19].

The features of a particular roof are taken into account by a coefficient  $C$  determined by the expression:

$$C = \mu C_e C_{alt}, \quad (6)$$

where  $\mu$  is the coefficient taking into account the roof profile, adopted mainly according to the recommendations of SNiP, but expanded with the involvement of the Eurocode data;

$C_e$  – coefficient taking into account, similarly to SNiP, the operating mode of the roof;

$C_{alt}$  – coefficient of geographic height  $H$ , taken as  $1.4H + 0.3$  for  $H \in 0.5$  km.

The generalized statistical data testified to significant territorial variability of the snow load, which significantly differed from its standardization of SNiP, according to which almost the entire territory of Ukraine belonged to the least snowy regions I ( $S_0 = 0.5$  kPa) and II ( $S_0 = 0.7$  kPa). Meanwhile, the experimentally substantiated design values of the snow load corresponding to the base average repetition period  $T = 50$  years vary from 0.76 kPa for the Kherson region to 1.79 kPa in the northeastern regions of Ukraine. Attention is drawn to the rather high values (1.20...1.80 kPa) of the snow load recorded at some southern meteorological stations. The analysis of experimental data, in addition, confirmed that in Ukraine there are especially snowy winters, for example, in 1963–64, 1966–67 and 1986–87. In some points, the largest weight of the snow cover exceeded 2.0 kPa, which, nevertheless, did not fall out of the total set of annual maximums.

The territorial zoning of Ukraine according to the characteristic values of the weight of the snow cover was carried out according to the method developed by V.A. Pashinsky [19]. A probabilistic model of a non-stationary normal random field was used, the ordinates of which were the values of the loads for individual meteorological stations located at distances of 30 ... 60 km. The smoothing procedure made it possible to obtain a smooth surface of the mathematical expectation of the snow load, free from random fluctuations in the data of individual meteorological stations. The regional values

of the design snow load were set so that the excess reserves of territorial zoning were minimal. As a result, six territorial regions with characteristic values from 0,8 to 1,8 kPa were allocated on the territory of Ukraine. At the same time, it was revealed that the actual design loads exceed the regional ones by no more than 12%, for 21% of meteorological stations. At the same time, due to the necessary generalization, the values increased by an average of 16,4% and in some cases exceeded the actual loads by 50%.

It should be emphasized that the limiting design values of the snow load included in the DBN in most cases exceed the corresponding values established by the SNiP. On the one hand, this leads to an increase in the cross-sections and material consumption of the supporting structures of the roofs, but on the other hand, to an increase in their level of reliability. At the same time, a noticeable increase in the calculated values of the snow load leads to a smaller increase in material consumption. So, for example, at  $T = 50$  years, the design values of the snow load increase on average by 58%, and the mass of steel trusses for a light roof – by only 22% [19].

Giving a general assessment of the Ukrainian codes DBN V.1.2-2006 "Loads and effects" in terms of snow load, it should be emphasized that they are compiled on a modern methodological basis, are close to the Eurocode, are based on representative statistical material, are more differentiated and have a scientific probabilistic basis more deeply developed than the codes of previous years.

In subsequent years, probabilistic studies of snow load continued in Ukraine, the practical results of which were recommendations for improving design codes. Kinash R.I. proposed an alternative method for zoning snow loads for the territory of Ukraine [18]. Proposals were developed for a more detailed snow zoning of the mountainous Carpathian region (within the boundaries

of the Transcarpathian region) with the introduction of additional 5 regions (from 7th to 11th) with characteristic snow loads in the range of 2.2 ... 3.0 kPa [31]. The probabilistic research of snow loads was continued by the scientific school of building structures reliability of the Yuriy Kondratyuk Poltava National Technical University [35]. Snow accumulation on the roofs with height discontinuity was studied, which gave a practical result in the form of a statistically substantiated combination coefficient of 0.8 for snow bags on the territory of Ukraine [32]. A probabilistic assessment of the influence of the building roofs thermal characteristics on the snow load value is carried out. The results of this work are presented in the form of a differentiated coefficient of roof operation [33]. Design snow loads on cold roofs of buildings with positive indoor temperatures were determined [34].

### Conclusions

It is shown that over the past eighty years, domestic codes for the design of building structures in terms of the regulation of snow loads have undergone significant changes and have expanded their statistical foundations. Territorial snow zoning has developed, the number of snow regions has increased, especially on the territory of Ukraine. The substantiation of the normative (characteristic) and design values of the snow load was modified on the basis of an increased return period. A probabilistic account of wind drift of snow from roofs has been developed and included in the codes, and a quasi-constant value of the snow load has been statistically substantiated. The high scientific level of domestic standards DBN V.1.2-2006 "Loads and effects", that have a modern statistical basis, which is associated with the Eurocode and provides the required level of reliability of building structures, is noted. New scientific results are highlighted that can be included in subsequent editions of snow load codes.

### References

1. Николаев А.Ф. (1935). Снеговые нагрузки на здания. *Строитель*, 8 (10), 18-26
2. Стрелецкий Н.С. (1938). Об исчислении запасов прочности сооружений. *Труды Московского инженерно-строительного института*, 1, 4-32
3. Стрелецкий Н.С. (1947). *Основы статистического учета коэффициента запаса прочности*. Москва: Стройиздат
4. Абовский В.П., Вексман А.М., Волков В.М., Матысек Г.В. (1954). Нерешенные вопросы проектирования промышленных зданий с интенсивными снегопадами. *Строительная промышленность*, 11, 30-31
5. Кан-Хут Э.Д. (1954). Вопросы уточнения снеговых нагрузок. *Строительная промышленность*, 12, 22-23
6. Кораблинов А.М., Краузе Л.С. (1957). Уроки аварий двух покрытий. *Строительная промышленность*, 7, 18-21
7. Гольденблат И.И., Корнев В.Г., Сизов А.М. (1956). О снеговых нагрузках по строительным нормам и правилам. *Строительная промышленность*, 6, 25-28
8. Отставнов В.А. (1960). О снеговых нагрузках на покрытия зданий. *Промышленное строительство*, 1, 58-61
1. Nikolaev A.F. (1935). Snow loads on buildings. *Builder*, 8 (10), 18-26
2. Streletsky N.S. (1938). On the calculation of the safety margins of structures. *Proceedings of the Moscow Civil Engineering Institute*, 1, 4-32
3. Streletsky NS (1947). *Fundamentals of statistical accounting for the safety factor*. Moscow: Stroyizdat
4. Abovskiy V.P., Veksman A.M., Volkov V.M. & Matysek G.V. (1954). Unresolved issues in the design of industrial buildings with heavy snowfall. *Construction industry*, 11, 30-31
5. Kan-Khut E.D. (1954). Clarification of snow loads. *Construction industry*, 12, 22-23
6. Korablinov A.M. & Krause L.S. (1957). Lessons from accidents of two coatings. *Construction industry*, 7, 18-21
7. Goldenblat I.I., Korenev V.G. & Sizov A.M. (1956). About snow loads according to building codes. *Construction industry*, 6, 25-28
8. Otstavnov V.A. (1960). About snow loads on building coverings. *Industrial construction*, 1, 58-61

9. Klepikov L.V. & Otstavnov V.A. (1962). Determination of loads in the calculation of building structures. *Structural mechanics and calculation of structures*, 5, 39-45
10. Bessonov V.S. (1964). Experimental work to prevent excessive accumulation of snow on the roofs of industrial buildings in areas with strong winds. *Proceedings of Universities. Building and architecture*, 11, 60-63
11. Khromets Yu.N. & Solodovnikov R.A. (1971). Methods for dealing with excess snow deposits on building surfaces. *Industrial construction*, 5, 28-30
12. Driving A.Ya. (1973). On the coefficient of overloading the snow load on light coatings. *Loads and reliability of building structures: Tr. TsNIISK*, 21, 53-57
13. Otstavnov V.A. & Rosenberg L.S. (1966). Possibilities for reducing snow loads on flat surfaces. *Industrial construction*, 12, 28-32
14. Bat A.A. (1977). Comments to the chapter SNiP II-6-74 "Loads and Impacts". *Industrial construction*, 5, 42-44
15. Zhukova N.K. (1979). Results of field observations of snow loads on spatial structures of pavements. *Proceedings of Universities. Building and architecture*, 9, 40-46
16. Neverov I.A., Zakharchenko S.M. & Klimenko V.Z. (1984). Snow loads on the lancet arched cover. *Industrial construction*, 7, 15-17
17. Koshutin B.N. & Strokotov B.P. (1984). On the possibility of reducing the design loads on flat surfaces of industrial buildings with skylights. *Industrial construction*, 5, 33-34
18. Kinash R.I. & Burnaev O.M. (1997). *Snow load in Ukraine*. Lviv: Publishing house of scientific and technical literature
19. Pashinsky V.A. (1999). *Atmospheric loads on building structures for the territory of Ukraine* Kyiv: UkrNDIProektstalkonstruktisiya
20. Gordeev V.N., Lantukh-Lyashchenko A.I., Pashinsky V.A., Perelmuter A.V. & Pichugin S.F. Ed. A.V. Perelmuter. (2008). *Loads and Loaings on buildings and structures*. Moscow: Publishing house ASV
21. Pichugin S.F. & Makhinko A.V. (2012). *Snow and ice loads on building structures*. Poltava: OOO ASMI
22. Nazarov Yu.P., Lebedeva I.V. & Popov N.A. (2006). Regional regulation of snow loads in Russia. *Structural mechanics and calculation of structures*, 3, 71-77
23. Otstavnov V.A. & Lebedeva I.V. (2004). The New Map of Ground Snow Loads for Russian Building Code. *Proc. of V International Conference on Snow Engineering*. Davos, Switzerland, 157-160
24. Malyi V.I. (2011). On the special attitude to snow load in Russian codes. *Industrial and civil engineering*, 8, 42-45
25. Pichugin S.F. (2016). *Calculation of reliability of building structures*. Poltava: TOV ASMI
26. Ledovskoy I.V. (2005). Analysis of the random process of snow accumulation on the ground. *Bulletin of Civil Engineers*, 3 (4), 29-35
27. Pichugin S.F. (1995). Probabilistic representation of loads on building structures. *Proceedings of Universities. Building*, 4, 12-18
28. Pichugin S.F. & Pashinsky V.A. (1999). On the possibility of representing the snow load in the form of a stationary random process. *Questions of the reliability of reinforced concrete structures*, Kuibyshev, 26-29
9. Клепиков Л.В., Отставнов В.А. (1962). Определение нагрузок при расчете строительных конструкций. *Строительная механика и расчет сооружений*, 5, 39-45
10. Бессонов В.С. (1964). Экспериментальные работы по предотвращению чрезмерных накоплений снега на кровлях промышленных зданий в районах с сильными ветрами. *Известия вузов. Строительство и архитектура*, 11, 60-63
11. Хромец Ю.Н., Солодовников Р.А. (1971). Способы борьбы с избыточными снегоотложениями на покрытиях зданий. *Промышленное строительство*, 5, 28-30
12. Дривинг А.Я. (1973). О коэффициенте перегрузки снеговой нагрузки на легкие покрытия. *Нагрузки и надежность строительных конструкций: Тр. ЦНИИСК*, 21, 53-57
13. Отставнов В.А., Розенберг Л.С. (1966). Возможности снижения снеговых нагрузок на плоские покрытия. *Промышленное строительство*, 12, 28-32
14. Бать А.А. (1977). Комментарии к главе СНиП II-6-74 «Нагрузки и воздействия». *Промышленное строительство*, 5, 42-44
15. Жукова Н.К. (1979). Результаты натурных наблюдений за снеговыми нагрузками на пространственные конструкции покрытий. *Известия вузов. Строительство и архитектура*, 9, 40-46
16. Неверов И.А., Захарченко С.М., Клименко В.З. (1984). Снеговые нагрузки на арочное покрытие стрельчатого очертания. *Промышленное строительство*, 7, 15-17
17. Кошутин Б.Н., Строкотов Б.П. (1984). О возможности снижения расчетных нагрузок на плоские покрытия производственных зданий с зенитными фонарями. *Промышленное строительство*, 5, 33-34
18. Кінаш Р.І., Бурнаєв О.М. (1997). *Снігове навантаження в Україні*. Львів: Видавництво науково-технічної літератури
19. Пашинський В.А. (1999). *Атмосферні навантаження на будівельні конструкції для території України* Київ: УкрНДІПроектсталь-конструкція
20. Гордеев В.Н., Лантух-Лященко А.И., Пашинский В.А., Перельмутер А.В., Пичугин С.Ф. Под общей ред. А.В. Перельмутера. (2008). *Нагрузки и воздействия на здания и сооружения*. Москва: Изд-во АСВ
21. Пичугин С.Ф., Махынко А.В. (2012). *Снеговые и гололедные нагрузки на строительные конструкции*. Полтава: ООО «АСМИ»
22. Назаров Ю.П., Лебедева И.В., Попов Н.А. (2006). Региональное нормирование снеговых нагрузок в России. *Стр. механика и расчет сооружений*, 3, 71-77
23. Otstavnov V.A., Lebedeva I.V. (2004). The New Map of Ground Snow Loads for Russian Building Code. *Proc. of V International Conference on Snow Engineering*. Davos, Switzerland, 157-160
24. Malyi V.I. (2011). On the special attitude to snow load in Russian codes. *Industrial and civil engineering*, 8, 42-45
25. Pichugin S.F. (2016). *Calculation of reliability of building structures*. Poltava: TOV ASMI
26. Ledovskoy I.V. (2005). Analysis of the random process of snow accumulation on the ground. *Bulletin of Civil Engineers*, 3 (4), 29-35
27. Pichugin S.F. (1995). Probabilistic representation of loads on building structures. *Proceedings of Universities. Building*, 4, 12-18
28. Pichugin S.F. & Pashinsky V.A. (1999). On the possibility of representing the snow load in the form of a stationary random process. *Questions of the reliability of reinforced concrete structures*, Kuibyshev, 26-29

29. Pichugin S.F. (2000). Probabilistic Description of Ground Snow Loads for Ukraine. *Snow Engineering. Recent Advances and Developments*. Rotterdam: A.A.Balkema, 251-256

30. Пашинський В.А. (1999). Квазіпостійні розрахункові значення навантажень на будівельні конструкції. *Коммунальное хозяйство городов: Научно-технический сборник*, 18, 78-81

31. Кінаш Р.І., Гук Я.С. (2011). Районування території Закарпатської області за максимальною висотою снігового покриву. *Современные конструкции из металла и древесины. Сборник научных трудов*, 3, 63-68

32. Pichugin S. & Dryzhyruk Y. (2010). Snow Load Investigation for Buildings of Different Heights. *Recent Advances in Research on Environmental Effects on Buildings and People*. Ed. by A. Flaga and T. Lipecki. PAWE, Cracow, Poland, 279-286

33. Пічугін С.Ф., Молька І.В., Дрижирук Ю.В. (2011). Вплив тепловтрат через дахи на величину снігового навантаження. *Збірник наукових праць. Галузеве машинобудування, будівництво*, 2 (30), 113-117

34. Пічугін С.Ф., Попович Н.М. (2012). Імовірнісна модель послідовності снігопадів для нормування снігового навантаження на холодні покрівлі. *Ресурсоєкономні матеріали, конструкції, будівлі та споруди. Збірник наукових праць*, 24., 377-384.

35. Pichugin S.F., Dryzhyruk Yu.V., Popovich N.M. & Chernetska I.V. (2015). *The features of snow loads on building roofs. Technical Transactions, 12. Civil Engineering, 2-B/2015*, 441-449

<https://doi.org/10.4467/2353737XCT.15.149.4186>

29. Pichugin S.F. (2000). Probabilistic Description of Ground Snow Loads for Ukraine. *Snow Engineering. Recent Advances and Developments*. Rotterdam: A.A.Balkema, 251-256

30. Pashinsky V.A. (1999). Quasi-constant design values of loads on building structures. *Municipal services of cities: Scientific and technical collection*, 18, 78-81

31. Kinash R.I. & Guk J.S. (2011). Zoning of the Transcarpathian region by the maximum height of snow cover. *Modern constructions from metal and wood. Collection of scientific works*, 3, 63-68

32. Pichugin S. & Dryzhyruk Y. (2010). Snow Load Investigation for Buildings of Different Heights. *Recent Advances in Research on Environmental Effects on Buildings and People*. Ed. by A. Flaga and T. Lipecki. PAWE, Cracow, Poland, 279-286

33. Pichugin S.F., Molka I.V. & Drizhiruk Yu.V. (2011). Influence of heat loss through roofs on the value of snow load. *Collection of scientific works. Industrial Engineering, Construction*, 2 (30), 113-117.

34. Pichugin S.F., & Popovich N.M. (2012). Probabilistic model of snowfall sequence for normalization of snow load on cold roofs. *Resource-saving materials, structures, buildings and structures. Collection of scientific works*, 24, 377-384.

35. Pichugin S.F., Dryzhyruk Yu.V., Popovich N.M. & Chernetska I.V. (2015). *The features of snow loads on building roofs. Technical Transactions, 12. Civil Engineering, 2-B/2015*, 441-449

<https://doi.org/10.4467/2353737XCT.15.149.4186>

UDC 624

## Experience and current issues of designing of steel and concrete composite structures of roof and floor systems

Storozhenko Leonid<sup>1</sup>, Gasii Grygorii<sup>2\*</sup>

<sup>1</sup> National University «Yuri Kondratyuk Poltava Polytechnic» <https://orcid.org/0000-0002-3764-5641>

<sup>2</sup> Sumy National Agrarian University <https://orcid.org/0000-0002-1492-0460>

\*Corresponding author E-mail: [grygorii.gasii@snau.edu.ua](mailto:grygorii.gasii@snau.edu.ua)

The current state of the building covering structures is thoroughly investigated, in particular, the world experience in the construction and building of various roof and floor structures, made of various materials, including composites, has been studied. A thorough results analysis of theoretical studies and experimental tests on the constructive solutions effectiveness determination conducted by domestic and foreign scientists has been carried out. Based on the received information about the features of the construction and technological solutions, there were determined the advantages and disadvantages of existing construction structures, the prospective development directions. Based on the result of actual scientific and technical literature analysis, the main research objectives are formulated.

**Keywords:** steel and concrete composite structures, a roof, a floor, a permanent shuttering, cross-sections

## Досвід і проблеми проектування сталезалізобетонних конструкцій покриття та перекриття

Стороженко Л.І.<sup>1</sup>, Гасій Г.М.<sup>2\*</sup>

<sup>1</sup> Національний університет «Полтавська політехніка імені Юрія Кондратюка»

<sup>2</sup> Сумський національний аграрний університет

\*Адреса для листування E-mail: [grygorii.gasii@snau.edu.ua](mailto:grygorii.gasii@snau.edu.ua)

Досліджено сучасний стан будівельних конструкцій покриття й перекриття, зокрема вивчено світовий досвід проектування, конструювання та будівництва таких конструкцій, у тому числі виготовлених із різних матеріалів. Виконано ґрунтовний аналіз результатів теоретичних досліджень та експериментальних випробувань щодо визначення ефективності конструктивних рішень покриття й перекриття, виконаних вітчизняними та зарубіжними вченими. Оскільки сталезалізобетонні конструкції зазнають бурхливого розвитку, модифікуються й удосконалюються, то вивчено проблему їх ефективності на всіх етапах життєвого циклу та проектного ресурсу. Проаналізовано новітні підходи до проектування сталезалізобетонних конструкцій покриття й перекриття. На підставі отриманих відомостей про особливості будови й технологічних рішень, переваги та недоліки існуючих конструкцій покриття й перекриття визначено перспективні напрями їх розвитку. У сталезалізобетонних конструкціях покриття й перекриття раціонально та повною мірою використовуються характеристики міцності матеріалів, тобто сталеві елементи розташовуються в зоні дії зусиль розтягу, а бетон – у зоні дії зусиль стиску. Такий поділ і розмежування різнорідних матеріалів вимагає заходів із забезпечення їх сумісної роботи. Сьогодні найбільш ефективним способом об'єднання сталевих деталей та бетону є застосування різноманітних анкерів: жорстких, гнучких і комбінованих. У загальному випадку несуча здатність сталезалізобетонних конструкцій, за винятком трубобетонних та схожих за будовою елементів, визначається саме несучою здатністю анкерних засобів на зріз і зсув. З огляду на зазначене останнім часом усе частіше при розробленні нових конструктивних рішень сталезалізобетонних елементів застосовується спосіб забезпечення сумісної роботи, суть якого полягає в об'єднанні сталевих каркасів із залізобетонними елементами в процесі бетонування без використання анкерів, тобто сталева конструкція забетонується. Такий підхід дозволяє отримати цілісну, неподільну конструкцію, несуча здатність котрої залежить від несучої здатності залізобетонних та металевих елементів.

**Ключові слова:** сталезалізобетонна конструкція, покриття, перекриття, незнімна опалубка, переріз



## Introduction

Steel and concrete structures are designs that have a long story of development, a wide scope, advantages, and shortcomings compared to other designs types. The scope and rate of such designs development are closely related to the significant amount of their features and difficulties caused by them. A part of the challenges concerns the design, construction, and further steel and concrete composite structures service, another part relevant to their structural concept features. All this demands the detailed and thorough analysis of the experimental and theoretical studies results, and obtained data synthesis with the purpose of establishing a shared understanding of steel and concrete composite structures stressing features, and further research trends allocation. Steel and concrete composite structures is a widespread composite material that is made of a concrete mix, and filler, and includes steel elements and reinforcement. Steel and concrete composite structures can be strengthened with rods, rigid and external reinforcement; also, they can be reinforced with different steel sections: tubes, plates, corners, steel sheets, etc.

Studying the stress-strained state, the search for effective ways of achieving steel and concrete members combined action, optimization, and design improvement taking into account the last achievements in science and technology are the main steel and concrete composite structures research trends.

A combination of positive reinforced and steel structures' physic-mechanical properties with simultaneous disposal of their shortcomings is the main advantage of steel and concrete composite structures.

Refer to the increased rigidity and bearing capacity unlike other designs to advantages of steel and concrete composite structures.

The finding of positive characteristics is the criterion that defines the structure efficiency. Therefore, in the steel and concrete composite structures, it is possible to reach a favorable strength indicator combination as steel during stretching as concrete on compression thanks to their combined action. The efficiency of such association is known and the application expediency in construction is proved and recognized long ago.

Thanks to such connections, steel and concrete composite structures are characterized by reduced sensitivity to damages and defects compared to reinforced concrete or steel. Besides, an established fact that they are capable of sustaining considerable loadings, even after achieving the yield point by the reinforcement. Also, treat steel and concrete composite structures advantages: high bearing capacity; low construction height; resistance to dynamic influences; technological effectiveness.

The steel and concrete composite structures designs are extremely various therefore they can be classified by different signs: for example, on kind of structures behavior, a way of production, or construction.

Also, steel and concrete composite structures can be classified by structural element type: supports or columns with the side hollows filled with concrete, and with external and internal rigid reinforcing; beams or crossbars with the side hollows filled with concrete,

and with external reinforcement with steel flat strip, and internal rigid reinforcing, including reinforced concrete structures with a permanent shuttering; the precast and monolithic steel and concrete composite slabs, including slabs with the metal decking or orthotropic plates, or with a steel frame; the reinforced combined concrete structures reinforced or strengthened by lattice, rod or other steel elements; the rafter combined steel structures with the reinforced concrete elements; elements of the spatial combined structures; elements of high-rise buildings and constructions; elements of long-span constructions, bridges, platforms, etc.; other special and engineering constructions and elements.

Steel and concrete composite structures gained the biggest distribution in bridge construction, and civil engineering. Steel and concrete composite structures in construction of buildings and structures are effectively used as a column, slabs, beams, crossbars, etc. Increasingly design features, properties, and resistance to damages and defects define the scope of steel and concrete composite structures.

However, it should be noted corrosive environments limit the steel and concrete composite structures scope.

It is known that corrosion of the steel and concrete composite structures open and unprotected steel parts and surfaces is one of the most frequent reasons for damages, which significantly reduce bearing capacity and affect the structure service suitability and durability.

## Review of the research sources and publications

Quite often steel members carry out the role of permanent shuttering. Steel and concrete composite structures as material are not new and the fact that it has high technical and economic rates is known for a long time, therefore, he didn't lose its relevance and presently is intensively investigated around the world [1–3].

In most cases, steel and concrete composite structures have the highest technical and economic effects compared to other structures [4].

Analysis of the sources showed that they are devoted to detailed individual problems research, but there are reviews devoted to the data generalization [5–8].

## Definition of unsolved aspects of the problem

Because steel and concrete composite structures experience rapid development around the world, are constantly modified and improved there was the obtained data analysis and synthesis problem. This problem is urgent as its solution will allow considering in a complex all factors at all life cycle stages in a particular design, building and service, the feature of behavior under load, and the stress-strain state.

## Problem statement

Study an experience and current issues of steel and concrete composite structures designing of roof and floor systems.



### Basic material and results

Steel and concrete composite structures are a special building structures class that found application in modern construction. As is known, a balance between the non-concreted steel members bearing capacities and concrete steel members belonging to the same structure is the feature that distinguishes steel and concrete composite structures from other structures.

At the steel and concrete composite structures design obviously, there is what their intense deformed state depends on physic-mechanical materials properties, which are their part, namely steel, and concrete. Steel is a uniform material, therefore, it has constants, within a class, physical and mechanical properties, as for concrete, they are very different in the physical and mechanical properties. The physical and mechanical concrete properties depend on its structure, which has the ability to change over time that in total under action external loadings cause the creep concrete deformation. Also, the concrete structure is affected by changing stresses and formatting of their concentration owing to communications between particles of concrete collapse. At compression, there are longitudinal compression stresses and cross stretching stresses from which action concrete collapses.

Except for material selection with necessary physical and mechanical properties, additional complexity at the design of steel and concrete composite structures, there is a problem of ensuring the combined action of concrete and steel. The combined action of these materials is ensured by coupling among themselves, only in that case materials will be deformed and work in common. The triaxial stress state availability is the most favorable condition under which it is possible to reach the necessary coupling between concrete and steel elements. This state is a well-known tube-concrete element characteristic where concrete is in a steel cage. Unlike tube-concrete elements, the special shear connectors application for the steel and concrete composite structures majority is a typical solution for the steel and concrete combined action problem.

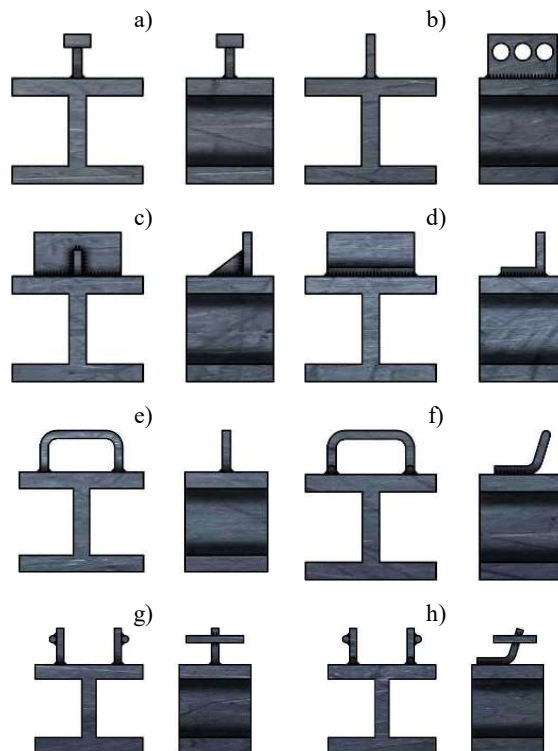
In general, many studies of scientists from different world countries are addressed to studying this issue. There are the largest shear connectors species, but the most typical and modern decisions into known shear connectors are short steel rods with a cap at the end – a headed stud shear connector (Fig. 1a) [9].

It should be noted the shear connectors can have various configurations and are produced practically from any steel fragment, a detail, or a plate (Fig. 1b).

Except for the typical design, shear connectors can be as a rigid connector (Fig. 1c, d), as loops (Fig. 1e, f); made from steel rods (Fig. 1g, h). The way of placement of shear connectors depends on the service of structures, and efforts that arise under loading. In order for the shear connector to be a flexural member, it must be placed perpendicularly, and if it is placed at an angle of 45° in the direction of the shear force, it will be in tension.

The type choice and shear connectors shape depends on the shear connectors' simplicity, also their ability to be connected to the steel parts and elements by welding,

and service conditions of the structure. As already mentioned, the most widespread types of shear connectors are headed stud shear connectors (Fig. 1a) and shear connectors made from short steel rods (Fig. 1g, h). Except for the basic purpose – to combine steel and concrete, the shear connectors can carry out the role of transverse reinforcement in designs with external reinforcement.



**Figure 1 – Certain types of shear connectors:**

- a – headed stud shear connector;
- b – shear connector made of the perforated plate;
- c – rigid connector; d – flexible connector;
- e – vertical loop; f – inclined loop;
- g – vertical bar; h – inclined bar.

Usage of various glue substances [10] is the less known way for ensuring combined action of steel and concrete structure parts.

A different important issue that is closely linked to the steel and concrete composite structures design is the assessment and rationing of their technical conditions. The relevance of the search for the solution to this problem is especially accurately outlined against the background of the actual wear and obsolescence of fixed assets of production, economic, educational, and other institutions. On the other hand, the importance of the solution of this problem predetermines the fact that designs are improved and developed more intensively, than methods of their calculations, and there are no standard recommendations and provisions, which regulate a technique of steel and concrete composite structures technical condition estimation. A bigger measure of the technical states concerns objects rationing questions, which are operated, but also does not lose the sharpness on the relation and to new construction. For new construction, definitions of a steel and concrete composite structures design resource are a current

problem also. There are recommendations concerning the definition of a steel and concrete composite structures design resource according to which at the steel and concrete composite structures design operational suitability indicators are set with a stock [11].

The specified technique provides acceptance of the steel service strategy and concrete composite structures and the resource coefficient introduction [11].

The service strategy of steel and concrete composite buildings and constructions or their members provides two options: 1) without capital repair throughout all characteristic terms of service; 2) carrying out capital repairs. The approach described in the paper [11], gives the chance to consider a time factor and allows optimizing construction and service structures costs.

Today the international bearing structures experience of construction from steel and concrete composite structures incredibly various also contains a significant amount of different objects, buildings, and structures in all construction fields. Despite universality and a variety of steel and concrete composite construction elements, the most frequent application they found was in industrial and civil engineering, especially in the floor structures.

Steel and concrete composite beams, which consist of a reinforced concrete plate, and a steel beam (Figure 2a) belong to the most widespread steel and concrete composite structures types. Scientists of the Frits laboratory of Lehigh University conducted thorough such designs research in the middle of the last century in the USA. The research results testify to high strength and technical and economic rates.

In such structures, the combined action of a steel element and reinforced concrete plate can be provided with different shear connectors types, but in terms of effective action conditions under shear forces, rather with rod shear connectors and connectors made of separate corner pieces, shear connectors as inclined loops are better and ensure combined elements action practically until the total structure break [12].

Steel beams with a reinforced concrete top belt (Figure 2b) are a kind of steel and concrete composite beams. The structures application reduces by 15 % cost and for 35 % labor of installation and construction [13].

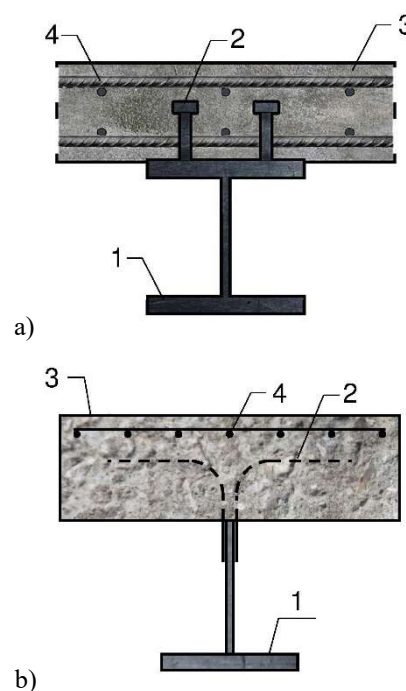
Steel and concrete composite beams that have external reinforcing with a sheet (Figure 3) are one more kind of composite structure made of steel and concrete. Such structures can have both a rectangular shape of section (Figure 3a, b) and T-type (Figure 3c), besides, they can be box-type. The bearing capacity of a steel and concrete composite box-shaped type beam compared to analogs, depending on the accepted reinforcing way is 2-6 times more [14].

To increase the rigidity and bearing capacity of the T-type steel and concrete composite beams, it might also be reinforced with tubes (Figure 3d) [15,16].

The steel and concrete composite beams usage that reinforced externally with sheet compared to typical reinforced concrete beams assists economy of high-strength longitudinal armature up to 20 % and 25 % at single and double reinforcement in construction respectively, and the structures advantage, which made steel

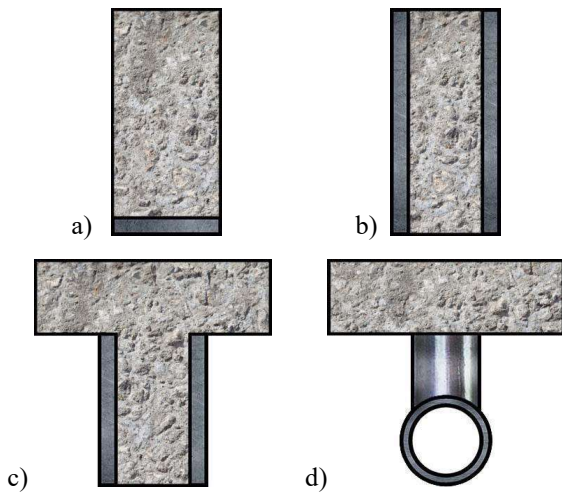
entirely lies in the steel economy of up to 35 % at identical bearing capacity [17]. The resistance to damages compared to the beams made of different materials and the fact that steel and concrete composite beams at similar damages have greater durability than reinforced or entirely steel structures is one more steel and concrete composite beam advantage. However, the structure's bearing capacity depends on service conditions and the mode of loading. Because of an experimental study of the influence of short-term cyclic and sign-variable loads on durability and deformability of steel and concrete composite beams, it is established that the bearing capacity decreases up to 20 % compared to the bearing capacity of beams at single loading. Besides the bearing capacity depends on the total number of cycles of loading and the level of the previous loading by negative bending moment [18].

In most cases, steel elements play a role in steel and concrete strengthening composite structures, but there are also such structures where this role is played by concrete. Beams that are formed from steel elements with the hollow (Figure 4) filled with concrete belong to such structures. The concrete coupling with a beam can be reached both using different shear connectors and using adhesives. In general, steel and concrete composite beams are highly bearing capacity. Experimental studies showed that the bearing capacity of the beams thanks to concrete in hollow increases compared to typical steel beams of a similar profile by 30-40 % in bend and for 40-50 % in shear [19].

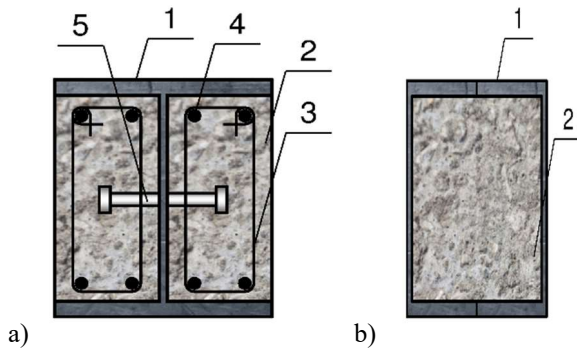


**Figure 2 – Types of steel and concrete composite beams:**

- a – a structure that consists of a reinforced concrete plate and a steel beam;
- b – a steel combined beam that held a reinforced concrete top flange;
- 1 – steel beam; 2 – shear connector;
- 3 – concrete slab; 4 – reinforcement.



**Figure 3 – Types of the cross-sections of steel and concrete composite beams:**  
 a – with external horizontal reinforcing;  
 b – rectangular with external vertical reinforcing;  
 c – T-type; d – type with reinforcing by a steel tube.



**Figure 4 – Steel and concrete composite beams with the hollows filled with concrete:**  
 a -- beam with an open profile;  
 b -- beam with a closed profile;  
 1 – rolled steel; 2 – concrete;  
 3, 4 – crosswise and longitudinal reinforcement;  
 5 – shear connectors.

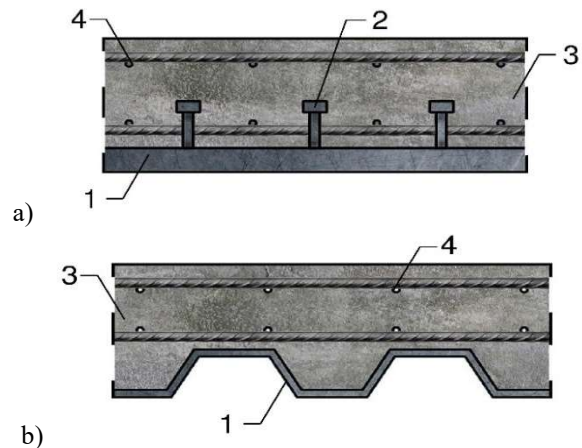
Composite structures, which consist of monolithic plates coupled to steel sheets (Figure 5) are widely used. Their main advantage is the small height of the cross-sections that are within limits of 2.5...5 % of their length, however, the bearing capacity of such steel and concrete composite plates at different consolidation ways significantly depends on the steel sheet thickness. It is experimentally established that the bearing capacity increases correspond to the increase in the thickness of a steel sheet [20].

Such structures were extremely often applied in high-rise construction as the bearing horizontal systems in recent years [21]. They were used in large quantities in the USA in the middle of the last century. Over time such systems began to be applied in Europe, in particular in Great Britain, began to consider a steel part of a structure (the pro-thinned-out flooring) not only as a permanent shuttering but also as external reinforcement [22]. In this case, there is a perception problem design

of the horizontal shifting efforts and to the prevention of separation of concrete from the sheet. At different times this issue was resolved differently, at first combined steel sheet and concrete action was reached thanks to the special sheet shape [23] over time began using the corrugated steel sheet with the drawing on the side [24]. In recent years the combined systems that can be formed from the special shape sheet with the applied relief image, reinforcing grids, and different fibers are actively investigated [25, 26].

To carry out these experimental studies and establishment of strength characteristics of steel and concrete composite slabs there were used samples with sizes of 1×1 m and 50 mm high. The steel sheet thickness varied within 1...3, 5 mm.

Considering good strength characteristics the most effective way is an application of special shear connectors that join steel elements by means of welding [27], but there are cases when such a shear connector could not apply or it is not economically expedient. Then non-standard structural concepts can serve as their alternative. An example of such shear connectors are items that are connected to the beam differently. Such shear connectors are produced as cold-formed steel Z or C-sections, which are connected to the beam with bolts or self-tapping screws.



**Figure 5 – Steel and concrete composite floor systems that consist of reinforced concrete slabs coupled to steel sheets:**

a -- orthotropic sheet; b -- steel sheet;  
 1 – sheet; 2 – shear connector;  
 3 – concrete; 4 – reinforcing.

The thin-walled composite slim-floor systems are a kind of such design. Their structural concept is in applying an innovative composite connection. This connection is reached by making reinforcing bars through openings in beams. Such technology is economic and effective as it is possible to use the full concrete elements potential. Results of experimental studies under the action of different loadings types, including dynamic and vibration, which demonstrate the increased bearing capacity and rigidity of such designs compared to analogs for 100 and 150 % [28] are confirmation to it.

Other steel and concrete composite structures representatives are a beams system with a box-shaped  $\Delta$ -similar cross-section [29]. The beam's feature is opening with a diameter of 75 mm or 150 mm, which is regularly distributed in length in a certain opening quantity with the edges bent inside. Thanks to the availability of such openings with curved edges, the materials combined action are ensured. Such beams can be applied both with combined thin-walled (Figure 6a) and with typical reinforced concrete hollow slabs (Figure 6b) [30].

The structures, which include slabs that consist of the profiled steel sheets and the spatial framework made of reinforcing bars as a lattice [31] are one more kind of steel and concrete composite bearing system.

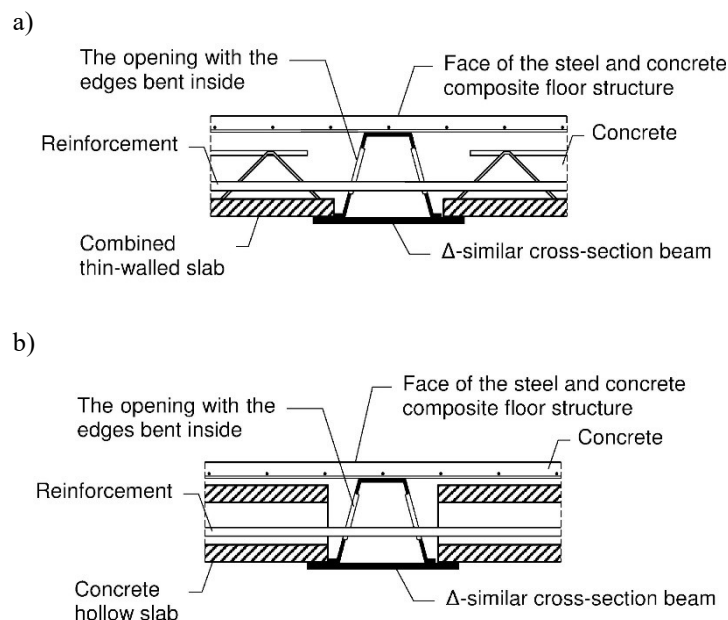
The systems have many advantages, such as profitability, convenience, and safety that allow them to reduce construction terms considerably compared to other systems. The structure can maintain the considerable concrete and construction equipment weight and is set directly on steel beams without additional support details [32]. Also, monolithic slabs with the profiled steel sheet can be mounted on different substructures or support structures like beams, crossbars, farms, etc. Besides the substructures can be reinforced concrete, steel, or steel-concrete. The steel and concrete composite slabs in association with steel farms or steel beams are an example of such a structure. Moreover, the design of the top knots can be diverse, most often applying steel rolled sections and thin-walled steel structures to the systems top belt production.

In research [33] a similar design is considered by the length of 44 m which is made of a spatial farm and a concrete slab. The finite element method is applied to

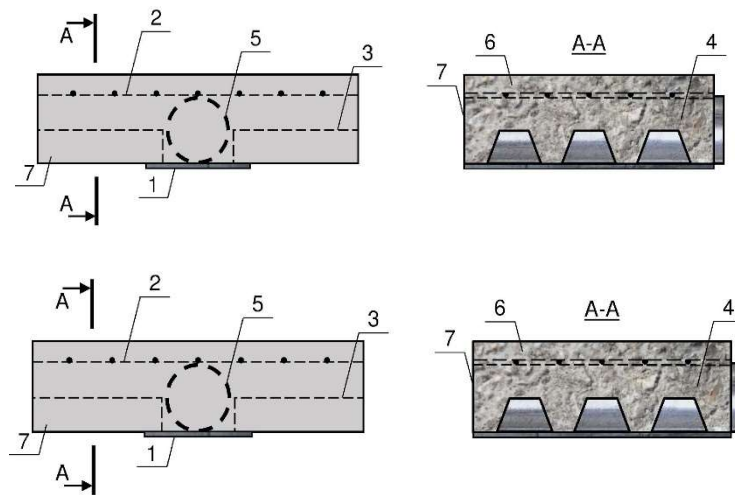
the theoretical analysis of the composite structure behavior. The results show that the concrete slab, when it is in combined action with the composite space truss, is compressed curved, and the internal forces in the composite truss elements are distributed evenly, thus, the materials strength properties are effectively used.

The interesting constructive concept is a system with usage of the steel tubes filled with concrete. This system consists of a monolithic slab that is connected to a profiled steel sheet, it sets over the truss with parallel belts where the top belt is filled with concrete [34, 35]. The steel and concrete composite slab can be lying as in the steel tube plane filled with concrete, (Figure 7) as on the steel tube top filled with concrete (Figure 8). In addition, according to the first scheme, the combined steel and concrete members action between themselves is implemented due to contact of a tube and concrete, and for the second, it is due to the shear connectors application. Experimentally it is proved that the structures have an increased bearing capacity.

The dependence between the failure load level (the load when the connection between concrete and steel members is lost) and a concrete class durability and concrete top layer thickness is established. It is established that at the increase in a concrete durability class the failure load for the first scheme increases up to 45 %, and for scheme 2 – up to 33 %. Besides, the shifting effort for the first scheme is almost four times more, than for scheme 2. Depending on the concrete top layer thickness, the failure load for the first scheme increases by up to 21 %, and for the second scheme – up to 26 % [36].

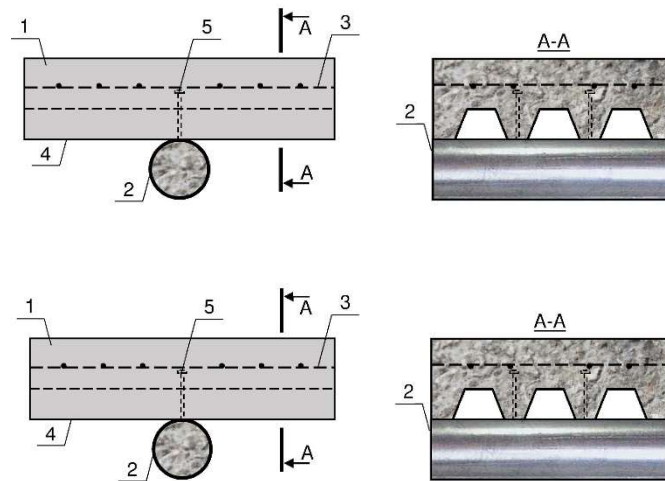


**Figure 6 – Steel and concrete composite systems consist of  $\Delta$ -similar beams and thin-walled (a) or hollow slabs (b) [29, 30].**



**Figure 7 – The structure with a monolithic steel and concrete composite slab that is lying in the plane of the tube filled with concrete [35]:**

1 – steel basic deck; 2 – reinforcing grid; 3 – the profiled steel sheet; 4 – concrete; 5 – the steel tube filled with concrete; 6 – the top layer of concrete; 7 – the face of the plate.

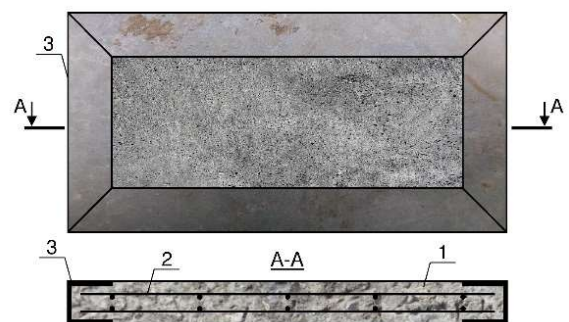


**Figure 8 – The structure with the monolithic steel and concrete composite slab that is lying on the tube filled with concrete [35]:**

1 – concrete; 2 – the steel tube filled with concrete; 3 – reinforcing grid; 4 – the profiled steel sheet; 5 – shear connector.

Along with the monolithic steel and concrete composite structures research, combined steel and concrete composite precast systems are studied. The combined structures use is the perspective direction for improving structural concepts of the bearing steel and concrete composite systems.

The slab with a steel frame (Figure 9) is one of the combined steel and concrete composite structure elements. It is experimentally established that the bearing capacity of such slab compared to a reinforced concrete slab of a similar section is more on 45–50 % [37]. Besides, due to a steel frame, the slab has increased rigidity.



**Figure 9 – The slab with a steel frame for the system of the precast flat slab construction [37]:**  
1 – concrete; 2 – reinforcing grid; 3 – steel frame.

It should be noted that the slab framed with steel members, except the key qualitative physic-mechanical parameters, has technological advantages, it is the low labor of production that is reached due to the frame use as a permanent shuttering. Experimentally confirmed advantages of such plates give the chance to apply them in the flat slab construction.

Other examples of the complex roof systems type are structures that consist of typical ridge reinforced concrete slabs and steel trusses. While the application of that structure the materials economy is reached if the combined action between slabs and trusses is provided. If trusses by the length of 30 and 36 m and slabs of 6 and 12 m are used, the steel economy reaches up to 18 %, concrete – up to 10 % [38], and in case of application of the long-span light grid steel and concrete composite slabs, the steel economy increases up to 25 % [39]. Among rod steel and concrete composite rafter designs, some consist of reinforced concrete beams and steel farms.

In general, the inclusion of typical reinforced concrete elements in combined action as the top belt with typical steel farms is an economically justified design. Even though these structures are effective, they have also essential shortcomings: firstly, it is the design complexity and the need for typical elements adaptation under new service conditions.

In general in industrial and civil engineering the technical and economic effect promotes the steel economy up to 33 % rather than entirely metal and up to 11 % compared to traditional reinforced concrete structures that have steel and concrete composite elements applications. Besides the given expenses decrease up to 30 % rather with steel and up to 50 % compared to reinforced concrete structures [40].

It is possible to claim efficiency and expediency of steel and concrete composite structures usage in the roof or floor systems construction, leaning on analysis results of current researches, as well as based on the different structural concepts review of the steel and concrete composite bearing elements, and widely used connections between steel and concrete details. However, for this purpose, it is necessary to execute thorough theoretical research of the spatial bearing systems and construction ways for most effective spatial systems allocation, which will be possible to be applied to shaping the roofs.

## Conclusions

For achieving the goal, the existing bearing systems and ways their shaping complex review was executed. As the result is the allocation of an among all bearing systems variety of the most effective in spatial behavior terms, low weight, material consumption, and architectural expressiveness, etc. Based on the steel and concrete composite structures review and the theoretical and experimental studies results, it is possible to notice that such structures are effective.

In such structures, materials strength characteristics are rationally and fully used, in general through the steel members are located in stretching elements, and concrete – in compression. Such an entirely different materials combination requires measures for ensuring their combined action.

Today in the most effective steel details and concrete members connection way is applications of different shear connectors: rigid, flexible, and combined. Generally, the steel and concrete composite structures bearing capacity, except for concrete-filled steel tubular structures and similar structures, is defined by the bearing capacity of the shear connectors in shearing or shifting.

Considering specified, for developing new steel and concrete composite systems structural concepts, the way of ensuring combined action between steel and concrete members the essence of which is the combination of a steel frame and reinforced concrete elements together during the concreting without the shear connectors usage is becoming increasingly applied, it means the steel structure is put in concrete solid. Such an approach allows creating integrity and indivisible structure in which bearing capacity depends on the bearing capacity of reinforced concrete or steel elements.

Steel and concrete composite structures have significant advantages and positive properties that allow applying them successfully in the different industrial and public buildings construction. In such structures the efficient materials use concept, and functions distribution is implemented, therefore the structure components are in the stresses that are inherent for them only, which means steel members are in tension, and concrete members are in compression. However, it is necessary to notice that the steel and concrete composite systems also have structural concepts imperfections. First of all, it is the complexity and massiveness of nodal connections. In certain cases, there is a need for shear connectors. It is possible to carry to shortcomings as well that such structures are monolithic, and it considerably limits a scope. In the case of the precast structures industry or on the building site, the span is limited and if concreting is carried out in design position – the construction process technology complexity due to concreting or welding overhead works, the need of timbering installation of, etc is increased.

## References

1. Galambos T.V. (2000). Recent research and design developments in steel and composite steel-concrete structures in USA. *Journal of Constructional Steel Research*, 55(1), 289-303  
[https://doi.org/10.1016/S0143-974X\(99\)00090-5](https://doi.org/10.1016/S0143-974X(99)00090-5)
2. Jianguo N. & Zhiwu Y. (1999). Research and practice of composite steel-concrete beams in China. *China Civil Engineering Journal*, 32(2), 3-8
3. Lam D. (2005). *Advances in composite construction in the UK*. Proceedings of the Second International Symposium on Worldwide Codified Design and Technology in Steel Structures. Hong Kong, 133-144
4. Gasii G., Hasii O. & Zabolotskyi O. (2017). *Estimate of technical and economic benefits of a new space composite structure*. MATEC Web of Conferences, 116, 02014  
<https://doi.org/10.1051/mateconf/201711602014>
5. Bonilla J., Bezerra L.M., Mirambell E. & Massicotte B. (2018). Review of stud shear resistance prediction in steel-concrete composite beams. *Steel and Composite Structures*, 27(3), 355-370  
<https://doi.org/10.12989/scs.2018.27.3.355>
6. Chrzanowski M., Odenbreit C., Obiala R., Bogdan T. & Degée H. (2019). Transfer of shear stresses at steel-concrete interface: Experimental tests and literature review. *Steel Construction*, 12(1), 44-54  
<https://doi.org/10.1002/stco.201800024>
7. Liew J.R., Yan J.B. & Huang Z.Y. (2017). Steel-concrete-steel sandwich composite structures-recent innovations. *Journal of Constructional Steel Research*, 130, 202-221  
<https://doi.org/10.1016/j.jcsr.2016.12.007>
8. Shan Z.W. & Su R.K.L. (2020). A review on composite actions of plate-reinforced composite coupling beams, *Advanced Steel Construction*, 16(2), 94-98  
<http://dx.doi.org/10.18057/IJASC.2020.16.2.1>
9. Shariati A., Ramli S.N.H., Suhatri M. & Shariati M. (2012). Various types of shear connectors in composite structures. *International Journal of Physical Sciences*, 7(22), 2876-2890  
<https://doi.org/10.5897/IJPSx11.004>
10. Стороженко Л.І., Горб О.Г., Білокуров П.С. (2014). Міцність клейкових з'єднань сталі та бетону. *Збірник наукових праць Української державної академії залізничного транспорту*, 149, 113-118
11. Клименко Є.В. (2014). До питання визначення проектного ресурсу сталезалізобетонних конструкцій. *Збірник наукових праць. Галузеве машинобудування, будівництво*, 3(42), 116-119
12. Крухмалев А.В. (2010). Напряженно-деформированное состояние сталежелезобетонных балок. *Наука и прогресс транспорта. Вестник Днепропетровского национального университета железнодорожного транспорта*, 33, 143-145
13. Крупченко О.А. (2008). *Напружено-деформований стан та міцність сталезалізобетонних двотаврових балок із залізобетонним верхнім поясом*. (Автореф. дис. канд. техн. наук). Полтавський національний технічний університет імені Юрія Кондратюка, Полтава
14. Сколибог О.В. (2006). *Сталезалізобетонні балки із зовнішнім листовим армуванням*. (Автореф. дис. канд. техн. наук). Полтавський національний технічний університет імені Юрія Кондратюка, Полтава
15. Gasii G.M. (2014). Technological and design features of flat-rod elements with usage of composite reinforced concrete. *Metallurgical and Mining Industry*, 4, 23-25
1. Galambos T.V. (2000). Recent research and design developments in steel and composite steel-concrete structures in USA. *Journal of Constructional Steel Research*, 55(1), 289-303  
[https://doi.org/10.1016/S0143-974X\(99\)00090-5](https://doi.org/10.1016/S0143-974X(99)00090-5)
2. Jianguo N. & Zhiwu Y. (1999). Research and practice of composite steel-concrete beams in China. *China Civil Engineering Journal*, 32(2), 3-8
3. Lam D. (2005). *Advances in composite construction in the UK*. Proceedings of the Second International Symposium on Worldwide Codified Design and Technology in Steel Structures. Hong Kong, 133-144
4. Gasii G., Hasii O. & Zabolotskyi O. (2017). *Estimate of technical and economic benefits of a new space composite structure*. MATEC Web of Conferences, 116, 02014  
<https://doi.org/10.1051/mateconf/201711602014>
5. Bonilla J., Bezerra L.M., Mirambell E. & Massicotte B. (2018). Review of stud shear resistance prediction in steel-concrete composite beams. *Steel and Composite Structures*, 27(3), 355-370  
<https://doi.org/10.12989/scs.2018.27.3.355>
6. Chrzanowski M., Odenbreit C., Obiala R., Bogdan T. & Degée H. (2019). Transfer of shear stresses at steel-concrete interface: Experimental tests and literature review. *Steel Construction*, 12(1), 44-54  
<https://doi.org/10.1002/stco.201800024>
7. Liew J.R., Yan J.B. & Huang Z.Y. (2017). Steel-concrete-steel sandwich composite structures-recent innovations. *Journal of Constructional Steel Research*, 130, 202-221  
<https://doi.org/10.1016/j.jcsr.2016.12.007>
8. Shan Z.W. & Su R.K.L. (2020). A review on composite actions of plate-reinforced composite coupling beams, *Advanced Steel Construction*, 16(2), 94-98  
<http://dx.doi.org/10.18057/IJASC.2020.16.2.1>
9. Shariati A., Ramli S.N.H., Suhatri M. & Shariati M. (2012). Various types of shear connectors in composite structures. *International Journal of Physical Sciences*, 7(22), 2876-2890  
<https://doi.org/10.5897/IJPSx11.004>
10. Storozhenko L.I., Gorb O.G. & Bilokurov P.S. (2014). Adhesive strength of steel and concrete. *Collection of Scientific Works of the Ukrainian State University of Railway Transport*, 149, 113-118
11. Klimenko Y.V. (2014). To the issue of definition of design resource of the steel-concrete composite structures. *Academic journal. Industrial Machine Building, Civil Engineering*, 3(42), 116-119
12. Krukmalov A.V. (2010). The strain- stress state of steel reinforced concrete beams. *Science and Transport Progress. Bulletin of Dnipropetrovsk National University of Railway Transport*, 33, 143-145
13. Krupchenko O.A. (2008). *Deflected mode and strength of double-Ts composite structures with upper belt produced from reinforced concrete*. (PhD thesis). Poltava National Technical Yuri Kondratyuk University, Poltava.
14. Skolybog O.V. (2006). *Steel reinforced beams with outer sheet reinforcement*. (PhD thesis). Poltava National Technical Yuri Kondratyuk University, Poltava.
15. Gasii G.M. (2014). Technological and design features of flat-rod elements with usage of composite reinforced concrete. *Metallurgical and Mining Industry*, 4, 23-25

16. Стороженко Л.І., Нижник О.В., Куч Т.П. (2009). Експериментальні дослідження сталезалізобетонних балок з армуванням трубами. *Дороги і мости*, 11, 319-324
17. Глазунов Ю.В. (2006). Экономическая целесообразность применения конструкций с внешним армированием. *Коммунальное хозяйство городов*, 73, 190-197
18. Голоднов К.А. (2013). Исследование сталежелезобетонных балок при повторных и знакопеременных режимах нагружения. *Строительство. Материаловедение. Машиностроение*, 69, 148-154
19. Яхін С.В. (2002). *Згинальні несучі конструкції зі сталевих двотаврів із порожнинами, заповненими бетоном*. (Автореф. дис. канд. техн. наук). Полтавський національний технічний університет імені Юрія Кондратюка, Полтава
20. Vatulya G.L. & Orel E.F. (2012). Effect of section parameters on the bearing capacity of steel-concrete structures. *Academic Journal. Industrial Machine Building, Civil Engineering*, 3(33), 30-34
21. Costa-Neves L.F., Silva J.G.S., Lima L.R.O. & Jordao S. (2014). Multi-storey, multi-bay buildings with composite steel-deck floors under human-induced loads: The human comfort issue. *Computers and Structures*, 136, 34-46  
<https://doi.org/10.1016/j.compstruc.2014.01.027>
22. Wright H.D., Evans H.R. & Harding P.W. (1987). The use of profiled steel sheeting in floor construction. *Journal of Constructional Steel Research*, 7(4), 279-295  
[https://doi.org/10.1016/0143-974X\(87\)90003-4](https://doi.org/10.1016/0143-974X(87)90003-4)
23. Mahachi J. & Dundu M. (2012). Prediction of the debonding/slip load of composite deck slabs using fracture mechanics. *Journal of the South African Institution of Civil Engineering*, 54(2), 112-116
24. Abbas H.S., Bakar S.A., Ahmadi M. & Haron Z. (2015). Experimental studies on corrugated steel-concrete composite slab. *Gradevinar*, 67(3), 225-233  
<https://doi.org/10.14256/JCE.1112.2014>
25. Abas F., Bradford M., Foster S. & Gilbert R. Ian (2016). Shear bond behaviour of steel fibre reinforced concrete (SFRC) composite slabs with deep trapezoidal decking: Experimental study. *Composite Construction in Steel and Concrete VII*, 561-580  
<https://doi.org/10.1061/9780784479735.043>
26. Altoubat S., Ousmane H. & Barakat S. (2015). Effect of fibers and welded-wire reinforcements on the diaphragm behavior of composite deck slabs. *Steel and Composite Structures*, 19(1), 153-171  
<http://dx.doi.org/10.12989/scs.2015.19.1.153>
27. Hicks S.J. & Smith A.L. (2014). Stud shear connectors in composite beams that support slabs with profiled steel sheeting. *Structural Engineering International*, 24(2), 246-253  
<https://doi.org/10.2749/101686614X13830790993122>
28. Hechler O., Braun M., Obiala R. et al. (2016). CoSFBC-Composite slim-floor beam: Experimental test campaign and evaluation. *Composite Construction in Steel and Concrete VII*, 158-172  
<https://doi.org/10.1061/9780784479735.013>
29. Peltonen S. & Leskelä M. (2006). Connection behaviour of a concrete dowel in a circular web hole of a steel beam. *Composite Construction in Steel and Concrete V*, 544-552  
[https://doi.org/10.1061/40826\(186\)51](https://doi.org/10.1061/40826(186)51)
30. Huo B.Y. (2012). Experimental and analytical study of the shear transfer in composite shallow cellular floor beams (PhD Thesis). City University London, London
16. Storozhenko L.I., Nyzhnyk O.V. & Kuch T.P. (2009). Experimental studies of composite steel-concrete beam structures with reinforcement by tubes. *Roads and bridges*, 11, 319-324
17. Glazunov Yu.V. (2006). Economic feasibility of using structures with external reinforcement. *Municipal economy of cities*, 73, 190-197
18. Golodnov K.A. (2013). Study of steel-reinforced concrete beams at repeating and alternating loading modes. *Construction, materials science, mechanical engineering*, 69, 148-154
19. Jahin S.V. (2002). *Bended I-beams with the cavities filled with concrete*. (PhD thesis). Poltava National Technical Yuri Kondratyuk University, Poltava.
20. Vatulya G.L. & Orel E.F. (2012). Effect of section parameters on the bearing capacity of steel-concrete structures. *Academic Journal. Industrial Machine Building, Civil Engineering*, 3(33), 30-34
21. Costa-Neves L.F., Silva J.G.S., Lima L.R.O. & Jordao S. (2014). Multi-storey, multi-bay buildings with composite steel-deck floors under human-induced loads: The human comfort issue. *Computers and Structures*, 136, 34-46  
<https://doi.org/10.1016/j.compstruc.2014.01.027>
22. Wright H.D., Evans H.R. & Harding P.W. (1987). The use of profiled steel sheeting in floor construction. *Journal of Constructional Steel Research*, 7(4), 279-295  
[https://doi.org/10.1016/0143-974X\(87\)90003-4](https://doi.org/10.1016/0143-974X(87)90003-4)
23. Mahachi J. & Dundu M. (2012). Prediction of the debonding/slip load of composite deck slabs using fracture mechanics. *Journal of the South African Institution of Civil Engineering*, 54(2), 112-116
24. Abbas H.S., Bakar S.A., Ahmadi M. & Haron Z. (2015). Experimental studies on corrugated steel-concrete composite slab. *Gradevinar*, 67(3), 225-233  
<https://doi.org/10.14256/JCE.1112.2014>
25. Abas F., Bradford M., Foster S. & Gilbert R. Ian (2016). Shear bond behaviour of steel fibre reinforced concrete (SFRC) composite slabs with deep trapezoidal decking: Experimental study. *Composite Construction in Steel and Concrete VII*, 561-580  
<https://doi.org/10.1061/9780784479735.043>
26. Altoubat S., Ousmane H. & Barakat S. (2015). Effect of fibers and welded-wire reinforcements on the diaphragm behavior of composite deck slabs. *Steel and Composite Structures*, 19(1), 153-171  
<http://dx.doi.org/10.12989/scs.2015.19.1.153>
27. Hicks S.J. & Smith A.L. (2014). Stud shear connectors in composite beams that support slabs with profiled steel sheeting. *Structural Engineering International*, 24(2), 246-253  
<https://doi.org/10.2749/101686614X13830790993122>
28. Hechler O., Braun M., Obiala R. et al. (2016). CoSFBC-Composite slim-floor beam: Experimental test campaign and evaluation. *Composite Construction in Steel and Concrete VII*, 158-172  
<https://doi.org/10.1061/9780784479735.013>
29. Peltonen S. & Leskelä M. (2006). Connection behaviour of a concrete dowel in a circular web hole of a steel beam. *Composite Construction in Steel and Concrete V*, 544-552  
[https://doi.org/10.1061/40826\(186\)51](https://doi.org/10.1061/40826(186)51)
30. Huo B.Y. (2012). Experimental and analytical study of the shear transfer in composite shallow cellular floor beams (PhD Thesis). City University London, London



31. Kim Y.J., Oh S.H., Yoon M.H. et al. (2009). Experimental investigation of deck plate system with non-welding truss type deformed steel wires (tox deck plate slab). *International Journal of Steel Structures*, 9(4), 315-327  
<https://doi.org/10.1007/BF03249505>
32. Wang C.M., Zhao X., Wu M. et al. (2013). Application of steel bar truss deck construction technology in a large steel project. *Applied Mechanics and Materials*, 368-370, 851-854  
<https://doi.org/10.4028/www.scientific.net/AMM.368-370.851>
33. Tang R.Q. & Huang Y. (2013). The static study on steel truss concrete slab composite structure. *Journal of Guizhou University (Natural Sciences)*, 5, 23-27
34. Kim I., Kim Y., Oh H. et al. (2016). Behavior of a CFT Truss girder with precast decks under negative bending moment. *Composite Construction in Steel and Concrete VII*, 214-225  
<https://doi.org/10.1061/9780784479735.017>
35. Perera S.V.T.J. (2008). *Shear capacity of composite deck slabs with concrete filled steel tubes* (Ph.D thesis). Muratuwa: University of Moratuwa
36. Perera S.V.T.J. (2013). *A composite floor truss top chord using concrete-filled steel tube (CFST)*. ICSBE-2012: International Conference on Sustainable Built Environment. Access mode: <http://dl.lib.mrt.ac.lk/handle/123/8937>
37. Стороженко Л.І., Нижник О.В., Клецов О.В. та ін. (2013). Експериментальні дослідження плит перекриття зі сталевим обрамленням у порівнянні зі звичайними залізобетонними плитами. *Ресурсоекономічні матеріали, конструкції, будівлі та споруди*, 25, 454-465
38. Абовская С.Н. (1992). *Новые пространственные сталежелезобетонные конструкции покрытия*. Красноярск: Стройиздат
39. Teslya V.A. & Gukin A.S. (2005). Steel and concrete composite slab SRS-15. *Bulletin of the Kuzbass State Technical University*, 3, 117-121
40. Глазунов Ю.В. (2008). Особенности и конструктивные свойства сталебетона. *Коммунальное хозяйство городов*, 85, 198-202
31. Kim Y.J., Oh S.H., Yoon M.H. et al. (2009). Experimental investigation of deck plate system with non-welding truss type deformed steel wires (tox deck plate slab). *International Journal of Steel Structures*, 9(4), 315-327  
<https://doi.org/10.1007/BF03249505>
32. Wang C.M., Zhao X., Wu M. et al. (2013). Application of steel bar truss deck construction technology in a large steel project. *Applied Mechanics and Materials*, 368-370, 851-854  
<https://doi.org/10.4028/www.scientific.net/AMM.368-370.851>
33. Tang R.Q. & Huang Y. (2013). The static study on steel truss concrete slab composite structure. *Journal of Guizhou University (Natural Sciences)*, 5, 23-27
34. Kim I., Kim Y., Oh H. et al. (2016). Behavior of a CFT Truss girder with precast decks under negative bending moment. *Composite Construction in Steel and Concrete VII*, 214-225  
<https://doi.org/10.1061/9780784479735.017>
35. Perera S.V.T.J. (2008). *Shear capacity of composite deck slabs with concrete filled steel tubes* (Ph.D thesis). Muratuwa: University of Moratuwa
36. Perera S.V.T.J. (2013). *A composite floor truss top chord using concrete-filled steel tube (CFST)*. ICSBE-2012: International Conference on Sustainable Built Environment. Access mode: <http://dl.lib.mrt.ac.lk/handle/123/8937>
37. Storozhenko L.I., Nyzhnik O.V., Klestov O.V. et al. (2013). Experimental studies of steel-framed floor slabs compared to conventional reinforced concrete slabs. *Resource-saving materials, constructions, buildings and structures*, 25, 454-465
38. Abovskaya S.N. (1992). *New spatial steel-concrete coating structures*. Krasnoyarsk: Stroyizdat
39. Teslya V.A. & Gukin A.S. (2005). Steel and concrete composite slab SRS-15. *Bulletin of the Kuzbass State Technical University*, 3, 117-121
40. Glazunov Yu.V. (2008). Features and structural properties of steel-concrete structures. *Municipal economy of cities*, 85, 198-202

UDC 624.072.2.016

## Flexural strength of span steel-reinforced concrete truss composite structures

Galinska Tatiana<sup>1\*</sup>, Ovsii Dmytro<sup>2</sup>, Ovsii Oleksandra<sup>3</sup>

<sup>1</sup> National University «Yuri Kondratyuk Poltava Polytechnic» <https://orcid.org/0000-0002-6138-2757>

<sup>2</sup> National University «Yuri Kondratyuk Poltava Polytechnic» <https://orcid.org/0000-0001-7007-1857>

<sup>3</sup> National University «Yuri Kondratyuk Poltava Polytechnic» <https://orcid.org/0000-0001-5833-4757>

\*Corresponding author E-mail: [Galinska@i.ua](mailto:Galinska@i.ua)

The scientific article proposes a method for calculating the bending strength of steel-reinforced concrete (SRC) composite span truss structures. This method allows calculating the flexural strength of the calculated sections of steel-reinforced concrete truss structures, taking into account their stress-strain state at the time of maximum load-bearing capacity or failure. The analysis of experimental and theoretical values of flexural SRC truss beam strength showed their adequate convergence, which allows the application of the calculation method in practice design SRC span truss structures and members.

**Keywords:** steel-reinforced concrete, span, composite, truss structures, flexural strength

## Міцність на згин прогінних сталезалізобетонних фермових композитних конструкцій

Галінська Т.А.<sup>1\*</sup>, Овсій Д.М.<sup>2</sup>, Овсій О.М.<sup>3</sup>

<sup>1,2,3</sup> Національний університет «Полтавська політехніка імені Юрія Кондратюка»

\*Адреса для листування E-mail: [Galinska@i.ua](mailto:Galinska@i.ua)

Наведено загальну методику розрахунку міцності на згин прогінних сталезалізобетонних фермових конструкцій. Дана методика дозволяє на основі екстремального критерія досягнення деформацій зони стиснення бетону величини  $\epsilon_u$  у крайній верхній грані полиці перерізу фермових композитних конструкцій, при якому міцність на згин ( $M_{Rd}$ ) буде максимальною, виконати розподіл випадків напружено-деформованого стану в розрахункових їх перерізах залежно від міцностних властивостей компонентів та їх об'єму (площі бетонної полиці та проценту її армування, площі еквівалентного сталюого елемента). В момент досягнення величини граничної деформації  $\epsilon_u$  відбуватися пластична стадія руйнування бетону полиці (Composite-PSD), при якій міцностні характеристики компонентів сталезалізобетонних фермових конструкцій будуть використовуватися в повному обсязі (випадок а). В той же час, при непропорційному конструктивному вирішенні перерізу сталезалізобетонної фермової конструкції, коли переріз чи міцностні характеристики одного із компонентів прийняті чи запроєктовані з визначеним запасом, руйнування в розрахункових перерізах конструкції може відбуватися на пружно-пластичній стадії (Composite-SC) (випадок с). Межею між пружно-пластичною і пластичною стадіями є випадок б, коли деформації в крайніх гранях розтягнутої і стисненої ділянок перерізу досягають одночасно граничних значень. В роботі викладені аналітичні залежності для послідовного розрахунку міцності на згин перерізів сталезалізобетонних фермових конструкцій з урахуванням їх напружено-деформованого стану в момент максимальної несучої здатності або руйнування. Проведений порівняльний аналіз експериментальних та теоретичних значень міцності на згин 21-ої композитної фермової балкової конструкції, які мали жорсткий зв'язок між своїми компонентами. Зіставлення експериментальних і теоретичних значень міцності на згин сталезалізобетонних фермових балок показало їх адекватну збіжність, що дозволяє застосовувати метод розрахунку на практиці при проєктуванні сталезалізобетонних прогінних композитних фермових конструкцій і елементів.

**Ключові слова:** сталезалізобетон, прогін, складений, фермові конструкції, міцність на згин



## Introduction

Span steel-reinforced concrete (SRC) truss structures of various combined cross-sections are widely used today in the construction of bridges and buildings and structures coverings. Structural solutions of SRC truss structures allow arranging air transport and pedestrian crossings with runs up to  $L=15\dots40$  m and more to  $L=60$  m.

The analysis of constructive decisions of modern truss bridges is carried out in the works of such scientists as: Nussbauera A., Schumachera A. and Hirta Manfreda A. [1, 2]; Daunera H.-G., Oribasi A. and Wery D. [3, 4].

In the work [5], the authors Zhijuan Tian, Yongjian Liu, Lei Jiang, Weiqing Zhu, and Yiping Ma collected 32 typical design cases of composite truss bridges and also summed up the historical results of developments.

The structural solutions analysis of span bridges, are carried out by scientists Mohammad Hossein Taghizadeha and Alaeddin Behraves in the work [6], showed the economic and structural efficiency of truss structures in comparison with traditional beam structures of bridges.

As a result of many years of monitoring the technical condition of bridges in Ukraine, the article authors Bodnar L., Koval P., Stepanov S., Panibratets L. [7] found that in 2019, 35% of bridges had got technical condition 5 (inoperable) and 48% - technical condition 4 (limited serviceability) and required repairing or replacement. Therefore, the main task at the moment is developing and implementing in the construction practice new effective structural solutions of girder truss structures, which are also used in bridge construction.

## Review of the research sources and publications

Scientists Martinez-Munoz D., Marti J. V. and Yepes V., as a result of studying more than 150 scientific works, conducted in work [8] the analysis of a condition and directions of the researches devoted to design and operation structures of steel-reinforced concrete bridges. The distribution of publications by research areas were [8]: design and behaviour - 66%; optimization - 13%; life cycle assessment - 8%; maintenance and repair - 6%; construction process - 5%; multi-criteria decision-making - 2%.

Experimental-theoretical study of the strength and deformability of span steel-reinforced concrete truss structures are devoted to the work of scientists: Reis A. and Pedro J. J. O. [9]; Bujnak J., Michalek P., Baran W. [10]; Luiz Alberto Araujo de Seixas Lea and Eduardo de Miranda Batista [11]; Luo L., Zhang X. [12]; Kuch T.P. [13]; Shkoliar F.S. [14]; Braz J. [15]; Videira O. [16]; Azmi M.H. [17]; Yiyuan Chen, Jucan Dong, Zhaojie Tong, Ruijuan Jiang, Ying Yue [18]; Zhijuan Tian, Yongjian Liu, Lei Jiang, Weiqing Zhu, Yiping Ma [5]; Zhang D., Zhao Q., Li F. & Huang Y. [19, 20].

## Definition of unsolved aspects of the problem

Nowadays, an important issue is the development of methods for calculating the flexural strength of span reinforced concrete truss structures depending on the stress-strain state of their calculated cross-sections at the time of failure.

## Problem statement

The work aims to develop a method for calculating the flexural strength of span steel-reinforced concrete truss structures.

## Basic material and results

*Basic prerequisites for the calculation of the span SRC truss structure.*

To develop a general method for calculating the flexural strength of a span steel-reinforced concrete (SRC) composite truss structure the following prerequisites were adopted:

- in the cross-section of the SRC truss structures, the steel profile has rigid vertical and inclined connections with the concrete slab;
- at the moment of failure, the cross-section of the SRC truss structure can have three cases of the limiting stress-strain state, at which:

case a:  $M_{pIRb}(\epsilon_{cu}, \epsilon_a > \epsilon_{au}) = \max$  – is the plastic stage;

case b:  $M_{Rb}(\epsilon_{cu}, \epsilon_a = \epsilon_{au}) = \max$  – the border between plastic stage and elastic-plastic stage;

case c:  $M_{Rb}(\epsilon_{cu}, \epsilon_a < \epsilon_{au}) = \max$  – elastic-plastic stage;

- the compressive force in the concrete  $N_c$  of the upper flange in the section of the SRC truss structures is determined as for reinforced concrete, taking into account the percentage of its reinforcement, according to the scientific proposals of D. Kochkarev [21] for the dependencies of Eurocode 4 [22];

- analysis of cross-sections SRC truss structures showed that most of their cross-sections can be generalized about the vertical axis to an equivalent I-section, see Fig.1 and Fig.2;

- depending on the position of the neutral line and the nature of fracture determining the bending strength, the main boundary cases of the stress-strain state of the cross-section of truss structures are distinguished, see Fig. 3.

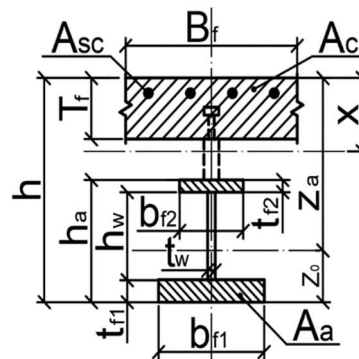
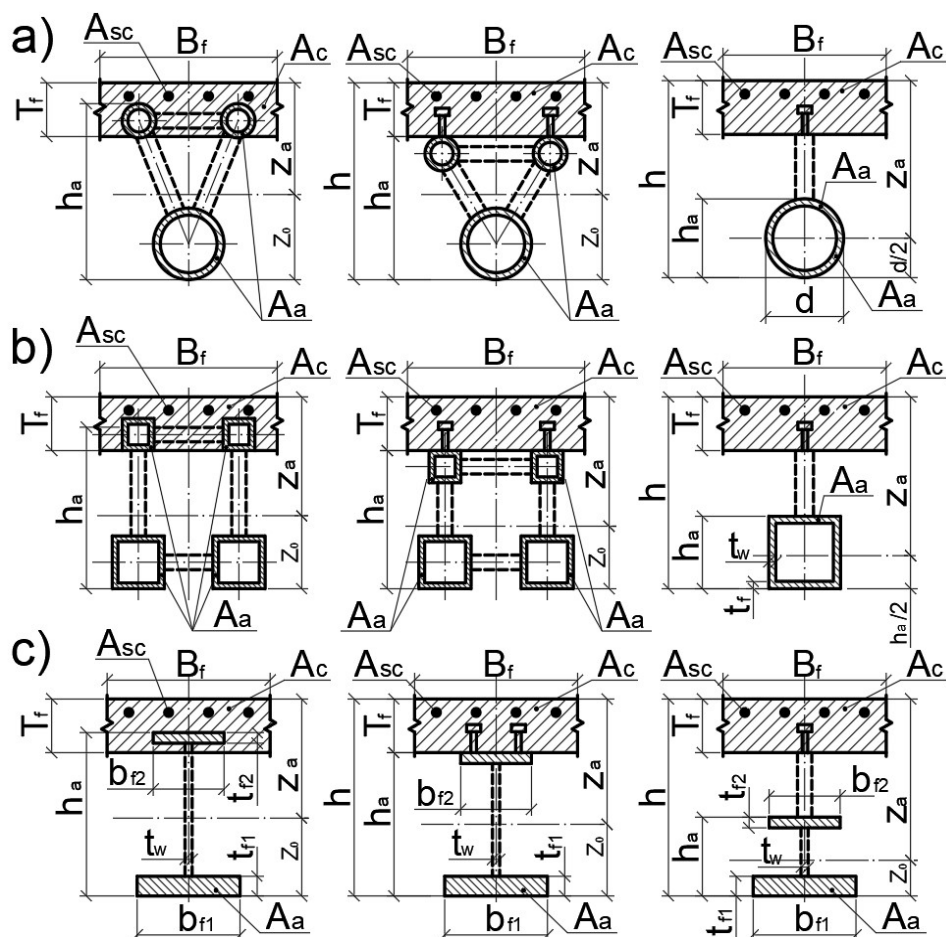


Figure 1 – Equivalent design cross-section of an SRC truss structure along the vertical axis



**Figure 2 – Cross-sections of SRC truss structures:**

- a) V- a similar shape of the section;
- b) II- a similar shape of the section;
- c) Equivalent a shape of the cross-section

The method foundations of calculating steel-reinforced concrete structures were previously laid in the works of the authors [23, 24].

*The sequence of calculation of the bending strength of the span SRC truss structures.*

According to the proposed method of calculating the bending strength, SRC truss structures determine the value of the limiting moment  $M_{Rb}$  and compare it with the external moment  $M$  from the action of the load:  $M_{Rb} \geq M$ .

First, we accept the parameters and cross-sectional dimensions of truss structures and technical characteristics of their components: ( $\varepsilon_{cu}$ ,  $\varepsilon_{au}$ ,  $E_c$ ,  $E_a$ ,  $f_{cd}$ ,  $f_y$ ,  $A_c = B_f T_f$ ,  $A_a = t_{f1} b_{f1} + h_w t_w + t_{f2} b_{f2}$ ,  $h_w = h_a - t_{f1} - t_{f2}$ ).

Determining the dependence ( $\alpha_a \mu$ ) by the formula (1):

$$\alpha_a \mu = E_a A_a / (E_c A_c); \quad (1)$$

Determining values of the internal forces  $N_{cf}$  and  $N_{pla}$ , respectively, by formulas (2) and (3):

$$N_{cf} = 0.85 f_{cd} B_f T_f; \quad (2)$$

$$N_{pla} = A_a f_y; \quad (3)$$

Checking the inequality condition (4):

$$\alpha_a \mu \geq \alpha_a \mu_{opt}; \quad (4)$$

where  $\alpha_a \mu_{opt}$  – coefficient, which is determined by the method given in the works [23, 24], and by the formulas (5), (6), (7), (8):

$$\alpha_a = E_a / E_c; \quad (5)$$

$$\mu_{opt} = \frac{[2\Delta_z \Delta_\varepsilon (1 + \Delta_h) - \Delta_\varepsilon - 1]}{\alpha_a [2\Delta_z (1 + \Delta_h) - \Delta_h (1 + \Delta_\varepsilon)]}; \quad (6)$$

$$\Delta_z = Z_a / (T_f + h_a / 2); \quad (7)$$

$$\Delta_\varepsilon = \varepsilon_{cu} / \varepsilon_{au}, \quad \Delta_h = h_a / T_f; \quad (8)$$

Next, determine the position of the neutral horizontal axis at the height ( $T_f$ ), when  $N_{cf} > N_{pla}$ .

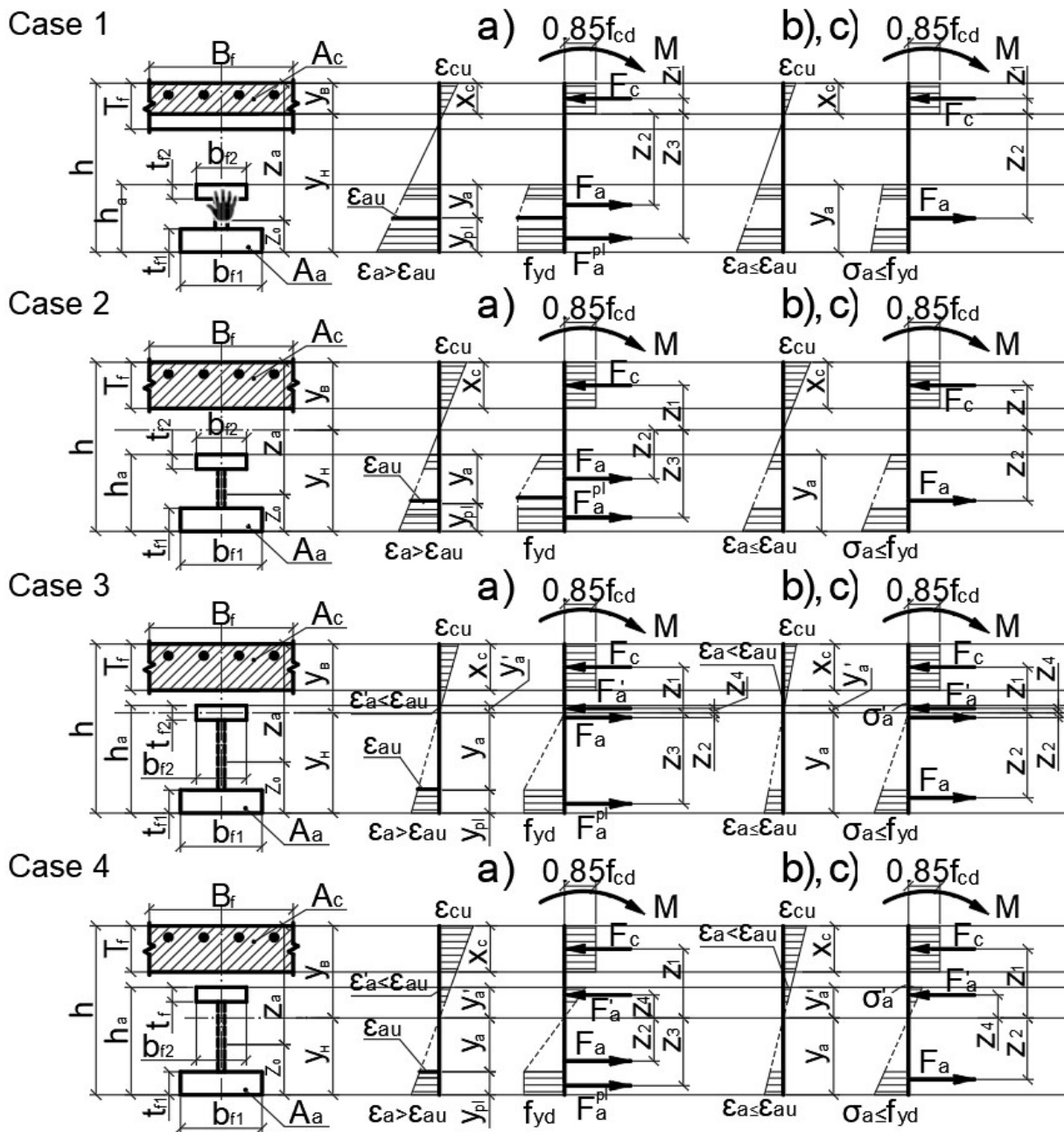


Figure 3– Limiting states of the equivalent section of a steel-reinforced concrete truss structure when determining the bending strength

When  $N_{ef} > N_{pl,a}$ , the neutral horizontal axis of the element is located within the height of the upper concrete shelf  $T_f$ , determining the compressed concrete zone ( $x_c$ ) height and bending moment ( $M_{Rd}$ ) for cross-section SRC truss structures at stress-strain state in cases 1a or 1b, c (Fig. 3).

Checking the conditions (9, 10). If conditions (9, 10) are satisfied, then the limit stress-strain state in the section span SRC truss structures corresponds to case 1a, see Fig.3.

Then, using dependence (11), the height  $x_c$  of the concrete compression zone is determined.

Using dependence (12) is determined the flexural strength  $M_{plRb}$  SRC truss structures.

$$\alpha_a \mu < \alpha_a \mu_{opt}; \quad (9)$$

$$N_{ef} \geq N_{pl,a}; \quad (10)$$

$$x_c = A_a f_y / (0.85 f_c B_f); \quad (11)$$

$$M_{plRb} = 0.5 A_a f_y (z_a - x_c / 2); \quad (12)$$

where:  $z_a$  – distance between the center of mass of the steel equivalent section and the middle of the compression zone section of the reinforced concrete slab.

If condition (9) is met and condition (10) is not met, need to calculate distance from the top edge of the compressive zone of the concrete to the neutral section line  $Y_B$  using the equation (13). If condition (14) is satisfied the SRC truss structure's limit state corresponds to case 2a (Fig. 3). Using dependence (15) is determined the flexural strength  $M_{plRb}$  SRC truss structures.

$$Y_B = A_a f_y / (0.85 f_c B_f) ; \quad (13)$$

$$Y_B \leq h_a - h_a ; \quad (14)$$

$$M_{plRb} = A_a f_y z_a + 0.85 f_c B_f T_f z_c ; \quad (15)$$

where:

$$z_c = Y_B - T_f / 2 . \quad (16)$$

If condition (9) is fulfilled and condition (10) is not fulfilled, then it is necessary to check condition (17). If condition (17) is satisfied, then we have case 3a of the limit state SRC truss structures (see Fig. 3).

The distance from the upper face of the compression zone of concrete to the section neutral line in the second approximation is calculated by the equation (18). The bending strength  $M_{plRb}$  of a section, the truss structures are determined according to equations (19) and (22).

$$h - h_a < Y_B \leq h - h_a + T_f ; \quad (17)$$

where:  $Y_B$  – the distance from the upper face of the compression zone of the concrete shelf to the section neutral line in the first approximation, which is calculated by the equation (13).

$$Y_B = (A_a f_y - 0.85 f_c B_f T_f) / (2 f_y b_f) + h - h_a ; \quad (18)$$

$$M_{plRb1} = A_a f_y z_{a1} - 2 f_a B_f (Y_B + h - h_a) z_{a2} ; \quad (19)$$

where:

$$z_{a1} = 0.5 (2 h - h_a - T_f) ; \quad (20)$$

$$z_{a2} = 0.5 (Y_B - h_a + h - T_f) ; \quad (21)$$

$$M_{plRb2} = 0.85 f_c B_f T_f z_c + 2 f_a B_f (Y_B + h_a) z_{a3} ; \quad (22)$$

where:  $z_c$  – the same as equation (20);

$$z_{a3} = 0.5 (h - Y_B) ; \quad (23)$$

If condition (9) is satisfied and conditions (10, 17) are not fulfilled, then there is a case 4a of the limit state of the SRC truss structures at the time of their failure (see Fig. 3).

The distance from the upper face of the compressed zone of concrete to the section neutral line in the second approximation is determined by the equation (24).

$$Y_B = (A_a f_y - 0.85 f_c B_f T_f - 2 f_y B_f T_f) / (2 f_y f_w) + h - h_a + T_f ; \quad (24)$$

The bending strength  $M_{plRb}$  for SRC truss structures are determined by equations (25) and (27).

$$M_{plRb1} = A_a f_y z_{a1} - 2 f_a B_f z_{a4} - 2 f_a t_w (Y_B + h_a - h - t_f) z_{a5} ; \quad (25)$$

where:  $z_{a4}$  – the same as the equation (20);

$$z_{a5} = 0.5 (Y_B - h_a + h - T_f - t_f) ; \quad (26)$$

$$M_{plRb2} = 0.85 f_c B_f T_f z_c + 2 f_a B_f T_f z_{a6} + 2 f_a t_w (Y_B + h_a - h - t_f) z_{a7} ; \quad (27)$$

where:  $z_c$  – the same as the equation (20);

$z_{a6}$  – the same as equation (23);

$$z_{a7} = 0.5 (h - Y_B - t_f) ; \quad (28)$$

If condition (9) is not satisfied and condition (29) is fulfilled, then the SRC truss structure's limit state corresponds to case 1b, c (see Fig. 3). The height  $x_c$  compression of the concrete zone of the cross-section is calculated by equation (30).

The bending strength  $M_{Rb}$  for SRC truss structures are determined by equations (31) and (32)

$$N_{cf} \geq 0.5 N_{pl a} ; \quad (29)$$

$$x_c = 0.5 A_a f_y / (0.85 f_c B_f) ; \quad (30)$$

at  $\varepsilon_a = \varepsilon_{au}$

$$M_{Rb} = 0.5 A_a f_y (z_{a8} - x_c / 2) ; \quad (31)$$

at  $\varepsilon_a < \varepsilon_{au}$

$$M_{Rb} = 0.5 A_a \sigma_a (z_{a8} - x_c / 2) ; \quad (32)$$

where:

$$\varepsilon_a = (\varepsilon_{cu} (h - x_c) / x_c) ; \quad (33)$$

$$\sigma_a = \varepsilon_a E_a . \quad (34)$$

If conditions (9, 29) are not met, it is necessary to calculate the distance from the upper face of the compressed zone of the concrete shelf to section line neutral  $Y_B$ , using the equation (35).

If condition (6) is satisfied, then there is a stress-strain state of the cross-section of the SRC truss structures in accordance with cases 2b, c (see Fig. 3).

The bending strength  $M_{Rb}$  section the truss structure is determined according to equations (36) and (37).

$$Y_B = 0.5 A_a f_y / (0.85 f_c B_f) ; \quad (35)$$

at  $\varepsilon_a = \varepsilon_{au}$

$$M_{Rb} = 0.5 A_a f_y z_{a9} + 0.85 f_c B_f T_f z_c ; \quad (36)$$

at  $\varepsilon_a < \varepsilon_{au}$

$$M_{Rb} = 0.5 A_a \sigma_a z_{a9} + 0.85 f_c B_f T_f z_c ; \quad (37)$$

where:  $z_c$  – the same as the equation (16);

$$\varepsilon_a = (\varepsilon_{cu} (h - Y_B) / Y_B); \quad (38)$$

$\sigma_a$  – the same as the equation (34);

If condition (9, 29) is not fulfilled, you need to check condition (18). If condition (18) is satisfied, then there is a limit stress-strain state SRC truss structures according to case 3b (see Fig. 3).

The value of the distance  $Y_B$  should be calculated by equation (35)

The distance from the upper face of the compressed zone of the concrete to the neutral line of intersection in the second approximation is calculated by equation (39).

$$Y_B = (0.5 A_a f_y - 0.85 f_c B_f T_f) / (\sigma_{a2}) + h - h_a; \quad (39)$$

where:

$$\varepsilon_{a2} = \varepsilon_{cu} t_f / Y_B; \quad (40)$$

$$\sigma_{a2} = \varepsilon_{a2} E_a \quad (41)$$

Flexural strength  $M_{Rb}$  for SRC truss structures are determined according to equations (42, 45) and (47).

at  $\varepsilon_{a1} = \varepsilon_{au}$

$$M_{Rb1} = 0.5 A_a f_y z_{a10} - \sigma_{a2} b_f (Y_B + h_a - h) z_{a11}; \quad (42)$$

where:

$$z_{a10} = h - h_a / 3 - T_f / 2; \quad (43)$$

$$z_{a11} = Y_B / 3 - T_f / 2 - 2 (h_a - h) / 3; \quad (44)$$

$$M_{Rb2} = 0.85 f_c B_f T_f z_c + \sigma_{a2} b_f (Y_B + h_a - h) z_{a12}; \quad (45)$$

where:  $z_c$  – the same as equation (35);

$$z_{a12} = (h + h_a - Y_B) / 3; \quad (46)$$

at  $\varepsilon_{a1} < \varepsilon_{au}$

$$M_{Rb1} = 0.5 A_a \sigma_{a1} z_{a10} - \sigma_{a2} b_f (Y_B + h - h_a) z_{a11}; \quad (47)$$

where:  $\varepsilon_{a1}$  – the same as equation (38);

$\sigma_{a2}$  – the same as equation (34).

If conditions (1, 29, 35) are not met, then there is a limit stress-strain state SRC truss structures, which corresponds to case 4 b, c (see Fig. 3).

The distance from the upper face of the compressed zone of concrete to section line neutral in the second approximation is determined according to the equation (48).

$$Y_B = (0.5 A_a f_y - 0.85 f_c B_f T_f - \sigma_{a2} b_f t_f) / (\sigma_{a3} t_w) + h - h_a + t_f; \quad (48)$$

where:

$$\varepsilon_{a2} = \varepsilon_{cu} (Y_B + h - h_a) / Y_B; \quad (49)$$

$$\sigma_{a2} = \varepsilon_{a2} E_a; \quad (50)$$

$$\varepsilon_{a3} = \varepsilon_{cu} (Y_B + h_a - h - t_f) / Y_B; \quad (51)$$

$\sigma_{a3}$  – the same as the equation (50);

Flexural strength  $M_{Rb}$  for SRC truss structures are determined according to equations (52, 56) and (60).

at  $\varepsilon_{a1} = \varepsilon_{au}$

$$M_{Rb1} = 0.5 A_a f_y z_{a13} - \sigma_{a2} t_f b_f z_{a14} - \sigma_{a3} t_w (Y_B + h_a - h - t_f) z_{a15}; \quad (52)$$

where:

$$z_{a13} = (2 h + Y_B) / 3 - T_f / 2; \quad (53)$$

$$z_{a14} = h - h_a + t_f / 3 - T_f / 2; \quad (54)$$

$$z_{a15} = (2 (h - h_a) + Y_B) / 3 + t_f - T_f / 2; \quad (55)$$

$$M_{Rb2} = 0.85 f_c B_f T_f z_c + \sigma_{a2} b_f t_f z_{a16} + \sigma_{a3} t_w (Y_B + h_a - h - t_f) z_{a17}; \quad (56)$$

where:  $z_c$  – the same as the equation (53);

$$z_{a16} = h_a - (h + t_f - Y_B) / 3; \quad (57)$$

$$z_{a17} = 2 h_a / 3 - t_f; \quad (58)$$

$$z_{a15} = (2 (h - h_a) + Y_B) / 3 + t_f - T_f / 2; \quad (59)$$

at  $\varepsilon_{a1} < \varepsilon_{au}$

$$M_{Rb1} = 0.5 A_a \sigma_{a1} z_{a13} - \sigma_{a2} b_f t_f z_{a14} - \sigma_{a3} t_w (Y_B + h_a - h - t_f) z_{a15}; \quad (60)$$

where:  $\varepsilon_{a1}$  – the same as the equation (38);

$\sigma_{a1}$  – the same as equation (34).

The calculated flexural strength ( $M_{Rd}$ ) in the calculated cross-section is compared with the magnitude of the bending moment ( $M$ ) from external forces acting on the SRC truss structure.

Bending strength in the SRC sections of the truss structure will be ensured if the requirement (61) is met:

$$M_{Rd} \geq M_{Rb1}. \quad (61)$$

If the bending strength condition (61) of the SRC truss structure sections is not met, then it is necessary to increase the size of their steel equivalent cross-section or take the materials of the components of the composite structure with higher values of strength characteristics and recalculate.

*Comparative analysis of experimental data of tests and theoretical calculations of flexural strength of SRC of truss structures.*

To compare the theoretical developments of the authors with the data of experimental studies of the bending strength of rafter structures, the results of experimental studies of the following scientists were used: Buinak J. et al. [10]; Leal L. et al. [11]; Luo L. et al. [12]; Kuch T.P. [13]; Scientist F.S. [14]; Braz J. [15]; Videira O.P. [16] and Azmi M.H. [17].

To analyze and summarize the results of comparing the theoretical and experimental values of bending strength of truss structures, statistical indicators were determined: arithmetic mean ( $\bar{X}$ ), standard deviation ( $\sigma_{n-1}$ ) and coefficient of variation ( $\nu$ ).

The results of the comparison of experimental tests ( $M^{test}$ ) and analytical calculations of the bending strength of SRC truss structures ( $M^{calc}$ ) are shown in table 1.

The following statistics were obtained by comparing the experimental and theoretical strength values of the

21 SRC truss beams, which had a rigid connection between the components.

With coefficients  $\gamma_c > 1.0$  and  $\gamma_M > 1.0$  that take into account the properties of components with parameters of the indeterminate model and size variations:  $\bar{X} = 1.229$ ;  $\sigma_{n-1} = 0.020$ ;  $\nu = 1.65\%$ .

With coefficients  $\gamma_c = 1.0$  and  $\gamma_M = 1.0$  that take into account the properties of components with parameters of the indeterminate model and size variations:  $\bar{X} = 1.085$ ;  $\sigma_{n-1} = 0.010$ ;  $\nu = 0.88\%$ .

**Table 1 – Comparison of experimental results with theoretical values of bending moments**

Specimen	Author	Year of publication	$M^{test}$ , kNm	$M_{\gamma>1,0}^{calc}$ , kNm	$\frac{M^{test}}{M_{\gamma>1,0}^{calc}}$	$M_{\gamma=1,0}^{calc}$ , kNm	$\frac{M^{test}}{M_{\gamma=1,0}^{calc}}$
-	Leal L.A.A.S.	2020	91,2	95,1	0,96	99,7	0,91
B-1	Luo L.	2019	385,6	300,6	1,28	364,6	1,06
B-2			405,9	300,6	1,35	364,6	1,11
B-3			408,7	300,6	1,36	364,6	1,12
-	Bujnak J.	2018	357,8	243,4	1,47	281,9	1,27
B-1.1	Shkoliar F.	2015	33,0	26,2	1,26	31,8	1,04
B-1.2			32,0	26,2	1,22	31,8	1,01
B-2.1			21,0	15,1	1,39	17,5	1,20
B-2.2			20,0	15,1	1,32	17,5	1,14
B-3.1			30,5	21,2	1,43	25,5	1,19
B-1	Kuch T.	2012	38,5	33,7	1,14	37,0	1,04
B-2-1			27,8	25,5	1,09	27,3	1,02
B-2-2-1			28,3	26,1	1,08	27,8	1,02
B-2-3			29,8	26,5	1,12	28,1	1,06
B-3-1			46,5	38,8	1,20	45,0	1,03
B-3-2-1			50,3	40,6	1,23	46,5	1,09
B-3-3			52,0	41,9	1,24	47,4	1,10
-	Braz J.	2009	352,5	314,7	1,12	338,2	1,04
-	Videira O.P.	2009	517,5	363,6	1,42	388,1	1,33
I	Azmi M.H.	1972	703,9	667,8	1,05	712,9	0,99
VI			526,5	485	1,08	516,0	1,02

## Conclusions

The scientific article proposes a method for calculating the bending strength of steel-reinforced concrete composite span truss structures. This method allows calculating the flexural strength of the calculated sections of steel-reinforced concrete truss structures, taking into account their stress-strain state at the time of maximum load-bearing capacity or failure. The analysis of experimental and theoretical values of flexural strength of SRC truss beams showed their adequate convergence, which allows the application of the calculation method in practice to design SRC span truss structures.



## References

- Schumacher A., Nussbauer A. and Hirt M.A. (2002). Modern Tubular Truss Bridges. *IABSE Symposium Report, January 2002*.  
doi:10.2749/222137802796337332 Source: OAI
- Hirt Manfred A. & Nussbauer Alain (2007). Tubular Trusses for Steel-Concrete Composite Bridges. Presented at: IABSE Symposium: *Improving Infrastructure Worldwide*, Weimar, Germany, 19-21 September 2007, 132-133  
<https://doi.org/10.2749/222137807796119988>
- Dauner H.-G., Oribasi A. & Wery D. (1998). The Lully Viaduct, a composite bridge with steel tube truss. *Journal of Constructional Steel Research*, v. 46, n. 1-3, pp. 67-68.  
[https://doi.org/10.1016/s0143-974x\(98\)00025-x](https://doi.org/10.1016/s0143-974x(98)00025-x)
- Dauner H.-G. (1998). Der Viadukt von Lully - Eine Neuheit im Verbundbrückenbau. *Stahlbau*, 67 (1), 1-14  
<https://doi.org/10.1002/stab.199800010>
- Zhijuan Tian, Yongjian Liu, Lei Jiang, Weiqing Zhu, Yinping Ma (2019). A review on application of composite truss bridges composed of hollow structural section members. *J. Traffic Transp. Eng.*, 6(1), 94-108  
<https://doi.org/10.1016/j.jtte.2018.12.001>
- Taghizadeha M.H. & Behraves A. (2015). Application of Spatial Structures in Bridge Deck. *Civil Engineering Journal*, 1(1)  
[10.28991/cej-2015-00000001](https://doi.org/10.28991/cej-2015-00000001)
- Боднар Л.П., Коваль П.М., Степанов С.М., Панібратець Л.Г. (2019). Експлуатаційний стан мостів України. *Автошляховик України*, 2, 57-67  
[10.33868/0368-8392-2019-2-258-57-68](https://doi.org/10.33868/0368-8392-2019-2-258-57-68)
- Martinez-Munoz D., Marti J.V. & Yepes V. (2020). Steel-Concrete Composite Bridges: Design, Life Cycle Assessment, Maintenance, and Decision-Making. *Advances in Civil Engineering*, 2020, Article ID 8823370  
<https://doi.org/10.1155/2020/8823370>
- Reis A. & Pedro J.J.O. (2011). Composite truss bridges: new trends, design and research. *Steel Construction*, 4(3), 176-182  
<https://doi.org/10.1002/stco.201110024>
- Bujnak J., Michalek P. & Baran W. (2018). Experimental and theoretical investigation of composite truss beams. *MATEC Web of Conferences*, 174, 04001  
<https://doi.org/10.1051/mateconf/201817404001>
- Lea L.A.A.S. and Batista E.M. (2020). Composite floor system with CFS trussed beams, concrete slab and innovative shear connectors. *REM, Int. Eng. J., Ouro Preto*, 73(1), 23-31  
<http://dx.doi.org/10.1590/0370-44672019730049>
- Luo L. & Zhang X. (2019). Flexural Response of Steel-Concrete Composite Truss Beams. *Advances in Civil Engineering*, 1502707  
<https://doi.org/10.1155/2019/1502707>
- Куч Т.П. (2012). *Напружено-деформований стан та несуча здатність сталезалізобетонних балкових конструкцій з винесеним армуванням трубами*. (Автореф. дис. ... канд. техн. наук). Полтавський національний технічний університет імені Юрія Кондратюка, Полтава
- Школяр Ф.С. (2015). *Напружено-деформований стан та несуча здатність залізобетонних балок з винесеним робочим армуванням*. (Автореф. дис. ... канд. техн. наук). Полтавський національний технічний університет імені Юрія Кондратюка, Полтава
- Braz J. (2009) Composite Truss Bridge Decks. (Master's thesis). Technical University of Lisbon, Lisbon
- Videira O. (2009). Composite Truss Bridge Decks. (Master's thesis). Technical University of Lisbon, Lisbon
- Schumacher A., Nussbauer A. and Hirt M.A. (2002). Modern Tubular Truss Bridges. *IABSE Symposium Report, January 2002*.  
doi:10.2749/222137802796337332 Source: OAI
- Hirt Manfred A. and Nussbauer Alain (2007). Tubular Trusses for Steel-Concrete Composite Bridges. Presented at: IABSE Symposium: *Improving Infrastructure Worldwide*, Weimar, Germany, 19-21 September 2007, 132-133  
<https://doi.org/10.2749/222137807796119988>
- Dauner H.-G., Oribasi A. & Wery D. (1998). The Lully Viaduct, a composite bridge with steel tube truss. *Journal of Constructional Steel Research*, v. 46, n. 1-3, pp. 67-68.  
[https://doi.org/10.1016/s0143-974x\(98\)00025-x](https://doi.org/10.1016/s0143-974x(98)00025-x)
- Dauner H.-G. (1998). Der Viadukt von Lully - Eine Neuheit im Verbundbrückenbau. *Stahlbau*, 67 (1), 1-14  
<https://doi.org/10.1002/stab.199800010>
- Zhijuan Tian, Yongjian Liu, Lei Jiang, Weiqing Zhu, Yinping Ma (2019). A review on application of composite truss bridges composed of hollow structural section members. *J. Traffic Transp. Eng.*, 6(1), 94-108  
<https://doi.org/10.1016/j.jtte.2018.12.001>
- Taghizadeha M.H. & Behraves A. (2015). Application of Spatial Structures in Bridge Deck. *Civil Engineering Journal*, 1(1)  
[10.28991/cej-2015-00000001](https://doi.org/10.28991/cej-2015-00000001)
- Bodnar L., Koval P., Stepanov S., Panibratets L. (2019). Operational state of bridges of Ukraine. *Highwayman of Ukraine*, 2, 57-67  
[10.33868/0368-8392-2019-2-258-57-68](https://doi.org/10.33868/0368-8392-2019-2-258-57-68)
- Martinez-Munoz D., Marti J.V. & Yepes V. (2020). Steel-Concrete Composite Bridges: Design, Life Cycle Assessment, Maintenance, and Decision-Making. *Advances in Civil Engineering*, 2020, Article ID 8823370  
<https://doi.org/10.1155/2020/8823370>
- Reis A. & Pedro J.J.O. (2011). Composite truss bridges: new trends, design and research. *Steel Construction*, 4(3), 176-182  
<https://doi.org/10.1002/stco.201110024>
- Bujnak J., Michalek P. & Baran W. (2018). Experimental and theoretical investigation of composite truss beams. *MATEC Web of Conferences*, 174, 04001  
<https://doi.org/10.1051/mateconf/201817404001>
- Lea L.A.A.S. and Batista E.M. (2020). Composite floor system with CFS trussed beams, concrete slab and innovative shear connectors. *REM, Int. Eng. J., Ouro Preto*, 73(1), 23-31  
<http://dx.doi.org/10.1590/0370-44672019730049>
- Luo L. & Zhang X. (2019). Flexural Response of Steel-Concrete Composite Truss Beams. *Advances in Civil Engineering*, 1502707  
<https://doi.org/10.1155/2019/1502707>
- Kuch T.P. (2012). *Stress-strain state and load-bearing capacity of reinforced concrete beam structures with exposed pipe reinforcement*. (Extended abstract of PhD dissertation). Poltava National Technical Yuri Kondratyuk University, Poltava
- Shkoliar F.S. (2015). *Tensely-deformed state and bearing capacity of reinforced concrete beams with remote working reinforcement*. (Extended abstract of PhD dissertation). Poltava National Technical Yuri Kondratyuk University, Poltava
- Braz J. (2009) Composite Truss Bridge Decks. (Master's thesis). Technical University of Lisbon, Lisbon
- Videira O. (2009). Composite Truss Bridge Decks. (Master's thesis). Technical University of Lisbon, Lisbon

17. Azmi M H. (1972). Composite open-web trusses with metal cellular floor. (Master's thesis). Mc Master University, Hamilton

18. Chen Y., Dong J., Tong Jucan., Jiang R. & Yue Y. (2020). Flexural behavior of composite box girders with corrugated steel webs and trusses. *Engineering Structures*, 209(2020), 110275

<https://doi.org/10.1016/j.engstruct.2020.110275>

19. Zhang D., Zhao Q., Li F., & Huang Y. (2017). Experimental and numerical study of the torsional response of a modular hybrid FRP-aluminum triangular deck-truss beam. *Engineering Structures*, 133, 172-185

<https://doi.org/10.1016/j.engstruct.2016.12.007>

20. Zhang, D., Zhao, Q., Huang, Y., & Li, F. et al. (2013). Flexural properties of a lightweight hybrid FRP-aluminum modular space truss bridge system. *Composite Structures* 108 (2014) 600-615

[10.1016/j.compstruct.2013.09.058](https://doi.org/10.1016/j.compstruct.2013.09.058)

21. Kochkarev D., Galinska T. (2017) Calculation methodology of reinforced concrete elements based on calculated resistance of reinforced concrete. *MATEC Web of Conferences 116*, 02020, 1-9

[10.1051/mateconf/201711602020](https://doi.org/10.1051/mateconf/201711602020)

22. Comité Européen de Normalisation (CEN), (2004b) "Eurocode 4: Design of Composite Steel and Concrete Structures-Part 1-1: General Rules and Rules for Buildings", European Standard BS EN 1994-1-1:1994. European Committee for Standardization (CEN), Brussels, Belgium

23. Galinska T., Ovsii D., Ovsii M. (2018). The combining technique of calculating the sections of reinforced concrete bending elements normal to its longitudinal axis, based on the deformation model. *International Journal of Engineering & Technology (UAE)*, 7(3.2), 123-127

[10.14419/ijet.v7i3.2.14387](https://doi.org/10.14419/ijet.v7i3.2.14387)

24. Galinska T.A., Murav'ov V.V., Ovsii N.A. (2014). Methodical bases of calculation of strength the normal cross section of reinforced concrete beams with concrete upper belt and external reinforcement, *17th Conference for Junior Researchers 'Science-Future of Lithuania. Transport Engineering and Management', Vilnius 2014*. Retrieved from

<http://jmk.transportas.old.vgtu.lt/index.php/conference/2014/paper/viewFile/352/352-1357-1-PB.pdf>

17. Azmi M H. (1972). Composite open-web trusses with metal cellular floor. (Master's thesis). Mc Master University, Hamilton

18. Chen Y., Dong J., Tong Jucan., Jiang R. & Yue Y. (2020). Flexural behavior of composite box girders with corrugated steel webs and trusses. *Engineering Structures*, 209(2020), 110275

<https://doi.org/10.1016/j.engstruct.2020.110275>

19. Zhang D., Zhao Q., Li F., & Huang Y. (2017). Experimental and numerical study of the torsional response of a modular hybrid FRP-aluminum triangular deck-truss beam. *Engineering Structures*, 133, 172-185

<https://doi.org/10.1016/j.engstruct.2016.12.007>

20. Zhang, D., Zhao, Q., Huang, Y., & Li, F. et al. (2013). Flexural properties of a lightweight hybrid FRP-aluminum modular space truss bridge system. *Composite Structures* 108 (2014) 600-615

[10.1016/j.compstruct.2013.09.058](https://doi.org/10.1016/j.compstruct.2013.09.058)

21. Kochkarev D., Galinska T. (2017) Calculation methodology of reinforced concrete elements based on calculated resistance of reinforced concrete. *MATEC Web of Conferences 116*, 02020, 1-9

[10.1051/mateconf/201711602020](https://doi.org/10.1051/mateconf/201711602020)

22. Comité Européen de Normalisation (CEN), (2004b) "Eurocode 4: Design of Composite Steel and Concrete Structures-Part 1-1: General Rules and Rules for Buildings", European Standard BS EN 1994-1-1:1994. European Committee for Standardization (CEN), Brussels, Belgium

23. Galinska T., Ovsii D., Ovsii M. (2018). The combining technique of calculating the sections of reinforced concrete bending elements normal to its longitudinal axis, based on the deformation model. *International Journal of Engineering & Technology (UAE)*, 7(3.2), 123-127

[10.14419/ijet.v7i3.2.14387](https://doi.org/10.14419/ijet.v7i3.2.14387)

24. Galinska T.A., Murav'ov V.V., Ovsii N.A. (2014). Methodical bases of calculation of strength the normal cross section of reinforced concrete beams with concrete upper belt and external reinforcement, *17th Conference for Junior Researchers 'Science-Future of Lithuania. Transport Engineering and Management', Vilnius 2014*. Retrieved from

<http://jmk.transportas.old.vgtu.lt/index.php/conference/2014/paper/viewFile/352/352-1357-1-PB.pdf>

UDK 624.074.5, 69.07

## Stress-strain state of space grid structure

Sribniak Nataliia<sup>1\*</sup>, Tsyhanenko Liudmyla<sup>2</sup>, Tsyhanenko Hennadii<sup>3</sup>, Halushka Serhii<sup>4</sup>

<sup>1</sup>Sumy National Agrarian University <https://orcid.org/0000-0003-3205-433X>

<sup>2</sup>Sumy National Agrarian University <https://orcid.org/0000-0002-6628-3635>

<sup>3</sup>Sumy National Agrarian University <https://orcid.org/0000-0002-3335-4804>

<sup>4</sup>Sumy National Agrarian University <https://orcid.org/0000-0001-8643-6937>

\*Corresponding author E-mail: [nataliia.sribniak@snau.edu.ua](mailto:nataliia.sribniak@snau.edu.ua)

One of the factors influencing the stress-strain state of the structure is the placement method of the columns and their step. The problem formulated in the article is to determine the design solution of the space grid structure with the least weight. The paper examines how the columns location, the number of support points, and the supports step affect the force values in the space grid structure rods and the supports (columns). The first variant of the model adopted a space grid structure supported in the corners of four columns. The second variant of the model adopted a space grid structure supported on two sides – six columns on each side. In the third variant, the structure is supported by 20 columns along the perimeter. It has been determined that the third method of supporting location is the most efficient.

**Keywords:** material capacity, optimization, space grid structure, stress-strain state regulation, tension regulator

## Напружено-деформований стан структурної плити

Срібняк Н.М.<sup>1\*</sup>, Циганенко Л.А.<sup>2</sup>, Циганенко Г.М.<sup>3</sup>, Галушка С.А.<sup>4</sup>

<sup>1</sup>Сумський національний аграрний університет

<sup>2</sup>Сумський національний аграрний університет

<sup>3</sup>Сумський національний аграрний університет

<sup>4</sup>Сумський національний аграрний університет

\*Адреса для листування E-mail: [nataliia.sribniak@snau.edu.ua](mailto:nataliia.sribniak@snau.edu.ua)

Структурні плити – це просторові стержньові конструкції. Форма структурної одиниці плити є подібною до форми природних кристалів, тому, очевидно, є ефективною та заслуговує на дослідження. Структура складається із просторових елементів за формою піраміди, що повторюються багаторазово. Структурні плити широко застосовуються для перекриття одноповерхових споруд і мають велике різноманіття конструктивних і архітектурних форм. Структурна конструкція є багато разів статично невизначуваною конструкцією. Одним із чинників, що впливають на напружено-деформований стан конструкції, є розташування колон. Схема, крок розташування колон, їх кількість впливають на величини зусиль в стержнях структури. Задача, що формулюється в статті, полягає у визначенні конструктивного вирішення структурної плити з найменшою вагою серед декількох конструктивних варіантів плит, що відрізняються різною кількістю опор, але мають однакові розміри в плані. В роботі досліджено, як саме розташування колон, кількість точок спирання та крок опор впливають на величини зусиль в усіх елементах структурної плити та в самих опорах (колонах). Базова структурна плита по верхньому поясу має розміри в плані 30×30 м. На базі цієї плити створено три розрахункові моделі, які відрізняються кроком колон та їх кількістю. При першому варіанті моделі прийняте спирання плити в кутах на чотири колони. Крок колон прийнято 27 м. При другому варіанті прийняте спирання плити по двом сторонам – на шість колон з кожного боку. Відстань між колонами 6 м. При третьому варіанті спирання структурна плита спирається на 20 колон по периметру, що розташовані з кроком 6 м. У висновках проаналізовано результати статичного розрахунку моделей структурної плити покриття з різним способом розташування опор. Визначено, що за критерієм металомісткості для розглянутих проектних рішень найбільш ефективний третій варіант розташування колон.

**Ключові слова:** структурна плита, регулювання НДС, структура, металоємність, оптимізація, регулятор напружень



## Introduction

In the world construction practice, many unique and unusual constructions of public and industrial function have been created. The load-bearing structures are considered separately for each of the structures

Metal space grid roof structures are widely used. These roof systems are distinguished not only by original architectural forms but also by progressive design solutions. Pipe profiles occupy a special place in the design of large-role roofs. They have an efficient cross-section of the rod and perceive axial forces. [1, 2].

Structural slabs (structures) are spatial rod structures [1] similar in structure with crystalline metal grates [3, 4].

They are characterised by many positive properties: multiple connections, versatility, the possibility of production on high-performance production lines, simplicity of transportation [5]. The structure consists of spatial elements in the shape of a pyramid which is repeated many a time and oft [8]. Multiple connections cause a number of advantages of structural designs in comparison with traditional structures, which are made up of roof trusses, secondary trusses, girders [8].

As noted in [1], the structures can be used as a roof structure for large buildings in the plan [6]. Internal forces in space grid structures, therefore, cross-section and weight of the structural elements, largely depends on the accepted design parameters. Finding the most effective design solution for the structural plate is one of the tasks to be solved in the initial stages of design [7]. The option that is chosen directly affects the further labor intensity of manufacture, installation, and, ultimately, the cost of the structure.

## Review of research sources and publications

Spatial structures are three-dimensional systems consisting of linear members, subjected to loads at their joints or along their length, and connected to each other using pin or moment connections. These structures can take various forms such as flat-double-layer grid (FDLG) or flat-multi-layer grid, braced barrel vault, or dome, or any other form (free-form). The decision to use rod systems as a roof structure is primarily associated with obtaining the most effective design solution for the space grid structure. The criterion for this decision may be material capacity. The choice of the orientation of the structural structure relative to the support contour directly affects the economic performance of the structure. For example, the internal forces in the chord of the structure are obtained by 27% less in the diagonal orientation of the structure relative to the square support contour than in the orientation of the structure parallel to the support contour. The maximum roof displacement is 4 times less than the displacement of the conventional trusses roofs [12]. In [12] it is indicated that the support of space grid structures with chord grids of triangular lattice on four or more nodes causes static indeterminate of the structure. In such a system, a change in the ratio of the rigidity of the rod causes a significant redistribution of internal forces in the rods. At the same time, there is no significant redistribution of internal forces in the statically determinate

structure (when the lower triangular grid is supported by three nodes and the quadrangular grid by four nodes)

In addition, in order to obtain a structure with minimum weight, the regulation of the stress-strain state can be carried out by varying many parameters.

Such parameters that can change are: the class of steel rod elements of the plate, the choice of the orientation of the space grid structures relative to the support contour, different types of chord grid (triangular, rectangular, rotated relative to each other by 45° chord grids from square grids); number of columns and their location (in the corners, on the sides of the plate, on the perimeter of the plate) [12], methods of connecting the rods of the structure. So, the criteria and factors influencing the change of internal forces in rods of structure and on: internal force value are many enough. Separately, each of the factors needs research and analysis, because such a criterion of design efficiency as metal capacity is the most important criterion in the first stage of finding the optimal design. The second criterion of efficiency is the labour content of the erection of the structure.

## The objective of the work and research methods

*The aim of the work* is to determine the least material capacity model of a spatial grid structure. Three options for the location of the support columns are accepted for stress regulators. The scheme, the interval of columns, the number of columns influence the force values in the rods of the structure.

*Objectives* that were formulated to achieve this goal:

- the creation of finite element models of space grid structures in the Lira-SAPR software for studying their structural behavior when changing the layout of columns and their number;
- selection of the cross-sections of the structural elements of the space grid structures models based on the results of static analysis;
- calculating the weights of each model of the space grid structure and determining the space grid structure model with the lowest weight. At the same time, the sufficient manufacturability of the model remains.

The *object* of the research is the space grid structure (structural rod plates of the roof) with chord grids of square lattices having a different number of supports.

The *subject* of the research is the stress-strain state of the structural rod plates of the roof with chord grids of square lattices, which have a different number of supports and their interval.

The *research method* is the method of computer modeling of structures using software systems that implement the finite element method (SP LIRA-SAPR).

The research *results* make it possible to determine the most effective of several possible space grid structures of the roof according to the criterion of effective material consumption, that is, according to the criterion of the lowest weight of the structure.

### Basic material and results

As indicated in the study [4], there are 20 main types of rod plates of interest for the practice of designing structural roof slabs (space grid structures).

Among this set, one can single out a system of the type of inclined cross trusses of two directions [9].

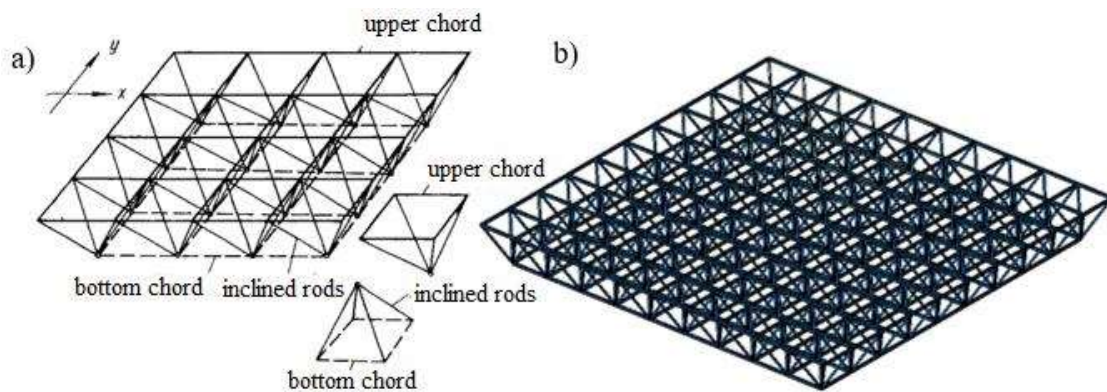
A structural slab (Fig. 1–2) with dimensions in the plan of  $30.0 \times 30.0$  m, having an orthogonal grid of chords with a cell of  $3.0 \times 3.0$  m and a height along the axes of the chords 3.0 m.

The structural plate (Fig.1–2) with a plan size of  $30.0 \times 30.0$  m, with an orthogonal grid of chords with a cell of  $3.0 \times 3.0$  m and chords height of 3.0 m is taken as the structure to be researched. Thus, the height of the structure is 1/10 of the span, which is the optimal height for simply supported structural plates [13]. The nodes of the upper and bottom chords are connected by diagonal rod elements.

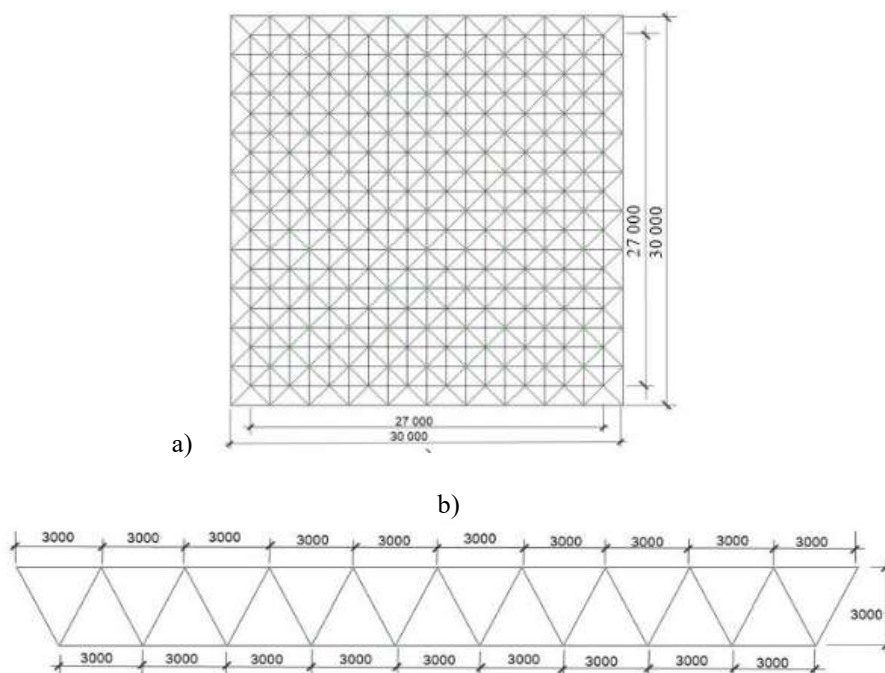
The crystals of the structural plate have the shape of a pyramid with a square base. The columns are 6,0 m high. The structural plate is supported on the columns along with the lower chords. The plate dimensions in the plan, the active load, the crystal type are taken as parameters, do not change.

The restrictions are the strength condition for the tensioned rods, the stability condition for the compressed rods, the limit slenderness and the limit deflection of the structure [14]. There are no intermediate supports in the structure (Fig. 2). The combination of all elements made in a hinged way, intersections of all elements – pipes electro-welded straight-seam according to GOST 10704-91.

The rod system on the square plan works in two directions and belongs to the most perfect types of space grid structures.



**Figure 1 – The system of the type of inclined cross trusses in two directions and with chord grids of square lattices is used to model the structural plate (a); the spatial model of the structural plate is researched investigated (b)**



**Figure 2 – Geometric scheme of the space grid structure: top view (plane XOY) (a); side view (plane XOZ or YOZ) (b)**

There are no monitors and level differences in the building. To ensure the removal of atmospheric precipitation, as a rule, the space grid structure is made with a two-sided slope.

However, this design feature is neglected in this static analysis.

When a square space is overlapped, the space grid structure makes full use of its load-carrying capacity. It is the square form exactly, not the rectangular form, that is, the ratio of sides 1:1 determines its work in two directions. Data is given that with the height-to-width aspect ratio of 1:0.8, the space grid structure begins to work in only one direction and the difference in forces in the elements along and across the span is 2,25 times [15].

The greater the difference in the height-to-width aspect ratio of the structure, the greater will be the uneven distribution of forces in its elements in two mutually perpendicular directions [8]. Thus, we will assume that in a structural plate with the height-to-width aspect ratio of 1: 1, the forces in its elements will be equal.

The number of columns and the method of their location on the plan will be taken as regulators of forces in the rods of the structure (Fig. 3). In model No.1, the distance between the columns is 27,0 m and the number of columns in the model is 4. In model No.2, the distance between the columns is 6,0 m and the number of columns in the model is 12. In model No. 3, the distance between the columns is 6,0 m, the number of columns in the model is 20.

The spatial model consisting of the space grid structure (plate) and columns was created for the static analysis. All elements of the structural plate were defined by the rods of a spatial truss with three statistical degrees of freedom: X, Y, Z, columns – spatial universal rods (FE No.10) with six statistical degrees of freedom: X, Y, Z, U<sub>x</sub>, U<sub>y</sub>, U<sub>z</sub>.

Analytical models according to fig. 3 are shown in fig. 4.

All rods of a structural plate are accepted from common steel, made from hot-rolled pipe profiles. Accepted steel class C245 [16] with the following characteristics:  $R_y = 24,0 \text{ kN/cm}^2$ ,  $R_{ym} = 24,5 \text{ kN/cm}^2$ ,  $E = 2,06 \cdot 10^8 \text{ kN/cm}^2$ ,  $\gamma = 77,0085 \text{ kN/m}^3$ ,  $\mu = 0,3$ .

The rods of the upper chord and bottom chord of the structural plate is made from hot-rolled pipe profile 242×32 mm, the inclined rods are made from hot-rolled pipe profile 168×25 mm. The columns have 6,0 m length and are made from a hot-rolled pipe profile 273×40 mm.

Construction loads are constant – roof load (from the steel sheets and the girders), the dead load of the structure, which was automatically set in the SP Lira-SAPR.

The live load is the snow load (characteristic for Sumy) is 1,64 kN / m<sup>2</sup>. Since the slope of the upper chord of the structure is  $\alpha < 30^\circ$ , a uniform distribution of the snow cover over the entire roof is assumed [1].

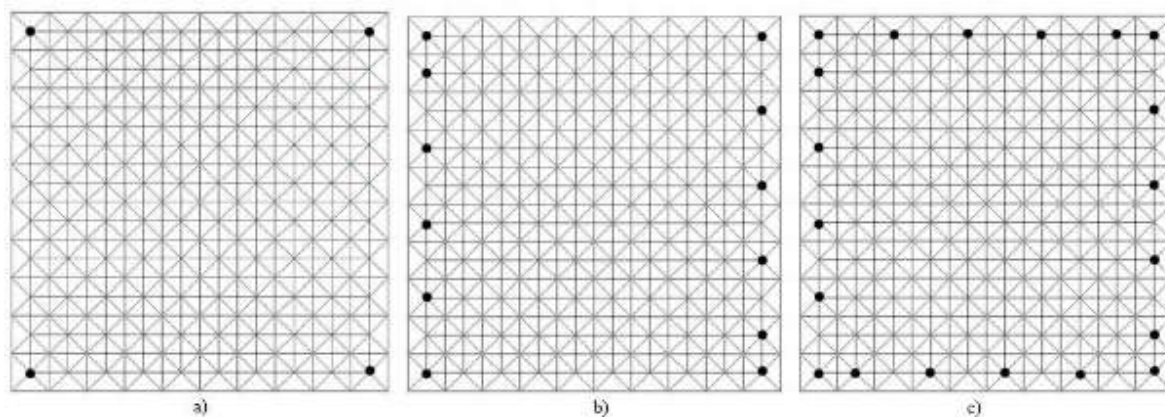
The steel sheets are based on the girders. Girders are attached to the upper chord of the space grid structure. Thus, in the analytical models, a point load from the steel sheet and snow was applied to the nodes of the upper chord of the space grid structure (Fig. 5).

All rods of a structural plate are accepted from common steel, made from hot-rolled pipe profiles. Accepted steel class C245 [16] with the following characteristics:  $R_y = 24,0 \text{ kN / cm}^2$ ,  $R_{ym} = 24,5 \text{ kN/cm}^2$ ,  $E = 2,06 \cdot 10^8 \text{ kN/cm}^2$ ,  $\gamma = 77,0085 \text{ kN/m}^3$ ,  $\mu = 0,3$ .

The rods of the upper chord and bottom chord of the structural plate is made from hot-rolled pipe profile 242 × 32 mm, the inclined rods are made from hot-rolled pipe profile 168 × 25 mm. The columns have 6,0 m length and are made from a hot-rolled pipe profile 273 × 40 mm. Construction loads are constant – roof load (from the steel sheets and the girders), the dead load of the structure, which was automatically set in the SP Lira-SAPR.

The live load is the snow load (characteristic for Sumy) is 1,64 kN/m<sup>2</sup>. Since the slope of the upper chord of the structure is  $\alpha < 30^\circ$ , a uniform distribution of the snow cover over the entire roof is assumed [1].

The steel sheets are based on the girders. Girders are attached to the upper chord of the space grid structure. Thus, in the analytical models, a point load from the steel sheet and snow was applied to the nodes of the upper chord of the space grid structure (Fig. 5).



**Figure 3 – Analytical model of location column:**

a – model No.1 (in four corners of the bottom chord), b – model No.2 (on both sides of the bottom chord), c – model No.3 (on four sides of the bottom chord with a step of 6,0 m)

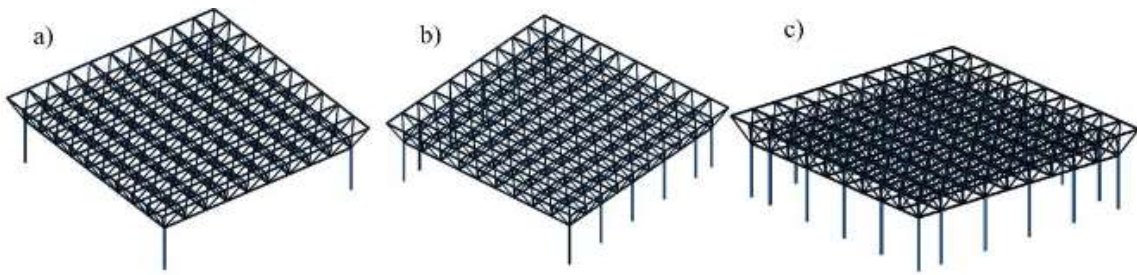


Figure 4 – Spatial analytical models of the space grid structure that are being researched: analytical model No.1 (a); analytical model No.2 (b); analytical model No.3 (c)

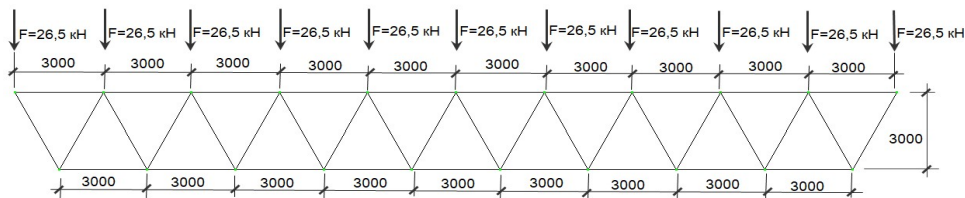


Figure 5 – The application scheme of nodal load on the space grid structure

The results of the numerical research of space grid structure

The static analysis was conducted to determine the stress-strain state of the whole structure. The selection of the cross section of tensioned elements was carried out based on strength analysis, compressed elements were carried out based on strength and durability analysis. The static analysis also took into account the limited slenderness of the elements and vertical linear displacements of the whole structure. Structure designed by the elastic method of analysis [1].

The upper chord rods are under the influence of the axial compression forces and the bottom chord rods are under the influence of the axial tension forces.

The axial force  $N$  in the inclined rods has an alternating value, so the rods are in both tension and compression. Fig. 6 shows the simple bar charts of the maximum forces in the rods of the structures.

Thus, the charts in Fig. 6 show that the forces in all chord systems and inclined rods decrease, but at this time there is an increasing number of structural supports. There are forces uniform in value in the rods of the chord systems.

Thus, the maximum compression forces in analytical model No.2 decreased in comparison with these forces in analytical model No.1 by 1,71 times, and the maximum compression forces in analytical model No. 3 decreased in comparison with these forces in analytical model No.1 by 3,12 times. The maximum tensile forces in analytical model No.2 decreased in comparison with these forces in analytical model No.1 by 1,85 times, and the maximum tensile forces in analytical model No.3 decreased in comparison with these forces in analytical model No.1 by 4,16 times. The maximum compression forces in the inclined rod in analytical model No.2 decreased in comparison to these forces in analytical model No.1 by 2,53 times, and the maximum compression forces in analytical model No.3 decreased in comparison to these forces in analytical model No.1 by 3,97 times.

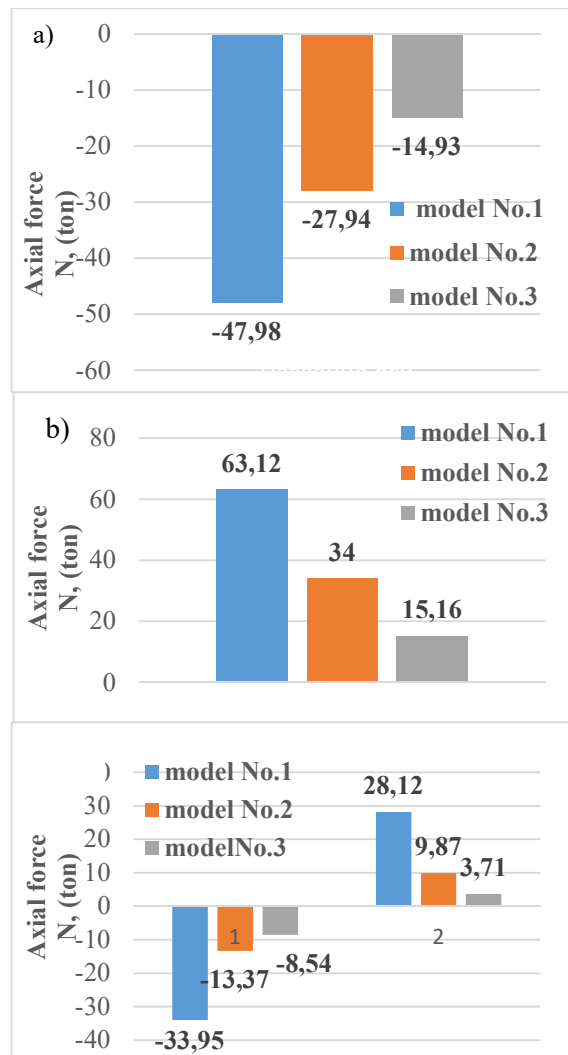


Figure 6 – Maximum forces «N» in the rods of the structures: axial forces in the rods of the upper chord (a); axial forces in the rods of the bottom chord (b); axial forces in the inclined rods (c)

The maximal tensile forces in model No.2 are 2,84 times less than those in model No.1 and the maximal tensile forces in model No.3 are 7,57 times less than those in model No.1. Fig. 7–8 shows the bar charts of forces in the columns.

Maximum compression forces in columns in analytical model No.2 are 2,7 times less than in analytical model No.1 and maximum compression forces in columns in analytical model No.3 are 3,77 times less than in analytical model No.1. The bending moments in columns also decrease with the increase of the support points for the space grid structure.

It should be noted that the forces in analytical models No.2 and No.3 (both in the structure rods and in the columns) decrease in comparison with the forces in the most stressful analytical model (analytical model No.1) by approximately the same value. Fig. 9 shows charts of vertical load deflections at the nodes of the structure in its cross-section.

For example, Fig. 9 shows that the least rigidity will be a structure in analytical model No.1, supported by four columns in the corners. The most rigid scheme will be analytical model No.3 – with the support of the structural plate around the perimeter. The general view of the deformed analytical models is given in Fig. 10.

The deformability of all models is within acceptable limits [17], and the maximum actual deflection for all analytical models does not exceed the maximum allowable value of 90 mm.

$$f_u = l / 300 = 27000 / 300 = 90 \text{ mm}$$

#### Cross-section analysis of structural rods

Strength analysis of steel elements with characteristic strength  $R_{yn} \leq 440 \text{ N/mm}^2$  with axial tension and compression, it should be performed according to the formula (1.4.1) [16]:

$$N / A_n \cdot R_y \cdot \gamma_c \leq 1 \quad (1)$$

Stability analysis of the elements under axial compression should be calculated by the formula (1.4.3) [16]:

$$N / \varphi \cdot A_n \cdot R_y \cdot \gamma_c \leq 1 \quad (2)$$

Thus, the required cross-section area with axial tensile strength:

$$A_n = N / R_y \cdot \gamma_c \quad (3)$$

Thus, the required cross-section area with axial compressive strength:

$$A_n = N / \varphi \cdot R_y \cdot \gamma_c \quad (4)$$

Tables 1 and 2 show the maximum axial forces occurring in the rods of the structure and the columns. Based on these data, we will find the necessary cross-sectional area of the rods according to the strength (1) and stability (2) conditions for a compressed rod.

The cross-sectional area of the rod required with the strength condition is calculated according to (3) and (4) and written in tables 1–4. We will also select a pipe profile according to the schedule of pipes (GOST 8639-82), calculate its weight and the total weight of the upper chord, bottom chord, inclined rods and columns.

Fig. 11 shows the ratio of the space grid structures and the weight of the columns.

As the number of supports increases, the weight of the roof plate decreases, and the weight of the columns increases (Fig. 12).

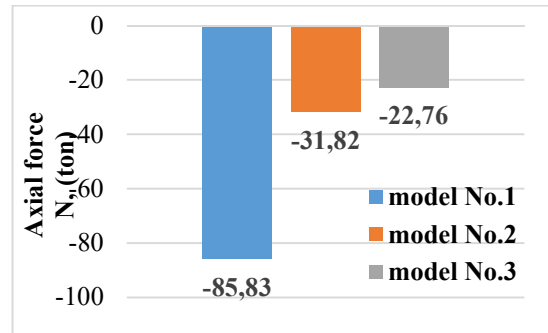


Figure 7 – Internal maximum forces "N" in the columns

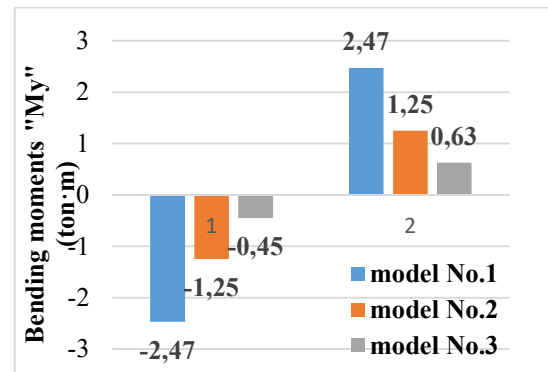


Figure 8 – Maximum bending moments "My" in columns

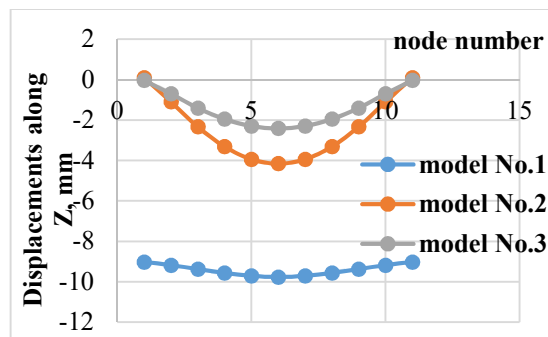


Figure 9 – Charts of the nodes vertical deflections of the structure in its cross-section



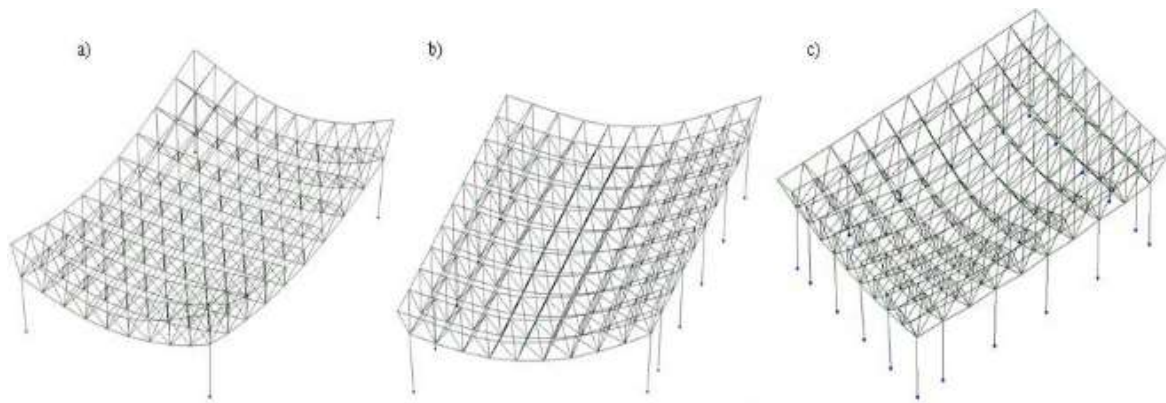


Figure 10 – Deformed structure: analytical model No. 1 (a); analytical model No. 2 (b); analytical model No. 3 (c)

Table 1 – Upper Chord Weight Count

Model №	Maximum forces N, kN	Cross-sectional area A, sm <sup>2</sup>	Pipe profile	Pipe profile, A, sm <sup>2</sup>	Weight of 1 r.mprofile, kg	Weight of 1 r.mprofile, ton	Chord-length, m	Weight, ton
1	470,68	19,61	80×7	19,6	15,38	0,01538	660	<b>10,15</b>
2	274,09	11,42	80×4	11,88	9,33	0,00933	660	<b>6,16</b>
3	146,46	6,10	50×3,5	37,74	4,94	0,00494	660	<b>3,26</b>

Table 2 – Bottom Chord Weight Count

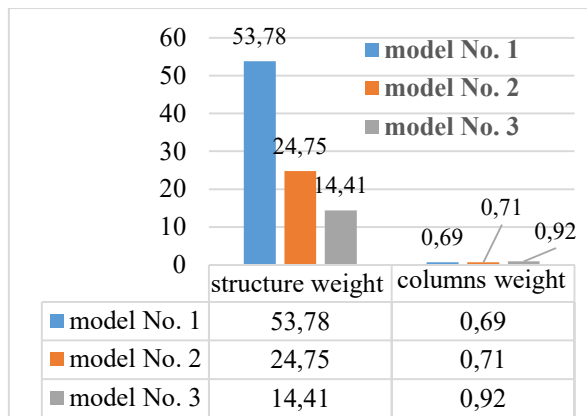
Model №	Maximum forces N, kN	Cross-sectional area A, sm <sup>2</sup>	Pipe profile	Pipe profile, A, sm <sup>2</sup>	Weight of 1 r.mprofile, kg	Weight of 1 r.mprofile, ton	Chord-length, m	Weight, ton
1	619,20	25,80	120×76	26,74	20,99	0,02099	540	<b>11,33</b>
2	333,54	13,90	60×77	14	11	0,011	540	<b>5,94</b>
3	148,71	6,20	50×73,5	6,3	4,94	0,00494	540	<b>2,67</b>

Table 3 – Inclined Rods Weight Count

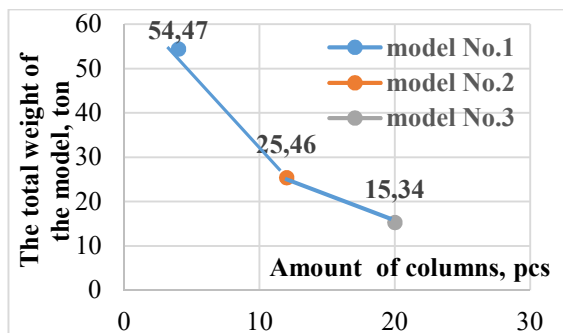
Model №	Maximum forces N, kN	Cross-sectional area A, sm <sup>2</sup>	Pipe profile	Pipe profile, A, sm <sup>2</sup>	Weight of 1 r.mprofile, kg	Weight of 1 r.mprofile, ton	Chord-length, m	Weight, ton
1	333,04	13,88	60×7	14	11	0,011	2936	<b>32,30</b>
2	131,15	5,46	50×3	5,48	4,31	0,00431	2936	<b>12,65</b>
3	83,78	3,49	35×3	3,68	2,89	0,00289	2936	<b>8,49</b>

Table 4 – Columns Weight Count

Model №	N, kN	A, sm <sup>2</sup>	Pipe profile	Cross-sectional area A, sm <sup>2</sup>	Weight of 1 r.mprofile, kg	Weight of 1 column, ton	Number of columns in the model	Total weight of columns in the model, ton
1	841,99	35,08	140×7	36,4	28,57	0,17142	4	<b>0,69</b>
2	312,15	13,01	70×5	12,57	9,87	0,05922	12	<b>0,71</b>
3	223,27	9,30	45×7	9,8	7,69	0,04614	20	<b>0,92</b>



**Figure 11 – The ratio of the weight of the space grid structure and the weight of the columns**



**Figure 12 – Weight changes in space grid structure depending on the number of columns according to the variants of their location**  
(model No. 1 – 4 columns, model No. 2 – 12 columns, model No. 3 – 20 columns)

## Conclusions

As the number of supports increases, the weight of the space grid structure itself decreases and the weight of the columns increases (see Tables 4–5). The model according to variant No.3 has the lowest weight, despite the largest number of columns in this model. As can be seen in Fig. 11 the weights of the columns in the weight of each model are values of the same order. The weight of the columns is from 0,7 to 0,9 tons, and the weight of the space grid structure differs by 2,17–3,8 times relative to the heaviest structure (according to model No.1). The most rigid is model No.3, the least rigid is model No.1 (when the space grid structure is supported by four columns at the corners). Based on the analysis of the obtained results, we can conclude that the criterion of metal consumption for the considered design solutions is the most effective third option for the location of the columns (along the perimeter of the lower chord of the space grid structure with a step of 6,0 m). In this case, the total weight of the whole structure would be the lowest. Prospects for further research are: the study of plate structures models with different variants of steel classes of construction and the labour content during the model erection.

## References

1. Василькин А.А., Денякова В.В. (2018). Регулирование напряженно-деформированного состояния структурной плиты покрытия. *ИВД*, 2(49)  
Взято з <https://cyberleninka.ru>
2. Пахомов А.И., Кочетова Е.А., Кобезский В.А. Основные аспекты структурных конструкций в современном проектировании. *Материалы VIII Международной студенческой научной конференции «Студенческий научный форум»*  
Взято з <http://scienceforum.ru/2016/article/2016019012>
3. Толмачев И.Н. (1981). *Структурные конструкции покрытий одноэтажных промышленных зданий*. Москва: МИИТ
4. Хисамов Р.И. (1981). *Расчет и конструирование структурных покрытий*. Киев: Будівельник
5. Лубо Л.Н., Миронков Б.А. (1976). *Плиты регулярной пространственной структуры*. Ленинград: Стройиздат
6. Колодежнов С.Н., Селиванова А.Н. (2017). Анализ висячих конструктивных систем подкрепления навеса в виде структурной плиты. *Строительная механика и конструкции*, 14, 61-71
7. Василькин А.А., Щербина С.В. (2015). *Автоматизированное решение задачи определения оптимальной высоты стальной фермы по критерию минимума массы при вариации высоты фермы*. Интеграция, партнерство и инновации в строительной науке и образовании (12-13.12.2014). Москва: МГСУ, 131-134
1. Vasil'kin A.A. & Denyakova V.V. (2018). Regulation of the stress-strain state of the structural roof slab. *IVD*, 2(49)  
Retrieved from <https://cyberleninka.ru>
2. Pahomov A.I., Kochetova E.A. & Koberzskij V.A. The main aspects of space grid structures in modern design. *Materials of the VIII International Student Scientific Conference "Student Scientific Forum"*  
Retrieved from <http://scienceforum.ru/2016/article/2016019012>
3. Tolmachev I.N. (1981). *Space grid structures of coatings of one-story industrial buildings*. Moscow: MIIT
4. Hisamov R.I. (1981). *Calculation and design of space grid coatings*. Kyiv: Budivelnik
5. Lubo L.N. & Mironkov B.A. *Slabs of regular spatial pattern*. Leningrad: Strojizdat
6. Kolodezhnov S.N. & Selivanova A.N. (2017). Analysis of suspended structural slab canopy reinforcement systems. *Structural mechanics and structures*, 14, 61-71
7. Vasil'kin A.A. & Shcherbina S.V. (2015). *Automated solution of the determining optimal height of a steel truss problem by the criterion of minimum mass with varying truss height*. Integration, partnership and innovation in building science and education (12-13.12.2014). Moscow: MGSU, 131-134

8. Никитюк А.В., Московкина А.А., Зуева И.И. (2011). Достоинства и недостатки структурных конструкций. *Вестник ПНИПУ. Строительство и архитектура*, 1  
Взято з <https://cyberleninka.ru>
9. Хисамов Р.И., Агафонкин В.С., Замалиев Ф.С. (1973). *Пособие по расчету и конструированию структурных покрытий из ферм*. Казань: Татполиграф
10. Трофимов В.И., Бегун Г.Б. (1972). *Структурные конструкции*. Москва: Стройиздат
11. Huybrechts S., Tsai S.W. (1996). Analysis and behavior of grid structures. *Composites Science and Technology*, 56(9), 1001-1015  
[https://doi.org/10.1016/0266-3538\(96\)00063-2](https://doi.org/10.1016/0266-3538(96)00063-2)
12. Chilton J. (1999). *Space Grid Structures*. Routledge  
<https://doi.org/10.4324/9780080498188>
13. Михайлов В.В., Сергеев М.С. (2011). *Пространственные стержневые конструкции покрытий (структуры)*. Владимир: ВИГУ
14. Парлашкевич В.С., Василькин А.А., Булатов О.Е. (2014). *Проектирование и расчет металлических конструкций рабочих площадок*. Москва: МГСУ
15. Трущев А.Г. (1983). *Пространственные металлические конструкции*. Москва: Стройиздат
16. ДБН В.2.6-198:2014 (2014). *Сталеві конструкції. Норми проектування*. Київ: Мінрегіонбуд
17. ДСТУ Б В.1.2-3:2006 (2006). *Прогини і переміщення. Вимоги проектування*. Київ: Мінрегіонбуд
18. Ashtul S.A. & Patil S.N. (2020). Review on Study of Space Frame Structure System. *International Research Journal of Engineering and Technology*, 7(4)
19. *Space Frame Structure; an analysis of its benefit by Constro Facilitator*.  
Retrieved from <https://www.constrofacilitator.com/space-frame-structure-an-analysis-of-its-benefit>
20. Murtha-Smith E. & Bean J.E. (1989). Double Layer Grid Space Frame Buckling. *International Journal of Space Structures*, 4(3), 117-127  
<https://doi.org/10.1177/026635118900400301>
21. Britannica, The Editors of Encyclopaedia. "Space frame". *Encyclopedia Britannica*,  
Retrieved from <https://www.britannica.com/technology/space-frame>
22. Li Z.X. (2013). Structure Mechanics Analysis with Different Construction Schemes in Large-Span Space Grid Structure. *Advanced Materials Research*, 788, 534-537  
<https://doi.org/10.4028/www.scientific.net/AMR.788.534>
23. Zhou Z., Wu J., Meng Sp. *et al.* (2012). Construction process analysis for a single-layer folded space grid structure in considering time-dependent effect. *International Journal Steel Structures*, 12, 205-217  
<https://doi.org/10.1007/s13296-012-2005-y>
24. Fu F., Parke G.A.R. (2018). Assessment of the Progressive Collapse Resistance of Double-Layer Grid Space Structures Using Implicit and Explicit Methods. *International Journal Steel Structures*, 18, 831-842  
<https://doi.org/10.1007/s13296-018-0030-1>
8. Nikityuk A.V., Moskovkina A.A. & Zueva I.I. (2011). Advantages and disadvantages of space grid structures. *PNRPU Bulletin. Construction and architecture*, 1  
Retrieved from <https://cyberleninka.ru>
9. Hisamov R.I., Agafonkin V.S. & Zamaliev F.S. (1973). *Tutorial for the truss roofing structural calculation and design*. Kazan': Tatpoligraf
10. Trofimov V.I. & Begun G.B. (1972). *Space grid structures*. Moscow: Strojizdat
11. Huybrechts S. & Tsai S.W. (1996). Analysis and behavior of grid structures. *Composites Science and Technology*, 56(9), 1001-1015  
[https://doi.org/10.1016/0266-3538\(96\)00063-2](https://doi.org/10.1016/0266-3538(96)00063-2)
12. Chilton J. (1999). *Space Grid Structures*. Routledge  
<https://doi.org/10.4324/9780080498188>
13. Mikhaylov V., Sergeev M.S. (2011). *Space grid structures for roofs*. Vladimir: VIGU
14. Parlashkevich V.S., Vasil'kin A.A. & Bulatov O.E. *Design and calculation of metal structures of working sites*. Moscow: MGSU
15. Trushchev A.G. (1983). *Spatial metal structures*. Moskva: Strojizdat
16. ДБН В.2.6-198:2014 (2014). *Steel structures. Design standards*. Kyiv: Minregionbud
17. ДСТУ Б В.1.2-3:2006 (2006). *Deflections and displacements. Requirements to designing*. Kyiv: Minregionbud
18. Ashtul S.A. & Patil S.N. (2020). Review on Study of Space Frame Structure System. *International Research Journal of Engineering and Technology*, 7(4)
19. *Space Frame Structure; an analysis of its benefit by Constro Facilitator*.  
Retrieved from <https://www.constrofacilitator.com/space-frame-structure-an-analysis-of-its-benefit>
20. Murtha-Smith E. & Bean J.E. (1989). Double Layer Grid Space Frame Buckling. *International Journal of Space Structures*, 4(3), 117-127  
<https://doi.org/10.1177/026635118900400301>
21. Britannica, The Editors of Encyclopaedia. "Space frame". *Encyclopedia Britannica*,  
Retrieved from <https://www.britannica.com/technology/space-frame>
22. Li Z.X. (2013). Structure Mechanics Analysis with Different Construction Schemes in Large-Span Space Grid Structure. *Advanced Materials Research*, 788, 534-537  
<https://doi.org/10.4028/www.scientific.net/AMR.788.534>
23. Zhou Z., Wu J., Meng Sp. *et al.* (2012). Construction process analysis for a single-layer folded space grid structure in considering time-dependent effect. *International Journal Steel Structures*, 12, 205-217  
<https://doi.org/10.1007/s13296-012-2005-y>
24. Fu F., Parke G.A.R. (2018). Assessment of the Progressive Collapse Resistance of Double-Layer Grid Space Structures Using Implicit and Explicit Methods. *International Journal Steel Structures*, 18, 831-842  
<https://doi.org/10.1007/s13296-018-0030-1>

UDC 624.012.82

## Work of masonry under the combined action of vertical and horizontal loads: an analysis of experimental studies

Dovzhenko Oksana<sup>1\*</sup>, Pohribnyi Volodymyr<sup>2</sup>, Usenko Dmytro<sup>3</sup>, Qiniso Mahlinza<sup>4</sup>

<sup>1</sup> National University «Yuri Kondratyuk Poltava Polytechnic» <https://orcid.org/0000-0002-2266-2588>

<sup>2</sup> National University «Yuri Kondratyuk Poltava Polytechnic» <https://orcid.org/0000-0001-7531-2912>

<sup>3</sup> National University «Yuri Kondratyuk Poltava Polytechnic» <https://orcid.org/0000-0001-7133-0638>

<sup>4</sup> National University «Yuri Kondratyuk Poltava Polytechnic» <https://orcid.org/0000-0001-6583-0353>

\*Corresponding author E-mail: [o.o.dovzhenko@gmail.com](mailto:o.o.dovzhenko@gmail.com)

The characteristic damage of masonry walls under the combined action of vertical and horizontal loads has been analyzed. Possible schemes of masonry destruction are considered. A diagonal shear is identified as a typical case of the destruction of piers under seismic impacts. The closeness of the loading conditions of the piers of the bearing walls under the action of the seismic force to those that arise in the frame when it is skewed is noted. The article considers the results of experimental studies of masonry specimens on the skew as models of the operation of piers under seismic impacts. The nature of destruction is analyzed, determining factors of influence. Based on the analysis of known experiments, proposals are presented for a kinematically possible scheme for the destruction of masonry walls, which is proposed as a base for the calculation

**Keywords:** diagonal shear, damage, seismic influences, schemes of destruction

## Робота кам'яної кладки при сумісній дії вертикальних і горизонтальних навантажень: аналіз експериментальних досліджень

Довженко О.О.<sup>1\*</sup>, Погрібний В.В.<sup>2</sup>, Усенко Д.В.<sup>3</sup>, Кінісо Махлінза<sup>4</sup>

<sup>1, 2, 3, 4</sup> Національний університет «Полтавська політехніка імені Юрія Кондратюка»

\*Адреса для листування E-mail: [o.o.dovzhenko@gmail.com](mailto:o.o.dovzhenko@gmail.com)

Проаналізовані характерні пошкодження кам'яних стін при сумісній дії вертикальних і горизонтальних навантажень. Розглянуто можливі схеми руйнування кладки. Особливу увагу приділено міжвіконним простінкам, котрі є однією із найбільш напружених й уразливих конструкцій цегляних будівель з точки зору сейсмостійкості. Виділено діагональний зсув як характерний випадок руйнування простінків при сейсмічних впливах. Наголошено на близькості умов завантаження простінків несучих стін при дії сейсмічної сили до тих, які виникають у каркасі при його перекосі. Розглянуто результати експериментальних досліджень кам'яних зразків на перекіс як моделей роботи простінків. Проаналізовано характер руйнування, визначальні фактори впливу: матеріал кладки, міцність каменю і розчину, внутрішні і зовнішні армування кладки, підсилення розчинними і бетонними аплікаціями, перехресними та горизонтальними залізобетонними смугами, вуглеволокном, діагональними металевими тяжами та інші. На основі аналізу відомих експериментів надані пропозиції щодо кінематично можливої схеми руйнування кам'яних простінків, котру запропоновано як базову для розрахунку варіаційним методом у теорії пластичності, розробленим у Національному університеті «Полтавська політехніка імені Юрія Кондратюка» для розрахунку міцності бетонних і залізобетонних, кам'яних та армокам'яних елементів при зрізі, місцевому стисненні та продавлюванні. В стадії руйнування простінок розділяється на чотири жорсткі диски: два клини під вантажною площадкою і два диски, окреслені зсувними ділянками клинів і площиною розколювання, котра з'єднує їх вершини. Клини рухаються назустріч один одному, а два інших диски віддаляються один від одного в напрямку, перпендикулярному до площини розколювання

**Ключові слова:** діагональний зсув, пошкодження, сейсмічні впливи, схеми руйнування



## Introduction

Ensuring seismic resistance is always one of the main tasks in the design and construction of buildings and structures in earthquake-prone areas. Recently, the applicability of this problem for Ukraine has significantly increased in connection with the frequent cases of earthquakes in Europe, including with a large number of human victims and significant material damage.

New seismic zoning maps ZSR-2004, put into effect in the norms [1] since 2006, provide for an increase in the proportion of territories subject to seismic effects. According to them, at this time, approximately 15% of the territory of Ukraine is earthquake-prone with design seismicity of more than 7 points.

The size of economic losses from seismic effects established as a result of the analysis for buildings with different structural schemes (with the same seismicity of the site) [2] indicates that buildings with masonry walls that are widespread in Ukraine are the most vulnerable to seismic effects and belong to the least seismic-resistant type. This is due, in particular, to the increased mass of structures and the presence of a large number of joints and seams, which leads to significant damage to building elements.

## Review of the research sources and publications

The results of recent studies [3 – 8] show that buildings with bearing masonry walls receive the following typical damages from the action of seismic loads: inclined and cruciform cracks in the piers of walls and unpierced walls; vertical cracks at the junction of the longitudinal and transverse walls with possible falling out of the walls; horizontal cracks in the walls, often at the level of the bottom of window areas, lintels or at the level of support of the floor; cracks in the places where reinforced concrete lintels were laid; cracks of a chaotic direction in the walls, which are a combination of the above (Fig. 1).

## Definition of unsolved aspects of the problem

Currently, there is no methodology for calculating masonry structures under the combined action of vertical and horizontal forces, which would be based on a common theoretical basis.

## Problem statement

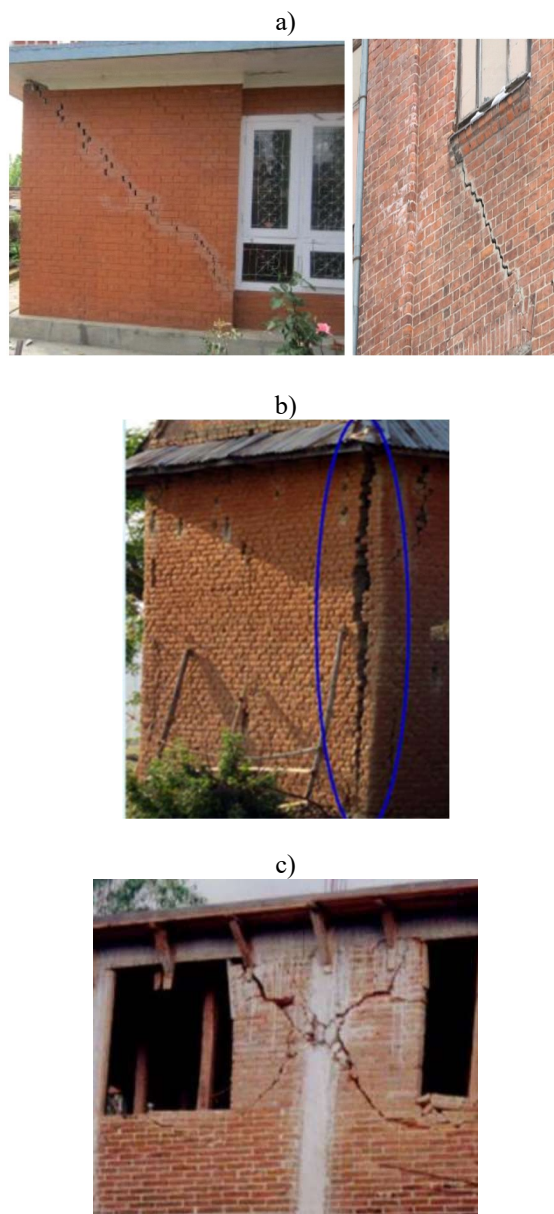
To create a reliable method for assessing the bearing capacity of masonry walls under the combined action of vertical and horizontal loads and informed decision-making regarding their effective reinforcement, it is necessary to analyze the nature of the destruction of structures and the results of their physical modeling in the experiment. The data obtained will serve as the basis for creating design diagrams of elements in assessing their strength.

## Basic material and results

Tumanov A. [9], based on the results of experimental studies, proposed a classification of cracks observed in masonry walls under the combined action of vertical and horizontal forces. The main types are:

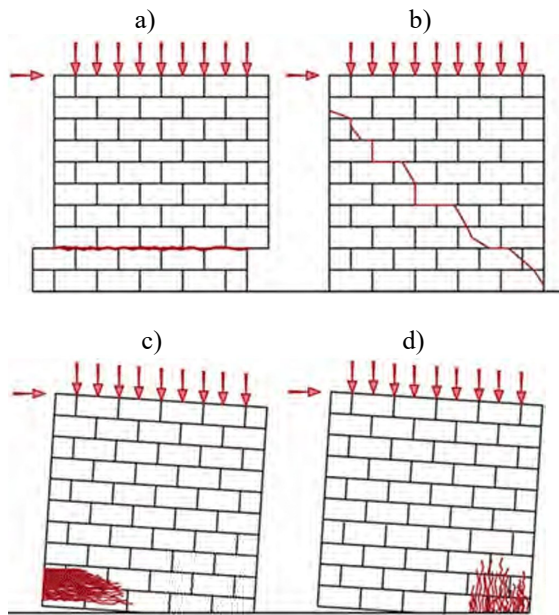
- main vertical cracks that divide the surface of the walls into separate vertical blocks;
- limiting inclined cracks that define the boundaries of an inclined compressed strip (destruction area);
- microcracks, the accumulation of which leads to crushing of the masonry;
- cracks in the tensile zone;
- cracks that characterize a shear of compressed masonry in inclined compressed strips.

The proposed classification of cracks can be considered as a criterion for the implementation of individual schemes of masonry destruction: displacement in the horizontal plane, diagonal shear, failure beyond the tensile zone, and crushing (Fig. 2).



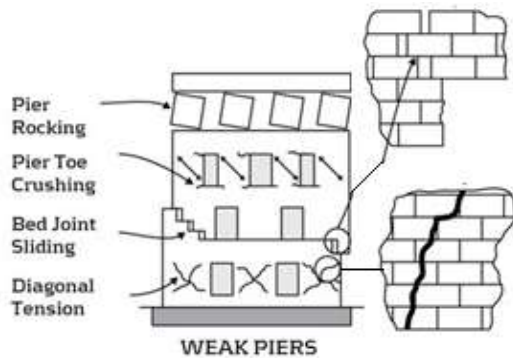
**Figure 1 – The nature of the destruction of masonry walls under seismic effects:**

- a – a diagonal cracks [3];
- b – a vertical crack at the junction of the longitudinal and transverse walls [7];
- c – a cruciform crack in the wall [8]



**Figure 2 – The nature of the destruction of masonry under the combined action of vertical and horizontal loads:**  
 a – displacement in the horizontal plane;  
 b – diagonal shear;  
 c – failure beyond the tensile zone;  
 d – crushing

One of the most vulnerable structures of masonry buildings in terms of seismic resistance are piers, cases of destruction are shown in Fig. 3 [10].

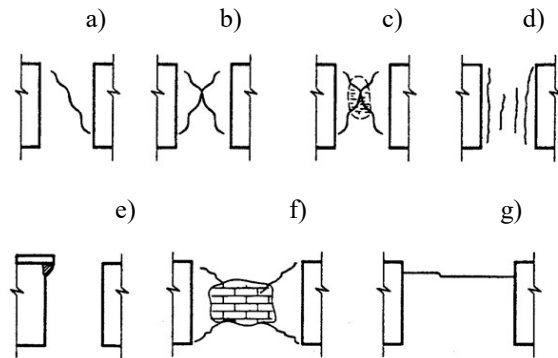


**Figure 3 – Cases of destruction the piers under seismic effects**

The width of the piers to a certain extent affects the location of the cracks (Fig. 4).

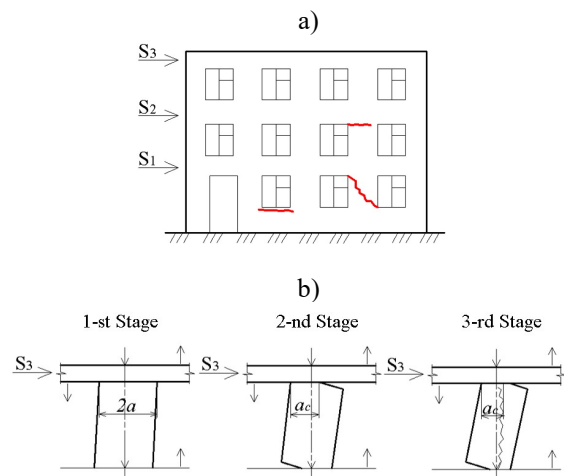
The most typical damage to walls is the formation of inclined and X-shaped cracks, which propagate mainly along the joints of the masonry, starting at the corners of the holes and other places where the walls weaken (change in stiffness). If the crack crosses the stones, then this is a sign of their insufficient strength, the layering of the masonry indicates a weak bond of the mortar to the stone. The value of crack opening can be different and is the main sign when assessing the degree of damage to a wall element.

According to [12], the piers of bearing walls under the action of a seismic force are under loading conditions that are close to those that arise in the frame when it is skewed.



**Figure 4 – Schemes of cracks location in the piers during earthquakes:**  
 a – e – damage in relatively narrow piers;  
 f, g – the same in relatively wide piers [11]

In the first stage of deformation of the masonry (Fig. 5), when the seismic forces are small, the piers work together with the above-window chord over the entire contact area. The vertical load is transferred from the upper to the lower piers at all levels along all horizontal sections.



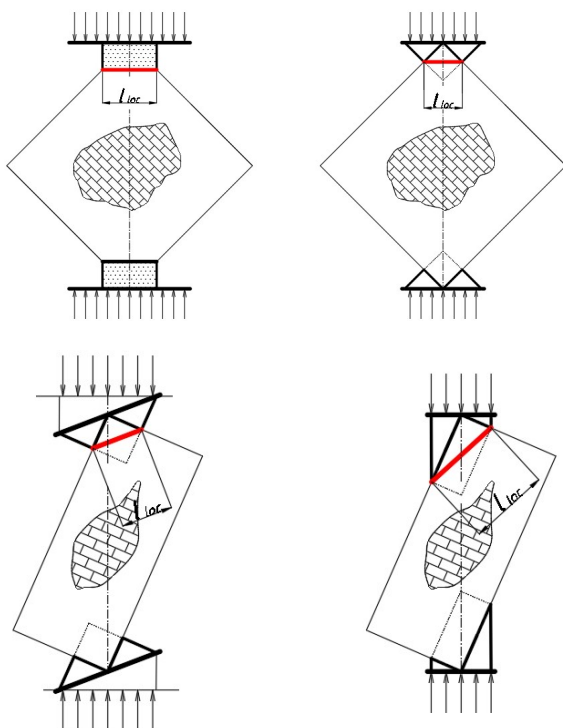
**Figure 5 – The work of the piers of bearing walls under the action of horizontal seismic force:**  
 a – characteristic damages;  
 b – stages of deformation of the piers

In the second stage, cracks form in the tensile zones of the horizontal section of the walls at the levels of the upper and lower parts of the window area adjacent to them, and the contact between the masonry is broken. At this stage, the transfer of vertical and horizontal loads in the mentioned sections is carried out only along with the length  $a_c < 2a$  (where  $a$  is half the width of the pier). With an alternating horizontal load, the bond in the masonry is broken along the contact between the top of the pier and the bottom of the chord due to the formation of cracks.

The third stage is characterized by a further reduction in the length of the compressed zone and the formation of a diagonal crack in the pier. One and the same pier on different floors of a building may be at different stages of deformation, which is associated with a change in the values and ratio of vertical and horizontal forces, as well as with possible differences in the strength and stiffness of the piers.

So, an experimental study of the work of piers for the combined action of vertical and horizontal loads can be carried out when testing masonry samples on the skew, first performed by Dmitriev A. in 1940 in the laboratory of masonry structures CRIIS [13]. He tested fragments of vibrational masonry walls from hollow ceramic stones. Since 1948 Polyakov S. studied the features of work of filling in frame-stone buildings: 57 samples with frame and continuous filling were tested. Since the publication of the monograph by Polyakov S. [14], many authors have carried out experimental studies of the strength and deformability of fragments of masonry made of bricks of various types, limestone, and other materials when skewed without frame framing. In most cases, the specimens were tested with a concentrated load applied along with one of their diagonals (Fig. 6). To prevent crushing of the loaded corners of the masonry, the latter were reinforced with steel or reinforced concrete bearing elements. With this test scheme, the strength indicators of the samples are influenced by the length of the support areas ( $l_{loc}$ ), through which the load is transferred to the sample.

Various methods of increasing the bearing capacity of elements under the combined action of vertical and horizontal forces were investigated.



**Figure 6 – Schemes used by researchers when testing masonry specimens for deformation during the application of a load along the diagonal**

Known experiments with vibrational masonry panels with sides dimensions 1060×1060, 1120×1120, 800×800, 800×1200, and 800×1600 mm [15] without reinforcement and with reinforcement with vertical bars and wire meshes through three courses of masonry, which did not increase the strength of the samples. The desired result was achieved with external reinforcement, and here the distance between the moment of the formation of a diagonal crack and the destruction of the element significantly increased.

Kabantsev A. and Tonkikh P. [16] manufactured and tested 7 series of experimental samples with dimensions 1060×1060×250 mm from solid brick with strength  $f_b = 10$  MPa on cement-sand mortar with strength  $f_m = 7.5$  MPa: control samples without reinforcement and reinforced with one or two sides. Carbon fiber FibARM Tape 230 and FibARM Tape 240 and binder FibArm Resin 230+ and FibArm Resin 530+ were used as reinforcement elements [15]. The use of an external reinforcement system made it possible to increase the bearing capacity of the masonry by 30 – 100%, depending on the strength of the carbon fiber, area, thickness, and a number of reinforcement layers. The destruction of these samples, in contrast to those reinforced with reinforced concrete and concrete applications, which are applied according to the usual technology and by the concrete shotcrete method [16], occurred along a diagonal crack outside, brittle, almost instantly after reaching the ultimate loads.

During the tests Derkach V. of unreinforced samples with dimensions of 500×500×140 mm made of bricks with strength  $f_b = 15$  MPa [17] the moment of formation of diagonal cracks coincided with the moment of destruction. At the same time, depending on the strength of the mortar, the following mechanisms of destruction were observed: splitting along the diagonal, in which the trajectory of the crack passes both along with the stones and along individual vertical and horizontal joints of the masonry (with a mortar with compressive strength  $f_m = 7.9 - 10.9$  MPa); splitting along the diagonal, in which the critical crack has a stepped trajectory and passes only along the horizontal and vertical joints of the masonry; displacement along the horizontal joints of the mortar (the last two types of destruction were observed when using a mortar with strength  $f_m = 3.1$  MPa).

The experiments of Demchuk I. [18] were carried out on masonry samples with dimensions of 500×500×65 mm for the manufacture of which solid and hollow (18%) bricks were used on standard mortars with compressive strength  $f_m = 3.1, 7.9,$  and  $10.9$  MPa. The results obtained indicate a decrease in the shear strength of the masonry  $f_{vv}$  at the mortar strength  $f_m = 3.1$  MPa.

Gasiev A. [12] produced and tested 3 series of samples with dimensions 1030×965×250 mm using a brick of average strength  $f_b = 12.5$  MPa on a mortar with strength  $f_m = 7.5$  MPa: control samples and reinforced with a sheet of carbon fiber brand MBACE FIB CF230 / 4900.200g / 5.100m with one and two sides of the specimen along its extended diagonal. The bearing

capacity in the first case of external reinforcement increases by about 1.5 times, and in the second by 2 times.

In the work of Izmailov Yu. [19], the results of experimental studies of the strength of four series of samples on the action of static and pulsating loads directed along the diagonal are presented. Both traditional masonry and vibrational brick elements were used. Strengthening was carried out by applying a plaster layer from a high-strength mortar to the side surfaces or reinforcing the plaster layer with steel meshes. Vibrations and the presence of plaster layers on the lateral surfaces of the samples increase the strength of the masonry up to 2 times; reinforcement postpones destruction from the moment of cracking, creating conditions for the development of plastic strain. Destruction of brick elements occurred along a diagonal crack, which spread along the joints, vibrational brick samples collapsed along a bandaged section; the destruction of the reinforced vibrational brick samples occurred along an inclined compressed strip. The effect on the resistance of the masonry was also analyzed by reinforcement with steel diagonal ties or during preliminary compression.

Experimental studies by Kadam S. and Singh Y. [6] included tests of six series of samples with strength characteristics of brick  $f_b = 21.06$  MPa and mortar  $f_m = 3.72$  MPa. The first two series had three reinforced masonry piers with dimensions of  $700 \times 700 \times 115$  mm (single-layer) and  $700 \times 700 \times 230$  mm (two-layer). Samples 3 – 6 series were reinforced from the outside (in one and two planes) with welded wire meshes located in a layer of concrete. Destruction of unreinforced specimens occurred behind a jagged diagonal crack and was sudden and externally brittle. The authors propose to consider this failure as a combination of diagonal shear and horizontal displacement. The behavior of reinforced specimens depended on their thickness, intensity, and method of reinforcement. The destruction began with the formation of a diagonal crack, the development of which was restrained for a certain time by reinforcement, which promoted more plastic failure in comparison with the samples without reinforcement. For specimens reinforced in one direction, the failure was accompanied by cracks that were localized along the edges of the specimen. At large displacements, there was a significant local crushing of the concrete adjacent to the welded mesh, which was torn in some places. For specimens reinforced in two directions, failure occurred along a crack that propagated along the length of the compressed diagonal of the specimens. At the last stage of loading, local crushing of the masonry in the places of load application was observed. The increase in the shear strength of the reinforced specimens in comparison with the reference was in the range of 0.57 – 1.48 MPa.

In the experiments of Dong K., Sui Z., Jiang J., Zhou X. [20], solid brick and ordinary mortar were used to make samples with dimensions of  $2100 \times 1560 \times 240$  mm and  $1560 \times 1560 \times 240$  mm (a total of 11 piers were tested). Three samples without reinforcement served as reference, the other 8 were reinforced with reinforced cross and horizontal strips from a solution 250 mm wide. The experiment varied: the

strength of the mortar of masonry and reinforcement strips, their thickness, the reinforcement ratio of the strips, the location of the reinforcement (on one or both sides), as well as the value of the vertical load. For the value of samples, a brick with dimensions of  $240 \times 115 \times 53$  mm with  $f_b = 10$  MPa and a mortar with  $f_m = 1$  MPa, 2.5 MPa, and 10 MPa for unreinforced elements were used. For reinforcement strips with a thickness of 40 mm and 60 mm, a mortar with  $f_m = 2.5$  MPa, 5 MPa, and 10 MPa was taken, respectively. The strips were reinforced with steel bars 6 – 12 mm in diameter. To simulate the work of the walls of the first floor of a seven-story building, a vertical load of 0.516 MPa was applied, the third – 0.4 MPa, and the seventh – 0.21 MPa. In the reference specimens, the first diagonal crack appeared in the center of the wall. It spread mainly along with horizontal and vertical layers of mortar, while in some places it crossed the brick. Sometimes a second diagonal crack could appear perpendicular to the first. Reinforced specimens collapsed from shear-compression along diagonal and vertical cracks, the latter appearing in unreinforced zones of the wall. When the maximum bearing capacity was reached, the strips retained their integrity and prevented the collapse of the samples during failure. The cracking load for the reinforced elements increased by 20 – 40%, and the ultimate load by 40 – 65%. An increase in the reinforcement ratio of the strips, the level of vertical stresses, and the strength of the mortar increased the shear resistance, while an increase in the ratio of the thickness to the width of the element, on the contrary, decreased it. The reinforcement increased the plastic properties of the masonry by 1.6 times with one-sided reinforcement and 2.8 times with two-sided reinforcement.

In the experiments of Mustafaraj E. and Yardim Y. [5], 6 specimens with dimensions of  $1200 \times 1200 \times 250$  mm was used with an average strength of a brick  $f_b = 24.03$  MPa and mortar  $f_m = 5.68$  MPa in compression. The samples were reinforced with a fiberglass mesh on both sides of the wall, followed by a layer of mortar. The test procedure was carried out in accordance with ASTM [21].

In the control unreinforced samples, destruction occurred along the compressed diagonal, mainly behind the mortar joints. However, in some cases, a combination of displacement along mortar horizontal joints over a length of about 500 mm was observed with a diagonal crack that propagated exclusively through the mortar joints. Specimens reinforced with fiberglass were destroyed along the compressed diagonal, their strength increased by an average of 1.3 times, while the plastic characteristics of the masonry increased.

So, analyzing the experimental studies of masonry on the skew, which can be considered as a simulation of the operation of masonry piers with the combined action of vertical and horizontal seismic forces, it should be noted that the most characteristic variant of failure (Fig. 7) is a diagonal shear in accordance with the classification (a crack can be stepped – extends only along vertical and horizontal mortar joints or rectilinear – crosses both the seams and the stone). Local crushing of masonry at the supports is also observed [16].



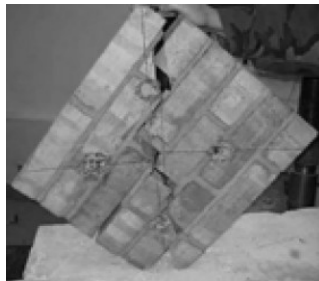


according to [17]



according to [12]

according to [6]



according to [3]



according to [5]

**Figure 7 – Diagonal shear of masonry in experimental studies on the skew**

Undoubtedly, the most complete data on the nature of deformation and destruction of masonry under the shear can be obtained experimentally. However, experiments require significant costs, and most importantly are parametrically limited, therefore, numerical calculations are an effective addition to physical experiments. A correct mathematical model is a tool for analyzing the influence of the selected parameters and their combination on the stress-strain state of the masonry. As a computational model, it is proposed to use the variational method in the theory of plasticity [22], which is widely used in calculations of concrete and reinforced concrete structures with a shear failure scheme [23 – 26]. And the failure obtained in experiments serves as a justification for the accepted kinematically possible failure scheme.

In the theoretical model, at the stage of destruction, the pier is divided into four hard disks: two wedges under the loading area (in the general case, the wedges should be non-sided) and two hard disks indicated by the shear sections of the wedges and a splitting plane that connects the tops of the wedges.

The wedges move towards each other; the other two disks move away from each other in a direction perpendicular to the splitting plane. There are four unknowns in the problem: two angles of inclination of the sections of shear of the wedges to the vertical, the ratio of the speeds of movement of hard disks, and the ultimate load.

### Conclusions

In the experiments performed, the nature of the destruction of masonry samples was investigated when they were skewed, the effect of the masonry material, the strength of the stone and mortar, the internal and external reinforcement of the masonry, its reinforcement with mortar and concrete applications, cross, and horizontal reinforced concrete strips, carbon fiber, diagonal steel tension bar on strength of elements were revealed under the combined action of vertical and horizontal loads.

The analysis of the material under consideration made it possible to propose a substantiated kinematically possible scheme for the failure of masonry elements when skewed, which will serve as the basis for using the method for calculating the strength of such structures by the variational method in the theory of plasticity, developed at National University «Yuri Kondratyuk Poltava Polytechnic».

### References

1. ДБН В.1.1-12-2014. (2019). *Захист від небезпечних геологічних процесів. Будівництво у сейсмічних районах України*. Київ: Держстандарт України
2. Ковров А. В., Шеховцов І.В., Петраш С. В. (2019). *Будівництво в сейсмічних районах України будівель і споруд зі стінами із цегли і великорозмірних блоків. Наука та будівництво*, 1, 18-24
3. National Society for Earthquake Technology Nepal (NSET) (2018). *Engineers Training on Design for Seismic Retrofitting of Masonry Building*, 13-17 August, Lalitpur, Nepal
1. DBN V.1.1-12-2014. (2019). *Protection Against Dangerous Geological Processes. Construction in Seismic Regions of Ukraine*. Kyiv: Gosstandart of Ukraine
2. Kovrov A.V., Shekhovtsov I.V., Petrash S.V. (2019). *Construction of Buildings and Structures with Walls Made of Bricks and Large-sized Blocks in Seismic Regions of Ukraine. Science and Construction*, 1, 18-24
3. National Society for Earthquake Technology Nepal (NSET) (2018). *Engineers Training on Design for Seismic Retrofitting of Masonry Building*, 13-17 August, Lalitpur, Nepal

4. Corradi M., Borri A., Castori G., Sisti R. (2014). Shear Strengthening of Wall Panels Through Jacketing with Cement Mortar Reinforced by GFRP Grids. *Composites Part B: Engineering*, 64, 33-42  
<https://doi.org/10.1016/j.compositesb.2014.03.022>
5. Mustafaraj E., Yardim Y. (2018). In-plane Shear Strengthening of Unreinforced Masonry Walls Using GFRP Jacketing. *Periodica Polytechnica Civil Engineering*, 62(2), 330-336  
<https://doi.org/10.3311/PPci.11311>
6. Kadam S., Singh Y., Bing L. (2012). Mechanical Properties of Externally Strengthened Masonry. *Proceedings of 15th world conferences on earthquake*
7. Meguro K., Soti R., Sathiparan N., Numada M. (2012). Dynamic Testing of Masonry Houses Retrofitting by Bamboo Band Meshes. *Journal of Japan Society of Civil Engineers*, 68 (4), 760-765  
<https://doi.org/10.2208/jscejsee.68.I.760>
8. Akshay G., Vaibhav S. (2020). Strengthening of Confined Masonry Structures for In-plane Loads: a Review. *IOP Conf. Series: Materials Science and Engineering*, 936, 012031  
<https://doi.org/10.1088/1757-899X/936/1/012031>
9. Туманов А.В. (2000). Прочность армированных стен из кирпичной кладки при совместном действии вертикальных и горизонтальных сил. (Дис. канд. техн. наук). Пенза
10. Earthquake Strengthening of Unreinforced Masonry Buildings in New Zealand. Взято з:  
<https://www.tinoseismic.co.nz/articles/earthquake-strengthening-unreinforced-masonry-buildings>
11. СП 31-114-2004. (2005). Правила проектирования жилых и общественных зданий для строительства в сейсмических районах. Москва : ЦИТП
12. Гасиев А.А., Грановский А.В. (2015). К вопросу об оценке несущей способности кирпичных простенков, усиленных холстами из углеволокнистой ткани, при действии сдвигающих усилий. *Промышленное и гражданское строительство*, 6, 36-42
13. Дмитриев А.С. (1960). Каменные конструкции. Современное состояние и перспективы развития. Москва: Госстройиздат
14. Поляков С.В., Сафаргалиев С.М. (1988). Сейсмостойкость зданий с несущими кирпичными стенами. Казахстан
15. Тонких Г. П., Кабанцев О.В., Кошаев В.В. (2005). Методика экспериментальных исследований по усилению зданий из каменной кладки железобетонными аппликациями. *Сейсмостойкое строительство. Безопасность сооружений*, 6, 76-82
16. Тонких Г.П., Кабанцев О.В., Кошаев В.В. (2007). Экспериментальные исследования несущей способности каменной кладки при главных нагрузках. *Сейсмостойкое строительство. Безопасность сооружений*, 6, 26-31
17. Деркач В.Н. (2012). Анизотропия прочности каменной кладки на растяжение при раскалывании. *Научно-технические ведомости СПбГПУ. Наука и образование*, 2(147), 259-265
18. Демчук И. Е. (2017). Прочность и деформации каменной кладки из керамического кирпича при сдвиге поперек горизонтальных швов. *Проблемы современного бетона и железобетона*, 9, 183-205  
<https://doi.org/10.23746/2017-9-12>
19. Измайлов Ю.В., Буровенко В.А., Кирпий А.Ф. (1990). Усиление зданий, поврежденных землетрясением. *Карпатское землетрясение 1986 г.*, 303-317
4. Corradi M., Borri A., Castori G., Sisti R. (2014). Shear Strengthening of Wall Panels Through Jacketing with Cement Mortar Reinforced by GFRP Grids. *Composites Part B: Engineering*, 64, 33-42  
<https://doi.org/10.1016/j.compositesb.2014.03.022>
5. Mustafaraj E., Yardim Y. (2018). In-plane Shear Strengthening of Unreinforced Masonry Walls Using GFRP Jacketing. *Periodica Polytechnica Civil Engineering*, 62(2), 330-336  
<https://doi.org/10.3311/PPci.11311>
6. Kadam S., Singh Y., Bing L. (2012). Mechanical Properties of Externally Strengthened Masonry. *Proceedings of 15th world conferences on earthquake*
7. Meguro K., Soti R., Sathiparan N., Numada M. (2012). Dynamic Testing of Masonry Houses Retrofitting by Bamboo Band Meshes. *Journal of Japan Society of Civil Engineers*, 68 (4), 760-765  
<https://doi.org/10.2208/jscejsee.68.I.760>
8. Akshay G., Vaibhav S. (2020). Strengthening of Confined Masonry Structures for In-plane Loads: a Review. *IOP Conf. Series: Materials Science and Engineering*, 936, 012031  
<https://doi.org/10.1088/1757-899X/936/1/012031>
9. Tumanov A.V. (2000). Strength of Reinforced Walls Done from Masonry under the Combined Action of Vertical and Horizontal Forces. (Dis. cand. tech. sciences). Penza
10. Earthquake Strengthening of Unreinforced Masonry Buildings in New Zealand. Retrieved from:  
<https://www.tinoseismic.co.nz/articles/earthquake-strengthening-unreinforced-masonry-buildings>
11. SP 31-114-2004. (2005). Rules for the Design of Residential and Public Buildings for Construction in Seismic Areas. Moscow: TSITP
12. Gasiev A.A., Granovsky A.V. (2015). To the Question of Assessing the Bearing Capacity of Brick Piers, Reinforced Canvases Made of Carbon Fiber Fabric, under the Action of Shear Forces. *Industrial and Civil Construction*, 6, 36-42
13. Dmitriev A.S. (1960). *Masonry Structures. Modern State and Development Prospects*. Moscow: Gosstroyizdat
14. Polyakov S.V., Safargaliev S.M. (1988). *Seismic Resistance of Buildings with Bearing Brick Walls*. Kazakhstan
15. Tonkikh G.P., Kabantsev A.V., Koshaev V.V. (2005). Experimental Research Technique for Reinforcing Masonry Buildings with Reinforced Concrete Applications. *Earthquake-resistant Construction. Safety of Structures*, 6, 76-82
16. Tonkikh G.P., Kabantsev A.V., Koshaev V.V. (2007). Experimental Studies of the Bearing Capacity of Masonry at Main Loads. *Earthquake-resistant Construction. Safety of Structures*, 6, 26-31
17. Derkach V.N. (2012). Anisotropy of Tensile Strength of Masonry During Splitting. *Scientific and Technical Statements of SPbSPU. Science and Education*, 2(147), 259-265
18. Demchuk I.E. (2017). Strength and Strain of Masonry from Ceramic Bricks During Shear Across Horizontal Joints. *Problems of Modern Concrete and Reinforced Concrete*, 9, 183-205  
<https://doi.org/10.23746/2017-9-12>
19. Izmailov Yu.V., Burovenko V.A., Kirpiy A.F. (1990). Strengthening of Buildings Damaged by an Earthquake. *Carpathian Earthquake 1986.*, 303-317

20. Dong K.B, Sui Z.-a, Jiang J., Zhou X. (2019). Experimental Study on Seismic Behavior of Masonry Walls Strengthened by Reinforced Mortar Cross Strips. *Sustainability*, 11(18), 4866  
<https://doi.org/10.3390/su11184866>
21. American Society for Testing and Materials (ASTM). ASTM E 519–02. (2015). *Standard Test Method for Diagonal Tension (Shear) in Masonry Assemblages*. West Conshohock, PA, PA: ASTM International
22. Митрофанов В.П., Довженко О.А., Погребной В.В. (2005). Вариационный метод расчета прочности каменной кладки при местном сжатии, *Строительство, материаловедение, машиностроение*, 32, 76-82
23. Довженко О.О., Погрибний В.В., Куриленко О.О. (2012). Про можливість застосування теорії пластичності до розрахунку міцності елементів із високоміцного бетону. *Коммунальное хозяйство городов*, 105, 74-82
24. Pohribnyi V., Dovzhenko O. & Maliovana O. (2018). The Ideal Plasticity Theory Usage Peculiarities to Concrete and Reinforced Concrete. *International Journal of Engineering & Technology*, 7(3.2), 19-26  
<http://dx.doi.org/10.14419/ijet.v7i2.26.14369>
25. Pohribnyi V., Dovzhenko O., Karabash L. & Usenko I. (2016). The Design of Concrete Elements Strength under Local Compression Based on the Variational Method in the Plasticity Theory. *Web of Conferences*, 116, 02026  
<http://dx.doi.org/10.1051/mateconf/201711602026>
26. Митрофанов В.П., Погребной В.В., Довженко О.О. (2002). Про можливість застосування передумови про ідеальну пластичність до бетону. *Вісник Одеської державної академії будівництва та архітектури*, 7, 118-124
20. Dong K.B, Sui Z.-a, Jiang J., Zhou X. (2019). Experimental Study on Seismic Behavior of Masonry Walls Strengthened by Reinforced Mortar Cross Strips. *Sustainability*, 11(18), 4866  
<https://doi.org/10.3390/su11184866>
21. American Society for Testing and Materials (ASTM). ASTM E 519–02. (2015). *Standard Test Method for Diagonal Tension (Shear) in Masonry Assemblages*. West Conshohock, PA, PA: ASTM International
22. Mitrofanov V.P., Dovzhenko O.A., Pogrebnoy V.V. (2005). Variational Method for Calculating the Strength of Masonry at Local Compression. *Construction, Materials Science, Mechanical Engineering*, 32, 76-82
23. Dovzhenko O.O., Pohribnyi V.V., Kurylenko O.O. (2012). On the Possibility of Using the Theory of Plasticity for Calculating the Strength of Elements from High-Strength Concrete. *Utilities of Cities*, 105, 74-82
24. Pohribnyi V., Dovzhenko O. & Maliovana O. (2018). The Ideal Plasticity Theory Usage Peculiarities to Concrete and Reinforced Concrete. *International Journal of Engineering & Technology*, 7(3.2), 19-26  
<http://dx.doi.org/10.14419/ijet.v7i2.26.14369>
25. Pohribnyi V., Dovzhenko O., Karabash L. & Usenko I. (2016). The Design of Concrete Elements Strength under Local Compression Based on the Variational Method in the Plasticity Theory. *Web of Conferences*, 116, 02026  
<http://dx.doi.org/10.1051/mateconf/201711602026>
26. Mitrofanov V.P., Pogrebnoy V.V. & Dovzhenko O.O. (2002). On the Possibility of Applying the Premise of Ideal Plasticity in Concrete. *Bulletin of the Odessa State Academy of Civil Engineering and Architecture*, 7, 118-124

UDC 624.042

## Proposals of diagrid structural systems

Chichulina Kseniia<sup>1\*</sup>, Chichulin Viktor<sup>2</sup>, Manoj Gupta<sup>3</sup>

<sup>1</sup> National University «Yuri Kondratyuk Poltava Polytechnic» <https://orcid.org/0000-0001-7448-0180>

<sup>2</sup> National University «Yuri Kondratyuk Poltava Polytechnic» <https://orcid.org/0000-0003-1838-7269>

<sup>3</sup> JECRC University, Jaipur (Rajasthan), India <https://orcid.org/0000-0002-4274-4927>

\*Corresponding author E-mail: [chichulinak@ukr.net](mailto:chichulinak@ukr.net)

The article describes various types of single-layer and double-layer diagrid structures. Types variants of diagrid structures that are used more for public buildings are given. The diagrid systems structural forms of existing types analysis, identified disadvantages and advantages of such structures. The calculating diagrid structural systems features using modern software systems are revealed. A new type of flat diagrid structures in the form of regular hexagons made of bent profiles is proposed. The variants of this structure type manufacturing and joining elements are considered. The bent channels and bolted dimensions or self-tapping screw systems are determined by calculation

**Keywords:** diagrid structural systems, structures, hexagon, bent elements, design model, bent channel

## Пропозиції ґратчастих структурних систем

Чичуліна К.В.<sup>1\*</sup>, Чичулін В.П.<sup>2</sup>, Манож Гупта<sup>3</sup>

<sup>1</sup> Національний університет «Полтавська політехніка імені Юрія Кондратюка»

<sup>2</sup> Національний університет «Полтавська політехніка імені Юрія Кондратюка»

<sup>3</sup> Університет JECRC (Джайпур, Індія)

\*Адреса для листування E-mail: [chichulinak@ukr.net](mailto:chichulinak@ukr.net)

Описано різні види ґратчастих одно- і двошарових конструкцій. Наведено різні варіанти типів ґратчастих конструкцій, що застосовуються більше для громадських будівель. Виконано аналіз існуючих типів конструктивних форм ґратчастих структурних систем, виявлено недоліки та переваги таких конструкцій. Представлено типові приклади споруд з використанням ґратчастих структурних систем, зокрема вежа Шухова в Україні, хмарочос «Геркін» в Лондоні, оперний театр в Пекіні, Британський музей у Лондоні, купол «Кліматрон» у США й ін. Виявлено особливості розрахунку сітчастих оболонок за допомогою сучасних програмних комплексів. Запропоновано новий тип плоских ґратчастих конструкцій у вигляді правильних шестикутників із гнутих профілів. Розглянуто варіанти виготовлення і з'єднання елементів такого типу конструкцій. Розміри гнутих швелерів та систем кріплення на болтах або самонарізних гвинтах визначаються розрахунком. Запропоновано конструкцію металевого одношарового покриття з елементами із гнутих швелерів. Така конструкція складається з типового монтажного шестикутного елемента, що вирізняється тим, що всі елементи виконані з однакового перетину швелерів, монтажні стики – на самонарізних гвинтах, що дозволяє зменшити металоемність з'єднання і прискорити монтаж, а також спростити транспортування. Конструкція покриття заводського виготовлення з дрібних типових чи великорозмірних плоских елементів застосовується для сталевого покриття споруд з профільованим настилом прогонами 12 м і більше. Для більших прогонів можна застосовувати гнуті елементи товщиною 4 – 6 мм, тоді допускається нарізання однакових елементів зі скошеними краями і зварювання їх між собою. Розміри елементів визначаються розрахунком відповідно обумовлених замовником прогонів. Розрахункові схеми цього типу конструкцій, побудовані в програмному комплексі SCAD, мають конфігурацію прямокутника або квадрата, а спирання відбувається по контуру чи з двох сторін; можливе застосування проміжних опор (колон)

**Ключові слова:** ґратчаста структурна система, конструкція, шестикутник, гнуті елементи, розрахункова модель, гнутий швелер



## Introduction

The use of space-rod structures is not a new technology: construction with their use has more than half a history century. Diagrid structural systems were most often used in civil construction, where it was required to cover spans of more than 30-40 m with minimal metal costs. At the beginning of the industry development, diagrid structural systems were used in their simplest geometric forms - domes.

This was due to the relative simplicity in calculating individual structural elements. The first domes were designed by Richard Fuller in the 40s of the last century. Fuller decomposed the dome structure into triangles, the sides of which are located on lines connecting two points on a curved surface. This design made it possible to cover the maximum possible space using the least amount of building materials. The works of R. Fuller brought their results: the world community drew attention to a new promising type of structures, which made it possible to create several interesting projects in the following decades [1].

A new vector of industry development was set relatively recently, due to the improvement and widespread computer technology introduction. The emergence of new computer-aided design systems and programs allowed us to go beyond the simplest diagrid structural systems configurations, to build not only domes, but also to give objects a shapes variety. Nowadays, huge data amounts can be processed automatically, and a large number of similar structural elements that differ in a small range of parameters can be created in semi-automatic mode with minimal human input. For this reason, with the diagrid structures various configurations appearing, the proposed topic is gaining more and more relevance.

## Review of research sources and publications

Diagrids are advanced framing systems composed of diagonal steel grids [1]. Developed a decade ago for spectacular buildings like the Swiss Re (the gherkin) in London, diagrid structures connect a breathtaking appearance with tangible advantages: a massive reduction in material use, a gain of available floor surface area and more flexibility. For the first time, this book gives a comprehensive account of the key aspects of this structural system. Diagonalized grid structures have emerged as one of the most innovative and adaptable approaches to structuring buildings in this millennium. The diagrid system variations have evolved to the point of making its use non exclusive to the tall building. Diagrid construction is also to be found in a range of innovative midrise steel projects. The paper [2] will examine developments in the recent history of diagrid buildings to include the design and detailing. Images by author unless otherwise noted in [3].

In recent time diagrid structures are often used as the main framework for high-rise buildings due to structural efficiency and unique geometry. System structural features allow to design the most innovative architectural solutions in the form and layouts of the building. Author of the article [4] considered the

possibility of using a diagrid system for construction of low-rise public buildings and the effectiveness of such a solution. The article [4] describes the shell frame design and the impact loads calculation. The calculation results were compared with a structure with a regular grid of columns. Conclusions about the effectiveness of the diagrid structures use are described.

The diagrid structural system has been widely used for recent tall buildings due to the structural efficiency and aesthetic potential provided by the unique geometric system configuration. The paper [5] presents a stiffness-based design methodology for determining preliminary member sizes of steel diagrid structures for tall buildings. The methodology is applied to diagrids of various heights and grid geometries to determine the optimal grid configuration of the diagrid structure within a certain height range. Constructability is a serious issue in diagrid structures because the nodes of diagrids are more complicated than those of conventional orthogonal structures. The paper [5] also presents various strategies to improve constructability of diagrids through prefabrication of the nodes.

Diagrid structural systems are emerging as structurally efficient as well as architecturally significant assemblies for tall buildings. The paper [6] presents a simple methodology for determining preliminary member sizes. The methodology is applied to a set of building heights ranging from 20 to 60 stories, and parameters for the optimal values of the grid geometry are generated for representative design loadings. These values are shown to be useful for architects and engineers as guidelines for preliminary design.

Diagrid structures are prevalently used for today's tall buildings due to their structural efficiency and architectural aesthetic potentials. The paper [7] studies structural performance of diagrid systems employed for complex-shaped tall buildings such as twisted, tilted and freeform towers. For each complex form category, tall buildings are designed with diagrid systems, and their structural efficiency is studied in conjunction with building forms. In order to investigate the impacts of variation of important geometric configurations of complex-shaped tall buildings, such as the rate of twisting and angle of tilting, parametric structural models are used for this study. Based on the study results, design considerations are discussed for the efficient use of diagrid structures for complex-shaped tall buildings.

Characteristics and stiffness-based preliminary design methodology of diagrid structures are discussed in [8]. The design methodology is applied to a set of diagrid structures, 40, 50, 60, 70, and 80 stories tall. The diagrid structure of each storey height is designed with diagonals placed at various uniform angles as well as gradually changing angles along the building height in order to determine the optimal uniform angle for each structure with a different height and to investigate the structural potential of diagrids with changing angles. Based on these design studies, design guidelines are provided for the optimal configuration of the diagrid structure grid geometry within a certain height range.

Diagrid systems have stronger structural efficiency than other systems like braced systems. Diagrid systems have unique geometric configuration used for various heights of tall structure. Geometric configurations and grid geometries of diagrid structure depends on the heights and angle of the diagrids. Joints of diagrid structure are more complicated than conventional structure therefore Construction of diagrid structure is complicated than conventional structure. In early days tall buildings have importance due to their architectural view and diagrid structure have better architectural view as well as good structural stability. Recent forms in tall structures have complex shapes like tapered, twisted and tilted. The paper [9] includes required data, model, Earthquake and Wind analysis of Braced Tube Structure and diagrid structure with Circular, Square and Rectangular plan. Then by keeping the same plan area and structural data for circular, square and rectangular plan, Earthquake and Wind analysis result of both Braced Tube and Diagrid Structures is carried out and by comparing the braced tube structures results and diagrid structures results conclusions drawn from the present investigation.

In the paper [10], an overview on application of such typology to high-rise buildings is carried out; in particular, in the first part of the paper, the diagrid systems peculiarities are described: starting from the analysis of the internal forces arising in the single diagrid module due to vertical and horizontal loads, the resisting mechanism of diagrid buildings under gravity and wind loads is described, and recent researches and studies dealing with the effect of geometry on the structural behavior are discussed. In the second part of the paper [10] a comparative analysis of the structural performance of some recent diagrid tall buildings, characterized by different number of stories and different geometries, namely the Swiss Re building in London, the Hearst Headquarters in New York and the West Tower in Guangzhou, is carried out, and some general design remarks are derived.

The paper [12] aims at discovering the evolutionary process of diagrid structures and their progresses which leads to major breakthroughs in architectural, structural and sustainability concepts. Indeed, these recent advances are investigated and reported for architects and engineers. The results, based on case studies, show that these structures have been able to address most of the designing requirements. They have also been used in different projects with totally different heights, areas and functions, suggesting diamond modules can be applied not only for high-rises but for a wide range of projects.

Recently diagrid structural systems have been adopted in tall buildings due to its structural efficiency and flexibility in architectural planning [13]. Compared to closely spaced vertical columns in framed tubes, diagrid structure consists of inclined columns on the exterior surface of the building. Due to inclined columns lateral loads are resisted by axial action of the diagonal compared to bending of vertical columns in framed tube structure. Diagrid structures generally do

not require cores because lateral shear can be carried by the diagonals on the building periphery.

Recently a diagrid structural system has been adopted in tall buildings due to its structural efficiency and flexibility in architectural planning. Diagrid structures consist of inclined columns on the exterior surface of buildings compared to closely spaced vertical columns in framed tubes. The lateral loads are resisted by axial action of the diagonal. In the paper [14], the comparison study of 20-storey simple frame building and diagrid structural system building is presented in [14].

#### **Definition of unsolved aspects of the problem**

For a long period of light metal structures development, scientists around the world have been studying the problems of designing diagrid structural systems and selecting methods for calculating them. The issue of developing new effective design solutions remains relevant and requires further research and suggestions.

#### **Problem statement**

The purpose of this work is to conduct a thorough analysis of existing design solutions for diagrid structural systems, as well as to identify their advantages and disadvantages. One of the main objectives of this study is to develop an easy-to-install coating of spatial hexagonal elements made of bent channels with reduced metal consumption and labor costs, assembly on the ground and installation of the coating as a whole. The research also aims to find optimal calculation methods using existing software packages.

#### **Basic material and results**

In the last 10-20 years, the so-called diagrid structural systems have become an increasingly popular solution when choosing a structural scheme of buildings with different purposes, shapes, heights and spans. In such structures, the usual vertical load-bearing elements, columns, along the perimeter of the building are replaced by inclined elements that form the diagrid structures of the building.

In this case, the internal columns are completely or partially excluded, and the loads from the floors and roof are borne by the beam or truss system, which transmits them to the diagrid structures. Also, additional diagrid elements can be created inside the building, which form a core of rigidity. Complete replacement of columns is possible due to the fact that the diagrid structural systems equally well perceive both vertical and horizontal loads on the building, as well as reduce shear and bending deformations due to the nature of the work of inclined elements.

Other design diagrid structural systems advantages include:

- increased stability, thanks to triangular elements;
- providing multiple load distribution options and reducing the possibility of failure;
- reducing the own structures weight;
- reduced material consumption.

From an architectural point of view, these structures also have a number of advantages:

- building unique shape creation both in plan and in height;
- architectural expressiveness due to diagrid elements, even with a simple building shape;
- large variation in the parameters of the load-bearing elements grid: size, angle of inclination, shape and cells number;
- large sunlight amount due to panoramic windows;
- creating column-free interiors.

Diagrid structural systems are load-bearing building structures that are made of metals, composite materials or wood. Today, the structures are relevant for the world's progressive architecture in the "high-tech" style. The mesh structure's advantage is the ability to block large spans or achieve a unique shape and architectural expression of building elements-facades and roofs.

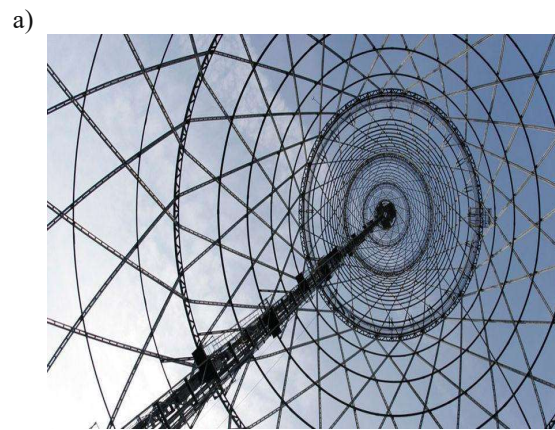
The world's first diagrid structural systems were used by engineer and inventor Vladimir Shukhov. He designed and built the 150-meter hyperboloid tower in 1922 (fig. 1, a). The inventor had a landmark-the Eiffel tower with a height of 325 m and a weight of 7300 tons. Shukhov managed to reduce the metal consumption per unit height of the structure by 14 times relative to the tower in Paris. He managed to increase the expressiveness of the building elements-facades and roofs.

Today, diagrid structural systems are used quite often. Especially in Europe, America and Asia, buildings and structures for various purposes are being actively built using mesh structures. These are the skyscraper in London "the Gherkin" (fig. 1, b), the Opera house in Beijing (fig. 1, c), the British Museum (fig. 1, d), diagrid structures of research centers in Canada, etc.

One of the reasons why diagrid structures are not often designed by our specialists is the complex modeling of structures in calculation complexes. It is important to take into account the geometric and physical nonlinearity in the work of mesh structures under the loads influence in order to obtain the most reliable picture of the spatial structures stress-strain state and stability [15].

Today, the studying methods issue for modeling diagrid structures using software and computer systems is relevant. To do this, it is necessary to consider the main modern modeling structures methods – discrete and continuous.

In a discrete model, edges are represented as diagrid, beam or three-dimensional finite elements. Today, the model can be used to successfully solve problems where restrictions are imposed on critical forces or moments. The reason is the modern computers computational capabilities. Software packages for finite element modeling, such as SCAD and others, allow you to use programming to generate diagrid structures models. These programs help you determine the degree of the diagrid structures parameters influence on the critical force or moment in a short time.



**Figure 1 – Examples of the diagrid structural systems:**

- a – the Shukhov Tower in Ukraine;
- b – "the Gherkin" in London;
- c – the Opera house in Beijing;
- d) the British Museum

The continuum diagrid structure model is characterized by frequently positioned edges. This system is conditionally replaced by a solid shell, the stiffness of which takes an average value. It depends on the layout and stiffness of the forming edges. When using the continuum model, the diagrid structural systems are described by the traditional orthotropic shells equations. In this case, the issue of a correct mathematical model constructing a continuous construction with the most accurate geometric and physical properties of the real construction is relevant.

A new industry development vector was set relatively recently, due to the improvement and widespread introduction of computer technology.

The emergence of new computer-aided design systems and programmable machines allowed us to go beyond the simplest mesh structures configurations, to build not only domes, but also to give objects a shapes variety. Nowadays huge data amounts can be processed automatically, and a large number of similar structural elements that differ in a small parameters range can be created in semi-automatic mode using programs with minimal human involvement.

A characteristic diagrid structures feature is the load-bearing structures absence in the form of various columns, beams. The structure is self-supporting and in most cases has higher load-bearing properties in comparison with other structures types. This is due to the uniform load distribution on all the structure rods, which virtually eliminates brittle destruction. The dome-based structure has good aerodynamic characteristics in addition to its high load-bearing properties, which expands the applications range.

The diagrid structures assembly is carried out in a faster time and requires a magnitude order less labor compared to traditional structures. Installation does not require special construction equipment, equipment and accessories, the main working tool is a wrench.

Membrane materials are often used to cover diagrid structures. The membrane is a high-tech, universal coating. These coatings are easy to transport and install, compact and non-flammable. In a harsh climate, it is possible to use insulated membranes. In addition to the membranes, steel sheet materials, sandwich panels, etc., cut in the form of triangles can be used for coating. They are attached to each other by bolted and riveted connections.

Structures glazing is widely used. Such a coating is most attractive from an architectural and aesthetic point of view, but the glass use as an enclosing structure always leads to higher prices and an increase in metal consumption due to a decrease in the movement tolerance of structural elements and precipitation.

The designing mesh structures process is carried out in specialized computer-aided design systems software complexes. These calculation programs meet all requirements and standards.

The creating a model process and calculating strength includes several stages:

1. The surface shape and size are determined depending on the building or structure purpose, the architectural and design concept, and the customer's

wishes. There are an infinite number of surfaces used in construction.

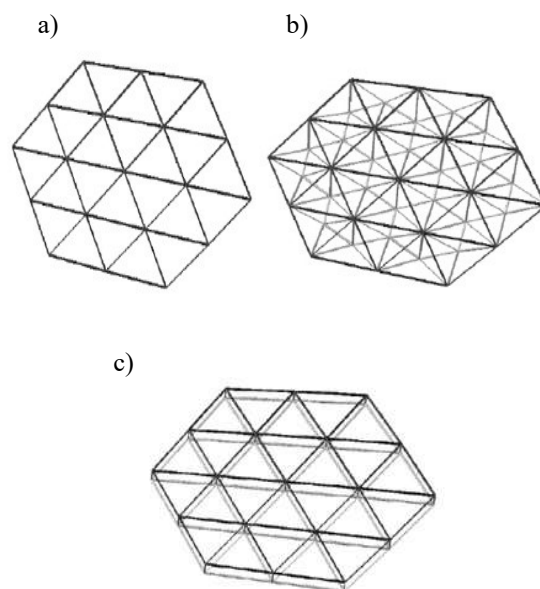
2. The pattern, shape, and size of the triangle grid cell can be different (Fig. 2). The most popular division into triangles, quadrilaterals, and hexagons is a structure based on the icosahedron vector division. A diamond-shaped partitioning system is also used, which is universal and suitable for any free-form mesh structures type. The mesh cells' frame consisting can be single-layer or multi-layer. The frame type is selected depending on the span size, seismic, climatic conditions, and other factors.

In diagrid structures with the less than 30 m diameter, a single-layer rod structure is used. For more than 30 m spans, as a rule, a two-layer truss of the first or second type is used, depending on the surface shape, external loads and the structural elements type choice.

3. When the construction model is ready, it is imported into the calculation program to determine the rod elements stiffness. Depending on the construction area, loads on the structure are selected in accordance with regulatory documents.

4. The last stage is the structure 3D model creation, design and working documentation calculation and development.

After creating the design model, it is imported into CAD, where all further design work will be performed. The construction and calculation of individual nodes and rods are carried out on the basis of the original model with fully integrated CAD tools and do not cause difficulties. However, for a structure containing tens of thousands of such elements, manual design will require a huge amount of time. In addition, the slightest change to the original design model will again require recalculation of all elements.



**Figure 2 – Structures:**

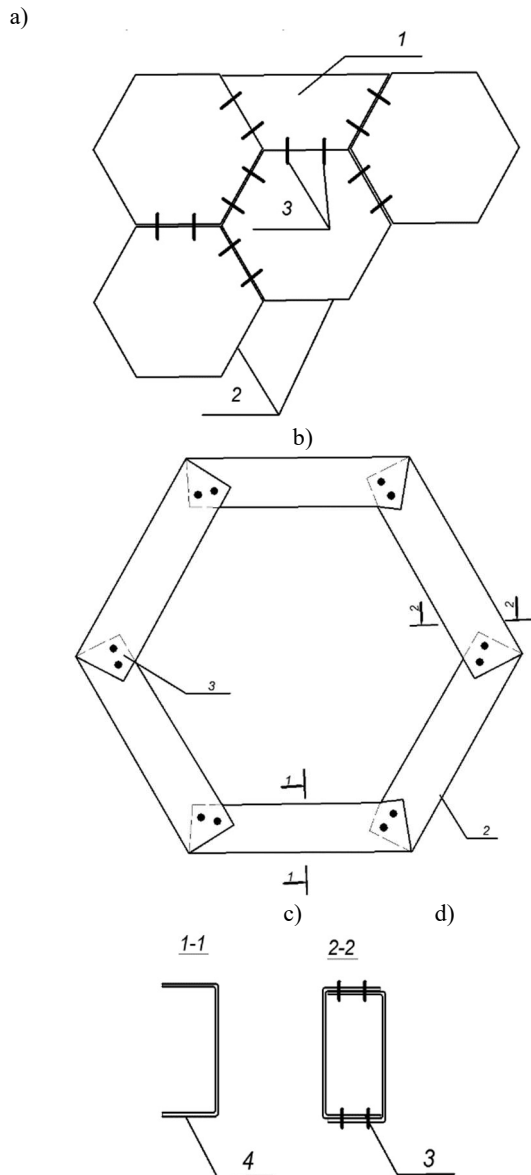
- a – single-layer structure;
- b – two-layer structure (diagonal);
- c – two-layer structure (with racks)



In the course of the study, the single-layer metal covering design with hexagonal elements made of bent channels was proposed (Fig. 3).

This diagrid design is used in flat and spatial cross systems.

This metal coatings construction type with triangular, quadrilateral elements is mainly used in diagrid domes, diagrid for various purposes. Such structures are common abroad and are effective for large spans and have the architectural expressiveness of buildings.

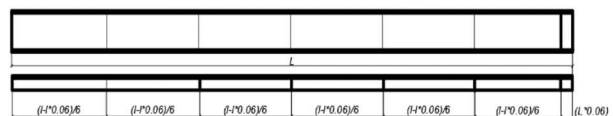


**Figure 3 – Construction of a single-layer metal covering with hexagonal elements made of bent channels:**

- a – a fragment of the coating made of hexagonal standard elements;
- b – a typical hexagonal element made of bent channel is connected on self-tapping screws;
- c – cross-section 1-1 of the bent channel,
- d – cross-section 2-2 of the connection of channel belts on self-tapping screws, (bolts according to calculation) [16]

Notes: end elements (1); hexagonal elements (2) obtained from a straight channel, then bent (4) and connected on self-tapping screws (3) for rigidity.

A special feature of the coating is the use of rectilinear bent channels, which can be cut and connected in the form of a hexagonal element separately (fig.4), or in the form of blocks with the best dimensions for transportation and subsequent installation. Assembly elements of these structures are manufactured in metal structure factories in the form of flat hexagonal elements to simplify delivery and are connected on the construction site using self-tapping screws or bolts according to the calculation.



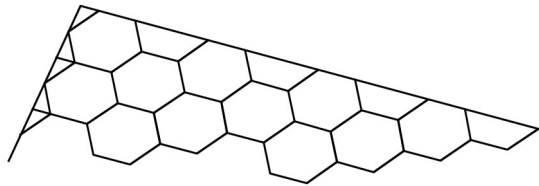
**Figure 4 – Diagram of a hexagon blank from a rectilinear bent channel**

The construction of a metal covering with spatial hexagonal elements from bent channels consists of: mounting end elements; mounting hexagonal elements obtained from a rectilinear channel marked on equal sections and at equal distances and a clipped shelf, then bent and connected on self-tapping screws for rigidity. Hexagons can be transported to the construction site separately, or connected in flat elements to simplify transportation and subsequent large-size installation. The structure is assembled on the ground and only then transferred to the design position on the walls or on the columns.

In general, all elements of the proposed design, performed according to the design calculation, are made of channels. A technological feature of the design of a metal covering with spatial hexagonal elements made of bent channels is the use of self-tapping screws on the construction site to obtain structures with minimal weight. Factory-made covering design made of small standard or large-sized flat elements. It is used for steel structures' covering with profiled flooring with spans of 12 m or more.

For larger spans, it is possible to use bent elements of a larger thickness of 4-6 mm, then we allow cutting identical elements with beveled edges and welding together. The element dimensions are determined by spans calculation, respectively, agreed by the customer. These type calculation schemes (fig.5) structures have a rectangle or square configuration. Support occurs along the contour or on both sides. It is possible to use intermediate supports (columns). In calculations, we accept the actual channel cross-sections. The criteria for load-bearing capacity are the ultimate strength and deformation.

Diagrid structural systems are used in the triangular and diamond-shaped grids form. An example of such an application is the dome "Climatron" of B.Fuller (fig. 6).



**Figure 5 – Fragment of the calculation scheme of the SCAD program**



**Figure 6 – The Dome "Climatron" (B. Fuller) [1]**

## Conclusions

The widespread diagrid structural systems use is constrained by the difficulties of designing, modeling, and calculating such structures. It is necessary to introduce new and atypical software complexes and related disciplines into the educational process in order to obtain in-depth knowledge in the programming and mathematical analysis field. The training of new highly specialized engineering personnel will allow us to put into practice the architects ideas.

Discrete and continuous models serve as complementary methods for modeling diagrid structures. The discrete model shows reliable results with a sparse grid step, or a small finite elements number. The continuum model is more suitable for a compacted grid and allows you to use the theory of differential equations to simplify the problem solution.

Diagrid structures are certainly one of the most promising areas in construction. They justify the name "structures of the XXI century", as they were dubbed by engineers. This is evidenced by the steadily growing structures number made using this technology and the customers interest. The technology potential is great, specialists predict special prospects for structures in the almost unlimited architectural forms possibilities, successful application in changing climatic conditions. But to realize this potential, many more developments in the materials science field, design automation, and building codes will need to be completed.

As the analysis result, the design of a single-layer metal covering with hexagonal bent channels elements was proposed.

## References

1. Boake T.M. (2014). *Diagrid Structures: systems, connections, details*. Basel, Switzerland: Birkhauser.
2. Boake T.M. (2013). *Diagrid Structures: Innovation and Detailing. Structures and Architecture (New concepts, applications and challenges)*, London, Taylor&Francis Group, 991-998.
3. Boake T.M. (2012). *CISC Guide for Specifying Architecturally Exposed Structural Steel, Canadian Institute of steel construction*: Copyright, 48.
4. Semashkina D.O. (2018). Diagrid systems for low-rise buildings, *Construction of Unique Buildings and Structures*, 1 (64), 36-49.  
<https://doi.org/10.18720/CUBS.64.3>
5. Moon K. (2009). *Design and Construction of Steel Diagrid Structures*. NSCC, School of Architecture. Yale University. New Haven. USA, 398-405.
6. Moon K., Connor J.J. & Fernandez J.E. (2009). Diagrid Structural Systems for Tall Buildings: Characteristics and Methodology for Preliminary Design. *The Structural Design of Tall and Special Buildings*, 16.2, 205- 223.  
<https://doi.org/10.1002/tal.311>
7. Moon K. (2011). Diagrid structures for complex-shaped tall buildings. *Procedia Engineering*, 14, 1343-1350.  
<https://doi.org/10.1016/j.proeng.2011.07.169>
8. Moon K. (2008). Optimal Grid Geometry of Diagrid Structures for Tall Buildings. *Architectural Science Review*, 51, 239-251.  
<https://doi.org/10.3763/asre.2008.5129>
1. Boake T.M. (2014). *Diagrid Structures: systems, connections, details*. Basel, Switzerland: Birkhauser.
2. Boake T.M. (2013). *Diagrid Structures: Innovation and Detailing. Structures and Architecture (New concepts, applications and challenges)*, London, Taylor&Francis Group, 991-998.
3. Boake T.M. (2012). *CISC Guide for Specifying Architecturally Exposed Structural Steel, Canadian Institute of steel construction*: Copyright, 48.
4. Semashkina D.O. (2018). Diagrid systems for low-rise buildings, *Construction of Unique Buildings and Structures*, 1 (64), 36-49.  
<https://doi.org/10.18720/CUBS.64.3>
5. Moon, K. (2009). *Design and Construction of Steel Diagrid Structures*. NSCC, School of Architecture. Yale University. New Haven. USA, 398-405.
6. Moon K., Connor J.J. & Fernandez J.E. (2009). Diagrid Structural Systems for Tall Buildings: Characteristics and Methodology for Preliminary Design. *The Structural Design of Tall and Special Buildings*, 16.2, 205- 223.  
<https://doi.org/10.1002/tal.311>
7. Moon K. (2011). Diagrid structures for complex-shaped tall buildings. *Procedia Engineering*, 14, 1343-1350.  
<https://doi.org/10.1016/j.proeng.2011.07.169>
8. Moon K. (2008). Optimal Grid Geometry of Diagrid Structures for Tall Buildings. *Architectural Science Review*, 51, 239-251.  
<https://doi.org/10.3763/asre.2008.5129>

9. Chittaranjan N. & Snehal W. (2020). Optimal Structural Design of Diagrid Structure for Tall Structure. *System Reliability, Quality Control, Safety, Maintenance and Management*, 263-271  
[https://doi.org/10.1007/978-981-13-8507-0\\_39](https://doi.org/10.1007/978-981-13-8507-0_39)

10. Mele E., Toreno M., Brandonisio G. & De Luca A. (2012). Diagrid structures for tall buildings: case studies and design considerations. *The Structural Design of Tall and Special Buildings*, 2, 124-145.  
<https://doi.org/10.1002/tal.1029>

11. Mele E., Montuori G.M., Brandonisio G. & De Luca, A. (2014). Geometrical patterns for diagrid buildings: Exploring alternative design strategies from the structural point of view. *Engineering Structures*, 71, 112-127  
<https://doi.org/10.1016/j.engstruct.2014.04.017>

12. Korsavi S. & Maqhareh M.R. (2014). The Evolutionary Process of Diagrid Structure Towards Architectural, Structural and Sustainability Concepts: Reviewing Case Studies. *Journal of Architectural Engineering Technology*, 3, 2-12.  
<https://doi.org/10.4172/2168-9717.1000121>

13. Khushbu J. & Pares V.P. (2013). Analysis and Design of Diagrid Structural System for High Rise Steel Buildings. *Procedia Engineering*, 51, 92-100.  
<https://doi.org/10.1016/j.proeng.2013.01.015>

14. Nishith B.P. & Vinubhai R.P. (2014). Diagrid structural system: Strategies to reduce lateral forces on high-rise buildings. *International Journal of Research in Engineering and Technology*. 3, 374-378.  
<https://doi.org/10.15623/ijret.2014.0304067>

15. Петренко Ф.И. (2018). *Расчёт сетчатых оболочек отрицательной гауссовой кривизны с учётом геометрической и физической нелинейности* (Автореф. дис. канд. тех. наук). МГУПС, Москва, 24.

16. Чичулін В.П., Чичуліна К.В. (2020). Патент 144877 Україна. *Конструкція металевого покриття з просторовими шестикутними елементами із гнутих швелерів*. Національний університет «Полтавська політехніка імені Юрія Кондратюка».

9. Chittaranjan N. & Snehal W. (2020). Optimal Structural Design of Diagrid Structure for Tall Structure. *System Reliability, Quality Control, Safety, Maintenance and Management*, 263-271  
[https://doi.org/10.1007/978-981-13-8507-0\\_39](https://doi.org/10.1007/978-981-13-8507-0_39)

10. Mele E., Toreno M., Brandonisio G. & De Luca A. (2012). Diagrid structures for tall buildings: case studies and design considerations. *The Structural Design of Tall and Special Buildings*, 2, 124-145.  
<https://doi.org/10.1002/tal.1029>

11. Mele E., Montuori G.M., Brandonisio G. & De Luca, A. (2014). Geometrical patterns for diagrid buildings: Exploring alternative design strategies from the structural point of view. *Engineering Structures*, 71, 112-127  
<https://doi.org/10.1016/j.engstruct.2014.04.017>

12. Korsavi S. & Maqhareh M.R. (2014). The Evolutionary Process of Diagrid Structure Towards Architectural, Structural and Sustainability Concepts: Reviewing Case Studies. *Journal of Architectural Engineering Technology*, 3, 2-12.  
<https://doi.org/10.4172/2168-9717.1000121>

13. Khushbu J. & Pares V.P. (2013). Analysis and Design of Diagrid Structural System for High Rise Steel Buildings. *Procedia Engineering*, 51, 92-100.  
<https://doi.org/10.1016/j.proeng.2013.01.015>

14. Nishith B.P. & Vinubhai R.P. (2014). Diagrid structural system: Strategies to reduce lateral forces on high-rise buildings. *International Journal of Research in Engineering and Technology*. 3, 374-378.  
<https://doi.org/10.15623/ijret.2014.0304067>

15. Petrenko F.I. (2018). *Calculation of diagrid structural of negative Gaussian curvature, taking into account geometric and physical nonlinearity*. (PhD in Engineering). MGUPS, Moscow, 24.

16. Chichulin V.P. & Chichulina K.V. (2020) Patent 144877 Ukraine: *Construction of a metal covering with spatial hexagonal elements made of bent channels*. National University «Yuri Kondratyuk Poltava Polytechnic».

UDC 624.075

## Properties and improvement directions of software of single-storey buildings with frame structures

Hudz Serhii<sup>1\*</sup>, Horb Oleksandr<sup>2</sup>, Pents Volodymyr<sup>3</sup>, Dariienko Viktor<sup>4</sup>

<sup>1</sup> National University «Yuri Kondratyuk Poltava Polytechnic» <https://orcid.org/0000-0002-4764-8635>

<sup>2</sup> National University «Yuri Kondratyuk Poltava Polytechnic» <https://orcid.org/0000-0003-3104-7621>

<sup>3</sup> National University «Yuri Kondratyuk Poltava Polytechnic» <https://orcid.org/0000-0001-9580-1457>

<sup>4</sup> Central Ukrainian National Technical University <https://orcid.org/0000-0001-9023-6030>

\*Corresponding author E-mail: [goods.sergiy@gmail.com](mailto:goods.sergiy@gmail.com)

The main stages of creating a spatial model of the steel frame are considered for industrial buildings or warehouses with a pitched roof. Different approaches to the analysis of internal forces of the first and second orders and the stability calculation for steel elements of building structures under the combined action of compression and transverse bending are highlighted using software applications. Ways to improve the process of creating a calculation model, design documentation, and working drawings are outlined. A comparison of specialized software products for calculating building models with portal frames (Autodesk Robot Structural Analysis Professional, PortalPlus, Consteel, Tekla Structural Designer, and Dlubal RFEM) is presented. Their advantages and disadvantages are indicated

**Keywords:** software, spatial model, portal frame, buckling, restraint

## Властивості та напрями вдосконалення програмного забезпечення для розрахунку одноповерхових будівель з рамними конструкціями

Гудзь С.А.<sup>1\*</sup>, Горб О.Г.<sup>2</sup>, Пенц В.Ф.<sup>3</sup>, Дарієнко В.В.<sup>4</sup>

<sup>1, 2, 3</sup> Національний університет «Полтавська політехніка імені Юрія Кондратюка»

<sup>4</sup> Центральнотехнічний національний технічний університет

\*Адреса для листування E-mail: [goods.sergiy@gmail.com](mailto:goods.sergiy@gmail.com)

Розглянуто основні етапи створення просторової моделі сталевих каркасів для промислових будівель або складів зі скатною покрівлею. Висвітлено різні підходи до проведення аналізу внутрішніх зусиль першого та другого порядків і виконання розрахунку стійкості сталевих елементів будівельних конструкцій при сумісній дії стиску й поперечного згину із застосуванням прикладних засобів програмного забезпечення. Намічено шляхи вдосконалення процесу створення розрахункової моделі, проектної документації та робочих креслень. Наведено порівняння спеціалізованих програмних продуктів для розрахунку моделей будівель із порталними рамами (Autodesk Robot Structural Analysis Professional, PortalPlus, Consteel, Tekla Structural Designer і Dlubal RFEM), указано їхні переваги та недоліки. Встановлено, що для збільшення точності розрахунків і наближення їх до дійсних умов роботи конструкції внутрішні зусилля потрібно визначати в просторовій моделі за нелінійною теорією другого порядку. У процесі обчислення коефіцієнта стійкості при згині доцільно врахувати крутильну або крутильну та зсувну жорсткість конструкцій, що розкріплюють стиснутий пояс елементів, схильних до втрати стійкості. Зокрема, хрестові в'язі частково сприймають, розподіляють і передають на основу горизонтальні навантаження на будівлю. Крім цього, вони забезпечують просторову жорсткість будівлі та слугують для розкріплення і зменшення розрахункової довжини елементів рами. В'язі можуть не тільки виконувати свою безпосередню функцію, але й ефективно використовуватися для розкріплення сталевих елементів з метою уникнення втрати стійкості, таким чином зменшуючи ступінь використання перерізу і витрати сталі. Розглянуто конструктивні заходи для усунення явища втрати просторової стійкості лінійних елементів поперечної рами каркаса будівлі при сумісній дії стиску, поперечного згину та кручення. Приєднані до елемента різного роду другорядні конструкції, в тому числі встановлені планомірно, збільшують його жорсткість і перешкоджають деформуванню. Проаналізовано вплив розкріплення на несучу здатність

**Ключові слова:** програмне забезпечення, просторова модель, портална рама, втрата стійкості, розкріплення



## Introduction

Conventional mathematical models do not characterize all the behavior features of the frame structure in the building framework, especially with significant rigidity of the connected elements. In such cases, the simulation often has little in common with the actual processes, does not correspond to the real picture of the stress-strain state, and needs refinement to adequately reflect the using degree of the cross-section by stress required to ensure the reliability of the structure as a whole. To increase the accuracy of calculations and bring them closer to the actual operating conditions of the structure, the internal forces must be determined in a spatial model by a nonlinear theory of the second order. It takes into account the geometric nonlinearity and is essentially the calculation of the deformed scheme, in which the equilibrium equations are written for the deformed state of the system. By buckling from compression, bending and torsion in the vertical or inclined element of the portal frame, which acts as a beam-column in a complex stress-strain state, several deformations occur simultaneously. The spatial deformed state of the rod consists of the angle of rotation around the longitudinal axis, as well as displacements in the direction of the horizontal axis  $y$  and vertical axis  $z$  in cross-section, respectively (curvature and deflection).

## Review of the research sources and publications

The transverse frames linear elements stability issue taking into account all possible factors, in the spatial setting for different types of loads, boundary conditions, and cross-sections is already practically solved in scientific and technical schools of Western Europe at the level of theory, rationing and programming. Issues of operation and behavior of thin-walled load-bearing elements of frame structures under complex loads are covered in great detail. So, the articles [1 – 4] are devoted to the advanced design and geometrical optimization of steel portal frames. The papers [5, 6] present the influence of the diaphragm effect on the behavior of pitched roof portal frames. The purpose of the research is to make a comparison between the simplified design model of a portal frame, where the supports simulating the purlins are considered with infinite axial rigidity, and a portal frame design model where the calculated stiffness of the cladding for the lateral supports is introduced manually. The approbation of the second-order theory in the works [7, 8] demonstrates that insufficient restrained structure in an elastic stage is very sensitive to the load and curvature change, therefore, by determining the bearing capacity consideration of braces rigidity possibly will be effective.

## Definition of unsolved aspects of the problem

Not solved before a part of the problem is the allocation of those points, to which need to pay special attention by the analysis, design, and calculation of portal frames for built model compliance with real work of structures at complex resistance. As a research task, it was decided to compare different software products for the design of the structures.

## Problem statement

We will analyse and identify ways to solve the problem of determining the load-bearing capacity of steel beams and columns, which are part of the portal frames and prone to loss of overall (spatial) stability, as well as the problem of expanding options and improving the design of single-storey buildings.

## Basic material and results

The tendency of the element to instability arises due to its considerable flexibility and insufficient fastening of the compressed flange by attached structures, which include: monolithic and prefabricated reinforced concrete slabs; steel flat and profiled flooring, sandwich panels and other enclosing structures; girders, purlins, floor beams, and other secondary beams; discrete bracings (horizontal cross bracings, strands). The first two types of structures can be attributed to continuous bracings, the other two belong to discrete ones. These structures reduce the calculated effective length of the beam and increase its overall stability. In construction, thin-walled structures that work in conjunction with the load-bearing flooring are widely used. For coatings of industrial and civil frame buildings due to high-efficiency light roofs are often used, consisting of purlins, which can support on the main beams (rafters) on top or adjacent to them at the same level, and steel profiled sheet, the rigidity of which when fixed to the upper flange is used to increase the stability and fixing of the beams from twisting. Also, the stabilization of the beams can be done through the arrangement of structural parts: rafter stays, flat and three-dimensional stiffeners, protrusions of the beams in the supporting areas, and the adjacency to the columns in the supports. Where the compressive flange is not laterally supported, additional elements should be provided to ensure a torsional or lateral restraint in selected cross-sections of the rafter. Such elements could be inclined bars (rafter stays) connecting the compressive flange with the purlins or longitudinal bars anchored at rigid parts of the overall structure.

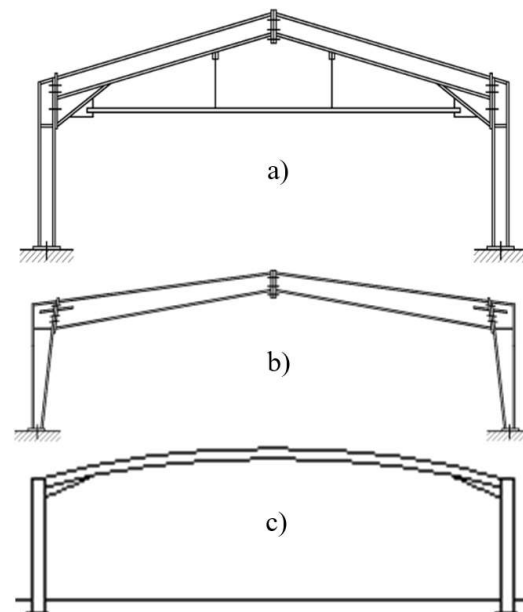
To check the stability of the steel element, it was decided to determine the stresses in the compressed flange and compare them with critical ones, which were equal to the calculated resistance of steel (yield strength) multiplied by the stability factor, which depends on the design scheme, geometric cross-sectional properties, and distance between points of compressed flange restraining. To determine the conditional flexibility for lateral-torsional buckling, depending on which the decreasing coefficient of bending stability is set according to European standards, it is necessary to know the elastic critical moment for lateral-torsional buckling. Its value for the I-beam hinged at the ends, loaded with an evenly distributed load, can be set following building codes. In other cases, it is recommended to quantify the critical moment by simulation. For a rod hinged at the ends, loaded with an evenly distributed load and reference bending moments, there is a method of determining the critical moment. Under such conditions and different boundary conditions and types of loads, it is recom-

mended to use a special free LTBeam program. A critical moment is required to calculate the insufficiently restrained bending steel I-elements by the lateral-torsional buckling. In addition, it is sometimes advisable to take into account the rotational or rotational and shear stiffness of structures that discretely or continuously restrain the compressed flange of the beam in most practical cases and reduce the deformation of its displacement. Taking into account the rounding at the junction of the flange to the web allows you to significantly increase the value of the torsional constant required for calculations. It can also be identified in this common computer program.

Taking into account the main factors that characterize the special operating conditions of the steel rod element with complex resistance and providing spatial stability for reliable operation of the structure without failures due to detailed analysis, allows you to more accurately determine the value of internal forces. This affects the overall stress-strain state of the structure and determines the calculated ratio of normal stresses, and therefore has a positive effect on the level of use and strength of the material.

In particular, the cross bracings partially receive, distribute and transmit the horizontal loads on the building pavement. Besides, they provide the spatial rigidity of the building and serve to secure and reduce the effective length of the frame elements. Bracings can not only perform their direct function but can also be used effectively to restrain steel elements to avoid loss of stability, thus reducing the use of cross-section and steel consumption.

The process of creating a calculated schematic model of a single-storey building should, taking into account the current state of development of computer technology, describe in as much detail, accurately, and conveniently as possible the structural relationships between the various elements of the building system. The process should include the following basic steps, maintaining a balance between structuring, the speed of obtaining the final results through automation, and ease of use (for example, testing the Frame Generator Autodesk Robot Structural Analysis Professional 2021). When creating steps and spans of load-bearing elements of the building in the window of the Frame Generator, which is the first stage of modeling, the number of structural elements in the transverse and longitudinal directions is indicated. If necessary, it is possible to create a geometric grid of complex shapes. In the next step, the geometry of the roof (flat, one- or two-slope), the size of the transverse frame, the type of supports (hinge, rigid clamping), cross-sections of columns and beams, steel grade are described. When choosing the type of rafter and its design, not all outline schemes are specified. In particular, the scheme with a puff (tied portal frame), the scheme with welded rafter and column cross-sections with linearly variable height, or the curvilinear scheme (curved rafter portal frame) is not presented. These schemes are shown in Figure 1.



**Figure 1 – Restraining points between bracings and buckling coefficients definition**

In a tied portal frame (Figure 1,a) the horizontal movement of the eaves and the bending moments in the columns and rafters are reduced. A tie may be useful to limit spread in a crane-supporting structure. The high axial forces introduced in the frame when a tie is used necessitate the use of second-order software when analysing this frame form.

Large spans over 30 m can also be overlapped with solid-wall frames. For such large hall dimensions, completely welded construction is shown in Figure 1,b. The welding of two flanges sheets and a web sheet for rafter and column cross-sections with linearly variable height is done using automatic welding machines, the fillet welds with larger length can produce economically. The high, slender webs of the welded I-section are prone to buckling, so buckling stiffeners may be required, as for the welded structures used in bridge construction.

Portal frames may be constructed using curved rafters (Figure 1,c), mainly for architectural reasons. Because of transport limitations, rafters longer than 20 m may require splices, which should be carefully detailed for architectural reasons.

The curved member is often modelled for analysis as a series of straight elements. Alternatively, the rafter can be fabricated as a series of straight elements. It will be necessary to provide purlin cleats of varying heights to achieve the curved external profile.

Next is the process of creating sections, grids, chords for through rafter (braces, racks, support braces). It is also necessary to cover the floor slabs (if any, their type, location, size of beams, columns, supports, slab cross-section of reinforced concrete platform). Eaves, cantilevers, and roof parapets are described by size, location, cross-sections. Creation of haunches between a column and a beam, haunch of beams in a roof ridge provides types of cross-sections, the sizes (height and width). Next is the design of the purlins: their number, deviations from the edges and the middle of the span,

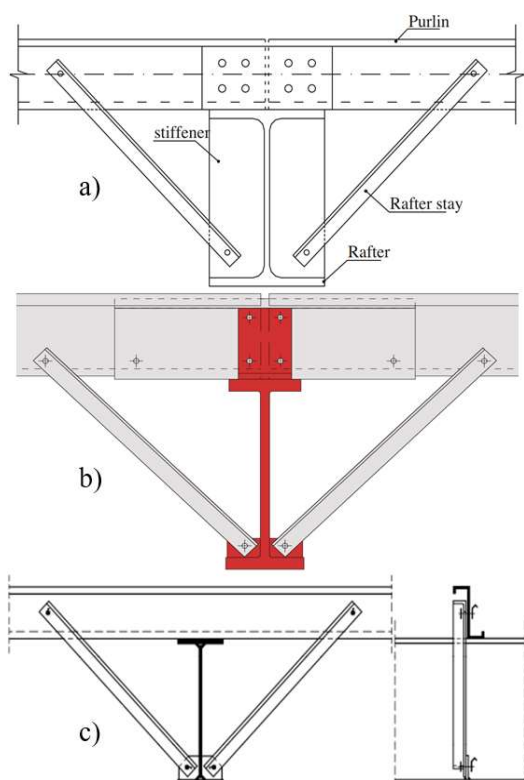
the type of scheme (single, continuous), the rafter stays, puffs. But the rafter stays are not reflected in the model and therefore do not have a geometric description. Layouts of vertical bracings and bracings on the roof require more detail, as well as the scheme of the outer wall (columns, beams, bracings can be in different variations).

During initial design, the rafter members are normally selected according to their cross-sectional resistance to bending moment and axial force. In later design stages stability against buckling needs to be verified and restraints positioned attentively.

The buckling resistance is likely to be more significant in the selection of column size, as there is usually less freedom to position rails to suit the design requirements; rail position may be dictated by doors or windows in the elevation.

If introducing intermediate lateral restraints to the column is not possible, the buckling resistance will determine the initial cross-section size selection. It is therefore essential to recognise at this early stage if the side rails may be used to provide restraint to the columns. Only continuous side rails are effective in providing restraint. For example, side rails interrupted by roller shutter doors, cannot be relied on as providing adequate restraint.

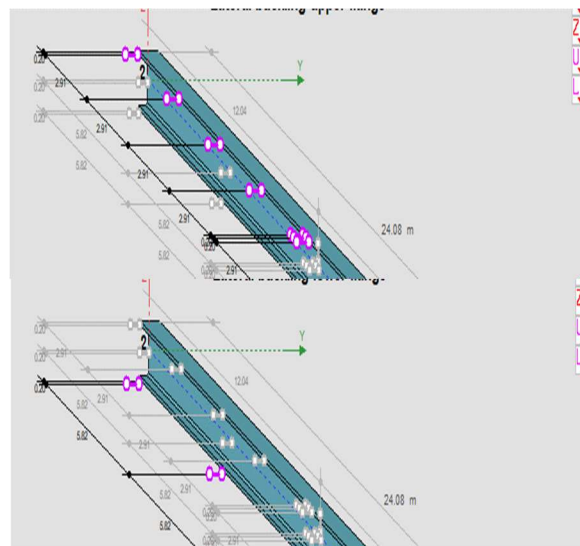
Where the compression flange of the rafter or column is not restrained by purlins and side rails, restraint can be provided at specified locations by column and the rafter stays to the inside flange (Fig. 2).



**Figure 2 – Torsional restraint of a rafter with a lower flange under compression through rafter-stays**

a – with stiffeners; b, c – with short local connectors

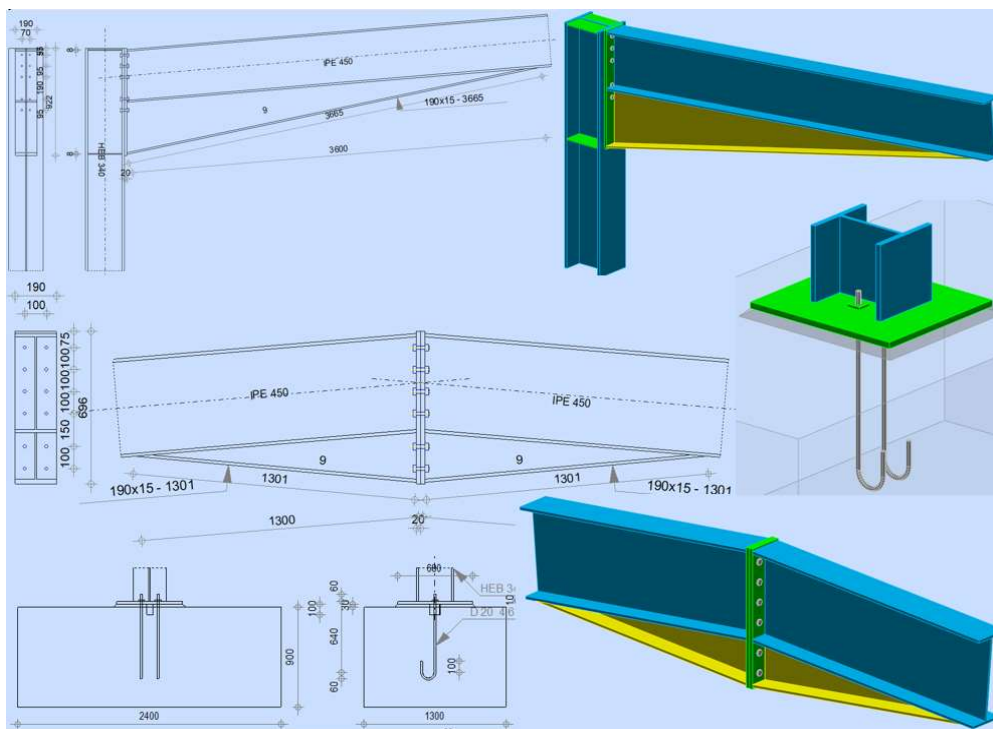
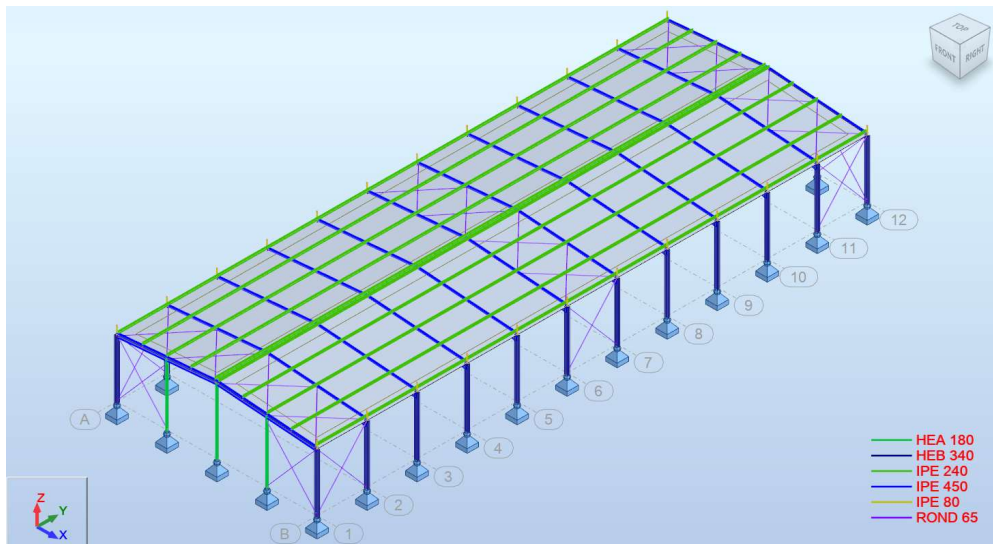
Purlins attached to the top flange of the rafter provide stability to the member in several ways: direct lateral restraint, when the outer flange is in compression; intermediate lateral restraint to the tension flange between torsional restraints, when the outer flange is in tension; torsional and lateral restraint to the rafter when the purlin is attached to the tension flange and used in conjunction with rafter stays to the compression flange. Initially, the out-of-plane checks are completed to ensure that the restraints are located at appropriate positions and spacing. Unfortunately, the restraining points are not set automatically (Fig. 3) after creating a model in the Frame Generator, which requires additional time.



**Figure 3 – Restraining points between bracings and buckling coefficients definition**

Although efficient portal frame analysis and design will use special software, which is likely to be using elastic-plastic analysis, initial manual elastic analysis is simple. In most circumstances, a reasonable estimate of the maximum bending moments will be obtained by considering only the vertical loads. Appropriate cross-sections can then be chosen based on this analysis. For the initial analysis, it is common to assume that the second moment of area of the column is 1,5 times that of the rafter section. For the pinned base frame, the bending moments at the eaves and apex can be calculated following [9, 10].

It is probably that many portal frames will be sensitive to second-order effects, which are likely to increase the design moments by up to 15%. If undertaking a preliminary analysis, bending moments from a first-order analysis should be amplified to allow for these effects. Calculation of boundary conditions, verification, and selection of cross-sections include stability testing by EN 1993-1-1. Loads in the Frame Generator can be constant, variable, crane, meteorological. The parameters of wind and snow include speed, pressure, terrain, unexpected precipitation. Explanatory notes, drawings, spatial view of the main components (with joints) are generated automatically (Fig. 4) but require some refinement and adjustment manually.



**Figure 4 – Design model of the building framework; drawings, spatial view of the main bolted and welded joints**

Let's compare different software for the portal frame design. Advantages of Autodesk Robot Structural Analysis Professional [11] are next:

- automation and speed of model creation;
- the Frame Generator with a user-friendly interface;
- integration with other products.

Disadvantages of Autodesk Robot:

- the need to refine the model;
- sharpening under reinforced concrete structures;
- simplified export to Advance Steel.

Advantages of Consteel, Tekla Structural Designer, and Dlubal RFEM:

- accuracy, versatility and systematization;
- profile for steel structures;
- the ability to create drawings (Tekla SD);

- the ability to consider the bracings stiffness and design of composite structures (Consteel and RFEM).

Disadvantages of Consteel, Tekla SD and RFEM:

- the difficulty of development due to the versatility;
- cost, limited area of application;
- no frame generator and long calculation (Consteel).

Advantages of PortalPlus [12]:

- quick calculation with details;
- clarity of presentation;
- lightness and free distribution.

Disadvantages of PortalPlus:

- no bracings;
- approximate definition of internal efforts;
- the limited scope of use and no guarantee.



## Conclusions

By the design of portal frames it can use the indicative data for parameter values:

- portal frame span: 20 – 50 m;
- portal frame step: 5 – 7,5 m;
- roof slope: 6° – 10°;
- construction height of solid-wall rafter: 1/25 – 1/45 of span;
- construction height of through rafter: 1/18 – 1/40 of span;
- ratio of column height to span: 1/4 – 1/7;
- column weight: 1,5 – 2 of rafter weight;
- length of the haunch area: 10% of span;
- height of the haunch: 2 rafter heights;
- step of purlins: 1,5-3 m.

## References

1. Hernández S., Fontán A.N., Perezán J.C. & Loscos P. (2005). *Design optimization of steel portal frames. Advances in Engineering Software*, 36(9), 626-633.  
<http://dx.doi.org/10.1016/j.advengsoft.2005.03.006>
2. Shah S.N.R., Aslam M. & Sulong N.H.R. (2016). Geometrically optimum design of steel portal frames. *University of Engineering and Technology Taxila. Technical Journal*, 21(4), 24-30.
3. Hradil P., Mielonen M. & Fülöp L. (2010). Advanced design and optimization of steel portal frames. *Journal of Structural Mechanics*, 43(1), 44-60.
4. Saka M.P. (2003). Optimum design of pitched roof steel frames with haunched rafters by genetic algorithm. *Computers & Structures*, vol. 81, no. 18-19, 1967-1978.  
[http://dx.doi.org/10.1016/S0045-7949\(03\)00216-5](http://dx.doi.org/10.1016/S0045-7949(03)00216-5)
5. Nagy Zs., Pop A., Moiş I., & Ballok R. (2016). Stressed skin effect on the elastic buckling of pitched roof portal frames. *In Structures*, vol. 8, 227-244.  
<http://dx.doi.org/10.1016/j.istruc.2016.05.001>
6. Wrzesien A.M., Lim J.B.P., Xu Y., MacLeod I.A. & Lawson R.M. (2015). Effect of Stressed Skin Action on the Behaviour of Cold-Formed Steel Portal Frames. *Engineering Structures*, 105, 123-136.  
<http://dx.doi.org/10.1016/j.engstruct.2015.09.026>
7. Kindmann R. & Krahwinkel M. (2001). Bemessung stabilisierender Verbände und Schubfelder. *Stahlbau* 70, 885-899.  
<https://doi.org/10.1002/stab.200102860>
8. Kuhlmann U. (2009). *Stahlbau-Kalender 2009: Schwerpunkt – Stabilität*. Berlin: Ernst & Sohn.  
<https://doi.org/10.1002/9783433600320>
9. Koschmidder D.M. & Brown D.G. (2012). *Elastic design of single-span steel portal frame buildings to Eurocode 3*. Steel Construction Institute.
10. Portal frames. Взято з [www.steelconstruction.info](http://www.steelconstruction.info)
11. Marsh K. (2016). *Autodesk Robot Structural Analysis Professional 2016: Essentials*. Marsh API.
12. Взято з <https://sections.arcelormittal.com>
1. Hernández S., Fontán A.N., Perezán J.C. & Loscos P. (2005). *Design optimization of steel portal frames. Advances in Engineering Software*, 36(9), 626-633.  
<http://dx.doi.org/10.1016/j.advengsoft.2005.03.006>
2. Shah S.N.R., Aslam M. & Sulong N.H.R. (2016). Geometrically optimum design of steel portal frames. *University of Engineering and Technology Taxila. Technical Journal*, 21(4), 24-30.
3. Hradil P., Mielonen M. & Fülöp L. (2010). Advanced design and optimization of steel portal frames. *Journal of Structural Mechanics*, 43(1), 44-60.
4. Saka M.P. (2003). Optimum design of pitched roof steel frames with haunched rafters by genetic algorithm. *Computers & Structures*, vol. 81, no. 18-19, 1967-1978.  
[http://dx.doi.org/10.1016/S0045-7949\(03\)00216-5](http://dx.doi.org/10.1016/S0045-7949(03)00216-5)
5. Nagy Zs., Pop A., Moiş I., & Ballok R. (2016). Stressed skin effect on the elastic buckling of pitched roof portal frames. *In Structures*, vol. 8, 227-244.  
<http://dx.doi.org/10.1016/j.istruc.2016.05.001>
6. Wrzesien A.M., Lim J.B.P., Xu Y., MacLeod I.A. & Lawson R.M. (2015). Effect of Stressed Skin Action on the Behaviour of Cold-Formed Steel Portal Frames. *Engineering Structures*, 105, 123-136.  
<http://dx.doi.org/10.1016/j.engstruct.2015.09.026>
7. Kindmann R. & Krahwinkel M. (2001). Bemessung stabilisierender Verbände und Schubfelder. *Stahlbau* 70, 885-899.  
<https://doi.org/10.1002/stab.200102860>
8. Kuhlmann U. (2009). *Stahlbau-Kalender 2009: Schwerpunkt – Stabilität*. Berlin: Ernst & Sohn.  
<https://doi.org/10.1002/9783433600320>
9. Koschmidder D.M. & Brown D.G. (2012). *Elastic design of single-span steel portal frame buildings to Eurocode 3*. Steel Construction Institute.
10. Portal frames. Retrieved from [www.steelconstruction.info](http://www.steelconstruction.info)
11. Marsh K. (2016). *Autodesk Robot Structural Analysis Professional 2016: Essentials*. Marsh API.
12. Retrieved from <https://sections.arcelormittal.com>

UDC 666.946.3

## Mineral binders and concretes based on technogenic waste

Haqverdieva Tahira<sup>1</sup>, Akhmednabiev Rasul<sup>2\*</sup>, Bondar Lyudmyla<sup>3</sup>, Popovich Nataliia<sup>4</sup>

<sup>1</sup>Azerbaijan University of Architecture and Construction

<sup>2</sup> National University «Yuri Kondratyuk Poltava Polytechnic» <https://orcid.org/0000-0002-8292-9504>

<sup>3</sup> National University «Yuri Kondratyuk Poltava Polytechnic» <https://orcid.org/0000-0002-1595-7740>

<sup>4</sup> National University «Yuri Kondratyuk Poltava Polytechnic» <https://orcid.org/0000-0001-6450-6332>

\*Corresponding author E-mail: [akhmednabiev4@gmail.com](mailto:akhmednabiev4@gmail.com)

Compositions of alkali-mineral binders based on wastes of alumina industry with application of research physicochemical methods have been developed. It has been established that impregnations with hot CaCl<sub>2</sub> solution accelerate the curing time. It has been established that the conditions of hardening significantly influence the physical-mechanical properties. The developed binding materials with a compressive strength of 40.0... 65.1 MPa belongs to hydration-condensation, alkaline-alkaline type. The results of studies on the ash slag influence from circulating fluidized bed boilers on the heavy concrete properties are presented. The studies were carried out using mathematical planning of the experiment. Mechanical concrete properties have been studied using in the study of freeze-thaw resistance, the dilatometry method was applied.

**Keywords:** alkali-mineral binders, compressive strength, DTA-analyses, fine-grained concretes, industry wastes, IR- spectrum, slags of TPP, X -ray analysis

## Мінеральні в'язучі та бетони на основі техногенних відходів

Ахвердієва Т.<sup>1</sup>, Ахмеднабієв Р.М.<sup>2\*</sup>, Бондар Л.В.<sup>3</sup>, Попович Н.М.<sup>4</sup>

<sup>1</sup> Азербайджанський університет архітектури та будівництва

<sup>2, 3, 4</sup> Національний університет «Полтавська політехніка імені Юрія Кондратюка»

Адреса для листування E-mail: [akhmednabiev4@gmail.com](mailto:akhmednabiev4@gmail.com)

Розроблено склади лужно-мінеральних в'язучих на основі відходів глиноземного виробництва із застосуванням фізико-хімічних методів дослідження. Вивчено процеси твердіння лужно-мінеральних в'язучих і бетонів на їх основі. Установлено, що просочення гарячим розчином CaCl<sub>2</sub> прискорюють термін твердіння. Визначено, що умови твердіння істотно впливають на фізико-механічні властивості й формування структури лужно-мінеральних в'язучих і бетонів. Доведено, що лужно-мінеральні в'язучі на основі алюмосилікатних відходів тверднуть у різних умовах. Процесом їхньої взаємодії є високоміцні, довговічні та водостійкі алюмосилікати, гідросилікати і гідроалюмосилікати. Приготовлено суміші з різним співвідношенням в'язучого й заповнювача (від 5:1 до 1:5), виготовлено зразки й після термічної обробки виконано випробування за стандартною методикою. Результати випробувань підтвердили, що розроблені в'язучі дозволяють одержати дрібнозернисті бетони із середньою густиною в сухому стані 1815 – 2311 кг/м<sup>3</sup>, межею міцності при стисненні 15 – 28 МПа. Досліджено властивості золошлаків котлів із циркуляційним киплячим шаром. Установлено, що при твердненні цементно-золошлакових смішей протягом 60 діб не утворюються шкідливі новоутворення типу гідроалюмосульфатів кальцію. У дослідженнях використовували портландцемент ППС 500 Н, пісок з модулем тонкості M = 1,05, гранітний щебінь фракцій 5 – 10 мм, пластифікатор «Fluid Premia-196». Дослідження здійснювалися з використанням математичного планування експерименту. При вивченні стійкості до замерзання-відтавання застосовували дилатометричний метод, а для критерію пористості – водопоглинення у вакуумній камері. Зазначено, що зі збільшенням ступеня заміщення піску золошлаками міцність бетону знижується на 3 – 10% порівняно з бетонами, що не містять шлаку. У результаті досліджень визначено оптимальні важкі бетонні композиції із застосуванням золошлаків ТЕС.

**Ключові слова:** ДТА-аналізи, дрібнозернисті бетони, золошлаки теплоелектростанцій, ІЧ-спектральний аналіз, лужно-мінеральні в'язучі, міцність на стиск, промислові відходи, рентгеноструктурний аналіз



## Introduction

To date, mankind has accumulated a large number of technogenic wastes, which can be notionally named new deposits. The largest amount of industrial waste is generated by the following enterprises: chemical industry; non-ferrous metallurgy; ferrous metallurgy; power industry; building materials industry; agro-industrial complex; forestry and woodwork and timber industry; textile industry; metal-processing industry, as well as human domestic activities.

Metallurgy is one of the main industries where large amounts of technogenic waste are generated. Some metallurgical wastes have already undergone high-temperature treatment, crystalline structures in the waste have been formed, and they do not contain organic impurities. Other wastes such as those of iron ore enrichment have not yet found their application in construction. Thus, for example, wastes of iron ores, wet enrichment, are still being stored in refuse dumps occupying large areas and polluting the environment. Technogenic products of the metallurgical industry, it is advisable to divide into wastes of ferrous and non-ferrous metallurgy, as well as hydrometallurgy sludge.

It is known that in the world, the degree of electric energy consumption, including thermal power plants, is growing every year. Billions tons of ash and slag have been accumulated in the territories of thermal power plants. The utilization of these wastes is an urgent task of humanity because they pollute the environment not only in places where they are accumulated, but also pose a threat to people's health all over the world.

The complex technological techniques development allows the waste use from the thermal power stations in the obtaining construction materials technology [2]. As a rule, waste from the coal burning in the thermal power plant boilers is gray-colored, and their chemical composition is represented by oxides of silicon, aluminum, iron, and calcium, as well as impurities in the form of magnesium, sulfur, sodium, and potassium oxides. The phase composition of the ash slag is represented mainly by aluminosilicate glass and also includes quartz, iron oxides.

The purpose of the study is to study the influence of ash salts from circulating fluidized bed boilers on the stability to freezing and thawing and, consequently, on the strength of heavy concretes designed for operation in the climatic conditions of Ukraine.

## Review of the research sources and publications

According to the research publications [1], the utilization rate of thermal power plants waste in CIS countries does not exceed 10 - 13%, whereas in Europe: Germany and Denmark it reached almost 100%, in the UK and Poland – 50 - 70%. This is due to the fact that ashes and slag waste in developed countries are the same commodities as heat and electricity.

The development of sophisticated technological techniques permits the use of thermal power plants waste in the technology of obtaining building materials [2]. The phase composition of the ash slag is mainly aluminosilicate glass and also includes quartz, iron oxides

[2]. Blast-furnace slag is mainly used in the cement industry. A great deal of work has been devoted to studying the process of their interaction with the minerals of Portland cement clinker, both domestic and foreign researchers. The expediency of blast furnace slag widespread use in the cement industry has been proven by numerous studies and practical recycling experience [3]. The processes of ashes and ash-slag interaction with the minerals of Portland cement clinker are the subjects of the modern researchers' studies [2, 4 – 7].

Efficient and prudent use of the components that make up mineral composites is an urgent scientific problem.

One of the fields of mineral origin waste management is their use in building materials technology. Some wastes can be used in cement production, while others can be a basis for other types of binders. The idea of producing alkaline-alkaline earth aluminosilicate hydraulic cement, as well as building concretes, belongs to the Ukrainian scholar V.D. Glukhovskiy [8].

Today, cement, including slag-alkali binders, is widely used in construction. It is known that slag-alkali binders and concrete based on them are considered to be high-strength, frost-resistant, and durable materials. Slag alkali cement differs from the known compositions by the fact that it can be manufactured based on various industrial wastes and an alkaline composition [9].

In Azerbaijan, the goal of many researchers in the field of building materials technology is to develop composite binders using industrial wastes.

One of the research projects we are carrying out in this field is developed based on alkali-mineral binders and concrete.

## Definition of unsolved aspects of the problem

Despite the large number of studies conducted, the utilization of industrial waste in Ukraine remains at a low level compared to European countries. Also, new technologies and, accordingly, new types of waste appear in the industry, which should be studied and areas of their use identified.

**The problem statement** is to develop an alkaline-mineral binder and high-strength concrete based on industrial waste

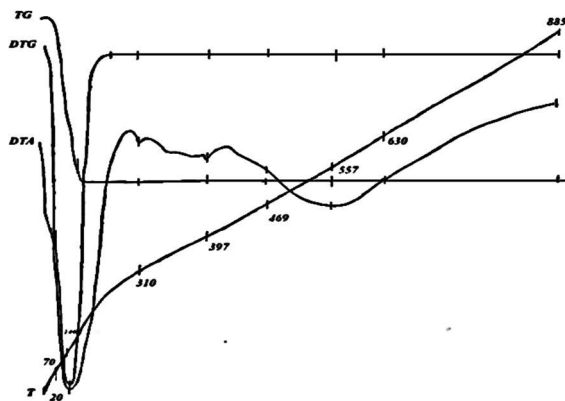
## Basic material and results

Industrial aluminosilicate wastes from the Ganja Alumina Refinery Plant are used as mineral raw materials for the production of alkaline-mineral binder and concrete. Liquid glass with a density of 1.215 g / cm<sup>3</sup> and a silicate module of 2.9 was used as the alkaline component, the chemical composition of which is characterized in percent for weight: Na<sub>2</sub>O + nSiO<sub>2</sub> – 22.5; SiO<sub>2</sub>, 16.87; Na<sub>2</sub>O – 5.63; H<sub>2</sub>O – 77.5.

It was established that the chemical composition of aluminosilicate waste is characterized by the following oxides in percent for weight: SiO<sub>2</sub> - 65.18; Al<sub>2</sub>O<sub>3</sub> 18.71; Na<sub>2</sub>O – 1.70; K<sub>2</sub>O – 1.06; MgO 0.60; CaO – 0.72; TiO<sub>2</sub> – 0.21; MnO – 0.07; Fe<sub>2</sub>O<sub>3</sub> – 7.56; p.p.p. – 4.76.

Sodium hydroxide NaOH, bentonite clay of the Dash-Salakhly deposit and Portland cement PC 500 of the Garadag plant was used as an additive, and quartz sand of the Imishli deposit of the Azerbaijan Republic with fineness modulus  $M_{kr} = 1.56$  was used.

The method to accelerate hardening, temperature and the processing mode is important for alkaline-mineral binders. The choice of processing temperature is based on the DTA data (fig. 1).



**Figure 1 – Thermogram of an alkaline-mineral composition based on aluminosilicate waste**

On the DTA curve, two endo-effects are observed having maxima of 70°C (weak) and 140°C (deep). This is because there are weakly coordinating water molecules in the system. In the range from 240°C to 885°C temperature, two particularly weak endo-effects

were recorded, having maxima of 310°C and 367°C and one weak endo-effect at 557°C temperature. There is dehydration of the original minerals here. The DTG curve is similar to the DTA curve range from 240°C to 885°C temperature, two particularly weak endo-effects were recorded, having maxima of 310°C and 367°C and one weak endo-effect at 557°C temperature. There is dehydration of the original minerals here. The DTG curve is similar to the DTA curve.

As it can be seen from the TG curves, when a sample is heated from 20 to 885°C, an intensive mass loss of only 56.6% occurs, including 1.2% in the range of 20–70 C, 55.4% in the range of 70–170°C. After a temperature of 170°C, the process stabilizes, and no mass loss is observed.

Based on the DTA results of the initial alkaline-mineral raw material, a treatment temperature of 140–150°C was adopted for 11 (2 + 7 + 2) hours.

It is known that, along with various hardening accelerators, impregnation with calcium chloride also accelerates the hardening of alkaline-mineral binders, especially since  $\text{CaCl}_2$  is economically more profitable. Based on a series of experiments on the processing of samples with calcium chloride solutions, the treatment model was established: processing after manufacturing the samples with a hot (60°C)  $\text{CaCl}_2$  solution with a density of 1.35 g/cm<sup>3</sup> for 1 h, then drying at the temperature of 140–150°C for 2.5 (0.5 + 1.5 + 0.5) h.

Compositions of alkaline-mineral binders and the conditions of their heat treatment are given in table 1.

**Table 1– Optimized composition of alkaline-mineral binder based on alumina silicate waste**

№	Hardening conditions	Composition, in percent per weight					Ultimate strength, MPa
		Liquid glass	NaOH	Portlandcement	Clay	Alumino-silicate waste	
1	Chamber drier 140-150°C	35.2	9.7	10.4	8.6	36.1	40.00
2	Air dry flow 140-150°C	32.0	9.4	9.4	8.0	41.2	44.75
3	Impregnation with $\text{CaCl}_2$ hot solution 60°C	29.0	8.4	8.4	7.3	46.9	53.23
4	Autoclave 9 atm., temperature 174.5°C	29.1	8.5	9.5	6.1	46.8	65.1

The table shows that binders, hardened in an autoclave have the maximum strength. Processing with a hot solution of calcium chloride provides strength lower than that in an autoclave, but also higher than in other conditions, within the experiment.

Thus, we can conclude that the alkaline-mineral binder based on aluminosilicate waste hardens under various conditions. The product of their interaction is high-strength, durable and water-resistant aluminosilicates, hydro silicates and hydro aluminosilicates.

The resulting binder material refers to hydration-condensation binders, such as alkaline-alkaline earth, with ratios of oxides:  $\text{R}_2\text{O} - \text{RO} - \text{R}_2\text{O}_3 - \text{SiO}_2 = (0.72 \mid 1.5): (0.4 \mid 0.73): 1: (2.03: 3.2)$ .

At the next stage, the possibility of obtaining concrete based on the developed binder was studied.

A mixture prepared with a different binder/aggregate ratio from 5:1 to 1:5, samples were made and tests were carried out after heat treatment (tab. 2).

**Table 2 – Optimized composition of fine-grained concrete based on alkaline mineral binder**

№	Hardening conditions	Composition, by weight %						Ultimate compressive strength, MPa	Density, kg/cm <sup>3</sup>
		Binder					Sand		
		Liquid glass	NaOH	Portlandcement	Clay	Alumino-silicate waste			
1	Chamber drier 140-150°C	19.6	5.4	5.4	4.6	19.5	45.5	15.73	1815
2	Air dry flow 140-150°C	19.5	5.5	5.3	4.7	24.1	40.9	18.77	2044
3	Impregnation with CaCl <sub>2</sub> hot solution 60°C	19.5	5.5	5.45	4.55	30.1	34.9	26.42	2254
4	Autoclave 9 atm., temperature 174.5°C	19.5	5.5	5.46	4.54	30.1	34.9	28.41	2311

The table shows that there is practically no difference between the strength indices of concrete hardened in an autoclave and treated with a hot solution of calcium chloride.

At the next stage, the possibility of obtaining concrete based on slag of circulating fluidized bath of TPP was studied.

The following materials were used in the work: Portland cement PC 500 N (42,5), sand with the fineness modulus  $M_f = 1.05$ ; slag from boilers with circulating fluidized bed; superplasticizer «Fluid Premia-196» based on modified polycarboxylates; as a coarse aggregate - crushed granite fraction of 5–10 mm taken from

Kremenchuk deposit. For more complete detection of the slag and studying the hyperplasticizer's influence on the concrete freeze-thaw resistance and strength, a three-level experiment planning matrix was implemented in the study.

When planning the experiment, the following input parameters were established:

- X<sub>1</sub> – cement consumption;
- X<sub>2</sub> – hyperplasticizer consumption;
- X<sub>3</sub> – degree of sand replacement with slag.

Terms of the experiment planning are presented in the table 3.

**Table 3 – Terms of the experiment planning**

Variable factors		Variation levels			Variation interval
Natural appearance	Coded appearance	-1	0	+1	
Cement consumption	X <sub>1</sub>	400	500	600	100
Additive consumption	X <sub>2</sub>	0.8	1.4	2.0	0.6
Degree of sand replacement with ash slag	X <sub>3</sub>	-1	0	1	0.5

Freeze-thaw resistance was determined by the rapid method. The dilatometry method for determining the freeze-thaw resistance by freezing in the kerosene medium was used in the work. According to this method, the freeze-thaw resistance is determined by the maximum difference between volumetric deformations of concrete and standard samples. The standard sample is an aluminum cube with a side length of 100 mm.

The concrete strength was determined by testing the 100-mm side sample-cubes on hydraulic presses. The concrete porosity was assessed by the degree of water adsorption in the vacuum chamber at the vacuum level of 0.7 Pa.

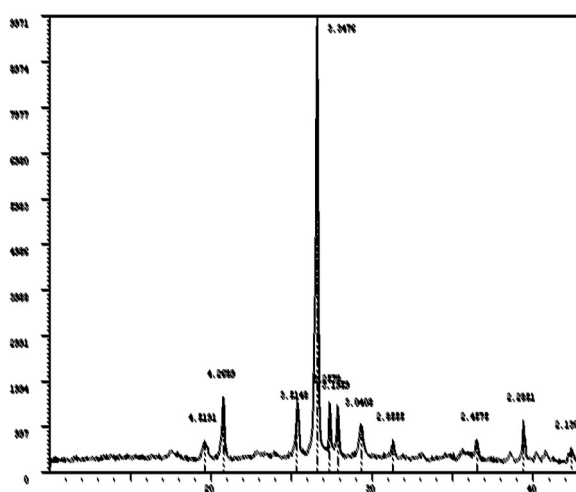
The chemical composition of the slag is shown in table 4. The properties of the slag were studied using

X-ray diffraction (XRD) fig.2 and spectral analysis methods fig. 3.

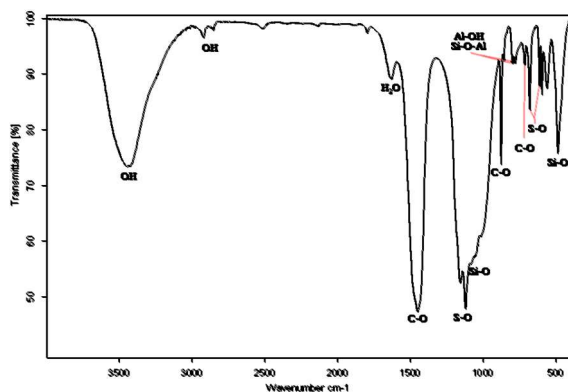
The table shows that the content of calcium oxide CaO=5, 17%, and silicon oxide SiO<sub>2</sub>=48.95%, according to these indicators, the slag can be attributed to acidic. The content of sulfur oxide SO<sub>3</sub> is more than 7% and according to this indicator, the slags are sulfate. The sulfur oxide may be in the composition of the slag in the form of gypsum CaSO<sub>4</sub>·2H<sub>2</sub>O or anhydride CaSO<sub>4</sub>. In both cases, they can react with the aluminate minerals of Portland cement and create hydrosulfite aluminates CA<sub>3</sub>S<sub>3</sub>H (ettringite) [14-16]. If they appear after cement hardens, the structure of the cement stone may be destroyed, which may lead to the destruction of concrete.

**Table 4 – The chemical composition of the slag**

Al	21.91	Al <sub>2</sub> O <sub>3</sub>	26.89
Si	44.37	SiO <sub>2</sub>	48.95
S	6.80	SO <sub>3</sub>	7.36
K	6.99	K <sub>2</sub> O	3.90
Ca	7.94	CaO	5.17
Ti	1.02	TiO <sub>2</sub>	0.81
Fe	9.57	FeO	6.12
Zn	0.04	ZnO	0.04
Mo	0.00	MoO <sub>3</sub>	0.00
In	1.36	In <sub>2</sub> O <sub>3</sub>	0.76
W	0.00	WO <sub>3</sub>	0.00



**Figure 2 – X-ray diffraction pattern of ash-slag**



**Figure 3 – Spectral pattern of ash slags**

Decoding of the X-ray diffraction pattern indicates that the maxima with vertices are 3.5149; 3.1959; 2.578; 1.8711; 1.1424 belong to anhydride CaSO<sub>4</sub> mineral, and with vertices – 3.3476; 2.4575; 2.2851; 2.1306; 1.9201; 1.6724 – belong to silicon oxide and correspond to the SiO<sub>2</sub> formula. Thus, the crystallized part of the slag consists of calcium minerals and silicon oxide. With the X-ray diffraction pattern, it is also evident that most of the slags are represented by amorphous structures, which can be combined under the name of vitreous phase, which promotes slag hydration.

The hydraulic activity of slags is associated with the presence of such compounds as lime in a free state or anhydride, which can react with water to form a water-resistant stone without introducing additional activators [7]. It is known that the different content of CaO affects both the change in the composition of the vitreous phase and the composition of the newgrowths crystallized, and the manifestation of hydraulic and pozzolanic properties of slags [7].

The IR spectra of slag contain bands characteristic of silicates and aluminosilicates with absorption bands in the region of 1050-1200 cm<sup>-1</sup>. The spectrum also contains a doublet characteristic of aluminosilicates within the range of wavenumbers 770-810 cm<sup>-1</sup>, which refers to vibrations of the Al-OH and Si-O-Al stretch oscillation. The deformation oscillations of the Si – O stretch are expressed in the absorption band within the range of wavenumbers 500–400 cm<sup>-1</sup>.

The presence of carbonates in the composition of slag is proved by the presence of absorption bands, which are caused by C – O oscillations: valency – an intense band on the wavenumber 1440 cm<sup>-1</sup>, a narrow intense band on 875 cm<sup>-1</sup>; deformation – a weak band at 713 cm<sup>-1</sup>, as well as bands at 2516 and 1795 cm<sup>-1</sup>.

Sulfate groups are determined by the intense absorption band within the range of wavenumbers 1090- – 1180 cm<sup>-1</sup> and 680–650 cm<sup>-1</sup>. According to the position of the maximum, it is possible to reliably determine the mineral in the sulfate group. In the composition of slag, judging by the spectrum, only anhydrous sulfates are present.

The high-frequency region of the absorption bands with the values: 2918; 2850 and 3443 cm<sup>-1</sup> refers to the stretch vibrations of connected OH-groups. The absorption band with a frequency of 1630 cm<sup>-1</sup> refers to the stretch vibrations of water molecules. The presence of bands corresponding to valent deformation vibrations of OH-groups and the valent vibrations of water molecules is associated with the phenomenon of moisture adsorption from the environment due to the high activity of minerals that are part of ash and slag composition.

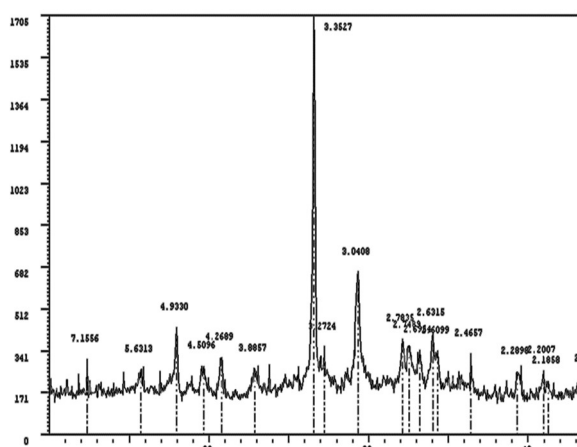
Thus, the studies have established that anhydrous calcium sulfate is present in the composition of ash and slag, and this may be anhydrite.

Studies have shown that ash slags belong to high-calcium ashes (CaO > 20 % wt), i.e. to basic ashes; as to the content of SO<sub>3</sub> – to sulfate (SO<sub>3</sub> > 5 % wt) ashes. The main sulfate mineral is anhydrite CaSO<sub>4</sub> [12].

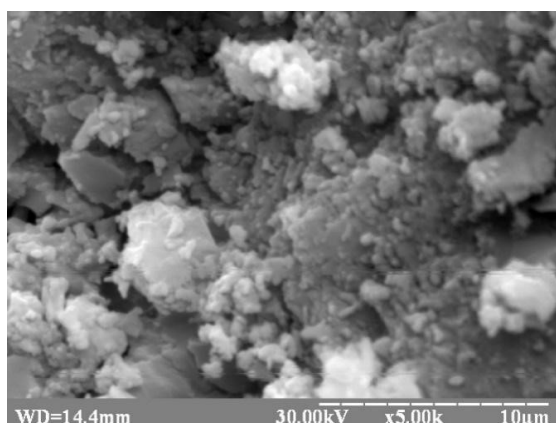
The processes of cement-ash compositions hydration should be subordinate to the established general fundamental laws, which, in particular, consist in the fact that, at ordinary temperatures, the ash silica glass is slowly hydrated, which leads to the formation of C4AN13-19 or calcium carboaluminate with excess CH in the liquid phase. Then it can go into the hydrogranate, aluminum hydroxide, or gibbsite. If these phases do not go into more stable hydrosulfoalluminates, the durability of the product will decrease [6,13].

A fragment of the graphs is shown in fig. 4.

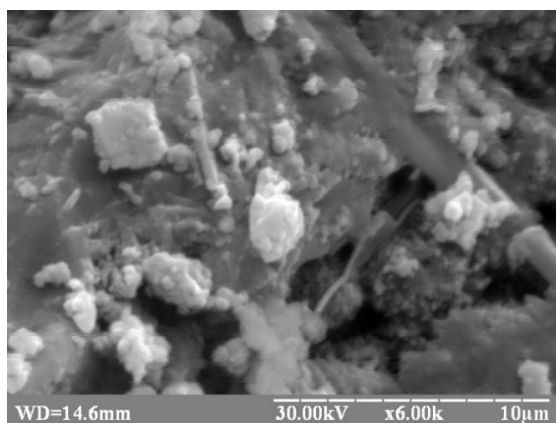
As can be seen from the X-ray diffraction pattern's fragment, the maxima inherent in ettringite in the cement stone at the age of two months are absent. Studies of cement-slag stone at the micro-level with a scanning microscope confirmed the absence of needle crystals inherent in hydro sulfoaluminate (figure 5-6).



**Figure 4 – X-ray diffraction pattern's fragment of cement-slag stone after hardening for 60 days in wet conditions**



**Figure 5 – Electron-microscopic photographs of the cement - slag stone fracture surface after its hardening for 60 days in wet conditions**



**Figure 6 – Electron microscopic photographs of the cement stone fracture surface after its hardening for 60 days in wet conditions**

Studying microscopic photographs of a pure cement stone compared to a cement slag stone, we can conclude the following: in a cement stone without slag, there are typical components of a cement stone-like Portlandite and calcium hydrosilicate. In micrographs of cement-slag stone the picture is almost the same, but with a large amount of portlandite. In our opinion, it is evidenced by an increase in the number of light crystals fig 5.

After no traces of hydro sulfoaluminate were found in the cement-slag stone, concrete samples were prepared according to the matrix of the experimental design (table 5).

**Table 5 – Experiment planning matrix**

№	x <sub>1</sub>	x <sub>2</sub>	x <sub>3</sub>
1	600	2.0	ash
2	400	2.	ash
3	600	0.8	ash
4	400	0.8	ash
5	600	2.0	sand
6	400	2.0	sand
7	600	0.8	sand
8	400	0.8	sand
9	600	1.4	0.5+0.5
10	400	1.4	0.5+0.5
11	500	2.0	0.5+0.5
12	500	0.8	0.5+0.5
13	500	1.4	ash
14	500	1.4	sand
15	500	1.4	0.5+0.5
16	500	1.4	0.5+0.5
17	500	1.4	0.5+0.5

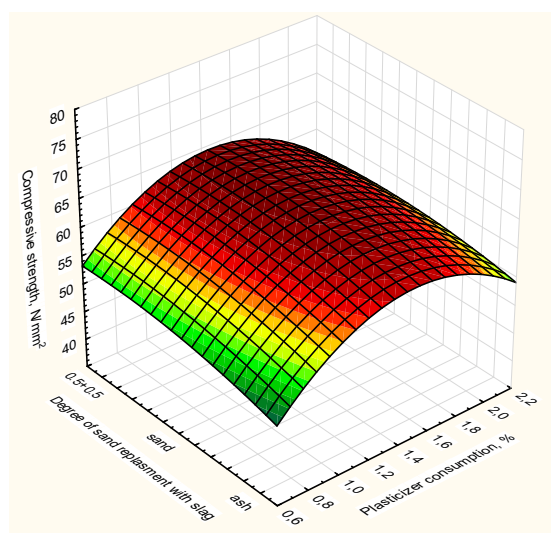
Mixing of the concrete mixture components was carried out in a compulsory-type concrete mixer with a skip capacity of 150 liters. Dosing of the mixture components was carried out using electronic scales with an accuracy of 0.1 kg. Dosed components of the mixture were charged into the mixer in the following sequence: crushed stone + sand (slag) + cement. The components were mixed without adding water for three minutes. In our work, we used a complex additive consisting of the plasticizer "Fluid premia 196" and the hardening accelerator TEMP-3. Dosing of the plasticizer was carried out according to the experimental matrix, and the amount of the hardening accelerator was constant 1% of the mass of cement. A mixture of water, accelerator and plasticizer was prepared in advance. A plasticizer and a hardening accelerator in measured amounts were added to water and mixed with a mixer for 30 seconds. The finished mixture was added to the concrete mixer. Mixing the components lasted 5 minutes. After 5 minutes, the mixture was discharged from the mixer. From the finished mixture, the samples were

made in the form of cubes with a side of 10 cm. The samples were compacted using vibration with an oscillation amplitude of 0.5 mm and a frequency of 50 Hz. A day later, samples were taken from the molds. Samples were laboratory cured for 28 days. After 28 days of curing, the samples were tested according to the experimental matrix.

The results of the samples testing for compressive strength are presented in Table 6 and fig. 7.

**Table 6 – Properties of concretes**

Batch	Compressi on strength N/mm <sup>2</sup>	Water absorption W <sub>m</sub> , %	Frost resistance, cycle
1	72,3	5,22	480
2	43,4	8,76	238
3	70,1	7,3	332
4	38,6	9,86	105
5	75,0	3,82	633
6	45,1	5,05	380
7	72,7	4,1	580
8	41,3	6,26	365
9	73,6	4,71	538
10	44,4	6,64	360
11	61,1	5,25	487
12	59,5	5,26	408
13	63,6	6,65	390
14	65,4	5,58	435
15	66,7	5,31	424
16	67,0	5,36	416
17	68,0	5,1	464



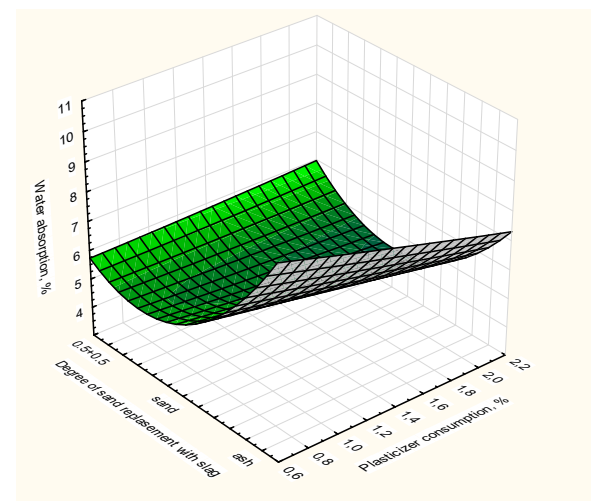
**Figure 7 – 3D Surface Plot of strength against the degree of sand replacement with slag and Plasticizer consumption**

Analysis of the samples testing results shows that when the sand is completely replaced with ash slag and at the minimum cement consumption within the limits of the experiment, the strength of the concrete is reduced by 6.5% (compositions 4 and 8). With a maximum amount of cement strength is reduced by only 3.6% (compositions 1 and 5). The concrete strength within the experimental design matrix varies from 38.6 to 75 N/mm<sup>2</sup>. With the mean values of the concrete components consumption, the strength of the samples varies from 44.4 to 73.6 N/mm<sup>2</sup>.

The fact of the strength reducing at the compression of the sample with increasing the sand replacement degree with slag can be explained by the fact that the slag is not so strong a mineral like quartz. Grains of slag have internal pores reducing their durability. The reduction of concrete strength is associated with the increased porosity.

Analysis of 3D Surface confirms that with increasing substitution of sand by slag, concrete strength decreases slightly. With an increase in the consumption of plasticizer to 1,4 – 1,6%, the strength of concrete increases. With a further increase in the consumption of plasticizers, the strength decreases. This fact can be explained by the fact that a large amount of plasticizer increases the plasticity of the concrete mixture and at the same time sedimentation of the mixture occurs.

Increasing porosity leads to an increase in water absorption. The results of research on water absorption of concrete in the experiment are presented in Table 6 and fig. 8.

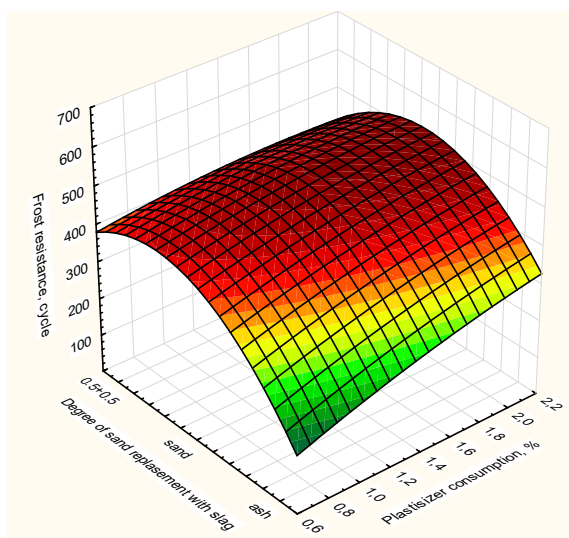


**Figure 8 – 3D Surface Plot of water absorption against the degree of sand replacement with slag and Plasticizer consumption**

The 3D Surface analysis shows that the maximum water absorption of 9.86% is observed in concrete batch 4, in which sand is completely replaced with slag. Specimens of batch 8, in which sand is not replaced by slag, but other components of concrete are the same, showing the water absorption of 7.26%, which is 26% lower. This fact confirms that slag contributes to increasing the porosity of the concrete.



An increase in the porosity of the concrete will reduce not only the strength but also frost resistance. The results of the concrete samples study for frost resistance are presented in fig. 9.



**Figure 9 – 3D Surface Plot of frost resistance against the degree of sand replacement with slag and Plasticizer consumption**

Analogues are compositions number 1 and number 5 with a maximum amount of cement and 4 and 8 with a minimum amount of cement. Frost resistance of samples number 1 is 480 cycles, that of number 8 is 633 cycles. The frost resistance reduction makes 24%. When comparing water absorption of the same compositions, the water absorption increase of composition 1 is 36%.

With the minimal amount of cement, the analogues are compositions 4 and 8. The frost resistance of composition 4 is three times lower than the frost resistance of composition 8. Analyzing the water absorption of these compositions, it can be stated that the water absorption increase of composition 4 makes 57%. It is obvious that the frost resistance of the concrete does not change in proportion to the water absorption change.

In concrete micropores sizing  $10^{-5}$  cm, usually, there is bound water that does not turn into ice even at extremely low temperatures (to  $-70$  °C), therefore micropores do not significantly affect the concrete's resistance to freezing-thawing. The latter depends on the particular macropores and their structure.

A number of laboratory studies have shown that concrete containing fly ash and ash slag may be less resistant to frost during freezing and thawing [17–19].

Concrete with fly ash can provide satisfactory resistance to freezing-thawing provided waterproof cement is used and W/C (water-cement ratio) does not exceed 0.45. In this case, of course, it is assumed that the concrete has an adequate porous structure [20].

The influence degree of ash and ash slag on the concrete properties depend not only on its amount in the mixture but also on other parameters, including the composition and ratio of other ingredients in the concrete mixture, the type and size of the particular component, the hardening conditions in the process of molding and hardening, as well construction methods [21].

In the studies, all the technological parameters were the same for all batches of samples. The concrete water/cement ratio did not exceed 0.45 due to the use of a plasticizer. Obviously, samples of concrete batch 4 showed the lowest frost resistance because, due to the small amount of cement and the maximal replacement of sand with ash slag, a relatively large macropore structure was formed in which the water freezes when the temperature drops.

Based on the studies performed, optimal compositions of heavy concretes were suggested with the use of ash slag instead of silica sand for the manufacture of small road products. All the concrete components provide frost resistance of products not less than 200 cycles, thus meeting the requirements of Ukrainian standards.

The optimal compositions of concretes are presented in table 7.

**Table 7 – Optimal compositions of concrete with the use of ash and slag boilers with circulating fluidized bed**

No	Class of conc.	Materials consumption per 1 m <sup>3</sup> of concrete mixture					
		Cement, kg	Crushed stone, kg	Sand, kg	Ash slag, kg	Plasticizer, kg	Water, liter
3	B25	400	1116	335	335	4.8	200
4	B30	420	1100	320	320	5.0	210
5	B35	450	1068	312	312	5.4	220
6	B40	490	1035	300	300	6.0	248
7	B45	525	1000	290	290	6.3	260
8	B50	580	950	280	280	6.9	290
9	B55	600	900	270	270	7.2	300

## Conclusion

The results of the studies permit the following conclusions.

1. Alkaline-mineral binders have been developed using local industry waste (liquid glass, NaOH, Portland cement, clay, aluminosilicate waste), hardening under various conditions; various factors influence the construction and technical properties of alkaline-mineral systems based on alumina production waste was studied and the composition of the alkaline-mineral binder was optimized.

2. It has been established that the hardening conditions have a significant effect on the physical-mechanical properties and structure-forming of alkaline-mineral binder and fine-grained concrete.

3. The compositions of fine-grained concrete based on alkaline-mineral binders and river sand have been developed, hardening under various conditions with the following physical-mechanical properties: mean dry density 1815.9 ... 2311.2 kg / m<sup>3</sup>, compressive strength 15.73 ... 28.41MPa.

4. It was established that in the chemical and mineralogical composition of the ash and slag of boilers with a circulating fluidized bed there are no salts and minerals that can adversely affect the hardening of cement-ash and slag compositions.

5. The results of X-ray diffraction analysis and microscopic studies prove that when hardening cement with slags, compounds such as hydrosulfite aluminates that can destroy concrete are not formed.

6. The use of slag as a fine aggregate in concrete leads to a decrease in strength by 3-5% and helps to reduce the water-cement ratio, which leads to an increase in the strength of concrete.

8. As a result of the studies, the optimal compositions of concrete were selected using slags as fine aggregate

9. It is advisable to use slag of boilers with a circulating fluidized bed as a fine aggregate in concrete in areas of their accumulation in terms of improving the environmental situation.

## References

1. Удосконалення системи поводження з відходами теплових електростанцій. Взято з <http://tef.kpi.ua>
2. Чулкова И.Л. (2011). *Повышение эффективности строительных композитов с использованием техногенного сырья регулированием процессов структурообразования* (дис. ... д-р техн. наук). Белгород
3. Волженский А.В., Бузов Ю.С., Колокольников В.С. (1973). *Минеральные вяжущие вещества*. Москва: Стройиздат
4. Ronald J.E. (2001). *Hydration of cement mixtures containing contaminants*. Design and application of the solidified product. Enschede: University of Twente
5. Swamy R. (1997). *Designs of Durability and Strength Through the Use of Fly Ash and Slag in Concrete*. Proc. of the Mario Collepardi Symposium on Advances in Concrete Science and Technology. Rome, Italy
6. Chen Wei (2007). *Hydration of slag cement. Theory, modelling and application* (dissertation to obtain the doctor's degree). Twente University
7. Кривенко П.В., Пушкарева Е.К., Гоц В.И., Ковальчук Г.Ю. (2012). *Цементы и бетоны на основе топливных зол и шлаков*. Киев: КНУБА
8. Глуховский В.Д. (1959). *Грунтосиликаты*. Киев: Госстройархиздат
9. Ахвердиева Т.А. (2008). Использование отходов Гянджинского глиноземного производства для получения бетонов на основе щелочно-минерального вяжущего. *Техника и технология силикатов*, 4, 23-25
10. Ахвердиева Т.А. (2009). Безобжиговые щелочно-минеральные вяжущие и бетоны на основе Джабраильского вулканического пепла. *Естественные и технические науки*, 2, 417-22
11. Akhverdieva T.A. (2010). Process of Strengthening and Structuration of Volcano Ashes, Liquid Glass, Sodium Hydroxide, Clay, Postplacement Mixture. *International Journal of Academic Research*, 1, 61-64
12. Binyu Zhang, Chi Sun Poon (2015). Use of Furnace Bottom Ash for producing lightweight aggregate concrete with thermal insulation properties. *Journal of Cleaner Production*, 99, 94-100  
<https://doi.org/10.1016/j.jclepro.2015.03.007>
1. Improvement of the waste management system of thermal power plants Retrieved from <http://tef.kpi.ua>
2. Chulkova I.L. (2011). *Increasing the efficiency of construction composites with the use of technogenic raw materials by regulating the processes of structure formation* (dissertation to obtain the doctor's degree). Belgorod
3. Volzhensky A.V., Burov Y.S. & Kolokolnikov V.S. (1973). *Mineral binders*. Moscow: Stroyizdat
4. Ronald J.E. (2001). *Hydration of cement mixtures containing contaminants*. Design and application of the solidified product. Enschede: University of Twente
5. Swamy R. (1997). *Designs of Durability and Strength Through the Use of Fly Ash and Slag in Concrete*. Proc. of the Mario Collepardi Symposium on Advances in Concrete Science and Technology. Rome, Italy
6. Chen Wei (2007). *Hydration of slag cement. Theory, modelling and application* (dissertation to obtain the doctor's degree). Twente University
7. Krivenko P.V., Pushkareva E.K., Gotz V.I. & Kovalchuk G.Y. (2012). *Cements and Concretes Based on Fly Ash and slag*. Kyiv: KNUBA
8. Glukhovskiy V.D. (1959). *Soil silicates*. Kyiv: Gosstroyarchizdat
9. Akhverdieva T.A. (2008). Use of waste from the Ganja alumina industry to produce concrete based on an alkaline-mineral binder. *Technique and technology of silicates*, 4, 23-25
10. Akhverdieva T.A. (2009). Unburned alkaline-mineral binders and concrete based on Jabrail volcanic ash. *Natural and Technical Sciences*, 2, 417-422
11. Akhverdieva T.A. (2010). Process of Strengthening and Structuration of Volcano Ashes, Liquid Glass, Sodium Hydroxide, Clay, Postplacement Mixture. *International Journal of Academic Research*, 1, 61-64
12. Binyu Zhang, Chi Sun Poon (2015). Use of Furnace Bottom Ash for producing lightweight aggregate concrete with thermal insulation properties. *Journal of Cleaner Production*, 99, 94-100  
<https://doi.org/10.1016/j.jclepro.2015.03.007>

13. Bondar V.A., Akhmednabiev R.R. & Akhmednabiev R.M. (2016). Influence of fly ash and slags of boiler with circulating fluidized bed on properties of concrete // *Academic journal. Series: Industrial Machine Building, Civil Engineering*, 2(47), 148-154

14. Bondar V., Shulgin V., Demchenko O. & Bondar L. (2017). Experimental study of properties of heavy concrete with bottom ash from power station [Electronic resource]. *MATEC Web of Conferees*, 116, 02007  
<https://doi.org/10.1051/mateconf/201711602007>

15. Aggarwal Yogesh & Rafat Siddique (2014). Micro-structure and properties of concrete using bottom ash and waste foundry sand as partial replacement of fine aggregates. *Construction and Building Materials*, 54, 210-223  
<https://doi.org/10.1016/j.conbuildmat.2013.12.051>

16. Yoon Seyoon, Monteiro P., Macphee D., Glasser F., Imbabi M. (2014). Statistical evaluation of the mechanical properties of high-volume class F fly ash concrete. *Construction and Building Materials*, 54, 432–442  
<https://doi.org/10.1016/j.conbuildmat.2013.12.077>

17. Roshazita Che Amat, Khairul Nizar Ismail, Norazian Mohamed Noor & Norlia Mohamad Ibrahim (2017). The Effects of Bottom Ash from MSWI Used as Mineral Additions in Concrete. *MATEC Web of Conferees*, 97, 01053  
<https://doi.org/10.1051/mateconf/20179701053>

18. Johnston C.D. (1987). Effects of Microsilica and Class C Fly Ash on Resistance of Concrete to Rapid Freezing and Thawing and Scaling in the Presence of Deicing Agents. *Concrete Durability*, 2, 1183-1204

19. Mehta P.K. (2004). *High-performance, high-volume fly ash concrete for sustainable*. Proceedings of International Workshop on Sustainable Development and Concrete Technology (Beijing, China). Ames: Iowa State University

20. Thomas M. & Eng P. (2007). Optimizing the use of fly ash in concrete. *Portland Cement Associations*, 1-24

21. Malhotra V.M. & Mehta P.K. (2002). *High-performance, high-volume fly ash concrete: materials, mixture proportioning, properties, construction practice, and case histories*. Ottawa, Canada

13. Bondar V.A., Akhmednabiev R.R. & Akhmednabiev R.M. (2016). Influence of fly ash and slags of boiler with circulating fluidized bed on properties of concrete // *Academic journal. Series: Industrial Machine Building, Civil Engineering*, 2(47), 148-154

14. Bondar V., Shulgin V., Demchenko O. & Bondar L. (2017). Experimental study of properties of heavy concrete with bottom ash from power station [Electronic resource]. *MATEC Web of Conferees*, 116, 02007  
<https://doi.org/10.1051/mateconf/201711602007>

15. Aggarwal Yogesh & Rafat Siddique (2014). Micro-structure and properties of concrete using bottom ash and waste foundry sand as partial replacement of fine aggregates. *Construction and Building Materials*, 54, 210-223  
<https://doi.org/10.1016/j.conbuildmat.2013.12.051>

16. Yoon Seyoon, Monteiro P., Macphee D., Glasser F., Imbabi M. (2014). Statistical evaluation of the mechanical properties of high-volume class F fly ash concrete. *Construction and Building Materials*, 54, 432–442  
<https://doi.org/10.1016/j.conbuildmat.2013.12.077>

17. Roshazita Che Amat, Khairul Nizar Ismail, Norazian Mohamed Noor & Norlia Mohamad Ibrahim (2017). The Effects of Bottom Ash from MSWI Used as Mineral Additions in Concrete. *MATEC Web of Conferees*, 97, 01053  
<https://doi.org/10.1051/mateconf/20179701053>

18. Johnston C.D. (1987). Effects of Microsilica and Class C Fly Ash on Resistance of Concrete to Rapid Freezing and Thawing and Scaling in the Presence of Deicing Agents. *Concrete Durability*, 2, 1183-1204

19. Mehta P.K. (2004). *High-performance, high-volume fly ash concrete for sustainable*. Proceedings of International Workshop on Sustainable Development and Concrete Technology (Beijing, China). Ames: Iowa State University

20. Thomas M. & Eng P. (2007). Optimizing the use of fly ash in concrete. *Portland Cement Associations*, 1-24

21. Malhotra V.M. & Mehta P.K. (2002). *High-performance, high-volume fly ash concrete: materials, mixture proportioning, properties, construction practice, and case histories*. Ottawa, Canada

UDC 624.131.543

## Base deformation's features during deep foundation pit excavation

Zotsenko Mykola<sup>1\*</sup>, Vynnykov Yuriy<sup>2</sup>

<sup>1</sup> National University «Yuri Kondratyuk Poltava polytechnic» <https://orcid.org/0000-0003-1886-8898>

<sup>2</sup> National University «Yuri Kondratyuk Poltava polytechnic» <https://orcid.org/0000-0003-2164-9936>

\*Corresponding author E-mail: zotcenco@hotmail.com

The problems of estimating the stress-strain state of the foundations during the deep foundation pits installation are considered. The results of finite element calculations in the plane formulation of the stability of the pit walls and the retaining structures' operation under dense urban development are presented. It is proved that the proposed method specifies the calculation of determining the impact of the new building on existing buildings and structures, which enables assigning the design of retaining structures from drilled piles on the conditions of normal further operation of existing facilities. It is established that the parameters of the structures retaining the walls of deep foundation pits in the presence of existing buildings, should be assigned based on the actual condition of these buildings and the allowable additional deformations.

**Keywords:** soil massif, dip foundation pit, stress-strained state, finite element method, retaining structure, drilled pile.

## Особливості деформування основ при влаштуванні глибоких котлованів

Зоценко М.Л.<sup>1\*</sup>, Винников Ю.Л.<sup>2</sup>

<sup>1</sup> Національний університет «Полтавська політехніка імені Юрія Кондратюка»

<sup>2</sup> Національний університет «Полтавська політехніка імені Юрія Кондратюка»

\*Адреса для листування E-mail: zotcenco@hotmail.com

Розглянуто проблеми оцінювання напружено-деформованого стану основ при проходженні глибоких котлованів. В основу алгоритму визначення додаткових деформацій існуючих будівель і споруд, розташованих навколо котловану, покладено принцип підсумовування деформацій від впливу усіх суттєвих факторів (зниження напружень у масиві навколо існуючих фундаментів при розробленні котлованів, бічний активний тиск ґрунту на існуючі фундаменти, втрата стійкості ґрунту навколо фундаменту, нерівномірне випирання ґрунту на дні котловану; витискання ґрунту з-під підшви фундаменту в бік котлована), що їх викликають. Після порівняння граничних і розрахункових додаткових деформацій цих будівель і споруд призначають заходи зі зниження негативного впливу нового будівництва. Наведено результати розрахунків методом скінченних елементів у плоскій постановці з використанням пружно-пластичної моделі ґрунту та узагальненого критерію міцності Мізеса-Шлейхера-Боткіна стійкості стін котлованів і роботи утримуючих споруд за умов щільної міської забудови. Доведено, що запропонована методика конкретизує розрахунок визначення впливу новобудови на існуючі будівлі та споруди, що дозволяє призначати конструкцію утримуючих споруд із буронабивних паль з умов подальшої нормальної експлуатації існуючих об'єктів. При моделюванні розглянуті варіанти влаштування паль у один та два ряди, а також використання ґрунтових анкерів. Встановлено, що параметри споруд, утримуючих стінки глибоких котлованів (тип, кількість, жорсткість, місцезосташування) при наявності поряд існуючих будівель, повинні призначатися, виходячи із фактичного стану цих будівель і допустимих додаткових для них абсолютних і відносних деформацій. Також встановлено, що слід враховувати послідовність робіт і характер навантажень, відповідні характеристики матеріалів конструкцій. Показано, що утримуюча споруда, при розрахунку за таким принципом, може мати більшу матеріалоемність, ніж та, яка розрахована лише за міцністю, але вона повністю виключить можливість руйнування існуючих навколо котловану будівель.

**Ключові слова:** ґрунтовий масив, глибокий котлован, напружено-деформований стан, метод скінченних елементів, утримуюча споруда, буронабивна паля.



## Introduction

At the present stage of the construction industry development in Ukraine, the reconstruction of large cities is being carried out intensively, which, in particular, includes new construction of houses of various purposes (including high-rise ones) with a developed underground part, underground structures of public and technical purpose (parks, shops, underground passages, warehouses), transport and communication tunnels, etc.

Groundworks are mostly performed in an open way.

## Review of the research sources and publications

Reconstruction, in this case, is understood as the placement of these objects among the existing buildings and structures in terms of compact urban development. The contours of the underground space, within which the foundation part of new buildings and structures is located, are directly close to the existing foundations [1 – 5].

Experience shows that as a result of such an approximation, the violation created before the new construction, stress-strain state (SSS) of the foundation is possible. This leads to cracks in the load-bearing structures of existing buildings, skew of the openings in the walls, displacement of floors, and so on. [1 – 5].

The main factors that arise as a result of new construction and cause the listed damages are changes in the SSS of the basis of existing buildings due to [1 – 8]:

- at the stage of construction of new foundations - foundation pit excavation;
- at the stage of further construction and operation - the emergence of additional stresses from the weight of the new building.

Of course, at the stage of the foundation construction, other influences on the basis of existing structures are possible, such as dynamic - from the operation of mechanisms, and even more with the dynamic immersion of piles and soil compaction; consequences of water lowering, etc. [1 – 5].

From the above analysis it follows that when building in dense conditions to ensure the preservation and subsequent normal operation of building structures existing in the building area of buildings and structures, additional requirements should be made to the choice of design solutions, technologies, and construction of new buildings [6 – 8].

This requires the development of special enclosing walls and retaining structures, in all cases, to reduce the settlement of existing buildings [1 – 5, 9 – 11].

This is also accompanied by an assessment of the SSS of the foundations of new buildings to determine the additional deformations existing along with the new buildings and structures during construction and operation [2 – 4, 12].

## Definition of unsolved aspects of the problem

When excavating pits and trenches near existing buildings, vertical and horizontal stresses in the soil mass around the existing foundations are reduced. This causes a decrease in the strength of the base due to the disappearance of the lateral load.

At the same time, there are some other negative phenomena, namely: lateral active soil pressure on the existing foundation (in buildings without basements); loss of soil stability around the foundation; uneven protrusion of soil at the bottom of the pit; squeezing the soil from under the base of the foundation towards the pit, etc. [6 – 8].

When deepening pits near buildings on pile foundations below their grilles, the soil may spill out of the inter-pile space and expose piles, which may eventually lead to uneven subsidence and destruction of grilles, floors, damage to inlets and outlets of communications [2, 5].

## Problem statement

Therefore, the goal of this paper was to improve the method of determining the impact of new buildings on existing buildings and structures, which would enable selection of the retaining structures design, based on the conditions of the further normal operation of existing buildings.

## Basic material and results

Thus, the main task in the design of buildings and structures in dense urban development is the principle of "do no harm".

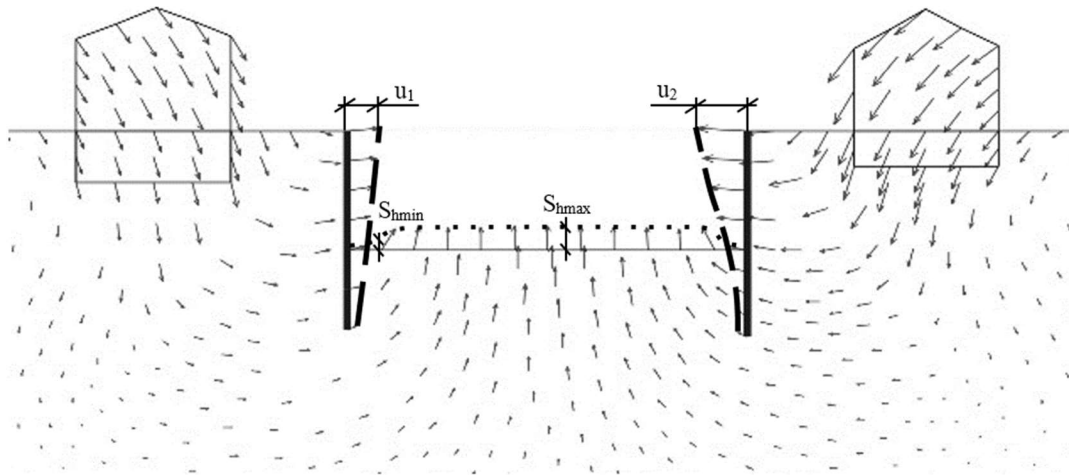
It is implemented in the following sequence:

- within the construction site, buildings and structures that may be affected by new construction are identified;
- technical inspection of certain existing buildings and structures is carried out in order to establish their technical condition, which determines their maximum additional deformations;
- for specific conditions, the negative factors of new construction which will affect the condition of existing buildings and structures are determined;
- from each factor the additional deformation of the building is defined, preference is given to methods of calculation which allow considering together the influence of more factors;
- total additional deformations of existing buildings and structures are defined as the sum of deformations from the influence of all identified factors;
- on the basis of boundary comparisons and calculated additional deformations, measures on reduction of the new construction negative influence are defined.

Further, it was considered the features of the SSS change of the existing buildings and constructions' basis only during the foundation pits' excavation for new construction.

As a result of the pits' excavation due to partial unloading of the base, there are deformations (Fig. 1), which can be divided into two groups:

- the first group of deformations is the protrusion of the pit bottom, with the maximum values they have in the center and the minimum at the periphery of the pit ( $S_{h \max}$  and  $S_{h \min}$ );
- the second group of deformations is associated with the operation of the pit slopes, they occur with the loss of their stability ( $u_1$  and  $u_2$ ).



**Figure 1 – Deformations development scheme during the foundation pit excavation**

In the standards for foundations of buildings and structures [7, 8] in this regard, in particular, it is said that "temporary and permanent attachments of deep pits, for which the requirements for displacement are set, must be calculated by the finite element method (FEM).

At the same time, it is necessary to consider the sequence of works and the load nature, to use the specified models of soil base, and also the corresponding characteristics of structural materials, and to provide measures for influence reduction of new construction on the existing building.

Modeling of retaining structures work can be carried out both by the plane, and spatial calculation scheme.

The choice of the scheme depends on the size of the structure in length. With a significant increase in the length of the supporting structures, the results of calculations in the flat and spatial settings are close in value.

Therefore, the assessment of SSS bases should be carried out with due regard to all the features of the supporting structures and the pit in the challenging urban and geological conditions.

Calculations of the pits' excavation at the second boundary condition make it possible to design more reliable retaining structures, excluding any destruction of existing buildings.

To establish the base's SSS, we used the software package "CONCORD - 4.2" (author – S.F. Klovnych) FEM in a plane setting [13].

The theoretical basis of the "CONCORD - 4.2" is a mathematical description of the soil as a continuous isotropic medium. The proposed soil model is a development of the theory of small elastic-plastic deformations by AA Illiushin and the deformation theory of G.A Geniiev.

This phenomenological model takes into account physical and geometric nonlinearity, dilatancy, compaction in the process of deformation, different resistance to compression and tension, pore and hydrostatic pressure, shrinkage, and swelling of the soil. When posing the problem of nonlinear soil mechanics, the following hypotheses are adopted [13]:

- manifestations of nonlinearity are taken into account: they contain plastic deformation of shape change under a complex stress state, the connection between the components of stress and strain deviators is nonlinear;

- plastic deformation takes into account dilatancy, ie the nonlinear relationship between the components of volumetric stress and strain tensors;

- unimpeded deformation of the soil during stretching.

The model of the soil is based on the relationship between octahedral tangential stress and displacement. The initial characteristics of the soil:

- specific cohesion  $c$ ;

- internal friction angle  $\phi$ ;

- deformation module  $E$ ;

- displacement module  $G$ ;

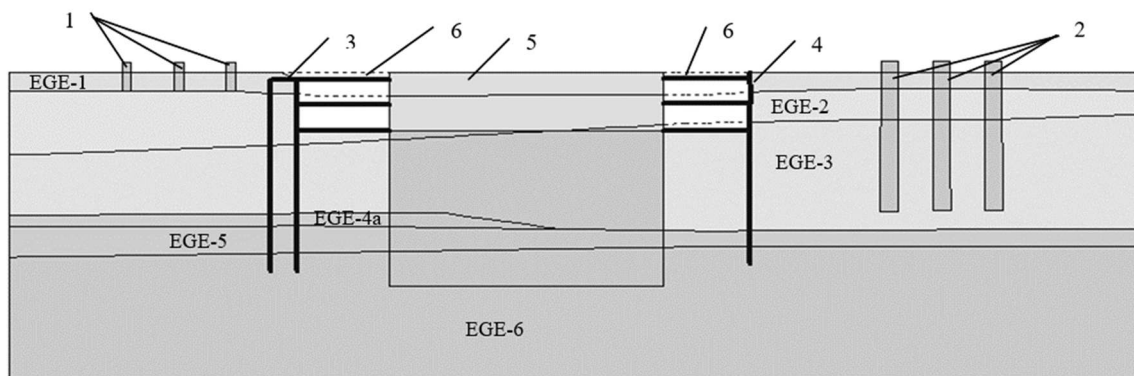
- spatial deformation module  $K$ , – change in the calculation process is a function of the SSS of the soil mass [13].

To describe the ultimate strength, a generalized Mises-Schleicher-Botkin criterion is used, which determines the value of the octahedral tangential stress depending on the octahedral normal stress  $\tau_0 = \sigma_0 \operatorname{tg} \phi_0 + c_0$ . The strength surface by this criterion describes the cone in the space of principal stresses [13].

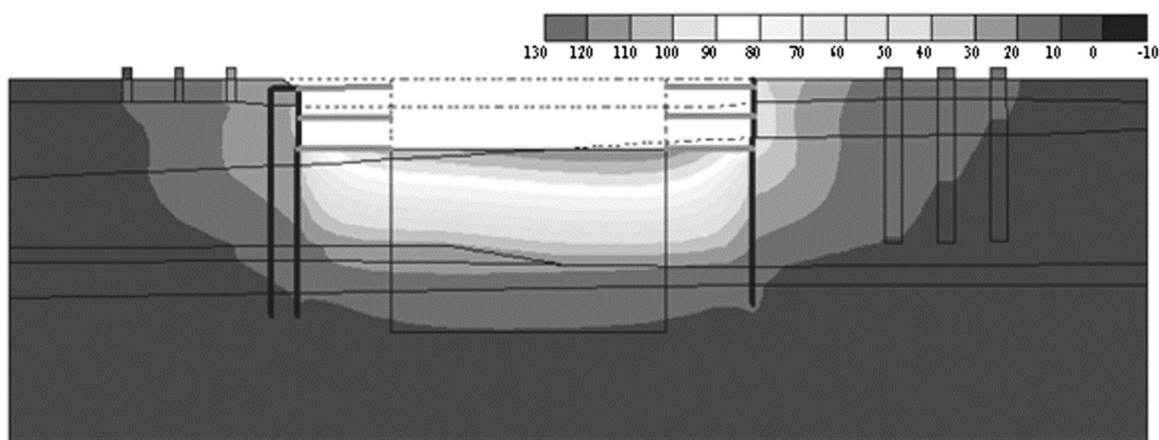
The algorithm of the software complex automatically takes into account the compaction of the base soil under the foundations during the operational period (for an existing building).

The application of the complex enables estimating the SSS of the system, to get an image of the possible impact of new construction on existing structures and buildings, to make decisions on preventing the undesirable impact of new construction on both existing and project facilities. [13].

The main problems in modeling the installation of deep pits will be considered by the example of the construction of a high-rise residential building in Kyiv. The calculation scheme for modeling the deformations of the base is shown in Fig. 2.



**Figure 2 – Calculation scheme: 1, 2 – foundations of existing buildings;  
3 – retaining wall of two rows of drilled piles; 4 – retaining wall of one row of drilled piles;  
5 – new building; 6 – parking**



**Figure 3 – Base displacement of the foundation pit setting up**

The base of the foundations is represented by six engineering-geological elements and includes sandstones and clays with a total thickness of up to 10 – 15 m, which are underlain by low-moisture fine dense sands.

An aquifer was found in the sandstone, which is caused by precipitation and leaks from aquifers. It is considered that piles rest on shallow dense sand.

The high-rise building is located in a dense urban development on a landslide-prone slope. The foundations of the building are piles with a grille performed as monolithic reinforced concrete 2 m thick slab. The length of the piles from the bottom of the grille is 22 - 25 m, diameter 800 mm.

By the technological solution, the piles are drilled. Existing buildings adjoin the new one on both sides at a distance of 4 m and 15 m.

A 10 m deep pit is used to erect the building's foundations and its underground part. To prevent the destruction of the walls of the pit and undesirable deformations of the existing building, the installation of retaining structures in the form of a retaining wall of drilled piles with a diameter of 1000 mm and a length of 23 - 25 m with the stiffness per 1 running meter of  $EA = 3,0 \cdot 10^6$  kN and  $EI = 4,7 \cdot 10^4$  kNm<sup>2</sup>.

In the simulation, the options for installation piles in one and two rows, as well as the use of soil anchors with stiffness indices at equivalent length are considered to be  $l_e = 10$  m  $EA = 9,8 \cdot 10^4$  kN.

The data in table 1 indicates that the parameters of retaining structures (type, number, stiffness, location) in the presence of existing buildings, should be selected based on the actual condition of these buildings and the allowable additional deformations.

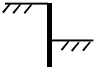
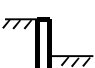
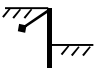

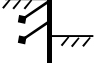
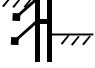
Accordingly, the retaining structure, calculated by this principle, may have a higher material consumption than that calculated only for strength, but completely eliminate the possibility of destruction of existing buildings around the pit.

So far there is no standard data on the limit values of deformations of existing buildings and structures from the impact of new construction in the conditions of dense urban development.

In our opinion, it is possible to use the data given in [6], which regulates the allowable settlement depending on the category of the existing building by its wear, i.e. on its actual condition.

According to the materials of the technical inspection, it is an existing building with four above-ground floors, frameless with load-bearing brick walls and strip foundations on a natural base.

**Table 1 – Deformations of the existing building due to the construction of the pit of the new building depending on the design of the retaining structure**

Variant	Bearing structure description	Foundation pit elevation, mm	Bearing structure top displacement, mm	Additional deformation	
				absolute subsidence, mm	settlement unevenness
1	 drilled piles in one row	119	214	24	0,0016
2	 drilled piles in two rows	117	139	20	0,0013
3	 drilled piles in one row with foundation bolts' row	97	8	12	0,0006
4	 drilled piles in two rows with foundation bolts' row	98	7	8	0,0003
5	 drilled piles in one row with foundation bolts in two rows	96	5	8	0,0003
6	 drilled piles in two rows with foundation bolts in two rows	96	3	5	0,00021

According to table 5 [6] the category by the condition of the load-bearing structures of the building is the second. The additional deformations limit of the existing buildings' foundation by table 4 [6] are  $[S] \leq 1.0$  cm, and their relative settlement difference is  $[\Delta S/L] \leq 0.0007$ .

According to the results of mathematical modeling by the FEM, it is established that at the stage of operation the new building will cause additional subsidence of the foundation of the existing building  $S_0 = 0.4$  cm, and the relative difference of the settlement  $-\Delta S/L = 0.0005$ .

When constructing a retaining structure according to items 4, 5 of the table. 1 total deformation of the foundation of existing buildings will be

$$S_0 = 0.8 + 0.4 = 1.2 \text{ cm} > [S] = 1.0 \text{ cm},$$

and

$$\Delta S/L = 0.0005 + 0.0003 = 0.0008 > [\Delta S/L] = 0.0007.$$

Thus, the conditions of the deformations' calculation for these variants of retaining structures (respectively, drilled piles in two rows with a row of anchors and drilled piles in one row with two rows of anchors) are not met.

In the construction of the retaining structure according to paragraph 6 of the table 1 total deformation of the foundation of existing buildings will be

$$S_0 = 0.5 + 0.4 = 0.9 \text{ cm} < [S] = 1.0 \text{ cm},$$

and

$$\Delta S/L = 0.0005 + 0.0002 = 0.0007 = [\Delta S/L] = 0.0007.$$

Therefore, the conditions of deformations' calculation for the sixth variant of retaining structures – drilled piles in two rows with two rows of anchors, are fulfilled.

### Conclusions

Thus, the above method specifies the calculation of determining the impact of the new building on existing buildings and structures, which enables assigning the design of retaining structures from the conditions of the further normal operation of existing facilities.

Parameters of geotechnical structures (type, quantity, rigidity, location) of retaining walls of deep pits in the presence of nearby existing buildings should be selected based on the actual condition of these buildings and allowable additional and relative deformations for their foundations.

It is also necessary to take into account the sequence of works and the nature of the loads, the relevant characteristics of the materials of structures.



## References

1. Briaud J.-L. (2013). *Geotechnical Engineering: Unsaturated and Saturated Soils*. Wiley
2. Улицкий В.М., Шашкин А.Г., Шашкин К.Г. (2010). *Геотехническое сопровождение развития городов*. Санкт-Петербург: «Георекострукция»
3. Ильичев В.А., Мангушев Р.А. (Ред.) (2014). *Справочник геотехника. Основания, фундаменты и подземные сооружения*. Москва: АСВ
4. Katzenbach R., Leppla S., Seip M. & Kurze S. (2015). Value Engineering as a basis for safe, optimized and sustainable design of geotechnical structures. *Proc. of the XVI ECSMGE Geotechnical Engineering for Infrastructure and Development*. Edinburg, 601-606  
<https://doi:10.1680/ecsmge.60678>
5. Мангушев Р.А., Никифорова Н.С. (2017). *Технологические осадки зданий и сооружений в зоне влияния подземного строительства*. Москва: АСВ
6. ВСН 490-87 (1988) *Проектирование и устройство свайных фундаментов и шпунтовых ограждений в условиях реконструкции промышленных предприятий и городской застройки*. Москва: Минмонтажспецстрой СССР
7. EN 1997-1:2004 (2004). *Eurocode 7: Geotechnical Design. Part 1: General Rules*. Brussels: European Committee for Standardization.
8. ДБН В.2.1-10: 2018 (2018). *Основи і фундаменти будівель та споруд. Основні положення*. Київ: Міністерство регіонального розвитку, будівництва та житлово-комунального господарства України.
9. Neves, M. & Pinto, A. (2015) *The use of CSM technology in permanent or temporary retaining structures with a cofferdam effect*. Proc. of the XVI ECSMGE Geotechnical Engineering for Infrastructure and Development. Edinburg.  
<https://doi:10.1680/ecsmge.60678>
10. Klein, P.Y. & Mathieu, F. *A soil remediation solution by deep soil mixing under low headroom conditions*. Proc. of the XVI ECSMGE Geotechnical Engineering for Infrastructure and Development. Edinburg  
<https://doi:10.1680/ecsmge.60678>
11. Kryvosheiev P., Farenjuk G., Tytarenko V., Boyko I., Kornienko M., Zotsenko M., Vynnykov Yu., Siedin V., Shokarev V., Krysan V. (2017). Innovative projects in difficult soil conditions using artificial foundation and base, arranged without soil excavation. *Proc. of the 19<sup>th</sup> Intern. Conf. on Soil Mechanics and Geotechnical Engineering*. Seoul, 3007-3010
12. Chau K. (2013). Numerical Methods. *Proc. of the 18<sup>th</sup> Intern. Conf. on Soil Mechanics and Geotechnical Engineering*. Paris, 647 – 654.  
[doi: 10.30977/bul.2219-5548.2020.89.0.59](https://doi:10.30977/bul.2219-5548.2020.89.0.59)
13. Клованич С.Ф. (2009). *Метод конечных элементов в нелинейных задачах инженерной механики*. Запорожье: ООО «ИПО «Запорожье»
1. Briaud J.-L. (2013). *Geotechnical Engineering: Unsaturated and Saturated Soils*. Wiley
2. Ulitskii V.M., Shashkin A.H. & Shashkin K.H. (2010). *Geotechnical provision of urban development*. Saint-Petersburg: «Georeconstruction»
3. Ilyichev V.A. & Mangushev R.A. (Ed.) (2014). *Handbook of geotechnics. Bases, foundations and underground structures*. Moscow: ASV
4. Katzenbach R., Leppla S., Seip M. & Kurze S. (2015) Value Engineering as a basis for safe, optimized and sustainable design of geotechnical structures. *Proc. of the XVI ECSMGE Geotechnical Engineering for Infrastructure and Development*. Edinburg, 601-606  
<https://doi:10.1680/ecsmge.60678>
5. Mangushev R.A. & Nykyforova N.S. (2017) *Technological settlements of buildings and structures in the underground construction influence zone*. Moscow: ASV
6. VSN 490-87 (1988). *Design and installation of pile foundations and sheet piles in the context of the industrial enterprises' reconstruction and urban development*. Moscow: *Minmontazhspetsstroy USSR*
7. EN 1997-1:2004 (2004). *Eurocode 7: Geotechnical Design. Part 1: General Rules*. Brussels: European Committee for Standardization.
8. DBN V.2.1-10: 2018 (2018). *Bases and foundations of buildings and structures. Main principles*. Kyiv: Ministry of Regional Development, Construction, and Housing of Ukraine.
9. Neves, M. & Pinto, A. (2015) *The use of CSM technology in permanent or temporary retaining structures with a cofferdam effect*. Proc. of the XVI ECSMGE Geotechnical Engineering for Infrastructure and Development. Edinburg.  
<https://doi:10.1680/ecsmge.60678>
10. Klein, P.Y. & Mathieu, F. *A soil remediation solution by deep soil mixing under low headroom conditions*. Proc. of the XVI ECSMGE Geotechnical Engineering for Infrastructure and Development. Edinburg  
<https://doi:10.1680/ecsmge.60678>
11. Kryvosheiev P., Farenjuk G., Tytarenko V., Boyko I., Kornienko M., Zotsenko M., Vynnykov Yu., Siedin V., Shokarev V., Krysan V. (2017). Innovative projects in difficult soil conditions using artificial foundation and base, arranged without soil excavation. *Proc. of the 19<sup>th</sup> Intern. Conf. on Soil Mechanics and Geotechnical Engineering*. Seoul, 3007-3010
12. Chau K. (2013). Numerical Methods. *Proc. of the 18<sup>th</sup> Intern. Conf. on Soil Mechanics and Geotechnical Engineering*. Paris, 647 – 654.  
[doi: 10.30977/bul.2219-5548.2020.89.0.59](https://doi:10.30977/bul.2219-5548.2020.89.0.59)
13. Klovanych S.F. (2009). *The finite element method in nonlinear problems of engineering mechanics*. Zaporozhye: LLC "IPO "Zaporozhye"

UDC 625.767

## Current trends in transport planning

Hasenko Lina<sup>1\*</sup>, Lytvynenko Tetyana<sup>2</sup>, Tkachenko Iryna<sup>3</sup>, Elgandour Mohamed<sup>4</sup>

<sup>1</sup> National University «Yuri Kondratyuk Poltava Polytechnic» <https://orcid.org/0000-0002-1310-914X>

<sup>2</sup> National University «Yuri Kondratyuk Poltava Polytechnic» <https://orcid.org/0000-0002-7229-201X>

<sup>3</sup> National University «Yuri Kondratyuk Poltava Polytechnic» <https://orcid.org/0000-0002-6605-5923>

<sup>4</sup> National University «Yuri Kondratyuk Poltava Polytechnic» <https://orcid.org/0000-0003-3800-056X>

\*Corresponding author E-mail: [lin02011@meta.ua](mailto:lin02011@meta.ua)

The settlements' infrastructure development, aimed at satisfying, first of all, the needs of motorists, is accompanied by powerful negative changes in the conditions of human life. Now problems of providing conditions for moving by individual environmental vehicles, pedestrian traffic and, in particular, for the low-mobility groups of the population are becoming more relevant. In the article is analyzed and summarized the world experience of urban street-road network reconstruction in accordance with the change of priorities that has occurred in the theory of transport planning. It singled out 2 basic options for the redistribution of space between pedestrians, cyclists, public and private transport: 1) narrowing of lanes for private transport; 2) reducing the number of lanes for private transport

**Keywords:** transport planning, street-road network, inclusive environment, individual eco-friendly vehicles, universal design principles

## Сучасні тенденції у транспортному плануванні

Гасенко Л.В.<sup>1\*</sup>, Литвиненко Т.П.<sup>2</sup>, Ткаченко І.В.<sup>3</sup>, Ельгандур М.<sup>4</sup>

<sup>1, 2, 3, 4</sup> Національний університет «Полтавська політехніка імені Юрія Кондратюка»

\*Адреса для листування E-mail: [lin02011@meta.ua](mailto:lin02011@meta.ua)

Розвиток інфраструктури населених пунктів, спрямований на задоволення насамперед потреб автомобілістів, супроводжується потужними негативними змінами в умовах людської життєдіяльності. Світовий досвід доводить, що навіть інвестуючи значні кошти у розвиток вулично-дорожньої мережі для розв'язання складних проблем автомобільного транспорту, неможливо вирішити проблему перевезень у великих містах, забезпечивши комфортне пересування автомобілів. Не випадково найкращі з точки зору транспорту міста у світі (Копенгаген, Берлін тощо) використовують так звану піраміду пріоритетів, яку радять застосовувати при прийнятті рішень, що стосуються проектування та реконструкції вулично-дорожньої мережі. На першому місці в цій піраміді стоять пішоходи, на другому – велосипедисти, на третьому – громадський транспорт, потім – комерційний транспорт, на останньому місці – приватний автотранспорт. Навіть виклики пандемії сприяли саме такому розподілу пріоритетів, коли в деяких великих містах Європи адміністративними заходами частину проїжджої частини вулиць віддали пішоходам та велосипедистам. В Україні останнім часом також спостерігається тенденція до зміни пріоритетів у теорії транспортного планування. Зміна пріоритетів знаходить відображення в оновлених нормативних документах України. У статті проаналізовано й узагальнено світовий досвід проектування та реконструкції вулично-дорожніх мереж населених пунктів відповідно до сучасних тенденцій у транспортному плануванні. У результаті аналізу закордонного і вітчизняного досвіду виокремлено два базові варіанти перерозподілу простору між пішоходами, велосипедистами, громадським та приватним транспортом: 1) звуження смуг для приватного транспорту (що дозволяють оновлені нормативні документи України); 2) зменшення кількості смуг для приватного транспорту (розглянуто три основні варіанти такого перерозподілу)

**Ключові слова:** транспортне планування, вулично-дорожня мережа, інклюзивне середовище, індивідуальні екологічні транспортні засоби, принципи універсального дизайну



## Introduction

The rapid rate of motorization creates a new situation in urban design. Illustration (fig.1) by Swedish artist Karl Jilg (which was commissioned by the Swedish Road Administration) shows how car-centric our reality is [1].

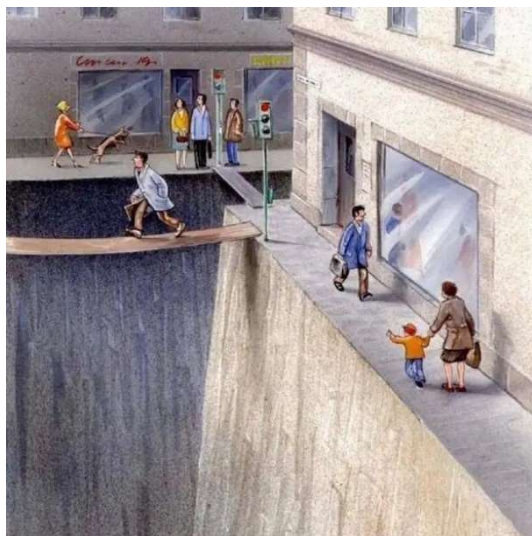


Figure 1 – Illustration by Swedish artist Karl Jilg

Now problems of providing conditions for moving by individual environmental vehicles, pedestrian traffic and, in particular, for the low-mobility groups of the population are becoming more relevant.

## Review of the research sources and publications

Recently, more and more researchers of transport planning use the term «Automobile Dependency» [2; 3]. In 1995 Permanent International Association of Road Congresses (PIARC) conducted a specialized XX World Road Congress, devoted exclusively to problems of urban transport planning. In the United States, at the state level, acts were adopted, in which special attention was paid to the organization and safety of pedestrian movement [4]: Intermodal Surface Transportation Act of 1991 (ISTEA), Transportation Equality Act of the 21st Century.

Many scientists from different countries are interested in the application of universal design principles (UDP) in street-road environment improvement. Scientists from Australia are researching universal design in housing [5; 6]. Indian scientists [7] have developed a design manual for a barrier-free environment in India. In Canada, there was a publication of the Barrier-free design guide in 2017 [8]. Researchers from Turkey have done an assessment of street design with universal design principles: case in Aswan [9]. In 2012 Norway hosted the largest conference on universal design held in Europe until then. The most interesting information from the conference has been collected in [10]. Canadian scientists think that it is necessary to provide environments designed to suit the needs of older adults [11]. Researchers from Indonesia have examined several design characteristics of themed streets in several coun-

tries from three different continents using UDP for giving proper directions to develop more user-friendly streets and they resumed that design direction can be suggested universally along with the richness of local aspects [12, 13].

The need to find alternatives to individual car transport means and ways to provide comfortable conditions for an individual eco-friendly friendly vehicles (IEV) movement is discussed in the works [14-17].

In the works [18-20] the classification of the main geometric structures of the street-road network is given, their influence on the parameters of transport systems functioning is evaluated and recommendations on the use of the city's territory for different planning schemes are given.

## Definition of unsolved aspects of the problem

But such classification based on the width and operational qualities cannot fully reflect all the processes taking place on the streets. The street should be not only a city transport artery but also the place of human interaction. The organization of street space should be guided by a number of requirements related to the activation of social and economic functions: improving the quality of life, mobility and activity of the inhabitants.

## Problem statement

The purpose of this study is to summarize the world experience of designing and reconstructing urban street-road networks and to formulate proposals for its improvement in accordance with the change of priorities that has occurred in the theory of transport planning.

## Basic material and results

An analysis of the urban planning history in the context of vehicle development [21] showed that before the development of motorization (in the US until the 30s of the twentieth century, and in Europe until the 50s) cities were smaller and more compact in area and population. Weak development of transport infrastructure hampered the development of the economy, the formation of centralized states. People walked, cycled, rode horses and donkeys, or traveled in cattle-drawn carriages.

With the development of road transport, the need for settlement compactness has lost relevance. In 1929, the Soviet sociologist M.O. Okhitovych came up with the idea of a "new resettlement". According to this idea, the appearance of the car is inevitable and leads to desurbanization. In the city, among the crowded buildings, the car cannot be used effectively. Service for residents should be provided by a system of orders and delivery directly to homes.

The gap between the growing number of cars and the narrow streets unsuitable for car traffic necessitated the redevelopment of settlements and the differentiation of city streets by class. Since 1940, road departments in the United States have begun to plan the road network: inventory all roads, determine the size and nature of road traffic, review road construction financing, determine the number of car owners and the nature of their

use, study road wear, survey to determine the destination of trips in cities [22].

In the areas that were built before the car boom, there are still convenient streets for pedestrians and cyclists, which connect the points of attraction with residential areas (fig. 2). Residential and industrial areas built during urbanization are much less conducive to pedestrian traffic. They mostly do not have sidewalks but have wide streets that are difficult to cross on foot or by bicycle (fig. 3).



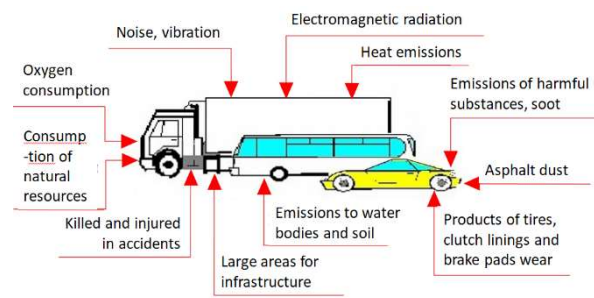
**Figure 2 – Cyclist and pedestrian-friendly street (USA)**



**Figure 3 – A wide suburban street that was built without taking into account bicycle and pedestrian traffic (USA)**

After the first hype around cars, more and more people began to realize that the constant continuous motorization and development of road construction are accompanied by powerful negative changes in human living conditions (fig. 4).

The Coronavirus crisis in 2020 gave us a glimpse of what life could be like in cities and on our streets without high levels of traffic and particularly high levels of car usage. Traffic levels fell and it became much easier for walking and cycling. Air pollution reduced and we could even see the blue skies again! It is imperative that we capture the benefits of more active travel as mobility levels return – and the majority of travel in many contexts can be by public transport, walking and cycling. But this will necessitate a strong policy approach – investing in high-quality public transport networks and giving more space to walking and cycling.



**Figure 4 – Harmful effects of road transport on the environment**

In our opinion, the creation of infrastructure for bicycle traffic is the preparation of settlements for future progress in the field of vehicles. Since scientists of the world are now actively working on the creation of various types of individual environment-friendly vehicles (IEFV) designed to replace or minimize the use of individual cars in settlements.

World experience shows that even investing heavily in the street and road network (SRN) development, the solution of road transport services complex problems, it is impossible to solve the problem of transportation in large cities by providing comfortable movement of cars. Not by chance the best in terms of transport cities in the world (Copenhagen, Berlin and others) use the so-called pyramid of priority (fig. 5), which advice to apply when making decisions in SRN designing and reconstruction [23].



**Figure 5 – The transport pyramid of inclusive street-road environment**

Taking into account the mass of the pedestrian movement (almost every citizen with one or another frequency used to move the walking) and its safety for the environment, on the highest step of this pyramid put pedestrians. The second step is cycling transport, which has the same advantages and problems as the pedestrian, but occupies a separate place in the pyramid because it allows you to overcome much larger distances (effective radius of bicycle use is 5 – 7 km) and needs parking spaces and, on separate streets, a separate infrastructure. The third step of the transport pyramid takes public transportation, which carries far more people than private cars, produces considerably fewer emissions (especially trolleybuses), takes much less space on the road and is not parked for a long time in the central part of the city. The social role of public

transport, which is much more affordable for private cars, is also great. To commercial vehicles, which deliver the required goods, in cities with an efficient transport system they give priority over private transport, since convenient conditions for this kind of transport stimulate business development and prevent the shortage of goods. Standard is the permission of commercial vehicles in certain hours, usually in the morning. The last step in the pyramid of priorities takes private cars, which, although provide a high mobility, comfort and unlimited travel range, has low efficiency. Large expenditure of energy efficiency relative to the weight he carries), causing noise and chemical pollution and occupies large areas.

Since 2018 priorities change that occurs in transport planning is beginning to be reflected in Ukrainian regulations. In the updated regulations, the requirements for the mandatory design of bicycle paths and lanes for new construction and reconstruction of streets are beginning to appear [24 - 26]. And also there are state building codes for buildings and structures inclusiveness [27].

So the question arises: how to implement change in priorities under the existing building settlements. We need to redistribute the space between pedestrians, cyclists, public and private transport. As a result of the foreign and domestic experience analysis, the authors proposed the following options for solving this problem. In order to give cyclists and pedestrians more space, we need to either narrow the lanes for private transport or reduce their number. Let's look at these two main ways.

### 1. The narrowing of lanes.

The change in priorities in Ukrainian normative documents is also evidenced by the narrowing of the regulatory minimum width of lanes on the roadway.

Thus, in the normative document DBN «Streets and roads of settlements», in effect since 2001, the minimum allowable lane width on main streets and roads of city and district significance in the most significant, significant, large, medium and small cities was 3.75 meters. Instead in document DBN «Streets and roads of settlements», in effect since 2018, minimum allowable lane width on main roads of city significance with continuous movement in the largest and large cities is 3.5 meters, and on main streets of city and district significance in the most significant, significant, large, medium and small cities, except streets with continuous movement, as well as on village roads and main streets is 3.00 meters.

Also, the minimum allowable width of the lane on local residential streets in this DBN in effect since 2001 was 3.5 and since 2018 is 2.75 meters.

That is, according to changes in regulations, free spaces from 0.25 to 0.75 m wide in each traffic lane appear on Ukrainian streets. That is, for example, on streets with 4 lanes, built according to the old regulations, released from 1 to 3 m.

The task of planners now is to reorient these spaces during the reconstruction of streets and provide them with functions that will meet, first of all, the needs of pedestrians, cyclists and public transport.

### 2. Reducing the number of lanes

The most popular in the United States option of reducing the number of lanes is «4-3 road diet», when a two-way street with two lanes in each direction becomes a three-lane (fig. 6) [28].



Figure 6 – Three lanes instead of four

The lane in the middle is reserved for those who go to the left. The remaining space can be used to create bicycle lanes, widen sidewalks or arrange dedicated lanes for public transport.

Converting four-lane roads to three lanes makes them substantially safer. This is evidenced by the following data [29].

- 3-lane roads are much safer for car drivers.

In 2013, a study of streets reconstructed on this principle was conducted in 17 cities. It turned out that in small cities, this version of the road diet reduces road accidents by 47%, and in large by 19% [28]. No reduction in street capacity was detected in any of the cases. Similar data are given in [29]. Converting roads from four lanes to three has been found to reduce collisions anywhere from 20 to 50 percent (fig. 7).

- 3-lane roads have a marginal impact on traffic flow. Such diet usually sees a reduction in car throughput in the 5% to 10% range. As the Federal Highway Administration report puts it, “under most average daily traffic conditions tested, road diets have minimal effects on vehicle capacity” [30].

- 3-lane roads slow speeds. The main difference between a 4-lane road and a 3-lane safe street is that traffic speeds go down and become far more uniform. It’s a proven fact that reducing speeds even a little bit, i.e. from 40 to 30 miles per hour, can make a huge difference in accident severity for pedestrians and bicyclists.

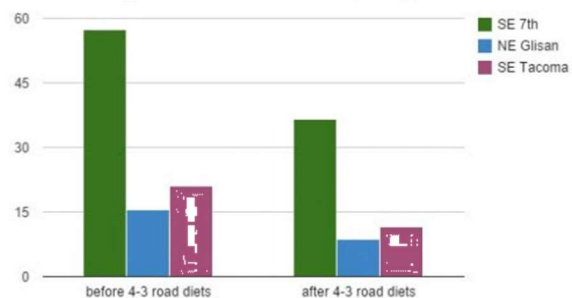


Figure 7 – Average traffic crashes per year

- 3-lane roads increase biking and walking. After a 4-3 road diet was fixed in San Francisco, “bicycle usage increased 37% during the PM peak hour, the number of pedestrians increased 49% during the PM peak hour, and public response has been overwhelmingly positive about this project” [29]. That’s just one example; also, it’s common sense.

- reducing the number of lanes is really cheap. Unlike expensive street reconstructions cities and counties can quickly, easily, and cheaply fix such redistribution of space.

For three-lane one-way streets with parking on both sides, there is a proposal for “3-2 road diet”, which offers to remove one of the lanes and narrow the parking a bit, and give the freed space for a two-way bike lane (fig. 8).



**Figure 8 – Two lanes instead of three**

Such traffic reorganization on one of the Brooklyn streets has reduced the speed of cars by 77% and the number of accidents by 63%. At the same time, the capacity of the street and the total travel time for motorists remained at the same level [28].

The first example of reducing the number of lanes in Ukraine was John Paul II Street in Ivano-Frankivsk, where they turned four lanes into two (fig. 9).

This «4-2 road diet» allowed the creation of safety islands to protect pedestrians, bike lanes for cyclists and a separate pocket for turns.



**Figure 9 – Two lanes instead of four**

Let's consider one more proof of expediency of lanes on city streets and road quantity reduction. Analysis of methods for calculating the required number of lanes [18, 31, 32] showed the following.

The capacity of the designed highway, required to pass the traffic flow of given traffic intensity, taking into account the perspective, is determined by the formula:

$$P_T = N / z, \quad (1)$$

where  $z$  is the perspective loading of the highway by traffic.

The capacity of a multi-lane roadway is defined as the sum of the capacities of its component lanes:

$$P = \sum P_i. \quad (2)$$

The capacity of each lane on the street is different. The closer the lane is to the center of the roadway, the less its capacity. This is primarily due to the restructuring, i.e. changing lanes.

The capacity of the  $i$ -th lane is determined by the formula:

$$P_i = P_1 \cdot k_{ni} \cdot k_c, \quad (3)$$

where  $P_1$  is the capacity of the first lane, units / hour;  $k_{ni}$  - the coefficient of reduction of the  $i$ -th lane capacity depending on its number, table 1;

$k_c$  is the coefficient of capacity reduction depending on the composition of the flow.

**Table 1 – Capacity reduction factor depending on the lane number**

lane number	1	2	3	4 and more
$k_{ni}$	1	0,85	0,7	0,5

Therefore, the capacity of the multi-lane roadway is defined as:

$$P_i = P_1 \cdot k_c \cdot \sum k_{ni}, \quad (4)$$

To pass the traffic flow of given traffic intensity, taking into account the perspective and load level, it is necessary that the capacity of the designed city highway with a multi-lane roadway ( $P$ ) was not less than the required capacity ( $P_T$ ). Given the dependences (1) and (4), we have:

$$P_1 \cdot k_c \cdot \sum k_{ni} \geq N / z. \quad (5)$$

Whence

$$\sum k_{ni} = N / P_1 \cdot k_c \cdot z. \quad (6)$$

According to table 1, it is necessary to take the number of bands ( $n$ ) at which the value of the total capacity reduction factor would be not less than that obtained by formula (6).

As we can see, the efficiency of the roadway decreases with the increasing number of lanes: from the position of capacity in four-lane carriageway almost not used one lane ( $\sum k_{ni} = 3.05$ ), and in six-lane - already two ( $\sum k_{ni} = 4.05$ ). Therefore, reducing the width of the roadway is justifiably appropriate, but requires further research.

## Conclusions

The settlements' infrastructure development, aimed at satisfying, first of all, the needs of motorists, is accompanied by powerful negative changes in the conditions of human life. Recently, more and more researchers of transport planning use the term «Automobile Dependency». World experience shows that even investing heavily in the street and road network (SRN) development, the solution of road transport services complex problems, it is impossible to solve the problem of transportation in large cities by providing comfortable movement of cars. Not by chance the best in terms of transport cities in the world (Copenhagen, Berlin and others) use the so-called pyramid of priority, which advice to apply when making decisions in SRN designing

and reconstruction. In the first place in this pyramid are pedestrians, in the second cyclists, in the third public transport, then commercial and in last place private cars. In the article is analyzed and summarized the world experience of urban street-road network reconstruction in accordance with the change of priorities that has occurred in the theory of transport planning. It singled out 2 basic options for the redistribution of space between pedestrians, cyclists, public and private transport:

- 1) lane narrowing for private transport;
- 2) reducing the lanes number for private transport.

## References

1. Garfield L. (2017). This ingenious illustration reveals how much space we give to cars. Business insider.
2. Barton H. & Tsourou C. (2000). Healthy Urban Planning. – WHO Regional Office for Europe / London & New York: Spon Press.  
<https://doi.org/10.4324/9780203857755>
3. Рейцен С.О. (2014). Організація і безпека міського руху. К.: ТОВ «СІК ГРУП УКРАЇНА»
4. Accessibility in Public Accommodations (1991). 581: Readily Achievable Checklist. ADA Compliance Guide. – USA: Thompson Publishing Group.
5. Bringolf J. (2008). Universal Design: Is it Accessible? *Multi: The RIT Journal of Plurality and Diversity in Design*, 1 (2), 45-52.
6. Ward M. & Bringolf J. (2019). Universal Design in Housing in Australia: Getting to Yes. *Transforming our World Through Design, Diversity and Education*, Publisher: Open Access by IOS Press, 209-355  
<http://dx.doi.org/10.3233/978-1-61499-923-2-299>
7. Byahut S., Mujumdar A., Patel A., Sheth A., Mitra A., Moothan R. and Pandya Y. (2005). *Design Manual for a Barrier-Free Built Environment*.
8. Alberta Municipal Affairs and Safety Codes Council Barrier-free design guide (2017).
9. Mai Eid Khalil A. (2016). An Assessment Of Street Design With Universal Design Principles: Case In Aswan / As-Souq. *MEGARON / Yildiz Technical University, Faculty of Architecture E-Journal*, 11(4), 616-628.  
<https://dx.doi.org/10.5505/megaron.2016.98704>
10. Skavlid S., Olsen H.P. & Haugeto A.K. (2013). *Trends in Universal Design, Norway, First Edition, Norwegian Directorate for Children, Youth and Family Affairs*, The Delta Centre.
11. Carr K., Weir P.L., Azar D. & Azar N. (2013). Universal Design: A Step toward Successful Aging. *Journal of aging research*, 3  
<https://doi.org/10.1155/2013/324624>
12. Harsritanto B., Indriastjario & Wijayanti (2017). Universal design characteristic on themed streets. *IOP Conference Series: Earth and Environmental Science*, Vol. 99 (1), 012025.  
<http://dx.doi.org/10.1088/1755-1315/99/1/012025>
13. Harsritanto B. (2018). Urban Environment Development based on Universal Design Principles. *The 2<sup>nd</sup> International Conference on Energy, Environmental and Information System (ICENIS 2017)*, 31, 09010.  
<https://doi.org/10.1051/e3sconf/20183109010>
1. Garfield L. This ingenious illustration reveals how much space we give to cars. Business insider: 2017.
2. Barton H. Healthy Urban Planning / H. Barton, C. Tsourou. – WHO Regional Office for Europe / London & New York: Spon Press, 2000. – 212 p.  
<https://doi.org/10.4324/9780203857755>
3. Reytsen Ye.O. (2014). *Organization and safety of urban movement*. K.: TOV «SIK HRUP UKRAYINA»
4. Accessibility in Public Accommodations (1991). 581: Readily Achievable Checklist. ADA Compliance Guide. – USA: Thompson Publishing Group.
5. Bringolf J. (2008). Universal Design: Is it Accessible? *Multi: The RIT Journal of Plurality and Diversity in Design*, 1 (2), 45-52.
6. Ward M. & Bringolf J. (2019). Universal Design in Housing in Australia: Getting to Yes. *Transforming our World Through Design, Diversity and Education*, Publisher: Open Access by IOS Press, 209-355  
<http://dx.doi.org/10.3233/978-1-61499-923-2-299>
7. Byahut S., Mujumdar A., Patel A., Sheth A., Mitra A., Moothan R. and Pandya Y. (2005). *Design Manual for a Barrier-Free Built Environment*.
8. Alberta Municipal Affairs and Safety Codes Council Barrier-free design guide (2017).
9. Mai Eid Khalil A. (2016). An Assessment Of Street Design With Universal Design Principles: Case In Aswan / As-Souq. *MEGARON / Yildiz Technical University, Faculty of Architecture E-Journal*, 11(4), 616-628.  
<https://dx.doi.org/10.5505/megaron.2016.98704>
10. Skavlid S., Olsen H.P. & Haugeto A.K. (2013). *Trends in Universal Design, Norway, First Editon, Norwegian Directorate for Children, Youth and Family Affairs*, The Delta Centre.
11. Carr K., Weir P.L., Azar D. & Azar N. (2013). Universal Design: A Step toward Successful Aging. *Journal of aging research*, 3  
<https://doi.org/10.1155/2013/324624>
12. Harsritanto B., Indriastjario & Wijayanti (2017). Universal design characteristic on themed streets. *IOP Conference Series: Earth and Environmental Science*, Vol. 99 (1), 012025.  
<http://dx.doi.org/10.1088/1755-1315/99/1/012025>
13. Harsritanto B. (2018). Urban Environment Development based on Universal Design Principles. *The 2<sup>nd</sup> International Conference on Energy, Environmental and Information System (ICENIS 2017)*, 31, 09010.  
<https://doi.org/10.1051/e3sconf/20183109010>

14. Broacha J., Dilla J. & Gliebe, J. (2012). Where do cyclists ride? A route choice model developed with revealed preference GPS data. *Transportation Research Part A: Policy and Practice*, 46 (10).  
<https://doi.org/10.1016/j.tra.2012.07.005>
15. Carreno, M., Ge, Y.-E., & Borthwick, S. (2014). Could green taxation measures help incentivise future Chinese car drivers to purchase low emission vehicles? *Transport*, 29(3), 260-268.  
<https://doi.org/10.3846/16484142.2014.913261>
16. Kampf R., Gašparik J. & Kudláčková N. (2012). Application of different forms of transport in relation to the process of transport user value creation. *Periodica Polytechnica Transportation Engineering*, 40 (2), 71-75.  
<https://doi.org/10.3311/pp.tr.2012-2.05>
17. Lytvynenko T. & Gasenko L. (2015). Peculiarities of Infrastructure Designing for the Movement of Individual Environmental Friendly Vehicles, *Periodica Polytechnica Transportation Engineering*, 43(2), 81-86.  
<https://doi.org/10.3311/PPtr.7593>
18. Лобанов Е.М. (1990). *Транспортная планировка городов*. М.: Транспорт.
19. Moughtin C. (2003). *Urban Design: Street and Square*. Architectural Press.
20. Marshall S. (2005). *Streets and Patterns: The Structure of Urban Geometry*. Spon Press.
21. Гасенко Л.В. (2015). Принципи містобудівної організації велоінфраструктури у середніх і великих містах: автореф. дис. на здобуття наук. ступеня канд. техн. наук: спец. 05.23.20 – містобудування та територіальне планування. – Київ
22. *University Course on Bicycle and Pedestrian Transportation* (2006). Federal Highway Administration. US Department of transportation. USA: FHWA-RT-05-133.
23. Довідник «Комфортне місто. Як спланувати велоінфраструктуру». (2014). Громадська організація «Асоціація велосипедистів Києва». АВК.
24. ДБН В.2.2-12:2019. *Планування та забудова територій* (2019). Київ: Мінрегіон України, ДП „Укрархбудінформ”.
25. ДБН В.2.3-5:2018. *Вулиці та дороги населених пунктів*. (2018). Київ: Мінрегіон України, ДП „Укрархбудінформ”.
26. ДСТУ 8906:2019. *Планування та проектування велосипедної інфраструктури*. (2020). Київ: ДП «УкрНДНЦ»
27. ДБН В.2.2-40:2018. *Інклюзивність будівель і споруд* (2018). Київ: Мінрегіон України, ДП „Укрархбудінформ”.
28. *Diet for cars*. Платформа розвитку міст.  
<http://urbanua.org/eksperty/zakordonni-eksperty/378>
29. Schmitt A. (2014). *The Airtight Case for Road Diets*. Streetsblog: USA
30. Huang H.F., Stewart J.R. & Zegeer C.V. (2004). *Summary Report: Evaluation of Lane Reduction "Road Diet" Measures and Their Effects on Crashes and Injuries*. FHWA  
<https://www.fhwa.dot.gov>
31. Литвин В.В., Грищенко Я.В. (2012). *Транспортне планування міст*. Методичні рекомендації до виконання практичних робіт для студентів денної форми навчання напряму підготовки 0701 Транспортні технології. – Дніпро: ДВНЗ «НГУ»
32. Безлюбченко О.С., Гордієнко С.М., Завальний О.В. (2008). *Планування міст і транспорт*. Харків: ХНАМГ
14. Broacha J., Dilla J. & Gliebe, J. (2012). Where do cyclists ride? A route choice model developed with revealed preference GPS data. *Transportation Research Part A: Policy and Practice*, 46 (10).  
<https://doi.org/10.1016/j.tra.2012.07.005>
15. Carreno, M., Ge, Y.-E., & Borthwick, S. (2014). Could green taxation measures help incentivise future Chinese car drivers to purchase low emission vehicles? *Transport*, 29(3), 260-268.  
<https://doi.org/10.3846/16484142.2014.913261>
16. Kampf R., Gašparik J. & Kudláčková N. (2012). Application of different forms of transport in relation to the process of transport user value creation. *Periodica Polytechnica Transportation Engineering*, 40 (2), 71-75.  
<https://doi.org/10.3311/pp.tr.2012-2.05>
17. Lytvynenko T. & Gasenko L. (2015). Peculiarities of Infrastructure Designing for the Movement of Individual Environmental Friendly Vehicles, *Periodica Polytechnica Transportation Engineering*, 43(2), 81-86.  
<https://doi.org/10.3311/PPtr.7593>
18. Lobanov E.M. (1990). *Transport planning of cities*. M.: Transport.
19. Moughtin C. (2003). *Urban Design: Street and Square*. Architectural Press.
20. Marshall S. (2005). *Streets and Patterns: The Structure of Urban Geometry*. Spon Press.
21. Hasenko L.V. (2015). Principles of cycling infrastructure urban organization in medium and large cities: dissertation abstract for the degree of PhD: specialty 05.23.20 – urban and territorial planning. - Kyiv.
22. *University Course on Bicycle and Pedestrian Transportation* (2006). Federal Highway Administration. US Department of transportation. USA: FHWA-RT-05-133.
23. *Handbook "Comfortable city. How to plan cycling infrastructure"*. (2014). Public organization "Association of Kyiv Cyclists". AVK
24. ДБН В.2.2-12:2019. *Planning and development of territories*. (2019). Kyiv: Ministry of Regional Development of Ukraine, SE "Ukrarkhbudinform”.
25. ДБН В.2.3-5:2018. *Streets and roads of settlements*: (2018). Kyiv: Ministry of Regional Development of Ukraine, SE "Ukrarkhbudinform”.
26. DSTU 8906:2019. *Cycling infrastructure planning and design*. (2020). Kyiv.: DP "UkrNDNC”.
27. ДБН В.2.2-40:2018. *Inclusiveness of buildings and structures*. (2018). Kyiv: Ministry of Regional Development of Ukraine, SE "Ukrarkhbudinform”.
28. *Diet for cars*. Urban development platform.  
<http://urbanua.org/eksperty/zakordonni-eksperty/378>
29. Schmitt A. (2014). *The Airtight Case for Road Diets*. Streetsblog: USA
30. Huang H.F., Stewart J.R. & Zegeer C.V. (2004). *Summary Report: Evaluation of Lane Reduction "Road Diet" Measures and Their Effects on Crashes and Injuries*. FHWA  
<https://www.fhwa.dot.gov>
31. Lytvyn V.V., Hryshchenko Ya.V. (2012). *Transport planning of cities*. Methodical recommendations for practical work for full-time students in the direction of training 0701 Transport technologies. Dnipro: SU "NGU”
32. Bezlyubchenko O., Hordiyenko S. & Zaval'nyy O. (2008). *Planning of cities and transport*. Kharkiv: HNAMEG



UDC 621.79101.670

## Experimental studies of long-term fatigue of steel sewer structures

Maksimov Serhii<sup>1</sup>, Makarenko Valerii<sup>2</sup>, Vynnykov Yuriy<sup>3</sup>, Makarenko Yulia<sup>4\*</sup>

<sup>1</sup> E.O. Paton Electric Welding Institute; <https://orcid.org/0000-0002-5788-0753>

<sup>2</sup> National University «Yuri Kondratyuk Poltava polytechnic»; <https://orcid.org/0000-0001-9178-9657>

<sup>3</sup> National University «Yuri Kondratyuk Poltava polytechnic»; <https://orcid.org/0000-0003-2164-9936>

<sup>4</sup> University of Manitoba, Winnipeg, Canada, <https://orcid.org/0000-0003-1252-4231>

\*Corresponding author E-mail: [green555tree@gmail.com](mailto:green555tree@gmail.com)

The results show that the experimental studies of long-term fatigue (strength) of steel structures of underground sewage structures in a chemically aggressive environment, simultaneously containing chemical ingredients and biologically aggressive bacteria. It is established that long-term fatigue (strength) of steel structures of underground sewage structures is significantly reduced during long-term operation, and especially when exceeding 20 years or more, in chemically aggressive environments of domestic sewage, which often leads to corrosion and mechanical damage. It is shown that in the course of long service life the indicators of long-term fatigue of reinforcing steel rods of reinforced concrete structures are significantly reduced, which causes the formation of cracks in the connection "reinforcement - concrete", which usually leads to the destruction of reinforced concrete pipes and structures as a whole.

**Keywords:** underground sewerage structure, steel structure, chemically aggressive environment, crack resistance, deformation, fluidity, tensile strength, viscosity.

## Експериментальні дослідження тривалої втомленості сталевих каналізаційних конструкцій

Максимов С.Ю.<sup>1</sup>, Макаренко В.Д.<sup>2</sup>, Винников Ю.Л.<sup>3</sup>, Макаренко Ю.В.<sup>4\*</sup>

<sup>1</sup> Інститут електрозварювання ім. С.О. Патона

<sup>2</sup> Національний університет «Полтавська політехніка імені Юрія Кондратюка»

<sup>3</sup> Національний університет «Полтавська політехніка імені Юрія Кондратюка»

<sup>4</sup> Університет «Манітоба», м. Вінніпег, Канада

\*Адреса для листування E-mail: [green555tree@gmail.com](mailto:green555tree@gmail.com)

Наведено результати експериментальних досліджень тривалої втомленості (міцності) сталевих конструкцій каналізаційних підземних споруд у хімічно-агресивному середовищі, які одночасно містять хімічні інгредієнти та біологічно-агресивні бактерії. В лабораторних випробуваннях використано арматурні стрижні діаметром 32 мм зі сталі марки 20ГС. Отримано нові емпіричні залежності між концентрацією гетеротрофних бактерій (ГТБ) у розчині та спротивом втомленості сталевих зразків, вирізаних із арматури залізобетонних конструкцій каналізаційних споруд, при їх циклічних випробуваннях на згин і кручення. Для порівняння аналогічні дослідження виконано для умов розчинів хлористого натрію. Встановлено, що тривала втомленість (міцність) сталевих конструкцій каналізаційних підземних споруд значно зменшується при тривалій експлуатації, а особливо при перевищенні терміну 20 років і більше, в хімічно-агресивних середовищах побутово-господарських стоків, що призводить часто до корозійно-механічних руйнувань. Доведено, що в процесі тривалого терміну експлуатації суттєво знижуються показники тривалої втоми арматурних сталевих стрижнів залізобетонних конструкцій, що спричиняє утворення тріщин в з'єднанні «арматура – бетон», яке, як правило, призводить до руйнувань залізобетонних труб і конструкцій в цілому. Отримані результати пояснено тим, що в процесі тривалої експлуатації каналізаційного устаткування відбувається окрихчення та деградація металу.

**Ключові слова:** каналізаційна підземна споруда, сталева конструкція, хімічно-агресивне середовище, тріщиностійкість, деформація, текучість, межа міцності, в'язкість



## Introduction

When constructing sewer systems, steel profile rolled products (pipes, T-shaped and I-beams, angles, etc.) are often used as the main type of structures [1].

In Ukraine, their share is about 90% [2, 3] and in the near future, this percentage will not change significantly, due to increasing service life of such structures sharply increases the wear of steel structures and corrosion damage of reinforcement in reinforced concrete structures, and therefore only pliable steel structures will be able to provide in most cases a satisfactory operational condition of underground sewage engineering structures [2]. The almost unique ability of these structures is to adapt to changing loads and therefore the force and temperature factors, without collapsing, allows us to consider them as the safest [3].

## Review of the research sources and publications

Significantly reduces the efficiency of steel reinforced concrete structures and constructions, their corrosion ability, in particular reinforcing bars [2-9].

Corrosion aggressiveness of sewage effluents is caused by the presence of chlorine ions, sulfuric acid anions, magnesium and calcium ions, anions of chloride salts and acids. In particular, in the sewerage systems of Kyiv, Chernihiv, Odesa, Kharkiv in domestic and industrial effluents there are (mg·dm<sup>3</sup>/eq) Cl<sup>-</sup> 1200-2100; SO<sub>4</sub><sup>2-</sup> 15-25; Mg<sup>2+</sup>+Ca<sup>2+</sup> 120-300; HCO<sub>3</sub><sup>-</sup> 10-25. Moreover, the coefficient of corrosion is on average 10-16, and the aggressiveness of the metal is SO<sub>4</sub><sup>2-</sup>+Cl<sup>-</sup> > 3 g/l.

Corrosion (destruction of metal) is the result of the interaction of the environment with metals. From the point of view of the mechanism of the corrosion process, corrosion happens chemical, electrochemical, and biochemical. Under industrial conditions, sewage structures can often be biological corrosion with a gradual transition to the electrochemical type of corrosion.

## Definition of unsolved aspects of the problem

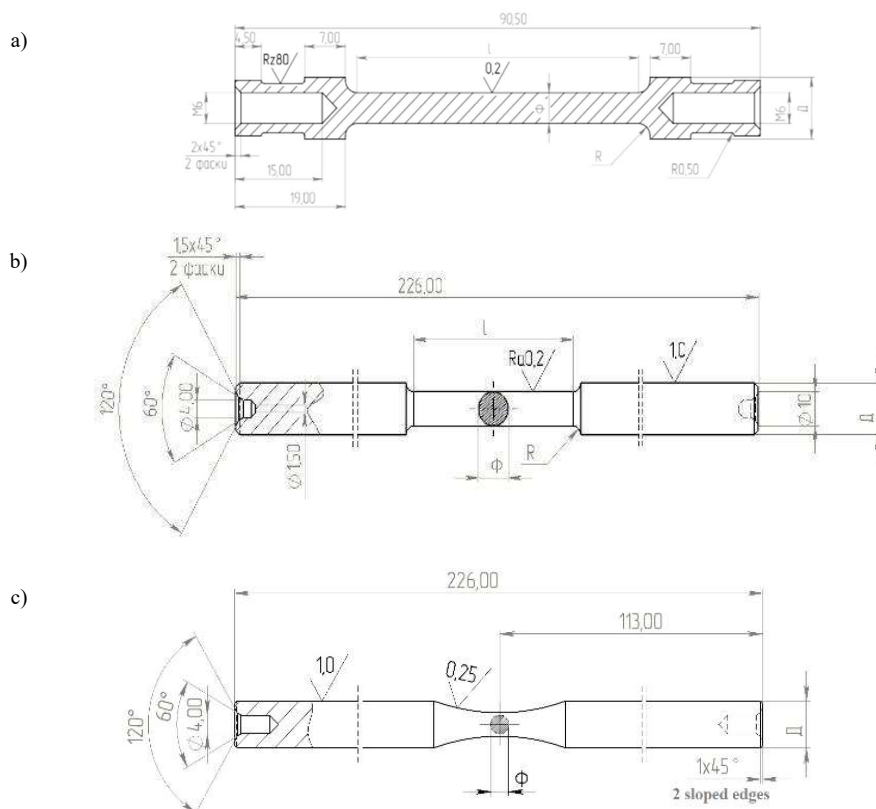
Analysis of literature sources [10 – 12] shows that to date there is no information on long-term fatigue (strength) of steel pipe structures, especially reinforcing rods of reinforced concrete sewers during a long life in aggressive chemically active environments, which simultaneously contains chemical ingredients and biologically aggressive bacterias.

## Problem statement

The purpose of the work is to establish quantitative dependencies to reduce long-term fatigue (strength) of steel structures of underground sewers under the conditions of their operation in chemically aggressive environments of domestic and industrial effluents.

## Material and methods of research

Samples for experimental tests for prolonged fatigue (strength) are shown in Fig.1. All samples were made of steel structures directly on the objects of sewage underground structures.



**Figure 1 – Samples for fatigue (long-term) strength tests:**  
a – sample for torsion tests; b – sample for tests under axial loading;  
c – a sample for bending tests during rotation

For the research were used carbon-low-alloy steel grade 08G2S with 0.07-0.092% C with the following characteristics:  $\sigma_B = 470-560$  MPa;  $\sigma_{0.2} = 315$  MPa ( $\sigma_{0.2min} = 245$  MPa) for ambient temperatures -20...-40°C. The carbon equivalent was  $CE = 0.21-0.32$ ;  $KCV = 28$  J (equivalent to FISI 1035 steel) [1, 7].

After normalization with heating to 860 °C and holding for 30 min from such steels made samples, which are shown in Fig.1. The samples were polished with a sanding skin with a grain size of 3/0, and then subjected to tempering in a vacuum chamber at 620 °C for 30 min to relieve residual stresses.

Experimental tests for corrosion fatigue (long-term strength) were performed under different types of loads.

The samples were tested on the setpoint of the Instron model (Great Britain). In particular, the tests were performed on a bend with zero average voltage and a cycle frequency of 20 Hz. The tests were performed in salt solutions with concentrations from 0.5% to 10%. To compare the results, tests were sometimes performed in the air.

Bacteria of the species of heterotrophic bacteria (GTB) were introduced into the water in the following quantities (in cells / ml):

$6.2 \cdot 10^6 - 2.2 \cdot 10^7 - 3.1 \cdot 10^8 - 25 \cdot 10^8 - 1.5 \cdot 10^9$ ;

and bacteria such as sulfate-reducing (CBD) in the amount (in cells/ml):

$1.0 \cdot 10^2 - 1.5 \cdot 10^2 - 1.5 \cdot 10^3 - 2.5 \cdot 10^4 - 1.5 \cdot 10^5 - 2.0 \cdot 10^6$ .

It should be noted that the samples made of industrial steels according to the requirements (Fig. 1) were the day before completely immersed in aqueous saline or bacterial solution circulating at a rate of 2.5 l / min between the test chamber (with a capacity of 1 l) and the reservoir, and kept for 720 h according to the requirements of the Specification of the International Corrosion Association (Specification TenquizOil and Gas Plant // ProzessPlant-Lurgi code: 65102-00-MAL-TENGUIZ II.Specification №.SPC-62900-XP-007) [1, 7, 12].

The volume of solution used for the experiments was 10 l, and after each test, the solution was replaced with a new one. The temperature of the solution during the tests was kept at 22 °C thanks to an electric automatic regulator. The dissolved oxygen content was not controlled.

During the operation of sewage systems, reinforced concrete gallery walls are in direct contact with moisture, in particular, chemically active waters and the surrounding atmosphere.

As a result, steel tubular and reinforced concrete structures (in particular, reinforcing bars) are subject to various types of corrosion, among which are atmospheric, underwater, underground, hydrogen, oxygen, gas and sulfuric acid, chloride, and microbiological (bacterial).

According to surveys and practice, corrosion processes of several types can occur simultaneously in sewer structures, in particular:

1. Atmospheric corrosion is particularly intense when the air temperature reaches 40 °C, the airflow is characterized by a significant air flow rate and relative humidity, often equal to 100%.

2. Underwater corrosion is the destruction of metal immersed in water. Under the water are the elements of the foundation attachments, which are adjacent to the drainage ditches and submerged products, the system of reservoirs, pipelines, etc. The presence of impurities of salts and acids in the water accelerates the process.

3. Underground corrosion occurs when reinforced concrete is exposed to underwater biologically aggressive environments and mineral particles. Hydrogen and gas types of corrosion are characteristic of metal structures in sewer structures.

In underground sewer conditions, metal corrosion is also classified by the nature of the destruction. Uneven corrosion is the most dangerous.

It is necessary to pay attention to the role of rolled scale and rust in processes of corrosion of metal designs, especially reinforcing cores of reinforced concrete designs in sewer conditions of long service life.

It is known that rust, in contrast to scale, occurs in the presence of moisture when  $t < 100$  °C, and therefore consists mainly of hydrated iron oxides. In general, the chemical composition of rust is expressed by the formula [12 – 15]:  $(FeO)_n \cdot (Fe_2O_3)_m \cdot (H_2O)_k$ .

Dissolved salts of iron and other cations are usually found in the rust layer. Due to the loose structure on the surface of the rust, moisture is retained for a longer time, which appears as a result of groundwater drainage, and therefore the corrosion rate increases.

As a result of the aggressive influence of underground sewer conditions, getting on separate parts of metal designs, water accumulates, forming stagnant zones (sites) that lead to their fast corrosion.

It is practically established those thin membranes of a liquid act more actively and aggressively, and therefore when narrow hair gaps are observed between metal parts. Then the corrosion processes are more intense.

The corrosion rate in hydraulic and sewage conditions is also affected by the temporary (carbonate) hardness of natural waters. Iron is corroded faster in soft water. Hard waters tend to precipitate insoluble salts, such as  $CaCO_3$  (especially in cathode regions), which prevents the diffusion of oxygen to the metal. [4 – 6, 13].

At the same time, easily soluble salts (chlorides, sulfates), which are in the soil or dissolved in groundwater, increase the corrosive aggressiveness of wastewater, accelerating the development of corrosion processes. This is due to the metal activation by presented ions in it. especially chlorine ions, which, adsorbing on the steel surface and displacing oxygen, contribute to the destruction of oxide membranes and make it difficult for the passivation of the surface.

An important role in this process is played by particles suspended in water, which by their corrosion activity can be divided into three groups:

1. Corrosion-active particles. These are in most cases particles of salts, such as sodium chloride, sodium sulfate, ammonium sulfate.

2. Corrosive-inactive particles adsorbing corrosive-active gases from the air. These are the particles of siltation of the bottom near aeration stations and observation wells, the presence of which on the metal greatly accelerates its corrosion.

3. Corrosion-inactive particles that do not adsorb harmful gases.

In some conditions of the sewer landscape, there is a phenomenon when the particles of solid waste and mineral rocks, in the absence of water inflow from the environment, create a protective membrane, under which corrosion processes are temporarily suspended.

The above-mentioned operating conditions of sewage equipment and various engineering metal structures change insignificantly within the sewage structures of Ukraine.

However, it should be noted that aggressive wastewater is the most corrosive and active in relation to the metal equipment, highly mineralized, containing a significant amount of ions  $Cl^-$  and  $SO_4^{2-}$ . Their total stiffness varies within 5...10 mg / eq, and alkalinity – pH = 6...7.2.

The content of mineral salts (sulfates and chlorides) in groundwater has a significant impact on the development of corrosion of metal structures, which ultimately affects their load-bearing capacity.

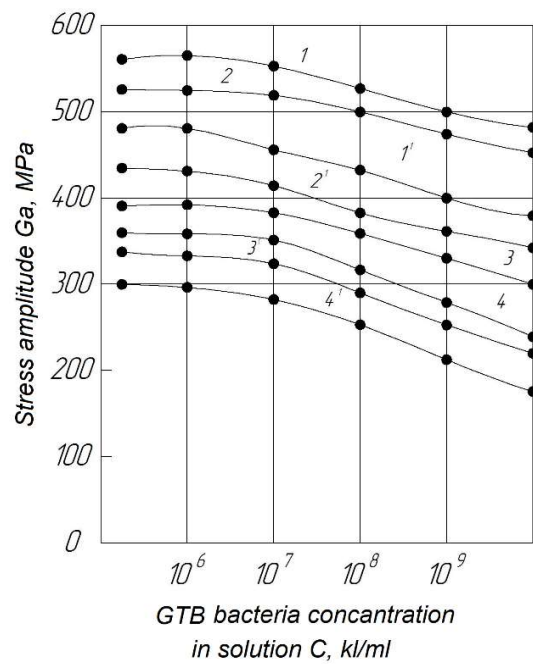
As a rule, the problem of ensuring the stability of already corroded areas of steel and reinforced concrete structures of sewer structures are solved one way – replace the old, corroded equipment with new ones. The optimal solution to this problem requires a detailed study of the corrosion process of engineering structures in the sewer (full-scale) conditions.

It should be noted that to assess the internal stresses in the existing metal structures of hydraulic structures was used a device model "Stresscan" company "Argosy Technologies" (USA), the principle of which is based on the properties of magnetoelasticity of ferromagnetic materials (Barkhausen noise). This device allows you to detect the parameters of the stress-strain state of the metal in the experimental location. Also, to quantify their danger, as well as identify areas with final plastic deformations and welding stresses. The principle of operation of this device is described in more detail in [3].

#### Research results and their discussion.

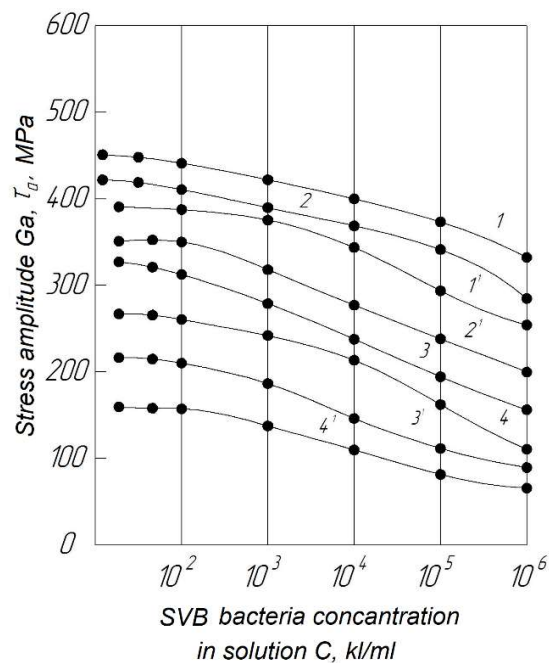
The results of experimental studies of long-term fatigue of various steel structures (steel 09G2) of sewer structures are shown in Fig. 2 – 7. In particular, in fig. 6 – 7 the data of fatigue strength of reinforcing cores of reinforced concrete constructions of sewer constructions are stated.

In the experimental tests were used reinforcing rods with a diameter of 32 mm made of steel grade 20GS.



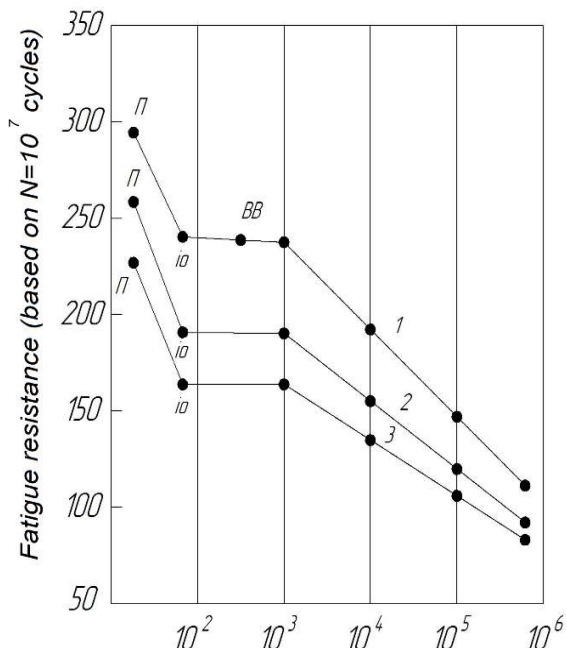
**Figure 2 – Curves of dependence between the concentration of GTB bacteria in solution and fatigue resistance at the base  $N=10^7$  cycles when tested by bending deformation during rotation.**

Designation: operation of sewer pipe structures (years): 1 – 10; 2 – 20; 3 – 30; 4 – 40; 1', 2', 3', 4' – (GTB solution +5% NaCl)



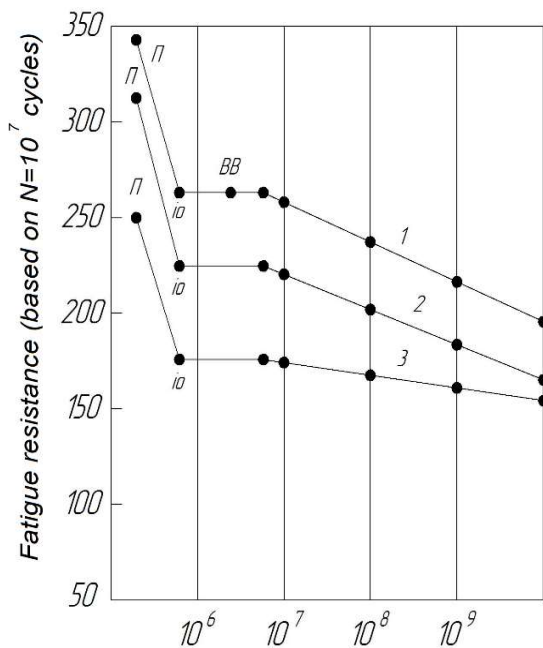
**Figure 3 – Curves of dependence between the concentration of CBS bacteria in solution and fatigue resistance at the base  $N=10^7$  cycles when testing samples by torsional deformation.**

Designation: operation of sewer pipe structures (years): 1 – 10; 2 – 20; 3 – 30; 4 – 40; 1', 2', 3', 4' – (GTB solution +5% NaCl)



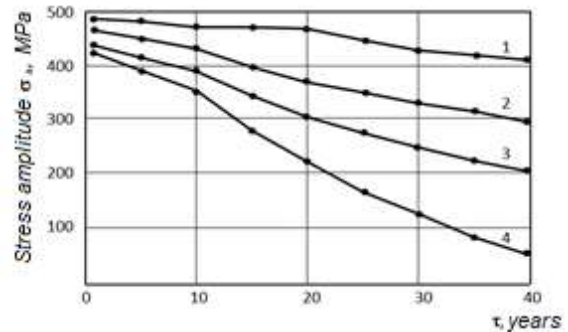
**Figure 4 – Curves of dependence between the concentration of bacteria of SVB in solution and resistance of fatigue on base  $N=10^7$  cycles during operation of sewer pipe structures lasting 40 years.**

Marking: 1 – bend during rotation;  
2 – axial load; 3 – torsion;  
BB - tap water; П – air; io - ion exchange water



**Figure 5 – Curves of dependence between the concentration of GTB bacteria in solution and fatigue resistance at the base  $N=10^7$  cycles during operation of sewer pipes of drainage duration of 40 years.**

Marking: 1 – bend during rotation;  
2 – axial load; 3 – torsion;  
BB – tap water; П – air; io – ion exchange water

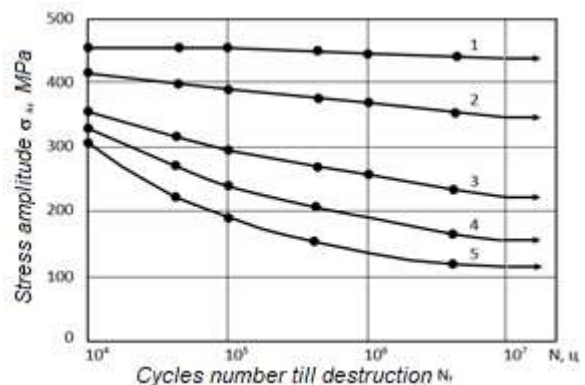


**Figure 6 – Graphs of dependence when testing for bending deformation of samples cut from the reinforcement of reinforced concrete structures of sewer structures.**

Fatigue tests at the base  $N=10^7$  cycles.

Marking: 1 – air test;  
2 – test in an environment with 3% NaCl;  
3 – tests in the environment with GTB bacteria ( $2.5 \cdot 10^6$  cells);  
4 – tests in the environment with CKD bacteria ( $5 \cdot 10^7$  cells).

Fittings with a diameter of 32 mm, steel of the 20GS brand



**Figure 7 – Graphs of dependence when tested in saltwater (NaCl -3% =30g/l) on deformation of axial loading, 20 Hz, the samples cut out of armature of reinforced concrete designs on constructions of sewer systems.**

Designation of service life of reinforced concrete structures (years):

1 – 15; 2 – 25; 3 – 35; 4 – 40 5 – 50;

Fittings with a diameter of 32 mm, steel of the 20GS brand

Analysis of the data is shown in Fig. 2 – 7, indicates that prolonged fatigue of steel and reinforced concrete structures of various sewage structures is significantly reduced when reaching 20 years or more, especially in an environment containing CBS bacteria, which, in turn, cause severe corrosion damage to the main pipe structures for sewage disposal in comparison with other simulated environments (Fig. 2 – 7).

Moreover, it is noteworthy that the samples, which are cut from metal with a long service life in hydraulic and sewer conditions (more than 20 years), are characterized by low long-term strength (Fig. 2 – 5).

The data presented in Fig. 7, clearly showed a sharp decrease in metal fatigue resistance in saline solutions, especially after 10 – 20 years of operation of steel reinforcing bars of reinforced concrete sewer structures. This result can be explained by the fact that in the process of long-term operation of metal structures, as well as in general sewage equipment is metal degradation caused by flooding, which, in turn, causes its embrittlement and, consequently, fragile destruction [10, 11].

## Conclusions

1. Thus, it is established that long-term fatigue (strength) of steel structures of underground sewage structures is significantly reduced during long-term operation (more than 20 years) in chemically aggressive environments of domestic sewage, which often leads to corrosion and mechanical destruction.

2. It is proved that in the process of long service life the indicators of long-term fatigue of reinforcing steel rods of reinforced concrete structures are significantly reduced, which causes the formation of cracks in the connection "reinforcement - concrete", which usually leads to the destruction of reinforced concrete pipes and structures as a whole.

## References

1. ДБН В.2.6-98:2009 (2009). *Конструкції будинків і споруд. Бетонні та залізобетонні конструкції. Основні положення проектування*. Київ: Мінрегіонбуд України
2. Гончаренко Д., Алейникова А. (2013). Водопроводные сети г. Харькова и возможные пути повышения их эксплуатационной долговечности. *MOTROL. Commission of motorization and energetics in agriculture: Polish Academy of sciences*, 15(6), 3-10
3. OFWAT (2004). *Maintaining Water and Sewerage Systems in England and Wales, Our Proposed Approach for the 2004 Periodic Review*. London
4. Алексеев С., Иванов Ф., Модры С., Шисль П. (1990). *Долговечность железобетона в агрессивных средах*. Москва: Стройиздат
5. Sanchez-Silva M. & Rosowsky D.V. (2008). Biodeterioration of construction materials: State of the art and future challenges. *J. of Materials in Civil Engineering*, 20 (5), 352-365
6. Bielecki R. & Schremmer H., (1987). *Biogene Schwefelsäure-Korrosion in teilgefüllten Abwasserkanälen*. Sonderdruck aus Heft 94 der Mitteilungen des Leichtweiß-Instituts für Wasserbau der Technischen Universität Braunschweig
7. Окада Т., Хаттори С. (1985). Зависимость между концентрацией соли в воде и сопротивлением коррозионной усталости конструкционной стали, содержащей 0.37% углерода. *Труды Американского общества инженеров-механиков*, 3, 98-107
8. Медовар Л.Б., Саенко В.Я., Ус В.И., Ярош В.М. (2020). Особенности конструирования биметаллических заготовок для производства арматурного профиля с коррозионно-стойким лакирующим слоем из стали 316L. *Промислове будівництво та інженерні споруди*. Київ: ДК «Український інститут сталевих конструкцій ім. В.М. Шимановського», 2-6
9. Винников Ю.Л., Макаренко В.Д., Кравець І.А., Миненко І.С. (2019). Дослідження причин зниження міцності трубопроводів ТЕЦ. *Проблеми тертя та зношення*. 1 (82), 63 – 68.  
[http://dx.doi.org/10.18372/0370-2197.1\(82\).13488](http://dx.doi.org/10.18372/0370-2197.1(82).13488)
1. DBN B.2.6-98:2009 (2009). *Constructions of buildings and structures. Concrete and reinforced concrete structures. Basic design provisions*. Kyiv: Ministry of Regional Development of Ukraine
2. Goncharenko D. & Aleinikova A. (2013). Water supply networks of Kharkiv and possible ways to increase their operational durability. *MOTROL. Commission of motorization and energetics in agriculture: Polish Academy of sciences*, 15(6), 3-10
3. OFWAT (2004). *Maintaining Water and Sewerage Systems in England and Wales, Our Proposed Approach for the 2004 Periodic Review*. London
4. Alekseev S., Ivanov F., Modry S. & Shissl P. (1990). *Durability of reinforced concrete in aggressive environments*. Moscow: Stroyizdat
5. Sanchez-Silva M. & Rosowsky D.V. (2008). Biodeterioration of construction materials: State of the art and future challenges. *J. of Materials in Civil Engineering*, 20(5), 352-365
6. Bielecki R. & Schremmer H., (1987). *Biogene Schwefelsäure-Korrosion in teilgefüllten Abwasserkanälen*. Sonderdruck aus Heft 94 der Mitteilungen des Leichtweiß-Instituts für Wasserbau der Technischen Universität Braunschweig
7. Okada T. & Hattori S. (1985). The relationship between the salt concentration in water and the corrosion resistance of structural steel containing 0.37% carbon. *Proceedings of the American Society of Mechanical Engineers*, 3, 98-107
8. Medovar L.B., Saenko V.Ya., Us V.I. & Yarosh V.M. (2020). Features of design of bimetallic preparations for production of a reinforcing profile with a corrosion-resistant cladding layer from 316L steel. *Industrial construction and engineering structures*. Kyiv: SC "Ukrainian Institute of Steel Structures. V.M. Szymanowski », 2-6.
9. Vynnykov Y.L, Makarenko V.D., Kravets I.A. & Minenko I.S. (2019). Investigation of the reasons for the decrease in the strength of CHP pipelines. *Problems of friction and wear*. 1 (82), 63 – 68.  
[http://dx.doi.org/10.18372/0370-2197.1\(82\).13488](http://dx.doi.org/10.18372/0370-2197.1(82).13488)

10. Макаренко В.Д., Палий Р.В., Галиченко Е.Н. (2004). *Физико-механические основы сероводородного коррозионного разрушения промышленных трубопроводов*. Монография. Челябинск: ЦНТИ

11. Макаренко В.Д., Ковенский И.М., Прохоров Н.Н. (2000). *Коррозионная стойкость сварных металлоконструкций нефтегазовых объектов*. Москва: ООО «Недра-Бизнесцентр»

12. Макаренко В.Д., Максимов С.Ю., Билик С.І., Винников Ю.Л., Кусков Ю.М., Кузьменко О.Г., Макаренко Ю.В. (2021) *Корозійні руйнування каналізаційних систем України*: Монографія. Київ: НУБіП України

13. Баженов Ю.М., Демьянова В.С., Калашников В.И. (2006). *Модифицированные высококачественные бетоны*. Москва: Изд-во АСВ

14. Маринин А.Н., Гарибов Р.Б., Овчинников И.Г. (2008). *Сопротивление железобетонных конструкций воздействию хлоридной коррозии и карбонизации*. Саратов: «РАТА»

15. Сахаров В.Н., Майоров В.Г. (2005). Современные методы антикоррозионной защиты металлоконструкций в гидротехнике. *Гидротехническое строительство*, 3, 46-50

10. Makarenko V.D., Paliy R.V. & Galichenko E.N. (2004). *Physico-mechanical bases of hydrogen sulfide corrosion destruction of field pipelines*. Monograph. Chelyabinsk: CNTI

11. Makarenko V.D., Kovensky I.M. & Prokhorov N.N. (2000). *Corrosion resistance of welded metal structures of oil and gas facilities*. Moscow: Nedra-Business Center LLC

12. Makarenko V.D., Maksimov S.Y., Bilyk S.I., Vynnykov Y.L., Kuskov Y.M., Kuzmenko O.G. & Makarenko Y.V. (2021) *Corrosion destruction of sewer systems of Ukraine*: Monograph. Kyiv: NULES of Ukraine

13. Bazhenov Yu.M., Demyanova V.S. & Kalashnikov V.I. (2006). *Modified high-quality concrete*. Moscow: DIA Publishing House

14. Marinin A.N., Garibov R.B. & Ovchinnikov I.G. (2008). *Resistance of reinforced concrete structures to the effects of chloride corrosion and carbonization*. Saratov: "RATA"

15. Sakharov V.N. & Mayorov V.G. (2005). Modern methods of anticorrosive protection of metal structures in hydraulic engineering. *Hydraulic construction*, 3, 46-50

UDC 692.23:699.82-026.72

## Aspects of calculation of resistance vapor penetration of enclosing structures

Yurin Oleg<sup>1</sup>, Mahas Nataliia<sup>2\*</sup>, Zyhun Alina<sup>3</sup>, Musiienko Olha<sup>4</sup>

<sup>1</sup> National University «Yuri Kondratyuk Poltava Polytechnic» <https://orcid.org/0000-0002-9290-9048>

<sup>2</sup> National University «Yuri Kondratyuk Poltava Polytechnic» <https://orcid.org/0000-0002-4459-3704>

<sup>3</sup> National University «Yuri Kondratyuk Poltava Polytechnic» <https://orcid.org/0000-0002-1743-2294>

<sup>4</sup> National University «Yuri Kondratyuk Poltava Polytechnic» <https://orcid.org/0000-0002-4903-4717>

\*Corresponding author E-mail: [mahasnataliia@gmail.com](mailto:mahasnataliia@gmail.com)

When determining the resistance to vapor penetration of the vapor barrier layer which is based on the zero balance of moisture accumulation per year and the value of the allowable increase in moisture content of the material during the period of moisture accumulation. The temperature and relative humidity of the outside air for the period of the three coldest months of the heating period or the period with average monthly negative temperatures are usually used in the calculations. Although, the duration of the moisture accumulation period may not coincide with this period, and the value of the resistance to vapor penetration of the vapor insulation in the enclosing structures may not be determined correctly. The clarification of the calculation methodology was suggested. It is necessary to determine the months, when moisture accumulation occurs in the insulation of the enclosing structure, after determining the average temperature and relative humidity of the outside air during these months and calculate the resistance to vapor penetration of the vapor insulation layer.

**Keywords:** resistance to vapor penetration, vapor barrier, moisture accumulation, enclosing structures

## Аспекти розрахунку опору паропроникненню пароізоляції огорожувальних конструкцій

Юрін О.І.<sup>1</sup>, Магас Н.М.<sup>2\*</sup>, Зигун А.Ю.<sup>3</sup>, Мусієнко О.В.<sup>4</sup>

<sup>1, 2, 3, 4</sup> Національний університет «Полтавська політехніка імені Юрія Кондратюка»

\*Адреса для листування E-mail: [mahasnataliia@gmail.com](mailto:mahasnataliia@gmail.com)

Робота присвячена уточненню методики визначення розрахункових параметрів зовнішнього повітря (температури та відносної вологості) та величини опору паропроникненню шару пароізоляції. При визначенні опору паропроникненню шару пароізоляції виходять з нульового балансу вологонакопичення за рік та величини допустимого підвищення вологості матеріалу протягом періоду вологонакопичення. Зазвичай використовують у розрахунках температуру та відносну вологість зовнішнього повітря за період трьох найбільш холодних місяців опалювального періоду або періоду із середньомісячними від'ємними температурами. Але тривалість періоду вологонакопичення може не співпадати з цим періодом і величина опору паропроникненню пароізоляції в огорожувальних конструкціях, з умови підвищення вологості матеріалу протягом періоду вологонакопичення, може визначатися не вірно. Для підвищення точності розрахунку пропонується використовувати період місяців, коли відбувається вологонакопичення в утеплювачі огорожувальної конструкції. Було проведено перевірку на прикладі суміщеного покриття житлового будинку, побудовані графіки зміни парціального тиску насиченої водяної пари ( $E$ ) та фактичного парціального тиску ( $e$ ) у місяці року, коли відбувається накопичення вологи в огороженні (утеплювачі), виконано розрахунки вологонакопичення в шарі утеплювача з визначеною величиною опору паропроникненню пароізоляції. Було запропоновано уточнення методики розрахунку. Так, на початку, за методикою наведеною у ДСТУ-Н Б В.2.6-192:2013, необхідно визначити місяці коли відбувається вологонакопичення в утеплювачі огорожувальної конструкції. Потім визначити середні температури та відносну вологість зовнішнього повітря протягом цих місяців та розрахувати опір паропроникнення шару пароізоляції.

**Ключові слова:** опір паропроникненню, пароізоляція, вологонакопичення, огорожувальні конструкції





## Introduction

Heat-shielding features of building envelopes meaningfully depend on humidity conditions. The moisture condition of external enclosing structures may be influenced by many values. One of these values is the vapor penetration resistance of the vapor barrier layer. The deterioration of the moisture condition of the fence is the result of the inaccuracy in determining the latter. Eventually, it reduces its heat-protective power features.

## Review of the research sources and publications

Many researchers have been investigating the method of determining the resistance to vapor penetration of a part of the enclosing structure located between the inner surface of the enclosure and the zone (or plane) of water condensation, or directly the vapor insulation layer. The most famous researchers who dedicated themselves to organizing around this issue are A. Perekhzhintsev, V. Kupriyanov, I. Safin, V. Gagarin, P. Khavanov, K. Zubarev. The results of their work are set out in [1-6], they propose to solve the problem of determining the resistance to vapor penetration of the vapor barrier layer by an analytical or graph-analytical method. The humidity mode of enclosing structures, including the resistance to vapor penetration of structural layers, considered by researchers Yu. Vytchikov, M. Saparev, A. Kostuganov, R. Černý, J. Poděbradská, J. Drchalová, M. Jerman [7-9] and others. The work is a continuation of the research of the authors [10-13], who study the temperature-humidity regime of enclosing structures and their impact on the energy efficiency of buildings in general.

## Definition of unsolved aspects of the problem

It is admitted that moisture accumulation per year and values of permissible increase in moisture content of material during the period of moisture accumulation are based on zero balance in the determination of resistance to vapor penetration of vapor insulation layer [14]. That is why the amount of moisture that accumulates in the enclosure during the year is equal to the amount of moisture removed from the enclosure; the increased moisture content of the material during the moisture accumulation period does not exceed the normalized value. Researchers, who deal with this issue, propose to use outside temperature and relative humidity in calculations for the three coldest months of the heating period or the period with average monthly negative temperatures. However, the duration of the moisture accumulation period may not coincide with this period. Therefore, the value of the vapor penetration resistance of the vapor insulation in the enclosing structures, based on the condition of increasing the moisture content of the material during the period of moisture accumulation, may not be determined quite right.

## Problem statement

The purpose of the work was to clarify the method of determining the calculated parameters of the external air (temperature and relative humidity) and the value of resistance to vapor penetration of the vapor barrier

layer. Thereby, the method of calculating moisture accumulation in the fence was used according to the [14] to manage this issue.

## Basic material and results

Modern standards for assessing the thermal and moisture condition of enclosing structures [15] require the fulfillment of two requirements.

The first requirement is to increase the moisture content of the material in the thickness of the structure layer

$$\Delta w \Delta w_p, \quad (1)$$

where  $\Delta w$  is the increase in moisture content of the material in the thickness of the structure layer, in which moisture condensation can occur, during the cold period of the year, % by weight;

$\Delta w_p$  is the permissible increase in humidity of the material in the layer of which moisture condensation can occur, % by weight, set according to table 8 [15] depending on the type of material.

The following condition must be implemented for a negative or zero annual balance of moisture in the thickness of the enclosing structures.

The second requirement is zero annual moisture balance in the thickness of the enclosing structures.

$$W_{wp} \leq W_{sp}, \quad (2)$$

where  $W_{wp}$  is the amount of moisture accumulated in the thickness of the enclosing structure, which condensed over the period of moisture accumulation of the year, kg/m<sup>2</sup>;

$W_{sp}$  is the amount of moisture vaporizing from the fence during the moisture release period of the year, kg/m<sup>2</sup>.

Vapor permeability resistance of vapor insulation layer in enclosing structures is determined by analytical or graphoanalytic method. The graphoanalytic method allows determining the resistance to vapor penetration of the vapor insulation layer only from requirement 2 (Figure 1).

Resistance permeability resistance of vapor insulation by the analytical method is determined according to [15] by the following formulas.

The first requirement

$$R_{e.vi} = \frac{0.0024 \cdot Z_0 \cdot (e_i - E_{w.c})}{\rho_c \cdot \delta_c \cdot \Delta W_p + \eta} - R_{e.i}, \quad (3)$$

where  $Z_0$  is the number of days of the period with negative average monthly ambient temperatures;

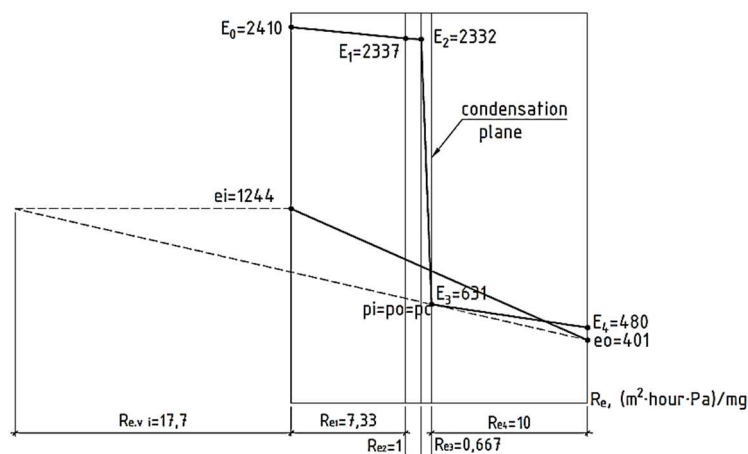
$e_i$  – internal air vapor partial pressure, Pa;

$E_{w.c}$  – partial pressure of saturated water vapor, Pa, in the condensation plane for the period with negative average monthly temperatures;

$\rho_c$  – density of the material layer in which condensable moisture accumulates, kg/m<sup>3</sup>;

$\delta_c$  – thickness of the layer of material in which condensable moisture accumulates, m;

$R_{e.i}$  – resistance to vapor penetration, m<sup>2</sup> hour Pa, parts of the enclosing structure located between the condensation zone and the internal surface of the enclosure.



**Figure 1 – Determination of vapor permeable layer resistance of vapor insulation**

Value  $\eta$  determined by formula

$$\eta = \frac{0.0024 \cdot Z_0 \cdot (E_{w.c} - e_i)}{R_{e.o}}, \quad (4)$$

where  $e_o$  – partial pressure of water vapor, Pa, outdoor air for the period with negative average monthly temperatures;

$R_{e.o}$  – vapor permeability resistance,  $m^2$  hour Pa, part of enclosing structure located between condensation zone and external surface of enclosing.

The second requirement

$$R_{e.vi} = \frac{e_i - E_{w.c.year}}{E_{w.c.year} - e_o} R_{e.i}, \quad (5)$$

where  $E_{w.c.year}$  – annual average partial pressure of saturated water vapor, Pa, in the condensation plane.

Typically, the resistance to vapor penetration of vapor insulation is defined by formulas (3) and (4), more frequently than formula (5). Therefore, we consider only formulas (3) and (4). They have gotten the duration of the moisture accumulation period and the average partial pressure of outdoor water vapor that is taken as a period with negative average monthly temperatures. However, the duration of the period with negative average monthly temperatures may differentiate from the period of moisture accumulation in the fence. This may affect the accuracy of determining the vapor permeability resistance of the vapor barrier layer. To verify this statement, the vapour penetration resistance value was calculated, the moisture accumulation value was determined with a certain vapour insulation resistance and an increase in the humidity of the insulation during the moisture accumulation period.

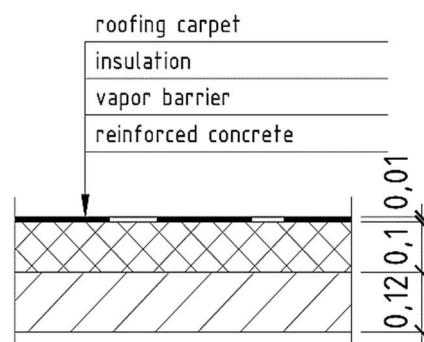
The examination was carried out for the combined coverage (Figure 2) of a residential building in Poltava.

Insulation was taken from mineral wool with density  $100 \text{ kg/m}^3$ . The period of months with negative temperatures consisted of three months: December, January, and February. The average outside air temperature for these months was  $t_o = -4.57^\circ\text{C}$ . Accordingly, the relative humidity was  $\phi_o = 84.7 \%$ .

Value of resistance to vapor penetration of the vapor insulation layer, which was determined by formulas (3) and (4), was  $R_{e.vi} = 2.37 \text{ m}^2 \text{ hour Pa/mg}$ .

Graphs of changes in the partial pressure of saturated water vapour ( $E$ ) and actual partial pressure ( $e$ ) during the months of the year when moisture accumulates in the enclosure (insulation) are given in Figure 3.

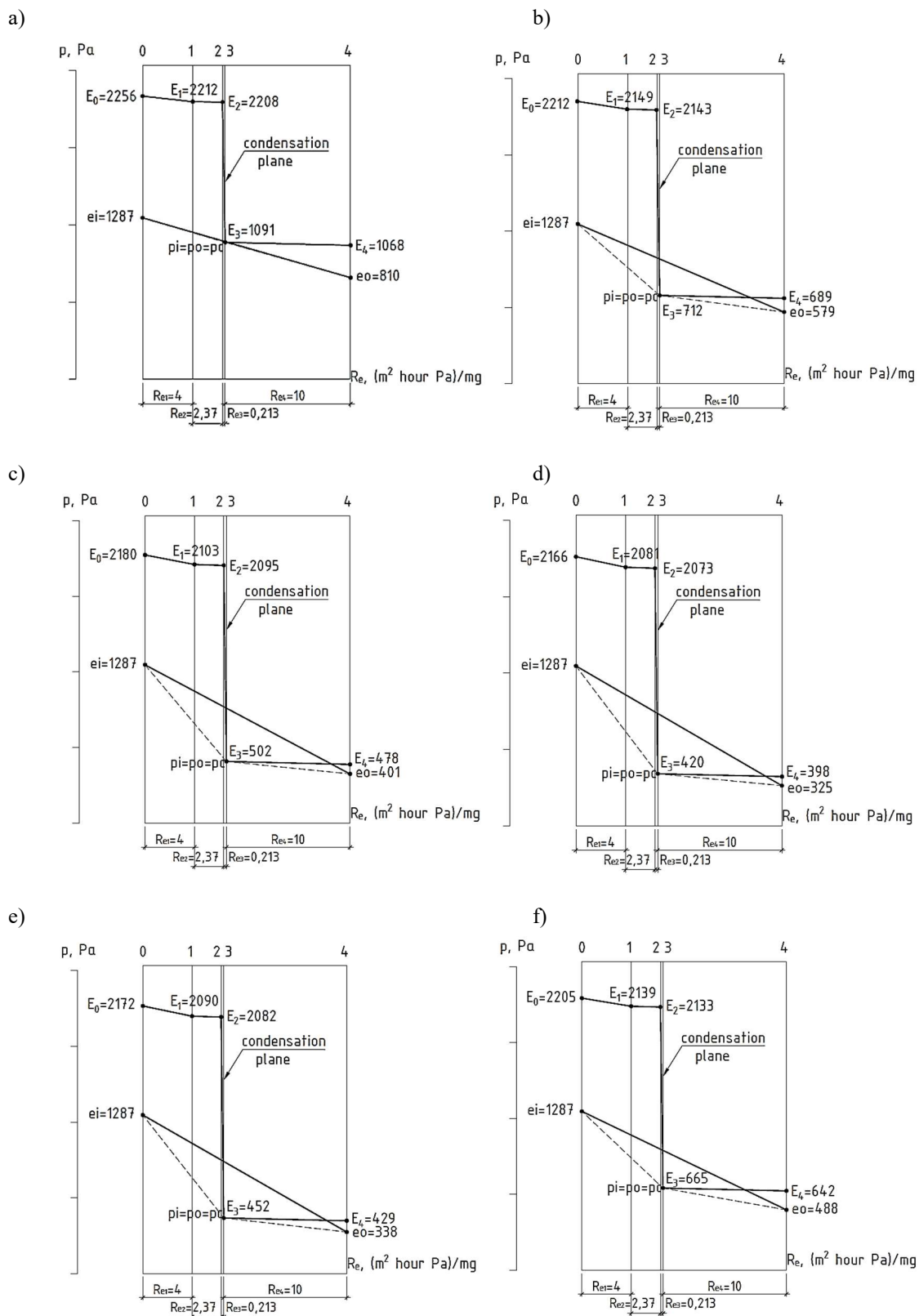
The results of the calculation of moisture accumulation in the mineral wool layer with a certain value of the vapor penetration resistance of the vapor insulation are shown in Table 1.



**Figure 2 – Design diagram of a combined coating**

**Table 1 – Amount of moisture that accumulates in the condensation plane**

Month of year	Amount of accumulated moisture $W_{wp}$ , $\text{kg/m}^2$
October	0.0013
November	0.055
December	0.0812
January	0.0909
February	0.0859
March	0.0571
	$W_{wp} = 0.371$



**Figure 3 – Graphs of changes in partial pressure of saturated water vapour ( $E$ ) and actual partial pressure ( $e$ ):**  
 a) in October; b) in November; c) in December; d) in January; e) in February; f) in March.

Moisture gain in insulators is  $\Delta w = 3.71\%$ , which exceeds the allowable value of heat insulation characteristics of material humidity increase  $\Delta w_p$ . Looking at eable 8 [15], this value is  $\Delta w_p = 2.5\%$  for mineral wool. It means that the resistance to vapor penetration of the vapor insulation is insufficient to implement requirement 1 (formula 1). It ought to be explained by the fact that moisture accumulation lasts six months, and the duration, which is accepted, when determining the vapor penetration resistance of the vapor insulation layer lasts only three months during the period with negative ambient air temperatures. In order to improve the accuracy of calculation of vapor penetration resistance of vapor insulation according to formulas (3) and (4), it is proposed to use the period of months when humidity increases in the insulator instead of a period with negative ambient air temperatures. The application of this change requires clarification of the calculation order. In the beginning, it is essential to identify the months when moisture accumulation occurs. It is necessary to figure out the average temperature and relative humidity of the outside air during these months. Afterward, it is quite important to determine resistance to vapor penetration of vapor insulation by formulas (3) and (4). Appropriate calculations have been made to verify the proposed changes.

To sum up, the period of damp accumulation lasts from October to March from previous studies. The average outside air temperature for these months was  $t_o = -0.73^\circ\text{C}$ . Accordingly, the relative humidity was  $\varphi_o = 82.5\%$ .

The value of resistance to the vapor penetration of the vapor insulation determined by formulas (3) and (4), is  $R_{e.vi} = 5.03 \text{ m}^2 \text{ hour Pa/mg}$ .

The results of the calculation of moisture accumulation in the mineral wool layer with a certain value of vapor penetration resistance of the vapor insulation are shown in Table 2.

**Table 2 – Amount of moisture that accumulates in the condensation plane**

Month of year	Amount of accumulated moisture $W_{wp}$ , kg/m <sup>2</sup>
October	0.005
November	0.036
December	0.056
January	0.063
February	0.059
March	0.037
	$W_{wp} = 0.256$

Moisture gain in heat insulation material is  $\Delta w = 2.56\%$ . This gain exceeds the allowable value of heat insulation characteristics of material humidity increase  $\Delta w_p = 2.5\%$ . This result is most likely due to the rounding of ambient temperature and relative humidity values used in the determination  $R_{e.vi}$  and with rounding

the amount of moisture accumulating in the heat insulation material in different months of the year. To prevent such a situation, it is proposed to increase the resistance to vapor penetration of the vapor insulation by 4%. It means that it is necessary to apply an increasing coefficient  $k_{inc} = 1.04$  in formula (3). Consequently, the formula will take the form

$$R_{e.vi} = \left( \frac{0.0024 \cdot Z_0 \cdot (e_i - E_{w.c})}{\rho_c \cdot \delta_c \cdot \Delta W_p + \eta} - R_{e.i} \right) k_{inc}, \quad (6)$$

Using this formula, the resistance to vapor penetration of the vapor insulation is  $R_{e.vi} = 5.23 \text{ m}^2 \text{ hour Pa/mg}$ .

The results of the calculation of moisture accumulation in the mineral wool layer with a certain value of the vapor penetration resistance of the vapor insulation are shown in Table 3.

**Table 3 – Amount of moisture that accumulates in the condensation plane**

Month of year	Amount of accumulated moisture $W_{wp}$ , kg/m <sup>2</sup>
October	0.005
November	0.035
December	0.054
January	0.062
February	0.057
March	0.036
	$W_{wp} = 0.249$

Moisture gain in insulators is  $\Delta w = 2.49\%$ , that does not exceed the allowable value of heat insulation characteristics of material humidity increase  $\Delta w_p = 2.5\%$ .

## Conclusions

During the usage of the vapor insulation layer in the calculation of vapor penetration resistance for the period of months with negative ambient air temperatures, the increase of insulation humidity exceeds the normalized value explained in [15]. This is because the duration of moisture accumulation is usually longer than the period with negative ambient temperatures.

It is proposed to use the period of months in formulas (3) and (4) when moisture accumulation occurs material of the enclosing structure of the heat insulation to improve the accuracy of the calculation.

It is also proposed to use an increasing coefficient  $k_{inc} = 1.04$  (Formula 6).

The implementation of this proposal strongly requires a change in the calculation method. In the beginning, it is necessary to determine the months according to the procedure given in [14], when moisture accumulation occurs in the insulation of the enclosing structure. Therefore, determine the average temperature and relative humidity of the outside air during these months and calculate the vapor penetration resistance of the vapor insulation layer by formulas (6) and (4).

## References

1. Перехоженцев А.Г. (2018). Нормирование и расчет паропроницаемости многослойных ограждающих конструкций зданий. *Academia. Архитектура и строительство*, №3, 130-134  
<https://doi.org/10.22337/2077-9038-2018-3-130-134>
2. Перехоженцев А.Г., Войтович Е.В. (2019). О качестве нормирования теплозащиты зданий. *Строительство и реконструкция*, №3(83), 100-111.  
<https://doi.org/10.33979/2073-7416-2019-83-3-100-111>
3. Куприянов В.Н., Сафин И.Ш. (2011). Проектирование ограждающих конструкций с учетом диффузии и конденсации парообразной влаги *Известия КазГАСУ*, №1 (15), 93-103
4. Куприянов В.Н., Сафин И.Ш. (2010). Паропроницаемость и проектирование ограждающих конструкций. *Academia. Архитектура и строительство*, №3, 385-390
5. Зубарев К.П. (2016). Расчет ограничения влаги в ограждающей конструкции с повышенным уровнем энергосбережения с утеплителем из минеральной ваты и основанием из кирпичной кладки за период с отрицательными средними месячными температурами наружного воздуха. *Инновационная наука*, №3, 71-73
6. Gagarin V.G., Khavanov P.A. & Zubarev K.P. (2020). The position of the maximum wetting plane in building enclosing structures. *IOP Conf. Ser.: Mater. Sci. Eng.* 896 012016  
<https://doi.org/10.1088/1757-899X/896/1/012016>
7. Vytychikov Yu.S., Saparev M.E. & Kostuganov A.B. (2021). Investigation of the humidity regime of multilayer enclosing structures of buildings and structures *IOP Conf. Ser.: Mater. Sci. Eng.* 1015 012035  
<https://doi.org/10.1088/1757-899X/1015/1/012035>
8. Černý R., Poděbradská J. & Drchalová J. (2002) Water and Water Vapor Penetration Through Coatings. *Journal of Building Physics*, 26(2), 165-177  
<https://doi.org/10.1177/0075424202026002975>
9. Jerman M. & Černý R. (2012). Effect of moisture content on heat and moisture transport and storage properties of thermal insulation materials. *Energy and Buildings* Vol. 53, 39-46  
<http://dx.doi.org/10.1016/j.enbuild.2012.07.002>
10. Юрін О.І., Галінська Т.А., Пашченко А.М., Камінська Л.С., Твердохліб В.С. (2014). Аналіз норм опору паропроникненню шару пароізоляції в покритті будівель холодильників. *Будівельні конструкції*, 80, 223-230
11. Авраменко Ю.О., Лещенко М.В., Магас Н.М., Мальношицький О.В., Семко В.О., Склярєнко С.О., Філоненко О.І., Юрін О.І., Семко О.В. (Ред.). (2017). *Утеплення, ремонт та реконструкція плоских покрівель цивільних будівель: посібник*. Полтава: Аструя
12. Філоненко О.І., Юрін О.І. (2018). *Енергетична ефективність будинків*. Полтава: Аструя
13. Semko O.V., Yurin O.I., Filonenko O.I. & Mahas N.M. (2020). Investigation of the Temperature–Humidity State of a Tent-Covered Attic. Proceedings of the 2nd International Conference on Building Innovations. *Lecture Notes in Civil Engineering*, 73. Springer, Cham.  
[https://doi.org/10.1007/978-3-030-42939-3\\_26](https://doi.org/10.1007/978-3-030-42939-3_26)
14. ДСТУ-Н Б В.2.6-192:2013. (2014). *Настанова з розрахункової оцінки тепловологісного стану огороджувальних конструкцій*. Київ: Мінрегіонбуд України
15. ДБН В.2.6-31:2016. (2016). *Теплова ізоляція будівель*. Київ: Мінрегіонбуд України
1. Perekhozhintsev A.G. (2018). Standardization and calculation of vapor permeability of multilayer building envelopes. *Academia. Architecture and construction*, no. 3, 130-134  
<https://doi.org/10.22337/2077-9038-2018-3-130-134>
2. Perekhozhintsev A.G. & Voitovich E.V. (2019). On the quality of standardization of thermal protection of buildings. *Construction and reconstruction*, no. 3 (83), 100-111.  
<https://doi.org/10.33979/2073-7416-2019-83-3-100-111>
3. Kupriyanov V.N. & Safin I.Sh. (2011). Design of enclosing structures taking into account the diffusion and condensation of vaporous moisture *Izvestia KazGASU*, No. 1 (15), 93-103
4. Kupriyanov V.N. & Safin I.Sh. (2010). Water vapor permeability and design of enclosing structures. *Academia. Architecture and construction*, no. 3, 385-390
5. Zubarev K.P. (2016). Calculation of the limitation of moisture in the enclosing structure with an increased level of energy saving with a mineral wool insulation and a brickwork base for a period with negative average monthly outdoor temperatures. *Innovative science*, no. 3, 71-73
6. Gagarin V.G., Khavanov P.A. & Zubarev K.P. (2020). The position of the maximum wetting plane in building enclosing structures. *IOP Conf. Ser.: Mater. Sci. Eng.* 896 012016  
<https://doi.org/10.1088/1757-899X/896/1/012016>
7. Vytychikov Yu.S., Saparev M.E. & Kostuganov A.B. (2021). Investigation of the humidity regime of multilayer enclosing structures of buildings and structures *IOP Conf. Ser.: Mater. Sci. Eng.* 1015 012035  
<https://doi.org/10.1088/1757-899X/1015/1/012035>
8. Černý R., Poděbradská J. & Drchalová J. (2002) Water and Water Vapor Penetration Through Coatings. *Journal of Building Physics*, 26(2), 165-177  
<https://doi.org/10.1177/0075424202026002975>
9. Jerman M. & Černý R. (2012). Effect of moisture content on heat and moisture transport and storage properties of thermal insulation materials. *Energy and Buildings* Vol. 53, 39-46  
<http://dx.doi.org/10.1016/j.enbuild.2012.07.002>
10. Yurin A.I., Galinska T.A., Pashchenko A.N., Kaminska L. & Tverdokhle V.S. (2014). Analysis of the norms of resistance to vapor permeation of the vapor barrier layer in the coating of refrigerator buildings. *Building structures*, 80, 223-230
11. Avramenko Yu.A., Leshchenko M.V., Mahas N.M., Malyushitsky O.V., Semko V.A., Sklyarenko S.A., Filonenko A.I., Yurin A.I., Semko A.V. (Ed.). (2017). *Thermal insulation, repair and reconstruction of flat roofs of civil buildings: allowance*. Poltava: Astra
12. Filonenko A.I. & Yurin A.I. (2018). *Energy efficiency of buildings*. Poltava: Astra
13. Semko O.V., Yurin O.I., Filonenko O.I. & Mahas N.M. (2020). Investigation of the Temperature–Humidity State of a Tent-Covered Attic. Proceedings of the 2nd International Conference on Building Innovations. *Lecture Notes in Civil Engineering*, 73. Springer, Cham.  
[https://doi.org/10.1007/978-3-030-42939-3\\_26](https://doi.org/10.1007/978-3-030-42939-3_26)
14. DSTU-N B V.2.6-192:2013. (2014). *Guidelines for the computational assessment of the thermal and moisture state of enclosing structures*. Kiev: Ministry of Regional Development of Ukraine.
15. DBN B.2.6-31: 2016. (2016). *Thermal insulation of buildings*. Kyiv: Ministry of Regional Development of Ukraine

UDC 697.12/.14:692.23-027.267

## Considering the availability of cold bridges in the design of thermal insulation shell of sandwich panels element-by-element assembly

Filonenko Olena<sup>1</sup>, Hasenko Lina<sup>2</sup>, Mahas Nataliia<sup>3\*</sup>, Mammadov Nurmammad<sup>4</sup>

<sup>1</sup> National University «Yuri Kondratyuk Poltava Polytechnic» <https://orcid.org/0000-0001-8571-9089>

<sup>2</sup> National University «Yuri Kondratyuk Poltava Polytechnic» <https://orcid.org/0000-0002-1310-914X>

<sup>3</sup> National University «Yuri Kondratyuk Poltava Polytechnic» <https://orcid.org/0000-0002-4459-3704>

<sup>4</sup> Azerbaijan Architecture and Construction University <https://orcid.org/0000-0002-0508-0439>

\*Corresponding author E-mail: [mahasnataliia@gmail.com](mailto:mahasnataliia@gmail.com)

The work is devoted to the refinement of engineering methods for calculating heat loss through structures made of prefabricated sandwich panels. At buildings installation in places of steel structures adjunction "cold bridges" and, as a result, condensate and mildew are formed. Heat loss due to "cold bridges" can reach up to 50% of the total house heat loss and affect its energy efficiency class. The paper presents typical energy-efficient structural units of enclosing structures made of sandwich panels and the results of these nodes temperature field modelling, which allow by the DSTU ISO 10211: 2005 method to determine the linear heat transfer coefficients, which can be used in engineering calculations of relevant structures transfer resistance and supplement Annex G in DSTU B V.2.6-189: 2013. Calculation of the linear coefficient of thermal conductivity for different variants of structures adjacency will avoid thermal failures and increase the energy efficiency class of buildings

**Keywords:** heat loss, insulation, linear heat transfer coefficients, temperature field

## Врахування наявності містків холоду при проектуванні теплоізоляційної оболонки з сендвич панелей поелементного збирання

Філоненко О.І.<sup>1</sup>, Гасенко Л.В.<sup>2</sup>, Магас Н.М.<sup>3\*</sup>, Мамедов Н.<sup>4</sup>

<sup>1, 2, 3</sup> Національний університет «Полтавська політехніка імені Юрія Кондратюка»

<sup>4</sup> Азербайджанський архітектурно-будівельний університет

\*Адреса для листування E-mail: [mahasnataliia@gmail.com](mailto:mahasnataliia@gmail.com)

Роботу присвячено уточненню інженерних методів розрахунку тепловтрат крізь конструкції зі збірних сендвич панелей. При монтажі будівель в місцях примикання сталевих конструкцій утворюються «містки холоду» і, як наслідок, можливе утворення конденсату і цвілі. Тепловтрати за рахунок «містків холоду» можуть досягати до 50% від загальних тепловтрат будинком і впливати на його клас енергоефективності. В українських нормативних документах не наведено методики визначення тепловтрат крізь конструкції, які складаються з сендвич-панелей поелементної зборки, з врахуванням конструктивних особливостей та значення лінійних коефіцієнтів теплопередачі. Для типових конструктивних вузлів у додатку Г ДСТУ Б В.2.6-189:2013 наведені лише значення лінійних коефіцієнтів теплопередачі для кам'яних конструкцій та їх елементів. У роботі наведено типові енергоефективні конструктивні вузли примикання сендвич-панелей до існуючих кам'яних стін, стін із сендвич-панелей до бетонного фундаменту, карнизів із сендвич-панелей, улаштування лотків внутрішнього водовідведення та результати моделювання температурного поля цих вузлів, що дозволяють за методикою ДСТУ ISO 10211:2005 визначити лінійні коефіцієнти теплопередачі, які можна застосовувати в інженерних розрахунках опору теплопередачі відповідних конструкцій та доповнити додаток Г ДСТУ Б В.2.6-189:2013. Моделювання конструктивних вузлів реалізовано методом скінчених елементів. Обрахунок лінійного коефіцієнту теплопровідності різних варіантів примикання конструкцій дозволить уникнути теплових відмов та підвищити клас енергетичної ефективності будівель

**Ключові слова:** тепловтрати, утеплювач, лінійний коефіцієнт теплопередачі, температурне поле



## Introduction

The use of mineral wool sandwich panels as enclosing structures allows constructing buildings with individual sizes and purposes, using typical design solutions. In addition, the use of such enclosing structures has an advantage over heavier enclosing wall panels and reinforced concrete floor slabs. However, there are also disadvantages, such as the possibility of heat loss through the prefabricated sandwich panels structure joints. At buildings installation in places of steel structures adjunction "cold bridges" and, as a result, condensate and mildew are formed. Heat loss due to "cold bridges" can reach up to 50% of the total house heat loss and affect its energy efficiency class. In the Ukrainian normative documents, there is no methodology for the heat loss designation for the structure, that is stored from the element-by-element sandwich panels' assembly, with the design features and values of linear heat transfer coefficients. For typical structural units in Annex G of DSTU B V.2.6-189: 2013 [13] only the values of linear heat transfer coefficients for stone structures and their elements are given. Therefore, the study of cold bridges' influence on the thermal insulation shell of the element-by-element sandwich panels' assembly design is an urgent task.

## Review of the research sources and publications

Enclosing structures in the sandwich panels form for the houses construction began to be actively used in the late 90s of the 20th century. The advantages of such structures include the construction speed, high-quality fabricated buildings, and low cost. The panels themselves are multilayer plates, which consist of two specially treated metal sheets, with the insulation between them. Most often, mineral wool acts as insulation. It has such advantages as resistance to moisture and flame, excellent heat, and sound insulation properties. The functional characteristics of enclosing structures largely depend on the temperature fluctuations range on the inner surface. Accurate forecasting of temperature conditions for buildings enclosing structures at periodic thermal effects allows avoiding thermal failures that were investigated in [1]. Theoretical studies of temperature fluctuations amplitude on the inner surface of sandwich panels and the possibility of condensate formation on it were investigated in [2], the limits of sandwich panels' application for external walls of refrigerators buildings were revealed. In [3] the thermal insulation capacity of civil buildings' external walls based on a framework from steel profiles and dependence of thermophysical characteristics of thermos profiles on type of perforation is investigated. In [4], the actual values of linear heat transfer of complex nodal points of enclosing structures for typical building thermal insulation structural elements, which significantly affect the reduction of thermal resistance, are calculated. The shortcomings in the calculation and construction of the described elements were analysed and the further development of engineering calculation methods for enclosing structures in the study of their complex ele-

ments was provided. In [5-10] examples of thermal insulation calculations, difficult nodes in enclosing structures are given.

## Definition of unsolved aspects of the problem

Sandwich panels, which are a multilayer enclosing element inhomogeneous in structure, have the main disadvantage from a thermophysical point of view – this is a significant number of assembly joints, through which heat loss occurs, condensate and mildew are formed. During building construction such "cold bridges" are not given enough attention, especially in custom solutions, such as reconstruction. In Ukrainian regulations, only a few values of linear heat transfer coefficients for standard designs of sandwich panels are given. The introduction of typical energy-efficient structural units of sandwich panels to existing stone walls or concrete foundations, sandwich panel cornices, installation of internal drainage trays, etc. will significantly increase the thermal protection of buildings. The results of modelling the temperature field of these nodes allow by the method of DSTU ISO 10211: 2005 [11] to determine the linear heat transfer coefficients that can be used in engineering calculations of heat transfer resistance of relevant structures and supplement Annex G in DSTU B V.2.6-189: 2013 [13].

## Problem statement

The purpose of this work is to clarify the calculating heat loss methods of sandwich panels, taking into account the linear heat transfer coefficients of their structural units and the development of design solutions for typical energy-efficient units.

Methods of thermophysical calculations are based on the calculation of two-dimensional temperature fields by the finite element method and on engineering methods for determining linear heat transfer coefficients.

## Basic material and results

Were analysed the enclosing constructions of the public building with the frame constructive scheme, the grid of columns is designed with a step 6×6 m. The roof of the building is combined with the coating. It has a small slope  $i = 0,1$  and designed from sheets of profiled flooring. Between the two sheets of profiled flooring (covering and roof) light mineral wool insulation and intermediate Z-beams are provided for installation directly on the construction site. The wall protection is made of light hinged three-layer sandwich panels of factory production with a height of 1500 mm: light mineral wool insulation between two layers of profiled flooring.

For typical structural units of the light wall enclosing structures and their elements in Annex G in [13] only the values of linear heat transfer coefficients are given. Therefore, when calculating the total heat transfer by the transmission through the area of the building according to [14]

$$Q_{tr} = H_{tr,adj} (\varrho_{int,set.H} - \varrho_e) t$$

takes into account the direct generalized coefficient of heat transfer by transmission to the environment,  $W/K$ , according to the formula (12) in [14]:

$$H_x = b_{tr,x} \odot_i A_i U_i, \quad (1)$$

where  $A_i$  – the area of the  $i$ -th element of the building shell,  $m^2$ ;

$U_i$  – generalized heat transfer coefficient of the  $i$ -th element of the building shell,  $W/(m^2 \cdot K)$ ;

$R_{\Sigma npi}$  – generalized heat transfer resistance of the  $i$ -th element of the building shell,  $m^2 \cdot K/W$ , that for opaque elements is determined in accordance with [13];

$b_{tr,x}$  – correction coefficient:  $b_{tr,x} = 1$  – when calculating  $H_D$ .

In the absence of information or insufficient amount of heat-conducting inclusions in the structure, it is recommended to use an adjusting correction to the heat transfer coefficient to take into account the impact of heat-conducting inclusions, according to the formula (21) [14]:

$$U_{op,corr} = U_{op,mn} + \otimes U_{tb}, \quad (2)$$

where  $U_{op,mn}$  – heat transfer coefficient of the opaque part of the structure (on the main field),  $W/(m^2 \cdot K)$ ;

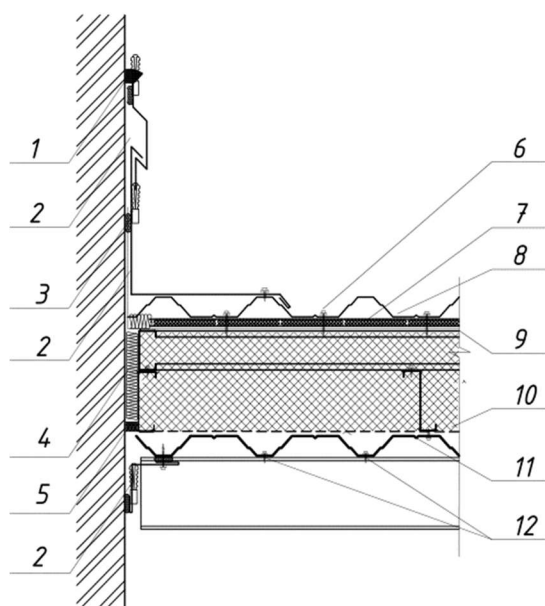
$\otimes U_{tb}$  – an additional component by default to the heat

transfer coefficient of opaque structures,  $U_{op}$ , taking into account the influence of heat-conducting inclusions,  $W/(m^2 \cdot K)$ , the calculated values are shown in table 4 of [14], and for the average value of the heat transfer coefficient for the opaque parts of the structures

$$U_{op,mn} < 0.4 \otimes U_{tb} = 0.15 W/(m^2 \cdot K).$$

Such a significant value of the additional component can reduce the actual value of the heat transfer resistance, so to increase the calculations accuracy, it is advisable to use the formula of the reduced heat transfer resistance of thermally inhomogeneous opaque enclosing structure (3) in [13]. Linear heat transfer coefficients can be determined by the recommendations for the design and calculation of energy-efficient design solutions of sandwich panel elements below. Determination of linear heat transfer coefficients is carried out based on calculations of two-dimensional temperature fields and methods according to [11-12].

The connection of the combined insulated roof to the stone walls of existing buildings during the reconstruction must be insulated to avoid freezing of the angle between the roof and the outer wall according to the scheme shown in figure 1.



**Figure 1 – The junction of the combined roof to the stone wall:**

- 1 – polyurethane sealant;
- 2 – shaped strip;
- 3 – anchor with a seal;
- 4 – polyurethane gasket;
- 5 – sealing mastic;
- 6 – self-tapping screw 5,5×50;
- 7 – thermal gasket 10 mm / 50 mm;
- 8 – roof panel PK-35/0,7;
- 9 – super diffusion membrane;
- 10 – vapour barrier;
- 11 – roof panel PK -60/0,7;
- 12 – self-tapping screw 5,5×25.

The linear heat transfer coefficients of this solution are shown in table 1.

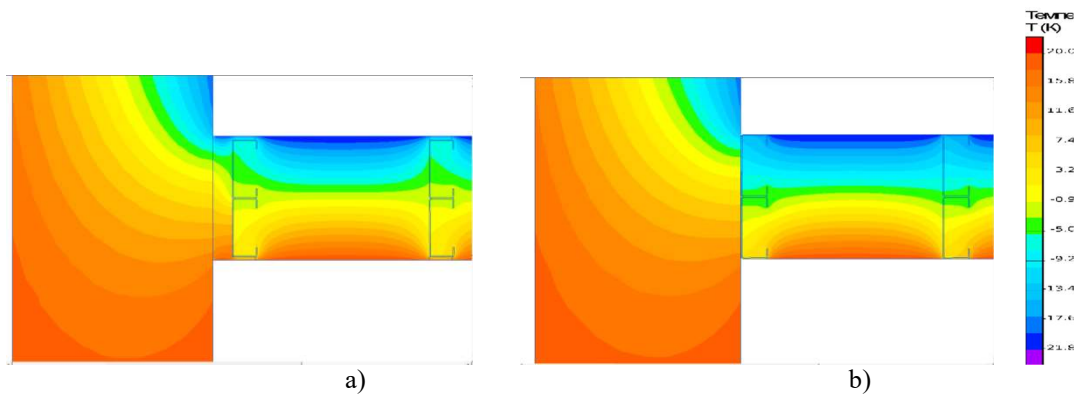
The result of the calculation of the temperature field with thermal liners for insulating metal elements from the surface with negative temperatures proved the need to comply with the design solution with a continuous insulating layer (see fig. 2).

Given that the main heat loss occurs through the uninsulated wall of the existing building, the linear coefficient is almost independent of the thermal characteristics of the roof.

**Table 1 – The junction of the combined roof to the stone wall**

Estimated thermal conductivity of the insulation in the combined roof, $W/(m \cdot K)$	Linear heat transfer coefficient, $W/(m \cdot K)$ , depending on the availability of thermal inserts	
	with thermal inserts	without thermal inserts
0,035	-0,184	-0,163
0,040	-0,181	-0,154
0,045	-0,178	-0,145
0,050	-0,175	-0,136





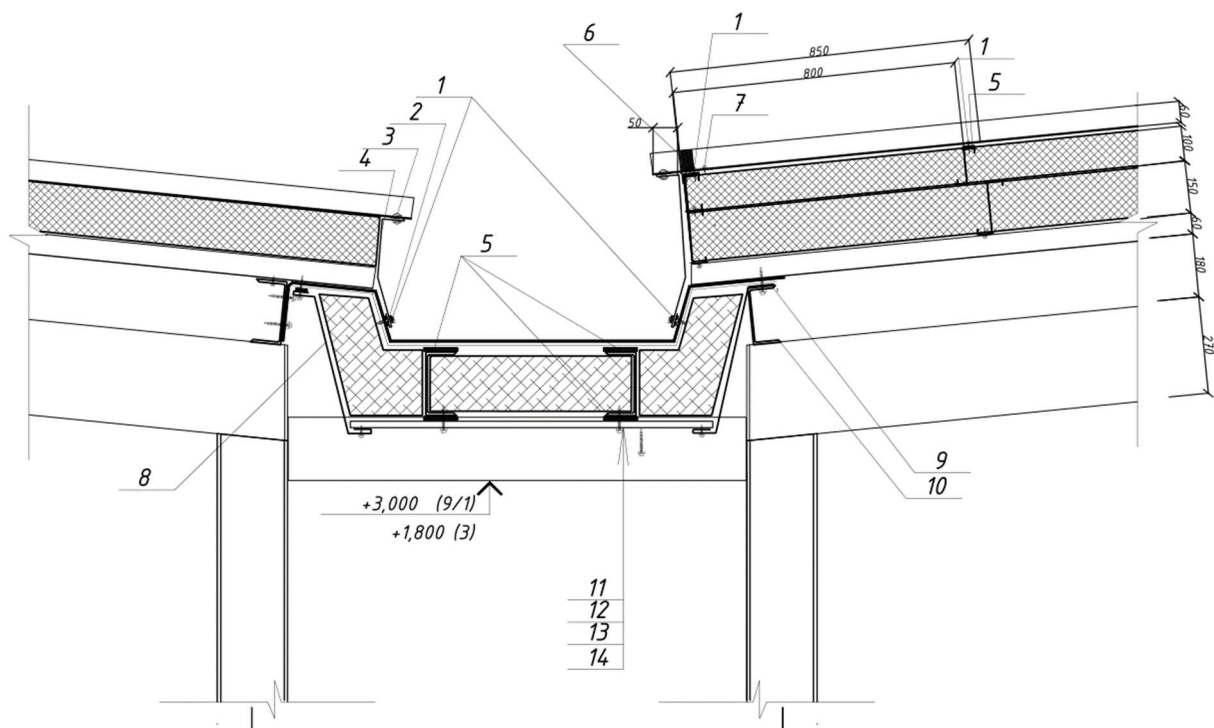
**Figure 2 – The temperature field of the junction of the combined roof to the stone wall, taking into account the thermal gaskets (a) and without additional thermal insulation of metal elements (b)**

The thermal insulation layer of the combined roof must be made inseparable from the thermal insulation of the insulated gutter according to the scheme shown in figure 3.

The linear heat transfer coefficients of this solution are shown in table 2. Design solutions for the installation of an external drainage system should have minimal impact on the integrity of the thermal and waterproofing layers of the roof (see fig. 4).

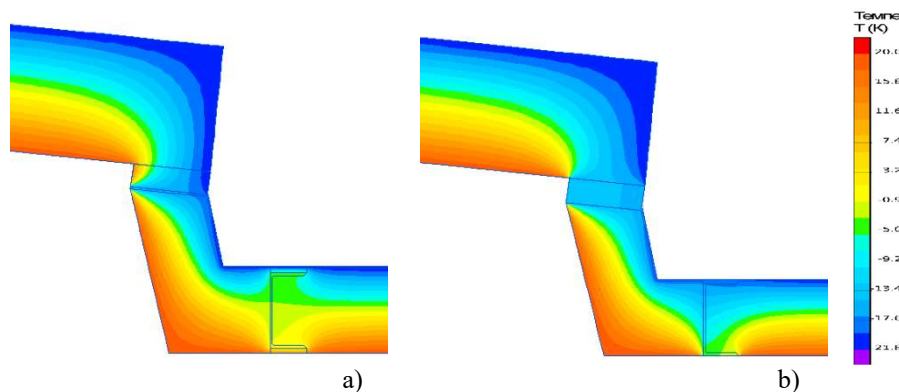
**Table 2 – The junction of the combined roof to the gutter**

Estimated thermal conductivity of the insulation in the combined roof, W/(m·K)	Linear heat transfer coefficient, W/(m·K), depending on the availability of thermal inserts	
	with thermal inserts	without thermal inserts
0,035	0,489	1,923
0,040	0,498	1,936
0,045	0,504	1,947
0,050	0,510	1,957



**Figure 3 – The junction of the combined roof to the gutter**

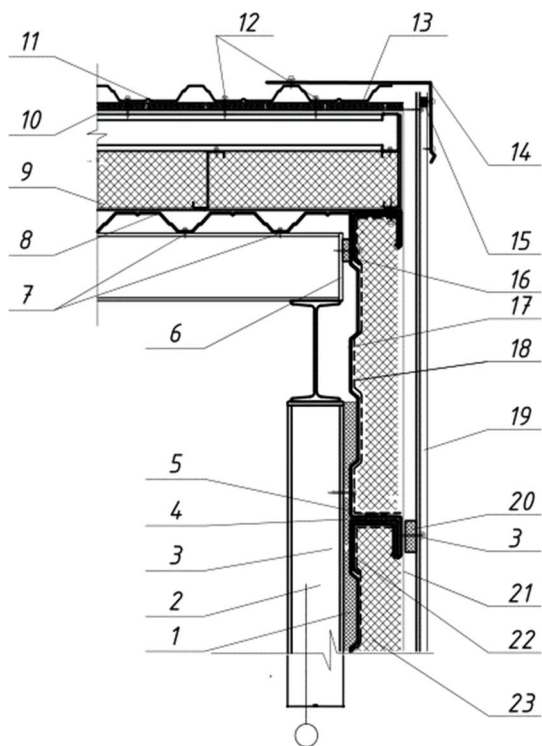
- 1 – self-tapping screw 5,5×50; 2 – sealant for external works; 3 – rivet (step 300 mm);
- 4 – shaped element 1; 5 – thermal gasket 10 mm / 50 mm; 6 – internal seal;
- 7 – self-tapping screw 4,8×16; 8 – shaped element 2; 9 – sealing tape; 10 – roofing beam;
- 11 – drainage gutter with electric heating, material - galvanized steel, thickness 4 mm;
- 12 – additional waterproofing layer; 13 – mineral wool of 180 mm in a polyethylene wrap;
- 14 – wall panel TP18.



**Figure 4 – The temperature field of the junction of the combined roof to the gutter, taking into account the thermal gaskets (a) and without additional thermal insulation of metal elements (b)**

The temperature field modelling proved the significant influence of the gutter design on the reduced heat transfer resistance of the combined roof due to the complex geometric shape and the presence of "cold bridges".

The thermal insulation layer of eaves nodes of the combined roof must be made inseparable from the thermal insulation of the building's outer wall according to the scheme shown in figure 5.



**Figure 5 – The junction of the combined roof to the outer wall (eaves node)**

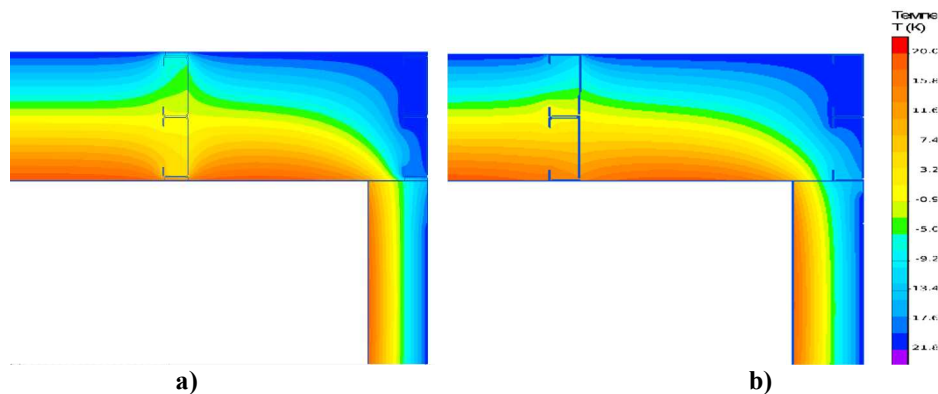
- 1 – seal "column - sandwich";
- 2 – carcass column;
- 3 – self-tapping screw 4,8×28 with gasket;
- 4 – horizontal sandwich seal;
- 5 – self-tapping screw with a washer 4,2×16;
- 6 – plate 6 mm;
- 7 – self-tapping screw 5,5×25;
- 8 – roof panel P-60/0,7;
- 9 – vapour barrier;
- 10 – super diffusion membrane;
- 11 – roof panel PK-35/0,7;
- 12 – self-tapping screw 5,5×50;
- 13 – thermal gasket 10 mm / 50 mm;
- 14 – eaves strip;
- 15 – external seal;
- 16 – thermal gasket;
- 17 – ordinary sandwich profile;
- 18 – vapour barrier;
- 19 – metal panel TP-18;
- 20 – thermal separation strip;
- 21 – wind-waterproofing membrane;
- 22 – stiffness element 150×96,2 mm;
- 23 – thermal insulation.

The linear heat transfer coefficients of this solution are shown in table 3. Design solutions of the eaves node should prevent the formation of cold bridges, which can affect the overall heat loss of the building (see fig. 6).

To prevent the cold bridges formation, which can affect the overall heat loss of the building, proved the feasibility of using thermal gaskets that reduce the linear coefficient of thermal conductivity.

**Table 3 – The junction of the combined roof to the outer wall (eaves node)**

Estimated thermal conductivity of the insulation in the combined roof and wall, W/(m·K)	Linear heat transfer coefficient, W/(m·K), depending on the availability of thermal inserts	
	with thermal inserts	without thermal inserts
0,035	0,629	1,133
0,040	0,635	1,184
0,045	0,642	1,234
0,050	0,649	1,285



**Figure 6 – The temperature field of the junction of the combined roof to the outer wall (eaves node), taking into account the thermal gaskets (a) and without additional thermal insulation of metal elements (b)**

### Conclusions

The use of the adjusting correction to the heat transfer coefficient to take into account the influence of heat-conducting inclusions according to the formula (21) DSTU B A.2.2-12: 2015 [14] leads to a reduction of the actual value of heat transfer resistance of multilayer structures by half. If it is necessary to obtain a certain energy efficiency class of the building as a whole, it leads to economically impractical overuse of thermal insulation material in structures and non-compliance with the condition of the thermal insulation layer continuity. The expediency of using thermal gaskets, that reduce the linear coefficient of thermal conductivity, to prevent the formation of cold bridges has been proved. The calculation of thermal conductivity linear coefficient for different options of connecting structures will avoid thermal failures and increase the energy efficiency class of buildings.

### References

1. Farenjuk G., Filonenko O. & Datsenko V. (2018). Research on Calculation Methods of Building Envelope Thermal Characteristics. *International Journal of Engineering & Technology*. 4.8, 97-102  
<http://dx.doi.org/10.14419/ijet.v7i4.8.27221>
2. Юрін О.І., Галінська А.Г. (2015). Визначення меж застосування сендвічпанелей RUUKKI в зовнішніх стінах будівель холодильників. *Сучасні технології та методи розрахунку в будівництві*, 3, 261-270
3. Чернявський В.В., Семко В.О., Юрін О.І., Прохоренко Д.А. (2011). Вплив перфорації легких сталевих тонкостінних профілів на теплофізичні характеристики огорожувальних конструкцій. *Збірник наукових праць. Галузеве машинобудування, будівництво*, 1(29), 194-199
4. Leshchenko M., Semko O., Shumska L. & Filonenko O. (2018). Insulation of Building Envelope Complicated Node Points. *International Journal of Engineering & Technology*, 4.8, 190-195  
<http://dx.doi.org/10.14419/ijet.v7i4.8.27239>
5. Sjoerd Nienhuys HA Technical Working Paper #2 – Calculation Examples of Thermal Insulation  
<https://www.researchgate.net/publication/232613788>
6. Landerheinecke K., Gany P. & Satter E. (2003). *Thermodynamik für Ingenieuren*. Viewegs Fachbücher der Technik
1. Farenjuk G., Filonenko O. & Datsenko V. (2018). Research on Calculation Methods of Building Envelope Thermal Characteristics. *International Journal of Engineering & Technology*. 4.8, 97-102  
<http://dx.doi.org/10.14419/ijet.v7i4.8.27221>
2. Yurin O.I. & Halins'ka A.H. (2015). Defining the limits of RUUKKI sandwich panels application in the external walls of refrigerator buildings. *Modern technologies and methods of calculation in construction*, 3, 261-270
3. Chernyavs'kyu V.V., Semko V.O., Yurin O.I. & Prokhorenko D.A. (2011). Influence of perforation of light steel thin-walled profiles on thermophysical characteristics of enclosing structures. *Academic journal. Industrial Machine Building, Civil Engineering*, 1(29), 194-199
4. Leshchenko M., Semko O., Shumska L. & Filonenko O. (2018). Insulation of Building Envelope Complicated Node Points. *International Journal of Engineering & Technology*, 4.8, 190-195  
<http://dx.doi.org/10.14419/ijet.v7i4.8.27239>
5. Sjoerd Nienhuys HA Technical Working Paper #2 – Calculation Examples of Thermal Insulation  
<https://www.researchgate.net/publication/232613788>
6. Landerheinecke K., Gany P. & Satter E. (2003). *Thermodynamik für Ingenieuren*. Viewegs Fachbücher der Technik

7. Dimoudi A., Androutsopoulos A. & Lykoudis S. (2006). Summer performance of a ventilated roof component. *Energy and Buildings*, 38, 610-617
8. Naji S., Celik O., Alengaram U.J. & Jumaat Zamin. (2014). Structure, energy and cost efficiency evaluation of three different lightweight construction systems used in low-rise residential buildings. *Energy and buildings*, 84, 727-739.  
<https://doi.org/10.1016/j.enbuild.2014.08.009>
9. Burch D. (1995). *An analysis of moisture accumulation in the roof cavities of manufactured housing*. Airflow Performance of Building Envelopes, Components, and Systems, ASTM STP 1255, American Society for Testing and Materials, Philadelphia, 156-177.
10. Wentling J. (2017). *Manufactured Housing. In: Designing a Place Called Home*. Springer, Cham.  
[https://doi.org/10.1007/978-3-319-47917-0\\_9](https://doi.org/10.1007/978-3-319-47917-0_9)
11. ДСТУ ISO 10211-1:2005 (2007). *Теплопровідні включення в будівельних конструкціях. Обчислення теплових потоків і поверхневих температур. Ч. 1. Загальні методи* (ISO 10211-1:1995, IDT). Київ: Мінреконбуд України
12. ДСТУ ISO 10211-2 (2008). *Теплопровідні включення в будівельних конструкціях. Обчислення теплових потоків і поверхневих температур. Ч. 2. Лінійні теплопровідні включення* (ISO 10211-2:1995, IDT). Київ: Мінреконбуд України
13. ДСТУ Б В.2.6-189:201 3(2013). *Методи вибору теплоізоляційного матеріалу для утеплення будівель*. (2013). Київ: Мінреконбуд України
14. ДСТУ Б А.2.2-12:2015 (2015). *Енергетична ефективність будівель. Метод розрахунку енергоспоживання при опаленні, охолодженні, вентиляції, освітленні та гарячому водопостачанні*. Київ: Мінреконбуд України
7. Dimoudi A., Androutsopoulos A. & Lykoudis S. (2006). Summer performance of a ventilated roof component. *Energy and Buildings*, 38, 610-617
8. Naji S., Celik O., Alengaram U.J. & Jumaat Zamin. (2014). Structure, energy and cost efficiency evaluation of three different lightweight construction systems used in low-rise residential buildings. *Energy and buildings*, 84, 727-739.  
<https://doi.org/10.1016/j.enbuild.2014.08.009>
9. Burch D. (1995). *An analysis of moisture accumulation in the roof cavities of manufactured housing*. Airflow Performance of Building Envelopes, Components, and Systems, ASTM STP 1255, American Society for Testing and Materials, Philadelphia, 156-177.
10. Wentling J. (2017). *Manufactured Housing. In: Designing a Place Called Home*. Springer, Cham.  
[https://doi.org/10.1007/978-3-319-47917-0\\_9](https://doi.org/10.1007/978-3-319-47917-0_9)
11. DSTU ISO 10211-1: 2005 (2007). *Thermally conductive inclusions in building structures. Calculation of heat flows and surface temperatures. Part 1. General methods* (ISO 10211-1:1995, IDT). (2007). Kyiv
12. DSTU ISO 10211-2 (2008). *Thermally conductive inclusions in building structures. Calculation of heat flows and surface temperatures. Part 2. Linear thermally conductive inclusions* (ISO 10211-2:1995, IDT). (2008). Kyiv
13. DSTU B V.2.6-189:2013 (2013). *Methods of selecting insulation material for thermal insulation of buildings*. Kyiv
14. DSTU B A.2.2-12:2015 (2015). *Energy efficiency of buildings. Method of calculating energy consumption for heating, cooling, ventilation, lighting and hot water supply*. (2015). Kyiv

UDC: 692.415:502.171

## «Green roofs» - historical experience and modern requirements

Filonenko Olena<sup>1\*</sup>, Avramenko Yurii<sup>2</sup>, Kidenko Vitalii<sup>3</sup>

<sup>1</sup> National University «Yuri Kondratyuk Poltava Polytechnic» <https://orcid.org/0000-0001-8571-9089>

<sup>2</sup> National University «Yuri Kondratyuk Poltava Polytechnic» <https://orcid.org/0000-0003-2132-5755>

<sup>3</sup> National University «Yuri Kondratyuk Poltava Polytechnic»

\*Corresponding author E-mail: [olena.filonenko.pf@gmail.com](mailto:olena.filonenko.pf@gmail.com)

The article considers the historical experience of creating "green roofs", as well as the requirements and conditions under which such roofs are currently designed. Historical examples and existing modern world objects show the expediency of creating and using green roofs of houses in Ukraine, which will significantly enrich the "fifth facade" of buildings and improve the overall appearance of cities. The lack of regulatory framework for the design of "green roofs", as well as some types of roofing technology problems that may arise during the operation of such roofs and the consequences that they have - environmental, economic, social, and technical. Determining the design conditions and the feasibility of using "green roofs" was chosen a structural scheme of combined coverage, which has all the necessary structural elements. It has been shown that the energy efficiency of this type of coating is provided. Determination of heat transfer resistance was carried out according to all regulatory requirements of SBC B.2.6 - 31: 2006. Constructions of houses and buildings, thermal insulation of buildings. The structural component of the designed "green roof" and the sequence of arrangement of some structural layers of this type of coating are considered. The efficiency and expediency of installation of "green" coatings on residential buildings, as well as the standard service life and warranty period of maintenance-free service of this coating, subject to regulatory requirements and operating conditions

**Keywords:** energy efficiency, green roofs, green structures, landscaping, environmental improvement

## «Зелені покрівлі» - історичний досвід та сучасні вимоги

Філоненко О.І.<sup>1\*</sup>, Авраменко Ю.О.<sup>2</sup>, Кіденко В.І.<sup>3</sup>

<sup>1,2,3</sup> Національний університет «Полтавська політехніка імені Юрія Кондратюка»

\*Адреса для листування E-mail: [olena.filonenko.pf@gmail.com](mailto:olena.filonenko.pf@gmail.com)

У статті розглядається історичний досвід створення «зелених покрівель», а також вимоги та умови, за яких такі покрівлі проектуються в даний час. На історичних прикладах та існуючих сучасних світових об'єктах показано доцільність створення та використання озелених покрівель будинків в Україні, що суттєво збагатить «п'ятий фасад» будівель та покращить загальний вигляд міст. Розглянуто відсутність нормативної бази для проектування «зелених покрівель», а також деякі види проблем технології озеленення покрівель, що можуть виникати в процесі експлуатації такої покрівлі та наслідки, що вони несуть – екологічні, економічні, соціальні та технічні. Для визначення умов проектування та доцільності використання «зелених покрівель» було обрано конструктивну схему суміщеного покриття, що має всі необхідні конструктивні елементи. Було показано, що енергоефективність даного типу покриття забезпечена. Визначення опору теплопередачі велося за усіма нормативними вимогами ДБН В.2.6-31:2006 «Конструкції будинків і споруд, теплова ізоляція будівель». Розглянуто конструктивну складову запроєктованої «зеленої покрівлі» та послідовність влаштування деяких конструктивних шарів даного типу покриття. Визначено ефективність та доцільність влаштування «зелених» покриттів на житлових будинках, а також нормативний строк служби та гарантійних термін безремонтної служби даного покриття, за умов дотримання нормативних вимог та умов експлуатації

**Ключові слова:** «зелена покрівля», озеленення, покращення навколишнього середовища, «зелена конструкція», енергоефективність



## Introduction

One of the modern architects' work areas is the construction of housing, in which a person could feel protected from the negative effects of the environment. Of course, the task is complex. And yet, the more materials offered to us by nature, surrounding us in everyday life, the more comfortable we feel. Realizing this, many architects use the experience of old architects in their designs. This is reflected in the desire of more and more people to regain the lost harmony with the natural environment, to preserve and increase the orderly depleted natural systems and landscapes. One of the areas of work to bring human habitation closer to wildlife is the installation of green roofs. Green roof - a place on the structure of the building, which is partially or completely covered with vegetation and fertile soil layer with the possibility of landscaping. Nowadays, this once primitive way of building a roof is increasingly turning into high-tech roofing, gaining popularity around the world. To roof landscaping, according to the developed classification, we also include landscaping of terraces [1].

"Green roofs" can now be considered as if the fifth facade, because their beauty often attracts more attention than the main facades of buildings. They are aesthetic, attractive, improve the appearance of the area and the city as a whole, and their environmental effect is beyond doubt. In addition, they create additional places for people to rest, among flowers and trees, without leaving their home and without using transport to get closer to nature. With the help of "green structures," you can mask the shortcomings of buildings and make them more harmonious and environmentally friendly. In addition, the use of such structures helps to harmoniously fit the building into the natural environment [1].

## Review of the research sources and publications

In Ukraine, "green technology" in general, and roof landscaping, in particular, have not become widespread yet. This leaves a certain imprint on research in this direction. Analysis of the literature showed that the research is theoretical, analytical, and generalizing. History of the issue, types of existing green structures are considered in the works of Kraynikovets O. [8], Kildisheva S. [5], Tkachenko T. [7], Shvec V. [10], Minyailo [13] offers ways to popularize the idea of roof landscaping in Ukraine, considers the prospects of "green structures" in Poltava. However, there are no serious research developments in Ukraine.

The main directions of development of this technology in Europe and the USA are presented in the works of Wong N. [1-2], Niachou A. [3], Taylor A. [9], Akbari H. [11].

## Definition of unsolved aspects of the problem

The lack of scientific base and popularization of the introduction of "green structures" in Ukraine is due to the lack of state support and the concept of the place, role, and importance of "green structures" to solve environmental, economic, and social problems of cities. The construction of "green structures" in Ukraine is sig-

nificantly hampered by the lack of a regulatory framework. The only norm that considers certain aspects of the use of "green roofs" is [14]. It provides only one version of the scheme of "green roof" and the calculation of loads from it.

Thus, the introduction of "green structures" in the "green" domestic construction is a promising direction, as evidenced by successful examples of the long-term existence of these structures in residential, educational, and commercial institutions. But the slowdown in the construction of green structures in Ukraine is due to the lack of research and development, regulatory framework, lack of concept of the role of "green structures" in sustainable urban development, lack of state support, as well as the difficult economic and political situation.

## Problem statement

The work aims to develop a typical energy-efficient solution of "green roof" structures based on the analysis of historical experience and foreign experience.

## Basic material and results

History of the "green roofs".

The prototype of the "green roof" can be considered the first home of a prehistoric man. Our ancestors placed grass on thatched roofs to improve thermal insulation, reduce the risk of outbreaks and ensure water runoff (Figure 1). Until recently, buildings in peasant yards in the northern regions of the Slavic countries were placed very close to each other, and their roofs were covered with a layer of soil and vegetation. The history of green roofs is quite old.



Figure 1 – Houses with sod roofs in the Faroe Islands

In Scandinavia and Iceland (over 1,000 years ago), dwellings with earthen roofs were common. Grass grew on the backfill, which served as additional insulation and allowed it to retain heat. In southern Europe, by contrast, roof landscaping was used for sun protection. This technology was especially suitable for warehouses and storage of agricultural products, wine cellars. Such buildings were built, in particular, in rural Austria in the late XIX - early XX century. In Babylon, the first "metropolis" of the ancient world, there was already a problem of environmental management. One-storey dense urban buildings have almost supplanted green urban areas. Small groves, orchards, and palm alleys surrounded only areas of rich nobles. But the city looked like a green oasis due to the system of green terraces, i.e. the famous Hanging Gardens of Semiramis [8].

The famous "Gardens of Semiramis", considered the seventh wonder of the world and built around 600 BC., were nothing more than "green roofs" of Babylonian palaces. The gardens in those days were terraces. The pillars were covered with stone slabs, which housed several layers of brick, bitumen, reeds, lead, and a thick layer of earth. The lower terrace was 45 x 40 m, the upper ones were smaller. The total height of the building was about 20-22 m. On the lower terrace grew plain plants, mostly trees, and on the upper there were mountain plants. Already, in this case, we are faced with the distribution of plants in tiers according to their environmental requirements and biological needs (Fig. 2) [8].



**Figure 2 – Hanging Gardens of Semiramis**

The most luxurious examples of hanging gardens are known in the Renaissance. Italy was especially famous for such gardens, where in Florence in the XV century in the gardens on the roof of Villa Medici grew exotic flowers, and in Mantua a huge hanging garden was built on the roof of the palace of the Duke of Gonzaga. Cardinal Andrea del Valle in 1530 built a museum in Rome in the form of a "hanging garden", and in Verona, Count Mafarey on the roof of his palace made a beautiful garden planted with various flowers and trees [1, 3-5]. In the XVI-XVII centuries, in northern Italy on the rocks of the island of Isola Bella, surrounded by the waters of Lake Maggiore, on the terraces of the castle were built hanging gardens, which became a model of garden art of the Late Renaissance. Under the terraces, where plants from almost all over the world were collected, there was a whole gallery of underground grottoes, where you could hide from the summer heat.

Thus, in the period from the era of the Ancient World (six centuries BC) and to the XIX century. Green roofs were used to solve aesthetic and utilitarian problems. The evolution of "green roofs" took place with the development of cities and society. In Europe, the ancient roof gardens were forgotten during the Middle Ages. The second birth of green roofs dates back to the XIX century when at the World's Fair in Paris, German architect Karl Rabitz surprised the audience by presenting a house with greenery instead of the traditional roof. Since then, appeared the concept of "living roof", "operated roof" - lawns or even gardens for recreation directly on the roof of the building. Karl Rabitz formulated the idea of landscaping roofs as the most important means of improving the urban environment.

The construction of flat "green roofs" took on a particularly large scale at the end of the 19th century, and in the early XX century, in connection with the advent of reinforced concrete and thanks to the work of the most prominent architects and urban planners, among whom were the Frenchman Le Corbusier and the American FL Wright [4]. Le Corbusier made "roofs-gardens" a necessary part of the architecture, developing and implementing a large number of projects using exploited green roofs, ranging from small villas to large residential complexes. Roof landscaping from the category of privileged private closed became open to the city and its inhabitants. That is, the social component was added to the utilitarian approach.

World standards for creating "green roofs"

In Europe, the United States, and Canada, roofs have been widely planted since the early 1980s. Initially, in a number of countries, landscaping was carried out as part of national programs aimed at enhancing biodiversity. Roof landscaping is currently recognized as one of the most relevant areas of landscape design. The governments of most developed countries do their best to encourage green roofs (especially in large cities). According to experts, the generally accepted priority in the creation of garden roofs now belongs to Germany, where about 14 million green roofs appear annually. In this country, one of the prerequisites for the design of new buildings – roofs landscaping, including a significant slope. Taxes have been introduced for homeowners who do not use roofs for gardens.

In England, in 2007, the mayor of London ordered the use of landscaping in all major projects, so that the total area of green roofs is growing every year. In Copenhagen (Denmark) since 2010, each roof is subject to landscaping. Tax benefits are provided for the implementation of such projects. In Austria, roof landscaping has been paid for by the municipality since 1983.

In Switzerland, every flat roof has been landscaped since 2002 (currently more than 1,900 roofs in Basel are landscaped, which is more than 25% of the total roof area).

In France, a law was passed in 2016 that obliges commercial property owners to cover the roofs of buildings with plants or solar panels. Thus, "green roofs" will provide the necessary level of thermal insulation to reduce the amount of energy needed to heat the building in the cold season or to cool in the summer.

In Bulgaria, the design of a roof garden is necessary to meet 20% of the rate of the landscaping of the land where the building is located.

In the United States in New York alone there are more than 7.5 thousand green roofs. New York Mayor Michael Bloomberg in 2010 announced his intention to green the roofs of city skyscrapers, turning them into parks. This initiative should help solve two pressing urban problems. First, improve air quality. Second, reduce the amount of runoff into storm sewers, which is poorly handled by worn-out drainage systems in New York. Although green roofs will cost the city \$ 6.8 billion, they will save \$ 2.4 billion over the next twenty years.

In Chicago, private homeowners are paid subsidies for roof landscaping. Chicago authorities have calculated that if you green all the roofs in the city, where the construction of buildings allows, it would bring to the city budget about \$ 100 million. per year due to energy savings.

In Canada, since 2009, every roof with an area of more than 2,000 m<sup>2</sup> has been subject to landscaping. In 2007, Toronto took 1st place in the list of cities in Canada with "green" roofs, when the total area of "green" roofs for the year was 83,000 square feet (7710.7 m<sup>2</sup>).

In Japan, since 2001, all roofs with an area of more than 100 m<sup>2</sup> are subject to landscaping: 20% of the roof with an area of 250 m<sup>2</sup> and 10% of the roof with an area of more than 1000 m<sup>2</sup>. "Green roofs" are also available in Taiwan and India.

In some countries of Europe, Asia, America there are associations of the landscaping of roofs, the main of which are:

- International Roofing Association (IGRA);
- Association of Roofing Landscape Architects of Germany (DDV);
- European Federation of Green Roof Associations (EFB).

In North America in 1999, the organization "Green Roofs for Healthy Cities - North America" was founded. There is even The Scandinavian Green Roof Association, which annually awards the best roof landscaping project. Every year, the International Congress of Roof Landscaping is held in different countries of the world, where development trends, the most relevant and promising areas of use, improvement of construction and design technologies, and new innovative projects are presented.

Introduction of "green structures" in Ukraine

In Ukraine, landscape and recreational planning of settlements is regulated by SBC B. 2.2-12: 2018, which has already appeared innovative means of increasing the area of landscaping: vertical gardens and parks (carpet and modular), mobile landscaping systems (mobile forms), green screens and walls, gardens of continuous flowering (work is underway on the second edition), as well as the State Sanitary Rules for Planning and Development of Settlements.

To date, there are no regulations on the introduction of "green structures" in the "green building" of Ukraine. Thus, all landscape design firms engaged in the market of Ukraine "roof landscaping" have no idea about the correctness of the design of "green structures", which leads to a gross violation of technology, safety, and reduced service life. Exceptions may be international companies (ZinCo, FlorDepot), operating in the Ukrainian market according to European standards and technologies.

Until 2000, there were virtually no examples of the introduction of "green structures" in Ukraine. Separate private "green roofs" began to appear in 2005. Over the past five years, there has been a rapid development of "green building" using "green structures". Recent projects cover not only the private construction sector. "Green constructions" began to appear in shopping

malls and offices, universities, and libraries (for example, the Ukrainian Catholic University in Lviv), as well as in residential complexes.

Existing green roofs on residential buildings are currently being approved in Ukraine as experimental housing. These include the "green roof" in Kyiv at the Royal Tower (Fig. 3) (2016) and Skyline (Fig. 4). The uniqueness of the roof on the Royal Tower is that it is intense and is located on the 32nd floor. Large woody plants up to 6 m tall are planted on the roof.



**Figure 3 – Green roof of the Royal Tower**

The Skyline has a terrace principle of landscaping. In recent years, especially popular roof landscaping of office buildings. The roof space is used as a recreational area for residents and guests of the house and is rented out for various events. Owners of some office buildings, for example, on Lobanovsky Avenue, where the "green roof" of the company "ZinCo" is located, use it for commercial purposes - for rent for various purposes.



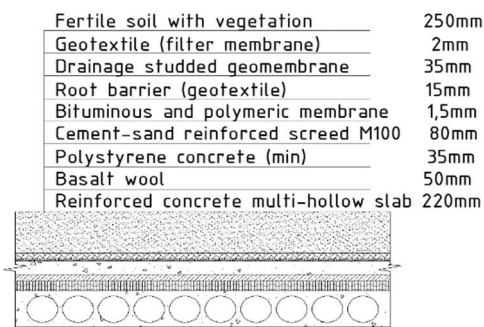
**Figure 4 – Green terraces of the Skyline house**

Among the "green structures" in business centers, there is an intensive "green roof" on Smolenskaya Street. In 2013, a project to create mini-farms on the roofs of high-rise buildings was actively discussed in Kyiv, but it never developed. However, the idea is promising, especially considering that in Kyiv there are more than 200 hectares of flat roofs that can be used as areas for small greenhouses. In addition, all roofs are usually covered with a black coating, which further retains solar heat, which can be used for greenhouses.

Designing a "green roof"

When developing the project of construction of a multi-storey residential building, a constructive solution of the "green roof" was applied according to this scheme (Fig. 5).



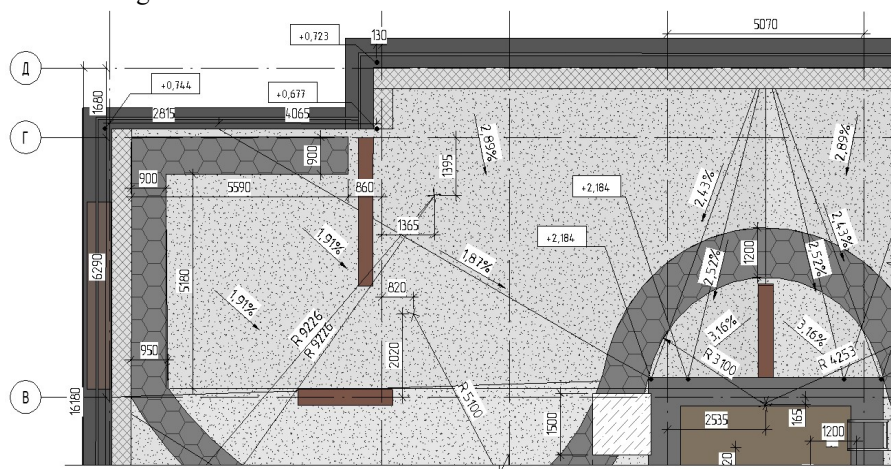


**Figure 5 - Constructive scheme of coverage**

In accordance with the calculated values and conditions defined in SBC B.2.6 - 31: 2006 [15], performing the thermal calculation of the combined coating, we obtain the heat transfer resistance of this structure. The normalized value will be equal to  $R_{qmin}=6.0 m^2 \cdot K/W$ , and accordingly calculated  $R=6.82 m^2 \cdot K/W$ , in such a way  $R_{\Sigma} \geq R_{qmin}$  that it will fully provide the conditions we need.

After these calculations, you can start designing a "green roof" for a multi-storey residential building. Taking into account all design features, according to SBC [15], aesthetic and recreational conditions that can be created on this type of roof, after the design we get a fundamentally individual and structurally provided "green roof".

The designed "green roof" (Fig. 6) has extensive landscaping, does not require special care. Almost around the perimeter of the roof is a green "fence" of boxwood.



**Figure 6 – Fragment of the designed "green roof"**

### Conclusions

Currently, scientific and technical development of "green structures" are carried out in the following areas:

- increase of energy efficiency of the building (improvement of heat-protective properties of buildings, passive cooling);
- reducing the amount of rainwater runoff by absorbing water "green roofs";
- improvement of the environment (reduction of thermal and chemical pollution of the atmosphere by eliminating "thermal islands", biological conversion of greenhouse gases into safe compounds);

To move around the roof, garden paths made of special rubber tiles arranged directly on the ground are designed. The rest of the territory is a garden lawn.

This "green roof" can be considered an extended area of relaxation and recreation. Grass cover and rubber paths allow all occupants of the house to be safe on the roof, including children, but under the supervision of adults. For greater security along the perimeter of the roof is a fence 1.3 m high.

The energy efficiency of such a roof structure will be ensured by multi-layered and elements that absorb less solar energy than roll coverings. Thus, the structure of the "green roof" will not overheat in the summer due to the soil layer, and in winter - to freeze, which will increase the service life of the entire structure and the house as a whole. As a vapor barrier in the construction of a "green roof" it is necessary to use rolled waterproofing materials without protective topping and to ensure the integrity of the waterproofing, and as the top layer of waterproofing should be used root-resistant material. The service life of this used roof structure will depend on the quality of work performed and materials used, but the warranty period of roofless maintenance (the period during which the roofing carpet, vapor, and insulation layers do not require current repairs, the cost of which would exceed 10% of capital costs construction) subject to compliance with regulatory requirements for the design of coatings and the full implementation of all requirements for the operation of the roof is 3 years [14].

– improving the aesthetic properties of buildings and the psycho-emotional state of man;

– applied use of "green structures" (for recreational purposes, doing business, growing medicinal and agricultural plants, grazing animals), etc.

The paper proposes to use "green" roofs and facades to solve the problems of cities related to urbanization.

The project proposal of the "green" roof was created and the energy efficiency of the proposed solution was proved by thermal calculation.

"Green" roofs are a dynamic system, the economic and environmental effect of which is very significant but not implemented in Ukraine.

## References

1. Wong N., Cheong D.K.W., Yan H., Soh J., Ong C.L., Sia A. (2003). The effects of rooftopgardens on energy consumption of a commercial building in Singapore. *Energy and Buildings*, 35, 353-364  
[https://doi.org/10.1016/S0378-7788\(02\)00108-1](https://doi.org/10.1016/S0378-7788(02)00108-1)
2. Wong N.H., Chen Y., Ong C.L., Sia A. (2003). Investigation of the thermal benefits of rooftop garden in the tropical environment. *Building and Environment*, 38, 261-270  
[https://doi.org/10.1016/S0360-1323\(02\)00066-5](https://doi.org/10.1016/S0360-1323(02)00066-5)
3. Niachou A., Papakonstantinou K., Santamouris M., Tsangrassoulis A. & Mihalakakou G. (2001). Analysis of the green roof thermal properties and investigation of its energy performance. *Energy and Buildings*, 33, 719-729  
[https://doi.org/10.1016/S0378-7788\(01\)00062-7](https://doi.org/10.1016/S0378-7788(01)00062-7)
4. Ле Корбюзье (1970). *Творчий шлях*. Москва: Стройиздат
5. Кільдішева С.В. (2006). Сучасні методи міського озеленення. Вертикальне і дахове озеленення. *Екологія урбанізованих територій*, 37-38
6. ДБН Б.2.2-12:2018 (2018). *Планування і забудова територій*. Київ: Укрархбудінформ
7. Ткаченко Т.Н., Мілейковський В.А., Дзюбенко В.Г. (2016). Перспективи «зеленого» будівництва та альтернативних форм озеленення в Україні. *Містобудування та територіальне планування*, 60, 324-334
8. Крайниковець О.В., Дідик В.В., Максим'юк Т.М. (2012). Сади на дахах. *Архітектура*, 728, 119-125
9. Taylor A., et al (2001). Coping with ADD: The Surprising Connection to Green Play Settings. *Environment and Behavior*, 33(1), 54-77  
<https://doi.org/10.1177/00139160121972864>
10. Швець В.В., Руденко К.С., Веремій О.Г. (2010). Формування екологічного каркасу міста. Укриття під зеленим покривом. *Сучасні технології, матеріали і конструкції в будівництві*, 2(27), 139-143
11. Akbari H. (2002). *Heat Island Reduction: An Overview - Effects of Trees and Implementation Issues. Presentation by Lawrence Berkeley Laboratory at the University of Pennsylvania*, LAPR 760  
[doi.org/10.1007/s11252-008-0054-y](https://doi.org/10.1007/s11252-008-0054-y)
12. Ameng Brown (2005). Report on the environmental benefits and costs of green roof technology for the city of Toronto. *Prepared For City of Toronto and Ontario Centres of Excellence*. Earth and Environmental Technologies (OCE-ETech)
13. Міняйло М.А., Філоненко О.І. (2015). Сади на дахах та їх соціально-економічний вплив. *Збірник наукових праць: будівництво, матеріалознавство, машинобудування*, 81, 111-118
14. ДБН В.2.6-220:2017 (2017). *Покриття будівель і споруд*. Київ: Міністерство регіонального розвитку, будівництва та житлово-комунального господарства України
15. ДБН В.2.6-31:2006 (2006). *Конструкції будинків і споруд. Теплова ізоляція будівель*. Київ: «Державний науково-дослідний інститут будівельних конструкцій» Мінрегіону України
1. Wong N., Cheong D.K.W., Yan H., Soh J., Ong C.L. & Sia A. (2003). The effects of rooftopgardens on energy consumption of a commercial building in Singapore. *Energy and Buildings*, 35, 353-364  
[https://doi.org/10.1016/S0378-7788\(02\)00108-1](https://doi.org/10.1016/S0378-7788(02)00108-1)
2. Wong N.H., Chen Y., Ong C.L. & Sia A. (2003). Investigation of the thermal benefits of rooftop garden in the tropical environment. *Building and Environment*, 38, 261-270  
[https://doi.org/10.1016/S0360-1323\(02\)00066-5](https://doi.org/10.1016/S0360-1323(02)00066-5)
3. Niachou A., Papakonstantinou K., Santamouris M., Tsangrassoulis A. & Mihalakakou G. (2001). Analysis of the green roof thermal properties and investigation of its energy performance. *Energy and Buildings*, 33, 719-729  
[https://doi.org/10.1016/S0378-7788\(01\)00062-7](https://doi.org/10.1016/S0378-7788(01)00062-7)
4. Le Corbusier (1970). *Creative Way*. Moscow: Stroyizdat
5. Kildisheva S.V. (2006). Modern methods of urban landscaping. Vertical and roof landscaping. *Ecology of urban areas*, 37-38
6. DBN B 2.2-12: 2018. *Planning and development of territories*. Kyiv: Ukrarhbuildinform
7. Tkachenko T.N., Mileyskovsky V.A. & Dzyubenko V.G. (2016). Prospects of "green" construction and alternative forms of landscaping in Ukraine. *Urban planning and spatial planning: scientific and technical*, 60, 324-334
8. Kraynikovets O.V., Didyk V.V. & Maksymyuk T.M. (2012). Garden on the roof. *Architecture*, 728, 119-125
9. Taylor A., et al (2001). Coping with ADD: The Surprising Connection to Green Play Settings. *Environment and Behavior*, 33(1), 54-77  
<https://doi.org/10.1177/00139160121972864>
10. Shvets V.V., Rudenko K.S. & Veremiy O.G. (2010). Formation of the ecological framework of the city. Shelter under a green cover. *Modern technologies, materials and structures in construction*, 2(27), 139-143
11. Akbari H. (2002). *Heat Island Reduction: An Overview - Effects of Trees and Implementation Issues. Presentation by Lawrence Berkeley Laboratory at the University of Pennsylvania*, LAPR 760  
[doi.org/10.1007/s11252-008-0054-y](https://doi.org/10.1007/s11252-008-0054-y)
12. Ameng Brown (2005). Report on the environmental benefits and costs of green roof technology for the city of Toronto. *Prepared For City of Toronto and Ontario Centres of Excellence*. Earth and Environmental Technologies (OCE-ETech)
13. Minyailo M.A. & Filonenko O.I. (2015). Gardens on the roofs and their socio-economic impact. *Collection of scientific works on construction, materials science, mechanical engineering*, 81, 111-118
14. DBN V.2.6-220:2017 (2017). *Covering of buildings and structures*. Kyiv: Ministry of Regional Development, Construction and Housing of Ukraine
15. DBN V.2.6-31:2006 (2006). *Constructions of houses and buildings. Thermal insulation of buildings*. Kyiv: "State Research Institute of Building Structures" of the Ministry of Regional Development of Ukraine

UDC 69:721.021.2

## Organizational and economic impact of implementation additive technologies in construction

Hanieiev Timur<sup>1\*</sup>, Korzachenko Mykola<sup>2</sup>, Bolotov Gennady<sup>3</sup>, Yushchenko Svitlana<sup>4</sup>

<sup>1</sup> Chernihiv Polytechnic National University <https://orcid.org/0000-0001-6037-5494>

<sup>2</sup> Chernihiv Polytechnic National University <https://orcid.org/0000-0002-5674-8662>

<sup>3</sup> Chernihiv Polytechnic National University <https://orcid.org/0000-0003-0305-2917>

<sup>4</sup> Chernihiv Polytechnic National University <https://orcid.org/0000-0003-0863-9020>

\*Corresponding author E-mail: [ganjejev.timur@gmail.com](mailto:ganjejev.timur@gmail.com)

The use of additive technologies in combination with other technologies that provide the transition from model to the finished product is actively used in the industry of many countries. The use of such technologies in combination with casting one allows you to make certain types of sculptures. Modeling of sculptures in specialized software packages without the participation of a sculptor is still not possible, so the most promising direction for town planning is the production of relatively simple in shape models of prominent historical and cultural buildings and entire cities. The ability to 3d print the developed model greatly simplifies and speeds up the production of a master model for further metal casting. The conducted cost analysis showed savings of 15-17% in the transition from manual production of a master model by a sculptor to modeling and 3d printing.

**Keywords:** additive technologies, economic efficiency, casting, master model, sculpture

## Організаційно-економічний вплив впровадження адитивних технологій в будівництві

Ганєєв Т.Р.<sup>1\*</sup>, Корзаченко М.М.<sup>2</sup>, Болотов Г.П.<sup>3</sup>, Ющенко С.М.<sup>4</sup>

<sup>1</sup> Національний університет «Чернігівська політехніка»

<sup>2</sup> Національний університет «Чернігівська політехніка»

<sup>3</sup> Національний університет «Чернігівська політехніка»

<sup>4</sup> Національний університет «Чернігівська політехніка»

\* Адреса для листування E-mail: [ganjejev.timur@gmail.com](mailto:ganjejev.timur@gmail.com)

Застосування адитивних технологій в комплексі з іншими технологіями, що забезпечують перехід від макетування до готового виробу активно використовуються в промисловості багатьох країн. Застосування таких технологій в комплексі з ливарними дозволяє виготовляти окремі види скульптур. Моделювання скульптур в спеціалізованих програмних пакетах без участі скульптора все ще не можливе, тому найперспективнішим напрямом для містобудування є виготовлення, відносно простих за формою, макетів визначних історико-культурних будівель та цілих міст. Можливість 3d друку розробленого макету значно спрощує та прискорює виготовлення майстер-макету для подальшого лиття металом. Роздільно здатність 3d принтерів в десятки мікрон дозволяє друкувати елементи майстер-макету з величезною деталізацією, а сучасні технології лиття забезпечують якість кінцевого виробу. Тобто основною перевагою від впровадження адитивних технологій в процес розробки та виготовлення макетів історичних будівель та споруд є мінімальне використання часу скульптора, відмова від роботи з скульптурними матеріалами на користь комп'ютерного моделювання та швидкий друк з значною деталізацією. Однак заміна роботи професійного скульптора на роботу спеціаліста з комп'ютерного моделювання значно звужує область застосування технології. Фактично раціональним є виготовлення копій старовинної забудови міст та окремих замків, церков, будинків. Розглянуті в роботі макети дозволяють припускати стрімкий розвиток такої технології в найближчому часі, а зважаючи на туристичний потенціал міст України технологія буде мати практичне застосування принаймні з два десятки років. Проведений аналіз витрат на прикладі бронзового макету «Чернігівська фортеця початку XVIII ст.» показав економію коштів в 15-17% при переході з ручного виготовлення майстер-макету скульптором на моделювання та 3d друк.

**Ключові слова:** адитивні технології, економічна ефективність, лиття, майстер-макет, скульптура



## Introduction

The advantages of the introduction of additive technologies in the development and manufacture of various models are undoubted, but the use of these technologies in combination with others, such as casting, to obtain a finished architectural product requires more experience and active discussion.

The development of master models for casting requires a lot of time and manual labor of the sculptor and the architect, but if there are repetitive or similar objects in the project, it is possible to apply a computer simulation with subsequent 3D printing. This approach significantly reduces the production time of the master model, and the high resolution of modern 3D printers increases their detailing.

## Review of research sources and publications

One of the modern trends in construction is to support the concept of inclusive urban space. As part of this concept, bronze models of historic buildings [1, 2] or individual historically important buildings have appeared in many cities with a rich historical past [3] (Fig. 1).

A distinguishing feature of such models with high digitalization and duplication of inscriptions in Braille is their tactility. It is especially important for children and persons with visual deficiency.

## Definition of unsolved aspects of the problem

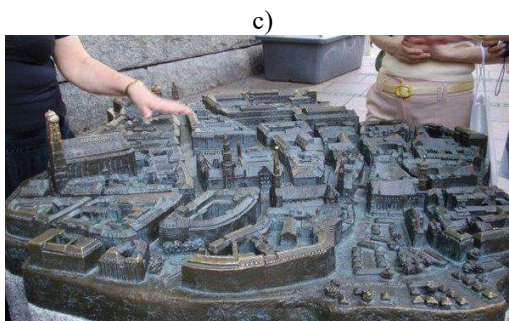
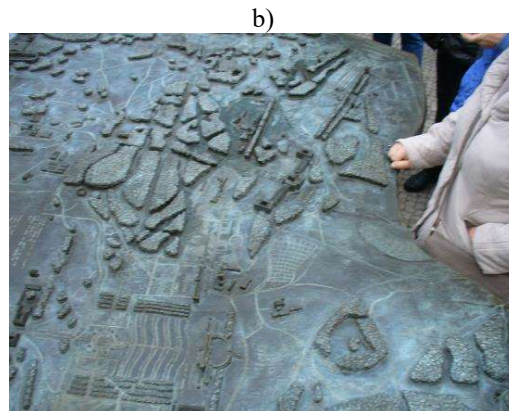
The question of expediency and limits of using 3D printing in architectural and town planning projects is still insufficiently covered. In the first place, there is the possibility of replacing the sculptor's manual with repetitive and simple in shape objects, but with a large number of small details.

## Problem statement

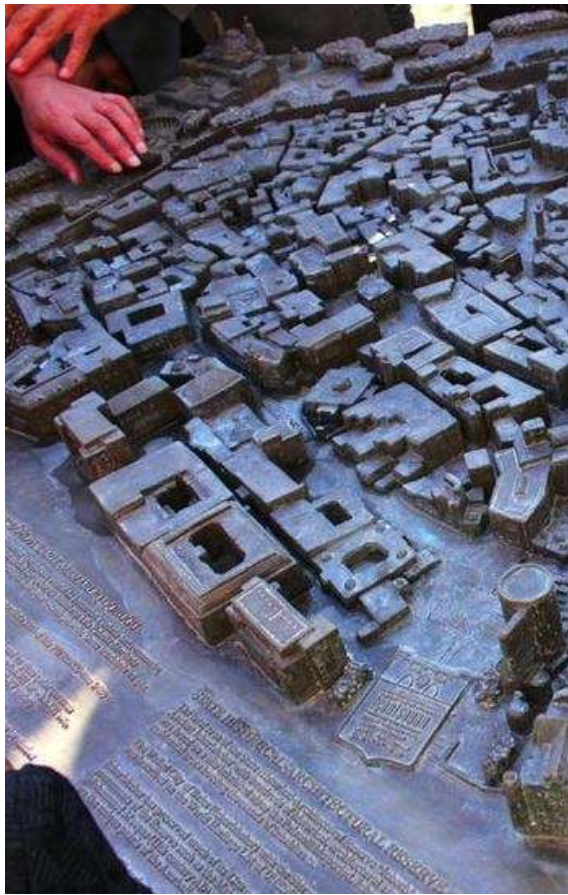
To determine the limits of the use of 3D printing in the manufacture of a master model for casting on the example of a bronze model "Chernihiv Fortress of the early XVIII century".

## Basic material and results

Development of projects in architecture and town planning is always a complex and multi-vector process that requires visualization of decisions [4]. The current level of CAD systems allows to realistically model urban development and landscape at the design stage of the construction object, and the availability of additive manufacturing technologies (Additive Manufacturing, AM) speeds up and reduces the cost of the model [5, 6]. In most projects, the use of AM-technologies is limited to this [7], but for projects with sculptural compositions, it becomes possible to make a master model for casting. The reorientation of AM from the field of visualization and presentation models to the final product is a global trend. So, the percentage of AM-technologies in the manufacture of master models for metal casting in 2004 was 8.1%, and in 2013 – 10.8% [7]. One of the successful examples of the additive technologies used is the tactile project of Cyril Rabat in Baku [8] (Fig. 2).



**Figure 1 – Examples of existing bronze models:**  
a – Church of St. Mary of the Perpetual Assistance, Ternopil (Ukraine) [2];  
b – Sanssouci Park (Germany) [1];  
c – Old part of Munich (Germany) [3]



**Figure 2 – Tactile model, Baku (Azerbaijan) [8]**

A model of the historic part of Baku was made in 2017 in co-authorship with German architect Egbert Broerken.

In Ukraine the opportunity to carry out work on the production of master models for casting by AM technology entirely appeared in 2019. The historical part of the city of Chernihiv was chosen as the object of visualization, modeling, and master model making. According to the plan, the model should combine the existing churches and cathedrals with the buildings that surrounded them at the beginning of the XVIII century, immersing the visitor in the history of the city. For this purpose, the model has been installed in the center of the entrance group to the park “Chernihiv Dytnets”, which allows visitors to simultaneously observe the preserved architectural monuments and their model (Fig. 3). The bronze model is located on a stone pedestal. In a circle, at the foot of the stone, there are also the historical coats of arms of Chernihiv and tables with historical dates.

The sculptural composition consists of two groups of sculptures located in a semicircle on both sides of the bronze model “Chernihiv Fortress of the early XVIII century”. One group of sculptures depicts Prince Mstislav and Nestor the Chronicler, another – Colonel Martin Nebab, who was a close associate of Hetman Khmelnytsky, and the founder of the Chernihiv publishing house Lazar Baranovich. The author of the sculptures is Kyiv sculptor Oleksiy Shevchenko.

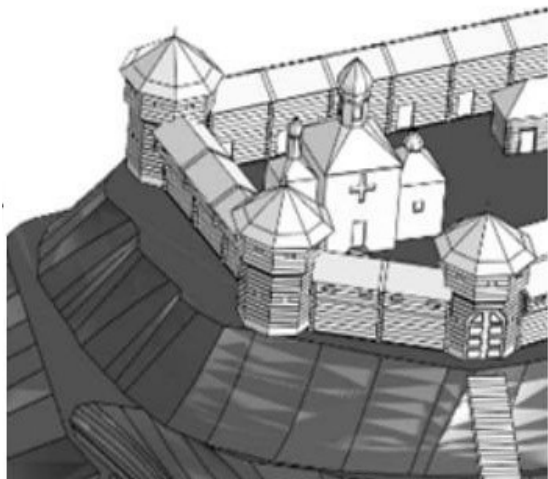
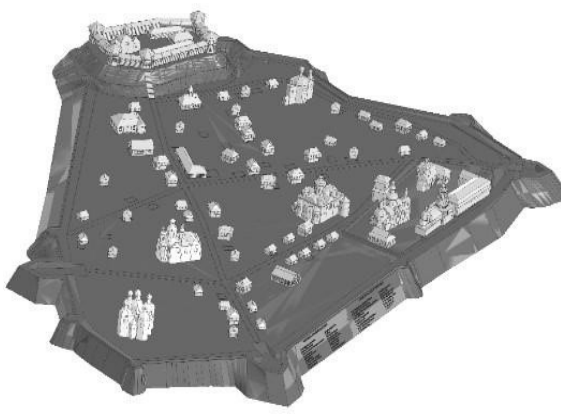
The author of the idea of the central part of the composition is the Chernihiv historian Oleksandr Bondar. The team of the Chernihiv Polytechnic National University was engaged in the introduction of AM-technologies in the project.

Modeling of elements was carried out according to the provided sketches. The presence of a digital model has greatly simplified and accelerated changes in the design of the model (Fig. 4). The significant advantage has been the presence in the model of three dozen buildings, represented by four repeating models, and the walls of the upper castle, formed by only three models. Changes in the placement of inscriptions and fonts also did not require the reworking of the master model. In addition, printing a series of identical elements significantly reduces printing time and the amount of waste.



**Figure 3 – Sculptural composition, Chernihiv (Ukraine), September 2020 [9, 10]**

The analysis of the economic efficiency of the project showed that the amount of cost savings for the production of a master model using 3D printing technology is 15-17% compared to the cost of manual labor of a professional sculptor. The production of master model elements was performed using FDM (Fused Deposition Modeling) technology, which according to ASTM F2792.1549323-1 (USA) belongs to the category of Material Extrusion technologies. FDM technology in this standard is described as a layered application of molten material using an extruder [11]. Additive technology laboratory printers, ZAVmaxPro models, were used for 3D printing. Glycol-modified polyethylene terephthalate (PETg) from 3DPlast was chosen as the printing material. The choice of material has been conditioned by its mechanical properties and low shrinkage during cooling. To reduce the printing time the height of the polymer layers was increased to 200  $\mu\text{m}$  and chemical smoothing of the finished surfaces was applied.



**Figure 4 – Intermediate variant of model design**

Each element of the master model was printed as separate parts (Fig. 5). The basis of the model together with the arrays of trees was made by milling MDF boards. The casting of the elements was performed on molten molds. Assembly of elements on the basis was performed by gas soldering.

Additionally, bronze plates with a description of the model elements were made by milling on CNC machines.

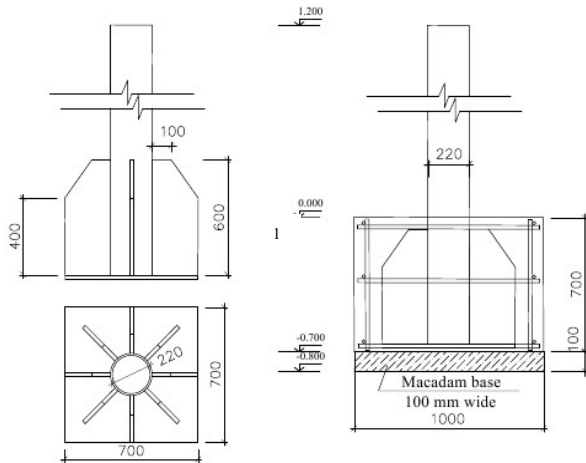


**Figure 5 – Printed elements of the master model before casting**

There are also certain requirements for the pedestals, on which the model must be placed.

The pedestals can be made in the form of a small pillar produced of brick, stone (mainly marble, granite), reinforced concrete, metal, or combined (for example, reinforced concrete lined with marble). Such pedestals usually do not require auxiliary requirements for the arrangement. The main condition is a secure attachment of the model and the base of the pedestal to the foundation. The depth of the foundation may be limited by town-planning conditions.

The authors propose to use a metal pipe with a diameter of 200-300 mm, which using metal plates has been reinforced to a reinforced concrete foundation with a depth of 0.7 m and by dimensions of 1 m per 1 m (Fig. 6). These dimensions allow you to keep the model from damage by vandals. The metal pipe can be painted, concreted, or faced with decorative materials (marble, granite).



**Figure 6 – Construction of the pedestal made of the metal pipe with a reinforced concrete foundation**

The decision to accept the massive elements can be dictated not only from architectural or design solutions but also from the point of view of anti-vandalism or at least for reasons of aesthetic appearance. It should be noted that the model has requirements not only for the safety of the environment (humans, animals, birds) but also requirements against vandalism.

When placing models in the city, special attention must be paid to the installation of a solid foundation for the objects. Although the model itself may be light, the pedestal on which the elements are placed can be large (several square meters) and usually made of marble, granite, or heavy concrete (the weight of such elements can reach several tons).

The weight of massive stones is usually distributed over the entire area of the pedestal, but if the estimation of the base reliability is incorrect, it can lead to excessive subsidence of the pedestal, especially in the presence of soils with special properties under the foundation base.

The stage of the concrete preparation of the pedestal and stages of installation of the pedestal and the ready model in Chernihiv are shown in Fig. 7, 8.



**Figure 7 – Concrete preparation under the pedestal for the model in Chernihiv [12]**



**Figure 8 – The stone with the bronze model of the Historic Dytynets in Chernihiv [13]**

In some cases, soil compaction or macadam or other concrete preparation under the base of the pedestal is not enough. In such cases, it is necessary to arrange artificial fixing of soil or replacement of weak soil on a more reliable basis.

The substantiation of rational decisions concerning the construction of a building on which the model is placed must be based on the complex analysis of the territory features taking into account the constructive decision of the object.

## Conclusions

The gradual introduction of AM technologies in complex and knowledge-intensive industries of developed countries is forcing our country to begin its research in various application fields of additive technologies.

One of the promising industries may be architecture and town planning. The most probable application for the given technology is the production of metal models of increased detailing and simplicity for modeling of forms.

The example of a bronze model “Chernihiv fortress of the early XVIII century” shows the possibility of accelerating the implementation of such projects through a complete transition to computer modeling and AM technology. Renunciation of the traditional process of the master model formation, in addition to saving time, also allows reducing the cost of the finished model by transferring from manual labor to an automated process and replacing the classic sculptural materials with polymer.

## References

1. *Парк Сан-Суси*. Взято з [https://www.tripadvisor.ru/LocationPhotoDirectLink-g187330-d501640-i148040065-Sanssouci\\_Park-Potsdam\\_Brandenburg.html](https://www.tripadvisor.ru/LocationPhotoDirectLink-g187330-d501640-i148040065-Sanssouci_Park-Potsdam_Brandenburg.html)
2. *Бронзовий Тернопіль*. Взято з <https://bronze.te.ua/>
3. *Бронзовый макет старой части города*. Взято з <http://www.openarium.ru/poi/28758556/>
4. Самойлов С.В. (2011). Освоение технологии производства художественного литья (изделий духовного назначения) из цветных металлов и сплавов. *Металл и литье Украины*, 9-10, 64-66
5. Ковалевский С.В., Гончарова Н.С. (2015). Развитие аддитивных технологий на основе послойного выращивания деталей машин. *Научный вестник Донбасской государственной машиностроительной академии*, 3, 149-154
6. Besklubova S., Skibniewski M.J. & Zhang X. (2021). Factors Affecting 3D Printing Technology Adaptation in Construction. *Journal of Construction Engineering and Management*, 147(5), 2034
7. *Характеристика рынка аддитивных технологий*. Взято з <https://extxe.com/9663/harakteristika-rynka-additivnyh-tehnologij>
8. *В Баку представлен уникальный проект – макет Ичеришехер в бронзе для слепых*. Взято з <https://news.day.az/society/907217.html>
9. *Ярослав Куц: скульптурна композиція на Валі – нова туристична принада Чернігова*. Взято з <http://svoboda.fm>
10. *Историко-скульптурная композиция на черниговском Валі готова!* Взято з <https://www.gorod.cn.ua>
11. *Классификация и терминология аддитивных технологий*. Взято з <https://extxe.com/9643/klassifikacija-i-terminologija-additivnyh-tehnologij/>
12. *На вході на Вал готують основу для встановлення макету Дитинця і скульптур*. Взято з <https://chernigiv-rada.gov.ua/news/id-43717/>
13. *При вході на Вал почали встановлювати скульптури і готувати місце під макет Дитинця*. Взято з <https://chernigiv-rada.gov.ua>
1. *Sanssouci park*. Retrieved from [https://www.tripadvisor.ru/LocationPhotoDirectLink-g187330-d501640-i148040065-Sanssouci\\_Park-Potsdam\\_Brandenburg.html](https://www.tripadvisor.ru/LocationPhotoDirectLink-g187330-d501640-i148040065-Sanssouci_Park-Potsdam_Brandenburg.html)
2. *Bronzed Ternopil*. Retrieved from <https://bronze.te.ua/>
3. *Bronze Model of the Old Town*. Retrieved from <http://www.openarium.ru/poi/28758556/>
4. Samoilov S.V. (2011). Mastering the technology for the production of artistic casting (spiritual products) from non-ferrous metals and alloys. *Metal and casting of Ukraine*, 9-10, 64-66
5. Ковалевский С.В., Гончарова Н.С. (2015). Development of additive technologies based on layered growing of machine elements. *Научный вестник Донбасской государственной машиностроительной академии*, 3, 149-154
6. Besklubova S., Skibniewski M.J. & Zhang X. (2021). Factors Affecting 3D Printing Technology Adaptation in Construction. *Journal of Construction Engineering and Management*, 147(5), 2034
7. *Description of additive technologies' market*. Retrieved from <https://extxe.com/9663/harakteristika-rynka-additivnyh-tehnologij>
8. *A unique project presented in Baku - model of Icherisheher in bronze for the blind*. Retrieved from <https://news.day.az/society/907217.html>
9. *Yaroslav Kuts: sculptural composition at the Val – new tourist allure of Chernihiv*. Retrieved from <http://svoboda.fm>
10. *Historical-sculptural composition on the Chernihiv Val is ready!* Retrieved from <https://www.gorod.cn.ua>
11. *Classification and terminology of additive technologies*. Retrieved from <https://extxe.com/9643/klassifikacija-i-terminologija-additivnyh-tehnologij/>
12. *At the entrance to the Val the basis for the installation of a model of the Baby and sculptures is preparing*. Retrieved from <https://chernigiv-rada.gov.ua/news/id-43717/>
13. *At the entrance to the Val the installation of sculptures and preparation a place for a model of the Dytynets has been begun*. Retrieved from <https://chernigiv-rada.gov.ua>



UDC 622.24

## The efficiency increase of equipment work for the cleaning block of washing fluid

Surzhko Tetiana<sup>1</sup>, Savyk Vasyl<sup>2\*</sup>, Molchanov Petro<sup>3</sup>, Kaliuzhnyi Anatoliy<sup>4</sup>

<sup>1</sup> National University «Yuri Kondratyuk Poltava Polytechnic» <https://orcid.org/0000-0001-8095-3984>

<sup>2</sup> National University «Yuri Kondratyuk Poltava Polytechnic» <https://orcid.org/0000-0002-0706-0589>

<sup>3</sup> National University «Yuri Kondratyuk Poltava Polytechnic» <https://orcid.org/0000-0001-5335-4281>

<sup>4</sup> National University «Yuri Kondratyuk Poltava Polytechnic» <https://orcid.org/0000-0003-4768-1272>

\*Corresponding author E-mail: [savycvasyl@ukr.net](mailto:savycvasyl@ukr.net)

The efficiency increase of equipment work for the cleaning block of washing fluid by the vibrating sieve modernization has been observed. The approach to the most acceptable values of constructive parameters of vibrating sieve using analytical methods and the usage of the rheological mixture model that allows determining the dynamic and technological characteristics of the vibrating machine and environmental impact on the form board and bottom has been implemented. The influence of the working body (grid) of the vibrating sieve on the rough cleaning of drilling mud from sludge has been investigated. A method for reducing complex hybrid systems to systems with a finite number of freedom degrees has been proposed, and the reduced parameters had the ability to adequately describe the wave processes of a continuous medium.

**Keywords:** the vibrating sieve, the drilling solution cleaning, the vibration exciter, the drilling solution, the rheological model, the working body, harmonic fluctuations, the resonant mode.

## Підвищення ефективності роботи обладнання блоку очищення промивальної рідини

Суржко Т.О.<sup>1</sup>, Савик В.М.<sup>2\*</sup>, Молчанов П.О.<sup>3</sup>, Калюжний А.П.<sup>4</sup>

<sup>1,2,3,4</sup> Національний університет «Полтавська політехніка імені Юрія Кондратюка»

\*Адреса для листування E-mail: [savycvasyl@ukr.net](mailto:savycvasyl@ukr.net)

Підвищення ефективності роботи обладнання блоку очистки промивальної рідини за рахунок модернізації вібростата. Зведення до найбільш прийнятних значень конструктивні параметри вібраційного сита за допомогою аналітичних методів та застосування реологічної моделі суміші, що дозволяють визначити динамічні та технологічні характеристики вібраційної машини, вплив середовища на борт і дно форми. Виявлено, що вібростата, які використовуються при очищенні бурового розчину, конструктивно можуть ефективніше впливати на розчин при контрольованому режимі роботи робочого органу, що дозволить збільшити при цьому інтенсивність дії вібрації. Досліджено, що амплітуда напружень суттєво залежить від фізико-механічних характеристик суміші, частоти і амплітуди коливань, товщини оброблюваного шару і співвідношення частот вимушених і власних коливань системи. Вивчено динаміку роботи вібраційних систем, що представляють собою реологічну модель у вигляді інтегрального суцільного середовища, з урахуванням різних впливів на робочий орган. Досліджено вплив робочого органу (сітки) вібраційного сита на грубу очистку бурового розчину від шламу. Запропоновано метод зведення складних гібридних систем до систем з кінцевим числом ступенів свободи, при цьому редуковані параметри мають здатність адекватно описувати хвильові процеси суцільного середовища. На підставі отриманих результатів дослідження запропонована методика інженерного розрахунку визначення динамічних і конструктивних параметрів вібростата для очистки бурового розчину в насосно-циркуляційній системі бурової установки.

**Ключові слова:** вібраційне сито, очистка бурового розчину, вібробуджувач, буровий розчин, реологічна модель, робочий орган, гармонійні коливання, зарезонансний режим



## Introduction

The work actuality is based on the importance of providing the high quality of wells drilling process in the oil and gas industry. It highly depends on the characteristics of re-generating systems (sifter-vibrating sieve, centrifuge, cyclones-sand separators, and others). The speed and quality of cleaning the drilling solution are up to constructive specialties of the vibrating sieve. Refining the cleaning drilling characteristics we offer to probe the vibrating sieve construction. Existing constructions have a row of disadvantages – particularly, an underdeveloped knot of imbalances that causes insufficiently qualified cleaning the drilling solution.

During wells drilling the cleaning of drilling solution from a drilled rock is the main operation. On its quality do physical and mechanical solution properties as well as the quality of prepared solution depend. During the rough solution, cleaning has been established that the most widespread way is using vibrating mechanisms of the set.

Cleaning the drilling solution it is actual to apply economic vibrating sieves with spacious fluctuations, for instance, a resonant type. But in existing vibrating sieves in the resonant of fluctuations, there is pulled the whole metal construction accompanied by the drilling solution in [1, 2] that needs big energetic expenditure. The effective mixture sealing is contributed by direct resonant fluctuations of form walls, which are here the active working body. For resonant fluctuations, we need less energy expenditure than for fluctuations of the whole set construction going along with the mixture. So, the development of cassette sets with the active working body is an actual and vital scientific and technical task. The circulating system of drilling sets includes ground devices and buildings that supply the wells washing by continuous circulation of washing fluid along the closed-circuit: pump – downhole – pump. The closed circulation prevents the pollution of natural habitat with drains of washing fluid that contains chemically aggressive and toxic components.

Circulating systems of drilling sets implicate mutually connected devices and buildings that are meant to implement the following functions:

- the preparation of washing liquids,
- the cleaning of washing liquid from drilled rock and other harmful additives,
- the pumping and operating the adjustment of physical and mechanical properties of washing fluid.

The composition of the circulating system includes sucking-in and pressure lines of drilling pumps, capacities to reserve the solution and needed materials for its preparation, gutters, settling tanks, equipment for solution cleaning, controlling-measuring appliances, and others. Circulating systems are mounted on detached blocks, which are involved in the suite of drilling sets. The block principle of manufacturing provides the compactness of the circulating system and eases its montage and technical service.

The most important requirements that are claimed to circulating systems of drilling sets – are the qualitative preparation and control as well as the sustainment necessary composition and physical-mechanic properties

of washing fluid for given geological and technical conditions. While sticking to these requirements we can reach high speeds of drilling and forestall accidents and complications in the well.

## Review of research sources and publications

The main parameters of a vibrating cleaning regime include the amplitude of vibrating displacements, fluctuations frequency, and time of vibrating influence on drilling solution. It is often the effect of vibrating sealing of mixture that is rated by the product of vibrating displacements amplitude and fluctuations frequency or vibrating displacements amplitude and square of fluctuations frequency, which are the vibrating speed and vibrating acceleration correspondingly [1, 2].

In his studies, V.I. Shmygalsiy [2] stated that the effect of vibrating impact is fully characterized by the criterion “intention of vibration”, which is the product of vibrating displacements amplitude square and cube of fluctuations frequency, by the way, the technological effectiveness of vertically directed harmonic fluctuations remains unchangeable during different connection of amplitudes and frequencies if the mentioned product is unchangeable. Also in publications K.O. Olehnovych learning the intention of periodic motion of working bodies for different types of vibrating machines introduced the criterion “specific power of dynamic impact” (p. d. i.). There were theoretical dependencies of the vibrating process, realized experimental studies and done their processing, produced the construction and suggested the rough calculation of cassette vibrating set with the active working body, accomplished the research of the active working body and got with the varied way equation of fluctuations.

These issues are not watched as for vibrating sieves, but their usage will highly raise the efficiency of drilling solution cleaning. Losses of washing liquid rise with the volume increase of drilled rock and liquid leaks while it is cleaning [4-6].

At the bottom and in the open trunk of the well the washing fluid is contaminated by fragments of drilled rock, clay, and solid particles. Excessive containment of solid and rough clay particles in it leads to the decrease of drilling speeds. For example, while the increase of containment of solid phases in the washing fluid is on 1 % the figures of chisels operation decline by 7 – 10 %.

## Definition of unsolved aspects of the problem

As a result of the abrasive influence of solid particles there accelerates the wearing-out and relevantly increases the expenditure of pumps, swivels, and downhole motors details. Consequently, there is increased workforce and material expenditures on repair, which impacts negatively on technical-economic figures of drilling. That's why cleaning devices must provide a thorough removal of drilled rock from the washing liquid. The washing fluid of optimal composition does not have to include particles of drilled rock, sand, and mud with the size 5 mkm and more. The admissible capability of cleaning devices must be not less than maximal pump giving.

Among requirements that are claimed to be circulating systems the most important are mechanization and automation of processes to prepare and clean washing fluids.

### **Problem statement**

The tasks of research in this work are the analysis of existing cleaning technologies and the next development of recommendations for the effectiveness assessment of usage in industrial conditions to raise the efficiency of drilling solution cleaning.

### **Basic material and results**

The cleaning of washing fluids is carried on by the way of successive removal of big and tiny fragments of drilled rock and other additives, which are included in the washing fluid that comes from the well. For full cleaning of washing fluids circulating systems are equipped with a complex of cleaning devices. The primary cleaning is done by the vibrating sieves, with the help of which there are done big particles away (with the size of more than 75 mkm). Fine ones are removed with the sand separator (40 mkm), mud separator (25 mkm), and centrifuge (5mkm), which are used in the next stages of cleaning.

The solution must correspond with the following requirements:

- remove destroyed rock to the surface;
- cool and smear a drilling chisel and equipment;
- transmit energy on placement at the bottom of machine and turbine;
- sustain and stabilize well walls;
- create hydrostatic pressure on the layer full of fluid and gas;
- decrease the weight of the pipes due to the effect of buoyancy;
- serve as the habitat while conducting logging;
- warn the disruption of well trunk while turbulent flow or partial dissolution of rocks;
- be compatible with overdrilled rocks and filled with their liquid and gas;
- warn the corrosion of chisel, drilling column, casing pipe, and surface equipment;
- prevent the filtration properties escalation of the productive layer.

The containment of the solid phase in the drilling solution characterizes the clay concentration (3 – 15 %) and weighting material (20 – 60 %). To provide the drilling efficiency (depending on precise geological-technical conditions) the properties of the drilling solution are adjusted by the correlation change of dispersed phase containment and dispersed habitat one and the addition of special materials and chemical reagents to them. To warn the water-oil-gas appearance during anomaly high layer pressures there is increased the density of drilling solution by adding special weighting materials or decreased it by the aeration of drilling solution or addition of foam-generators to it. The containment of the solid phase in the drilling solution is regulated by the three-step system of cleaning on vibrating sieves, sand separators (cyclones), and mud separators (sedimentary centrifuges); gas-like agents are separated

in degassers. Besides it, to adjust the containment of solid-phase we add selective flocculants to it.

While being cleaned on vibrating sieves particles of drilled rock are sieved under the impact of vibrations that are arisen by eccentric or inertial vibrators. The most widespread are inertial vibrators, which permit to adjust easily the amplitude of the fluctuations by changing the imbalances position. The vibrator drive consists of electro-machine and V-belt transmission. Particles of washing fluid being bigger than net cells of vibrating sieve anchor on it and are delivered to the dump (the sludge capacity) through the transporting gutter. The cleaning solution having overcome the sieve reaches receiving capacities of the circulating system.

According to the number of vibrating frames there are allocated one-, double and tripled vibrating sieves with one-, two- and three-tier horizontal or incliningly situated sieves. Vibrating frames are set with individual vibrators and equalizers for equal sharing of solution along the width of the sieve. In multi-tier vibrating sieves washing fluid comes from the well to the higher sieve with larger cells and then to lower ones with fewer cells. Consequently, the productivity on the unit of surface increases, and simultaneously, its wearing-out declines.

For washing fluids of high viscosity, the cleaning effectiveness rises during the increase of vibrations amplitude and inclining angle of the sieve. Multi-tier sieves are provided with the device for independent regulation of inclining angle of sieves. To soften hits and protect from big loadings the vibrating frame is hung to the prop frame with the help of spiral springs or rubber shock absorbers. Vibrating frame fluctuations happen along with the closed round or elliptic trajectory. The facing motion of the vibrating frame and washing fluid contributes to the self-cleaning of the sieve. The recovery of permissible capability in vibrating sieves occurs by periodical cleaning of the sieve with water or blowing with cramped air.

The permissible capability and cleaning depth of washing fluid depends on the surface and size of net cells. The biggest surface is on wicker sieves of steel wires or nylon threads. The sieve longevity is up to the wearing-out and corrosion-fatigue tightness of used wires and treads as well as the equality of sieve strain in the vibrating frame. While boosting the thickness of wires there is an increase in their toughness and wearing-out. But, synchronously, there is the decrease of sieve surface and, decently, the permissible capability of the vibrating sieve.

In vibrating sieves there are applied nets with such sizes of cells: 0.16×0.16; 0.2×0.2; 0.25×0.25; 0.4×0.4; 0.9×0.9 mm. While choosing the cell size it is worth considering the necessary stage of cleaning, the permissible capability of vibrating sieve, and density of washing fluid.

The net is attached to the vibrating frame with the help of a cassette or two drums situated at the frame ends. At one end the net is wound with the saving of length, which is used for permission of injured while exploiting fields of the working surface of the net.

The cassette attachment supplies the equal strain of the net in longitudinal and transverse directions. The waving of the working surface in the net and its non-touch connection to the vibrating frame lead to premature injuries. Vibrating sieves allow cleaning fully washing fluids from particles with the size of more than 0.125 mm and removing it to 50 % of the drilled rock.

For widespread vibrating machines with resonant harmonic fluctuations the criterion can be shown in such a way:

$$N_0 = \left( \frac{m_0 r_0}{M_n} \right)^2 \frac{\omega^3}{2\pi}, \quad (1)$$

where  $m_0 r_0$  – the static moment of imbalances;  
 $M_n$  – the got mass of fluctuation system that is the masses total of the working body, form, and some part of the mixture;

$\omega$  – the angle speed of fluctuations.

This criterion has an energetic character, is conveniently linked with dynamic and constructive parameters of vibrating-forming machines, and allows to correlate their technological effectiveness at the stage of projecting.

Having multiplied the denominator and numerator of dependence (1) and the angular speed of fluctuations  $\omega$  and mentioned while it  $m_0 r_0 \omega = F_0$ , we have got the correlation of made powers for different frequencies of fluctuations while unchangeable power of dynamic impact

$$\frac{F_{01}}{\omega_1} = \frac{F_{02}}{\omega_2} \quad \text{or} \quad F_{01} = F_{02} = \sqrt{\frac{\omega_2}{\omega_1}}. \quad (2)$$

Shown dependencies (2) demonstrate the advantage of low-frequent fluctuations, which means that having declined the frequency of fluctuations while having the same power of dynamic impact we can get “softer” vibration regimes on record to the made power and amplitude value of vibrating acceleration.

Browsed above criteria of vibration intensity permit considering technological possibilities of the vibrating set, but have not obtained the general and full recognition from scholars and builders.

The development of machine formation has led to the fact that now the vastest are vibrating sets with vertically directed fluctuations with the frequency of fluctuations  $f = 50$  Hz and amplitude  $A = 0,3 \dots 0,7$  mm.

Processes, which perform while vibrating, depending on the viscosity of habitat as well as the shape, size, character of the particle's surface, amount of solid phase, and the most important – the value and frequency of impulses that are transmitted by mixture fragments [6, 9].

There has been a row of studies to define the mixture impact on the operation dynamics of the working body in vibrating systems. In publications [25, 26, 50, 63] the accountability of mixture impact on the working body is calculated by the coefficient of connection  $\alpha$ , which is up to work parameters of vibrating compeller:

$$M \frac{d^2 y}{dt^2} + b \frac{dy}{dt} + Cy = F, \quad (3)$$

where  $M$  – the got mass of system vibrating particles that is determined from the dependence:

$$M = M_{st} + M_f + \alpha M_b, \quad (4)$$

where  $M_{st}$  – the mass of moving trunk;

$M_f$  – the form mass;

$\alpha$  – the coefficient of connection;

$M_b$  – the mixture mass;

$C$  – the given coefficient of tightness for spring elements;

$b$  – the given coefficient of movement prop of the working body;

$F$  – the made power.

The dependence (3) is right when observing the mixture as the system with focused parameters.

Accounting for the waving fact the definition of fluctuations regimes, which go on in the mixture, is dedicated to publications [1-11], the solution of which is done according to the internal properties of the system.

In the work, there have been learned the spread of waves spring-plastic deformations and defined rheological characteristics of mixture considering tensions of sealing layer. Therefore, the tension that arises in the sealing layer is determined according to the formula:

$$\sigma(x, t) = \rho g(H - x) + \sigma(x) \cdot \sin[\omega(t + \gamma x) - \beta_3], \quad (5)$$

where  $\rho$  – the mixture toughness;

$g$  – the acceleration of free fall;

$H$  – the product, which is forming;

$x$  – the current value of height;

$\sigma(x)$  – the amplitude of tensions in the sealing layer;

$\omega$  – the frequency of the fluctuations;

$t$  – the current time;

$\gamma$  – the coefficient of the extra slide;

$\beta_3$  – the complex coefficient that includes dynamic parameters of vibrating machine and habitat.

The amplitude of tensions is highly up to physical and mechanical characteristics of the mixture, frequency, fluctuations amplitude, layer thickness, which is being processed, and frequencies correlation between made and own system fluctuations.

The observation of operation dynamics in vibrating systems, which are the rheological model being shown as a one-piece integral environment considering diverse impacts on the working body (harmonic, hitting-vibrating, and poly-phase ones), is given in the publications [1, 2, 10] where there has been offered the method of knowledge between compounded hybrid systems and systems with the eventual number of freedom stages while reductive parameters have the ability to describe adequately waving processes of one-piece habitat.

The equation of the dynamic system “machine-habitat” has the sight:

$$(m + m_b a_1)x + (b + m_b \omega d_1)x + Cx = F \cdot \sin(\omega t), \quad (6)$$

where  $m$  – the mass of moving particles;

$a_1$  and  $d_1$  – coefficients of reactive and active resistance of mixture correspondingly that implicate parameters of waving process and are defined according to the dependence [1, 2]:

$$a_1 = \frac{\alpha \cdot \sin 2\alpha \cdot h + \beta \cdot \sin 2\beta \cdot h}{h \cdot (\alpha^2 + \beta^2) \cdot [ch2\alpha + \cos 2\beta \cdot h]} \quad (7)$$

$$d_1 = \frac{\alpha \cdot \sin 2\beta \cdot h + \beta \cdot \sin 2\alpha \cdot h}{h \cdot (\alpha^2 + \beta^2) \cdot [ch2\alpha + \cos 2\beta \cdot h]},$$

where  $h$  – the height of the mixture layer,  
 $\alpha$  – the coefficient that defines the extinguishment of the wave,  
 $\beta$  – the coefficient that determines the length of the wave.

The dynamic pressure in such a case is defined on record to the formula:

$$\sigma = \rho H X_0 \omega_2 \alpha_1^2 + d_1^2, \quad (8)$$

In publications [7, 9, 11] the rheological model of the mixture is shown by the body Shofild-Skott-Bler, which is the successive connection of the models belonged to Bingham and Kelvin:

$$\eta_1 \eta_2 \dot{\gamma} + \eta_1 \gamma = (\tau - \tau_0) + \left( n_1 + n_2 + \frac{n_2}{\xi} \right) \tau + n_1 n_2, \quad (9)$$

where  $n_1, n_2$  – the time of relax and time of spring deformation postponement relevantly;  
 $\xi$  – the dimensionless coefficient of viscosity;  
 $\eta_1$  – the coefficient of real viscosity, which characterizes the flow of mixture sample;  
 $\tau$  – the tangential tension;  
 $\tau_0$  – the maximal tension of slide.

While  $\tau > \tau_0$  the model (9) is like the spring-viscous-plastic body that explains the mechanism of mixture vibration dilution, which allows revealing regularities of switching the last one to diluted state and establish parameters of the dynamic tense state that supply such transmission.

As shown above, rheological models of mixture allow us to define the dynamic and technological characteristics of vibrating machines and environmental impact on the form board and bottom.

The solution of the given task is shown in the publications [3, 11], in which the rheological model is shown as the researched partly-line function and has the sight:

$$\left\{ \begin{array}{l} x - \frac{1}{\rho} \left( \frac{d\sigma_x}{dx} + \frac{d\tau_{xy}}{dy} \right) = \frac{dV_x}{dt} + V_x \frac{dV_x}{dx} + V_y \frac{dV_y}{dy}; \\ y - \frac{1}{\rho} \left( \frac{d\tau_{xy}}{dx} + \frac{d\sigma_y}{dy} \right) = \frac{dV_y}{dt} + V_x \frac{dV_y}{dx} + V_y \frac{dV_y}{dy}; \\ \frac{1}{\rho} \left( \frac{d\rho}{dt} + V_x \frac{d\rho}{dx} + V_y \frac{d\rho}{dy} \right) + \frac{dV_x}{dx} + \frac{dV_y}{dy} = 0 \\ \frac{2\tau_{xy}}{\sigma_x - \sigma_y} = \frac{\frac{1}{2} \left( \frac{dV_x}{dy} + \frac{dV_y}{dx} \right) \pm \frac{dV_x}{dx} \operatorname{tg} \varphi}{\frac{dV_x}{dx} \mp \frac{1}{2} \left( \frac{dV_x}{dy} + \frac{dV_y}{dx} \right) \operatorname{tg} \varphi} \end{array} \right. \quad (10)$$

where  $x, y$  – relevant projections of masses powers;  
 $\sigma, \tau$  – normal and tangential tensions relevantly;  
 $\rho$  – the toughness of habitat.

The task solution for the vibrating sealing (10) leads to the following: there is the lining with the method of

characteristics, then it is shown in a canonical view and solved with the method of ultimate odds. With the help of this method as the result of defining initial and limited conditions, we can observe the whole process of sealing as well as the loadings that influence the machine and form board [3].

Conditionally the process of sealing is divided into several stages. In the publication [7] there is shown the three-step division of the sealing process, while which at the first step there is the intensive convergence of mixture particles and fast air removing that remains between them in an uncompressed state; at the second one there is removed the part of compressed air as the result of cement dough dilution; at the third step, there is the thixotropic dilution of cement dough with the remnants dispersion of compressed air and free water as well as the filling of free space in the form. In the works [7, 8] there have been proposed to pick out the next processes that occur while processing the mixture: at the first one there is the re-compacting of components, at the second stage there appear shells and liquid phase on the surface of big filler and at the last one, there is the compressing cramp of the mixture.

In the work [6] there have been offered to allocate two phases: the first – there is the re-compacting of big components (rubble) and creation of macrostructure and the second includes the deeper thixotropic change in the small dispersed (cement) system and formation of microstructure. This approach bases on the imagination of mixture as a composting material that has macro and micro peculiarities [6].

In the works [6, 12] there is demonstrated the explanation of fluctuations regimes for the mixture. At the first stage, there are recommended fluctuations of low frequency with the big amplitude of fluctuations while overcoming the powers of dry friction clutch in mixture particles. For this, we do not need small amplitudes (1 ... 5 mm) and the acceleration (1,5 ... 3,5) g to subdue the limited tension of the slide depending on habitat properties and sizes of big filler [7, 14]. At the second step, there is the extra sealing, which will go intensively while big thixotropic changes. To dilute the dissolved component there are actual high frequencies or the introduction of plasticized additives.

Using harmonic fluctuations to process mixtures, one or another stage dominates. So, the flow is faster on the first stage with low frequencies and big amplitudes, but during high frequencies and small amplitudes, it is on the contrary (the second one) [7]. This change can be removed by using asymmetric fluctuations regimes that are realized with the frequency of 25 Hz and lower, and big amplitudes, near which there arises a row of high frequencies and small amplitudes. As the result of an asymmetric regime there happens the connection of two stages, which means intensifying the process [1, 6, 9, 10].

During the impact of low-frequent regimes, there is the less intensive dilution of dissolved components. On the other hand, big amplitudes facilitate mutual displacement of particles, and the general time of sealing decreases [6, 12, 13].

For moving mixtures in conditions of low frequencies, powers of viscous resistance will be higher than while middle frequencies, but not important. In studies to find out rational accelerations for diverse frequencies, it has been established that while increasing the vibration frequency we need to raise the high acceleration. Therefore, for frequencies 10 ... 15 Hz the rational acceleration is (1,5 ... 3,0) g, but for frequencies 40 ... 50 Hz it is (3,0 ... 4,0).

While applying moving mixtures it is especially important to remove the stratification. The usage of asymmetric fluctuations regimes with the frequency from 10 to 25 Hz and acceleration in limits of 10-35 m/s<sup>2</sup> decreases the stratification at 2 ... 2,5 times for moving and at 3 ... 3,5 ones for very moving mixtures comparing to symmetric regimes of vibrating ( $f = 50$  Hz,  $A = 0,2 \dots 0,5$  mm) [6, 8]. While there appears the possibility to use effectively additives and plasticizers, decrease the cement expenditure and decline the noise level and vibration while contracting the sealing regime to 15 ... 30 s [1, 3, 10].

The sealing is functionally dependent on the acceleration that is accepted as one of the main factors, which define this process, which is essential during creating the vibrating set. The fewer values of acceleration and scopes for rational frequencies and amplitudes are, which will allow the highest effect of sealing, the more optimal the vibrating system will be [6, 7, 8]. Besides the acceleration, the efficiency of vibration impact was also rated by the vibrating speed, specific power, intension, and other connections of displacement and fluctuations frequency [1, 3, 6-16].

## Conclusions

1. There has been a possibility to increase the efficiency of equipment work for the cleaning block of washing fluid.

2. There have been observed processes happening during the vibration, which are dependent on the environment viscosity.

3. There has been learned the dynamics of vibrating systems work that are the rheological model being shown as a one-piece integral environment.

4. There have been explained the fluctuations regimes for the solution.

## References

1. Стебельська Г.Я. (2015). Геологічні умови розвідки та розробки покладів високов'язких нафт та природних бітумів. *Вісник Харківського національного університету імені В.Н. Каразіна*, 1157, 53-57
2. Шмигальський В.Н., Горячих М.В. (2011). Изобретения не по специальности и профессии заявителя. *Материалы II Международной НПК учёных, руководителей, специалистов и преподавателей «Украина и современный мир» (13.05.2011)*. 74-77
3. Nesterenko M., Nazarenko I. & Molchanov P. (2018). Cassette installation with active working body in the separating partition. *International Journal of Engineering and Technology (UAE)*, 7(3), 265-268  
doi:10.14419/ijet.v7i3.2.14417
4. Nesterenko M., Maslov A. & Salenko J. (2018). Investigation of vibration machine interaction with compacted concrete mixture. *International Journal of Engineering and Technology (UAE)*, 7(3), 260-264  
doi:10.14419/ijet.v7i3.2.14416
5. Lyakh M.M., Savyk V.M. & Molchanov P.O. (2017). Experimental and industrial research on foamgenerating devices. *Розробка родовищ корисних копалин*, 5, 17-23
6. Nesterenko M.P., Molchanov P.O., Savyk V.M. & Nesterenko M.M. (2019). Vibration platform for forming large-sized reinforced concrete products. *Scientific Bulletin of the National Mining University*, 5, 74-78  
<http://doi.org/10.29202/nvngu/2019-5/8>
7. Biletskyi V.S., Shendrik T., Sergeev P. (2012). *Derivatography as the method of water structure studying on solid mineral surface*. Geomechanical Processes During Underground Mining. London: CRC Press Taylor & Francis Group
1. Stebelska G.Ya. (2015). Geological conditions of exploration and development of deposits of highly viscous oil and natural bitumen. *Visnyk Kharkivskogo natsionalnogo universytetu imeni V.N. Karazina*, 1157, 53-57
2. Shmigalsky V.N. & Goryachikh M.V. (2011). Inventions not in the applicant's specialty and profession. *Materials of the II International Scientific and Industrial Complex of scientists, leaders, specialists and teachers "Ukraine and the modern world" (May 13, 2011)*, 74-77
3. Nesterenko M., Nazarenko I. & Molchanov P. (2018). Cassette installation with active working body in the separating partition. *International Journal of Engineering and Technology (UAE)*, 7(3), 265-268  
doi:10.14419/ijet.v7i3.2.14417
4. Nesterenko M., Maslov A. & Salenko J. (2018). Investigation of vibration machine interaction with compacted concrete mixture. *International Journal of Engineering and Technology (UAE)*, 7(3), 260-264  
doi:10.14419/ijet.v7i3.2.14416
5. Lyakh M.M., Savyk V.M. & Molchanov P.O. (2017). Experimental and industrial research on foamgenerating devices. *Розробка родовищ корисних копалин*, 5, 17-23
6. Nesterenko M.P., Molchanov P.O., Savyk V.M. & Nesterenko M.M. (2019). Vibration platform for forming large-sized reinforced concrete products. *Scientific Bulletin of the National Mining University*, 5, 74-78  
<http://doi.org/10.29202/nvngu/2019-5/8>
7. Biletskyi V.S., Shendrik T., Sergeev P. (2012). *Derivatography as the method of water structure studying on solid mineral surface*. Geomechanical Processes During Underground Mining. London: CRC Press Taylor & Francis Group

8. Korobko B.O. (2016). Investigation of energy consumption in the course of plastering machine's work. *Eastern-European Journal of Enterprise Technologies (Energy-saving technologies and equipment)*, 4/8(82), 4-11 <http://journals.uran.ua/eejet/article/view/106873>
9. Nesterenko M.P., Nesterenko T.M. & Skliarenko T.O. (2018). Theoretical studies of stresses in a layer of a light-concrete mixture, which is compacted on the shock-vibration machine. *International Journal of Engineering & Technology (UAE)*, 7/3.2, 419-424 <http://dx.doi.org/10.14419/ijet.v7i3.2.14564>
10. Маслов О.Г., Сербін В.О., Лук'яненко В.П. (2015). Визначення раціональних параметрів вібраційної машини для формування бетонних блоків. *Вісник КрНУ імені Михайла Остроградського*, 1(90)/1, 98-103
11. Орловский В.М., Савик В.М., Молчанов П.О., Похилко А.С. (2018). Облегченный тампонажный материал. *Научный вестник национального горного университета*, 4(166), 36-42
12. Rivin E.I. (2003). *Passive vibration isolation*. New York: ASME Press
13. Kelly G. (2011). *Mechanical Vibrations*. Toronto: Cengage Learning
14. Shigeyuki D., Goryozono Y. & Hashimoto S. (2012). Study on consolidation of concrete with vibration. *Physics Procedia*, 25, 325-332. <https://doi.org/10.1016/j.phpro.2012.03.091>
15. Banfill P.F.G., Teixeira M.A.O.M. & Craik R.J.M. (2011). Rheology and vibration of fresh concrete: Predicting the radius of action of poker vibrators from wave propagation. *Cement and Concrete Research*, 41(9), 932-941 <https://doi.org/10.1016/j.cemconres.2011.04.011>
16. Juradian S., Baloevic G. & Harapin A. (2014). Impact of vibrations on the final characteristics of normal and self-compacting concrete. *Mat. Res.* [online], 17(1), 178-185 <http://dx.doi.org/10.1590/S1516-14392013005000201>
8. Korobko B.O. (2016). Investigation of energy consumption in the course of plastering machine's work. *Eastern-European Journal of Enterprise Technologies (Energy-saving technologies and equipment)*, 4/8(82), 4-11 <http://journals.uran.ua/eejet/article/view/106873>
9. Nesterenko M.P., Nesterenko T.M. & Skliarenko T.O. (2018). Theoretical studies of stresses in a layer of a light-concrete mixture, which is compacted on the shock-vibration machine. *International Journal of Engineering & Technology (UAE)*, 7/3.2, 419-424 <http://dx.doi.org/10.14419/ijet.v7i3.2.14564>
10. Maslov O.G., Serbin V.O. & Lukyanenko V.P. (2015). Determination of rational parameters of the vibrating machine for the formation of concrete blocks. *Bulletin of Mykhailo Ostrohradskyyi KrNU*, 1(90)/1, 98-103
11. Orlovsky V.M., Savik V.M., Molchanov P.O. & Pokhilko A.S. (2018). Lightweight grouting material. *Scientific Bulletin of the National Mining University*, 4(166), 36-42
12. Rivin E.I. (2003). *Passive vibration isolation*. New York: ASME Press
13. Kelly G. (2011). *Mechanical Vibrations*. Toronto: Cengage Learning
14. Shigeyuki D., Goryozono Y. & Hashimoto S. (2012). Study on consolidation of concrete with vibration. *Physics Procedia*, 25, 325-332. <https://doi.org/10.1016/j.phpro.2012.03.091>
15. Banfill P.F.G., Teixeira M.A.O.M. & Craik R.J.M. (2011). Rheology and vibration of fresh concrete: Predicting the radius of action of poker vibrators from wave propagation. *Cement and Concrete Research*, 41(9), 932-941 <https://doi.org/10.1016/j.cemconres.2011.04.011>
16. Juradian S., Baloevic G. & Harapin A. (2014). Impact of vibrations on the final characteristics of normal and self-compacting concrete. *Mat. Res.* [online], 17(1), 178-185. <http://dx.doi.org/10.1590/S1516-14392013005000201>

## CONTENTS

1	<b>Probabilistic basis development of standardization of snow loads on building structures</b> Pichugin Sergii	5
2	<b>Experience and current issues of designing of steel and concrete composite structures of roof and floor systems</b> Storozhenko Leonid, Gasii Grygorii	15
3	<b>Flexural strength of span steel-reinforced concrete truss composite structures</b> Galinska Tatiana, Ovsii Dmutro, Ovsii Oleksandra	26
4	<b>Stress-strain state of space grid structure</b> Sribniak Nataliia, Tsyhanenko Liudmyla, Tsyhanenko Hennadii, Halushka Serhii	35
5	<b>Work of masonry under the combined action of vertical and horizontal loads: an analysis of experimental studies</b> Dovzhenko Oksana, Pohribnyi Volodymyr, Usenko Dmytro, Qiniso Mahlinza	44
6	<b>Proposals of diagrid structural systems</b> Chichulina Kseniia, Chichulin Viktor, Manoj Gupta	52
7	<b>Properties and improvement directions of software of single-storey buildings with frame structures</b> Hudz Serhii, Horb Oleksandr, Pents Volodymyr, Dariienko Viktor	60
8	<b>Mineral binders and concretes based on technogenic waste</b> Haqverdieva Tahira, Akhmednabiev Rasul, Bondar Lyudmila, Popovich Natali	66
9	<b>Base deformation's features during deep foundation pit excavation</b> Zotsenko Mykola, Vynnykov Yuriy	76
10	<b>Current trends in transport planning</b> Hasenko Lina, Lytvynenko Tetyana, Tkachenko Iryna, Elgandour Mohamed	82
11	<b>Experimental studies of long-term fatigue of steel sewer structures</b> Maksimov Serhii, Makarenko Valerii, Vynnykov Yuriy, Makarenko Yulia	89
12	<b>Aspects of calculation of resistance vapor penetration of enclosing structures</b> Yurin Oleg, Mahas Nataliia, Zyhun Alina, Musiienko Olha	96
13	<b>Considering the availability of cold bridges in the design of thermal insulation shell of sandwich panels element-by-element assembly</b> Filonenko Olena, Hasenko Lina, Mahas Nataliia, Mammadov Nurmammad	102
14	<b>«Green roofs» - historical experience and modern requirements</b> Filonenko Olena, Avramenko Yurii, Kidenko Vitalii	109
15	<b>Organizational and economic impact of implementation additive technologies in construction</b> Hanieiev Timur, Korzachenko Mykola, Bolotov Gennady, Yushchenko Svitlana	115
16	<b>The efficiency increase of equipment work for the cleaning block of washing fluid</b> Surzhko Tetiana, Savyk Vasyl, Molchanov Petro, Kaliuzhnyi Anatoliy	121



## ЗМІСТ

1	<b>Розвиток імовірнісних засад нормування снігового навантаження на будівельні конструкції</b> Пічугін С.Ф.	5
2	<b>Досвід і проблеми проектування сталезалізобетонних конструкцій покриття та перекриття</b> Стороженко Л.І., Гасій Г.М.	15
3	<b>Міцність на згин прогінних сталезалізобетонних фермових композитних конструкцій</b> Галінська Т.А., Овсій Д.М., Овсій О.М.	26
4	<b>Напружено-деформований стан структурної плити</b> Срібняк Н.М., Циганенко Л.А., Циганенко Г.М., Галушка С.А.	35
5	<b>Робота камяної кладки при сумісній дії вертикальних і горизонтальних навантажень: аналіз експериментальних досліджень</b> Довженко О.О., Погрібний В.В., Усенко Д.В., Кінісо Махлінза	44
6	<b>Пропозиції ґратчастих структурних систем</b> Чичуліна К.В., Чичулін В.П., Манож Гупта	52
7	<b>Властивості та напрями вдосконалення програмного забезпечення для розрахунку одноповерхових будівель з рамними конструкціями</b> Гудзь С.А., Горб О.Г., Пенц В.Ф., Дарієнко В.В.	60
8	<b>Мінеральні в'язучі та бетони на основі техногенних відходів</b> Ахвердієва Т., Ахмеднабієв Р.М., Бондар Л.В., Попович Н.М.	66
9	<b>Особливості деформування основ при влаштуванні глибоких котлованів</b> Зоценко М.Л., Винников Ю.Л.	76
10	<b>Сучасні тенденції у транспортному плануванні</b> Гасенко Л.В., Литвиненко Т.П., Ткаченко І.В., Ельгандур М.	82
11	<b>Експериментальні дослідження тривалої втомленості сталевих каналізаційних конструкцій</b> Максимов С.Ю., Макаренко В.Д., Винников Ю.Л., Макаренко Ю.В.	89
12	<b>Аспекти розрахунку опору паропроникненню пароізоляції огорожувальних конструкцій</b> Юрін О.І., Магас Н.М., Зигун А.Ю., Мусієнко О.В.	96
13	<b>Врахування наявності містків холоду при проектуванні теплоізоляційної оболонки з сендвич панелей поелементного збирання</b> Філоненко О.І., Гасенко Л.В., Магас Н.М., Мамедов Н.	102
14	<b>«Зелені покрівлі» - історичний досвід та сучасні вимоги</b> Філоненко О.І., Авраменко Ю.О., Кіденко В.І.	109
15	<b>Організаційно-економічний вплив впровадження адитивних технологій в будівництві</b> Ганєєв Т.Р., Корзаченко М.М., Болотов Г.П., Ющенко С.М.	115
16	<b>Підвищення ефективності роботи обладнання блоку очищення промивальної рідини</b> Суржко Т.О., Савик В.М., Молчанов П.О., Калюжний А.П.	121